# Cell-Based Assays in Flowing and Sessile Drops


Aishah R. Prastowo

Brasenose College

University of Oxford

A thesis submitted to the Department of Engineering Science

for the degree of *Doctor of Philosophy*

2018

# Abstract

Cell-based assays have been performed in aqueous drops within a bulk immiscible fluid phase, as an alternative to multi-titer plates. Many microfluidic functions have been developed to manipulate these drops, for example, to merge pairs of drops, and sort drops based on size or fluorescence they emit. Whilst these functions have been successfully demonstrated in the proof-of-principle stage, challenges remain in combining them into one working platform for real-life applications. As many microfluidic devices are designed for only one specific application, adjustments are required to perform different tasks. For applications involving cell culture, one must be mindful that cells are subjected to a very different environment in microfluidic devices compared to conventional culture. Small culture volume results in large surface-to-volume ratio which would affect transport of molecules within the drops and with the interfaces. Furthermore, materials used in many microfluidic devices are usually different from those used in conventional culture. Motivated by these challenges, here a passive drop merging method in a single Teflon tube and a liquid handling method using sessile drops on a Petri dish are developed. Biocompatibility of these methods for cell-based assays are assessed using mammalian cells. The first method uses fluid mechanics of three or more immiscible fluids to control the relative speed of individual drops, rather than complex channel geometries. Fluids and surfactants were screened to find a biocompatible combination for this method. The second method concerns performing cell-based assays in sessile drops, overlaid with FC-40, on tissue-culture-treated polystyrene dishes. The impact of this arrangement on cells, and the alternation of the pinning line/interface by Fetal Bovine Serum (FBS) is examined in some details. It is found that constituents of FBS accumulate at the interface which results in an alternation on the pinning line properties that is beneficial to such assays.

# Acknowledgements

I greatly thank my supervisor Prof. Edmond Walsh for his support, guidance and advice, Prof. Peter Cook for hosting me in his lab and for his advice as well, Dr. Alex Feuerborn for his mentorship and support, and lab members for our discussion and good times together. I am also thankful for the welfare support I received from Brasenose College (Kate Tempest, Dr. Dominic Keech, Prof. Elspeth Garman and Prof. Harvey Burd), as well as family and friends. I gratefully acknowledge the financial support from Indonesian Endowment Fund for Education (*Lembaga Pengelola Dana Pendidikan, LPDP*) who awarded me with *Beasiswa Pendidikan Indonesia*.

# Table of Contents

# Introduction

Microfluidic devices manipulate fluids in small volumes or within small channels [1]. Water-soluble reagents can be manipulated in a microfluidic device as drops within a bulk immiscible fluid phase [2]. Many sub-devices have been developed to manipulate these drops and perform specific function, such as for merging [3-5], mixing [6, 7] and sorting [8] them. The development of drop-based microfluidic techniques and microfluidics in general is highly associated with life science applications [9]. Some applications include DNA amplification [10], single-cell diagnostics [11], and cell-cell communication research [12]. However, as discussed in a recent review [9], the vast majority of microfluidic papers are still being published in engineering journals rather than biology or medicine ones. This fact indicates a gap in translating microfluidic technology into life science applications, as also discussed in other reviews [1, 2, 13].

While many microfluidic devices or sub-devices functions have been successfully demonstrated in the proof-of-principle stage, one of the main challenges in microfluidic technology transfer is to integrate these sub-devices into one working platform [2, 14]. Compared to the conventional biology lab techniques, there is a lack of standardization between microfluidic devices. Many microfluidic devices are designed for only one specific application – and due to their complexity, a lot of adjustments need to be done to perform different tasks. Moreover, these devices usually require sophisticated machinery and specialised experts for both their fabrication and operation [15, 16], which are barriers for adopting the technology to conventional labs.

On the other hand, devices that have been developed by mostly engineers would need an extra assessment to ensure their suitability for biology and medicine applications [13, 17]. For example, the materials commonly used by microfluidic engineers (e.g., polydimethylsiloxane; PDMS) are not the same as those usually used in biology labs (e.g.,

polystyrene) [17]. For drop-based microfluidics, at least two types of fluids are involved, and surfactants are often used to stabilize the interface(s) [18, 19]. Therefore, the system's biocompatibility now also depends on the interaction between fluids and surfactants (e.g., the gas and temperature exchange between fluids, and the effect of surfactant/molecule adsorption at fluidic interfaces). Collaborative work between engineers and biologist is essential not only to assess the biocompatibility of existing microfluidic devices, but also to effectively translate such devices to real-life applications [13, 20].

Motivated by the challenges above, there is an apparent need on the development of a biocompatible microfluidic system for cell-based assays, using accessible platform for facile adaptation from conventional lab methods. Drop-based microfluidics has much potential for this purpose, as drops can act as compartments analogue to test tubes or wells (in multi-well plates) in the conventional labs. Protocols ensuring the device's biocompatibility need to be established, where the condition of the cells should be demonstrated as comparable to when using conventional methods. Accessible and versatile microfluidic methods, along with their demonstrated biocompatibility, would accelerate the technology transfer into real-life applications.

## I. Biology of cell culture

### I.1. Adherent and suspension cells

Cell culture is a method of growing cells in an artificial environment [21]. It enables the study of animal cells behaviour *in vitro*, as a model of the *in vivo* conditions. Culturing cells *in vitro* has some conveniences in terms of controlling cell environment, characterising specific cell types (homogeneity), the economical aspect (as it can be easily scaled up for massive screening), and having less moral/ethical issues than animal experimentation [22]. Culturing cells require different environmental conditions according to the cell type. In

general there are five environmental factors that can influence cell culture condition: (1) the nature of the substrate on which the cells grow, (2) contact with other cells, (3) the culture media composition, (4) the gas phase composition, and (5) incubation temperature [22].

Most mammalian cell lines are anchorage-dependent, which means they need to be cultured attached on a solid/semi-solid surface, usually as a monolayer (adherent cells). Other cell lines can be cultured floating in the culture media (suspension cells), either naturally (e.g. blood cells) or adapted from adherent cells [21, 22]. The characteristics of both types are listed in Table 1.

Table 1 Comparison of adherent and suspension cell culture, extracted from reference [21]

| Adherent cell culture | Suspension cell culture |
|---|---|
| Needs a substrate for the cells to attach on | Floats in the culture media |
| Growth rate/proliferation can be easily observed visually under the microscope | Requires cell counting to determine the growth rate/proliferation |
| Requires enzymatic or mechanical dissociation procedures when being sub-cultured | Does not require dissociation when being sub-cultured |
| Growth is limited by the surface area | Growth is limited by the volume of culture media |

The adhesion of cells on a surface is mediated by an extracellular matrix (ECM), which can either be artificially introduced to the surface or secreted by the cells themselves [22]. During the adhesion process, the cells undergo morphological change due to the distribution and reorganisation of the cytoskeleton [23]. Most adherent cells need to attach and spread on the surface before they begin to proliferate [22].

### I.2. Role of plasma serum in cell adhesion

Proteins such as vitronectin and fibronectin found in serum supplements (e.g., Fetal Bovine Serum; FBS) in cell media can bind to solid surface and aid cell attachment [24]. In serum-free media, some cell types can still attach to the surface, but generally serum is needed to provide growth factors and other nutrients [25, 26]. Despite its popular use in cell biology as cell media supplement, the composition of FBS is not precisely defined, and can

differ from one batch to another, which is attributed to its natural source [27]. Price et.al (1982) analysed the composition of 43 samples of FBS from different suppliers, which results are extracted in Table 2, with the range showing the minimum and maximum concentration of each respective compound [28].

Table 2 Some components of FBS and their variations, extracted from reference [28]. Only components with concentration more than 1 mg/100 ml are shown here.

| Component | Concentration per 100 ml (average) | Range |
|---|---|---|
| Total protein | 3.8 g | 3.2 – 7.0 |
| Albumin | 2.3 g | 2.0 – 3.6 |
| Glucose | 125 mg | 85 – 247 |
| Cholesterol | 31 mg | 12 – 63 |
| Blood urea nitrogen | 16 mg | 14 – 20 |
| Calcium | 13.6 mg | 12.6 – 14.3 |
| Haemoglobin | 11.3 mg | 2.4 – 18.1 |
| Inorganic phosphorous | 9.8 mg | 4.3 – 11.4 |
| Creatinine | 3.1 mg | 1.6 – 4.3 |
| Uric acid | 2.9 mg | 1.3 – 4.1 |

Serum protein binding at the surface is a complex process which involves the interaction/competition between hydrophilic and hydrophobic proteins, and the uncertainty in the constitution of the serum itself. For example, fibronectin (FN), one of the attachment factors in FBS, can bind to both hydrophobic and hydrophilic (solid) surfaces but in different ways [29]. Low concentration of FN binds better on hydrophobic surface (non-treated polystyrene) than hydrophilic one (tissue-culture treated plates), but in presence of normal concentration of serum in cell culture, little FN adsorption is detected in both types of surfaces. Increase of FN on the surface was observed when cells are present on hydrophilic surface, where cells attached and grew, while no such attachment/growth was observed on the hydrophobic surface [30]. Meanwhile, cells are found to attach on hydrophobic surface when both albumin and FN are present in the media, and not when one was added after the other [29].

## II. Cell culture in microfluidic device

### II.1. Micro-scale culture

The advantages of using microfluidic devices for culturing cells over conventional methods (in flasks or multi-well plates) have been stated repeatedly in the literatures [17, 31-33]: smaller dimension means the reduction of reagents and waste involved, and special machinery can be embedded to increase control, throughput and automation. However when cultured in micro-scale, cells are exposed to a different environment from conventional bulk cell culture method; one of the reasons is high surface-to-volume ratio [34]. Therefore, some adjustments should be made, for example perfusing media more often and changing the working cell density/concentration [35].

Culture volume in microfluidic devices is typically within the range of sub-microliters, while conventional methods can involve from hundreds of microliters (e.g. 96-well plate) to tens of millilitres (e.g. culture flask) volumes. This resulted in a much smaller ratio of culture volume to cell volume, thus reduced the amount of accessible free media per cell. To compensate the effect of reaching saturated condition faster (due to proliferation, media consumption, and waste accumulation), many microfluidic devices adopted strategies to perfuse media over the cells, either regularly or periodically [33, 36, 37]. Walker et al. (2004) [38] introduced some consideration factors when designing such systems, as cells can be affected by shear stress, and the transport of molecules is on a different scale from macro-cultures. They proposed a concept of "effective culture volume" (ECV), in which the cell culture environment is defined by combining these factors: (1) mass transport, (2) diffusion and convection, and (3) protein adsorption at the interfaces. However, the relation of the said factors, ECV, and cell behaviour is still only qualitatively defined.

## II.2. Substrate materials

Apart from dimension issues, the quality of cell culture in microfluidic devices is also being influenced by the choice of materials. On its early years, cell culture was done on glass apparatus [39, 40]. Polystyrene has become popular alternative material for cell culture equipment since the rise of plasticware, mainly due to its practicality: polystyrene-based culture-wares are cheaper, thus more accessible to many researchers and feasible for single uses [17, 41, 42]. Without any treatments, polystyrene surfaces are not suitable to support cell adhesion [42, 43]; however, treatments to make them suitable are usually proprietary. It has been suggested that manufactures usually use corona discharge, gas-plasma or microwave plasma to incorporate oxygen onto polystyrene surfaces, increase their hydrophilicity and promote cell adhesion [42, 43]. Interfacial free energy between the surface and cell culture media is suggested to predict the suitability of surface for cell adhesion [43]: low interfacial free energy leads to lower adsorption of proteins inhibiting adhesion. Although the surface properties can slightly vary between manufacturers due to different treatments, polystyrene culture-wares remain popular, so most cell culture data published currently are based on cell behaviour on polystyrene surfaces [17].

PDMS has been popularized by early microfluidic researchers as a material for fabricating microfluidic devices because it is optically transparent and easy for reproducing devices from a pre-fabricated mold [17, 35, 44, 45]. Like polystyrene, without treatment PDMS surface is hydrophobic and unsuitable for cell adhesion. Different treatments have been applied such as, among others, plasma exposure, protein physisorption, and chemical immobilization [35, 44, 46]. Currently there is no standard procedure to treat PDMS surface for cell culture, and new treatment methods are still being introduced [46].

In terms of biocompatibility, often PDMS is assumed to be non-toxic, however reports suggested that some artifacts may present as a result of the interaction between PDMS and

fluids or molecules involved in the culture [35]. For example, Lee, et al. [47] compared the growth of four types of mammalian cells on PDMS surfaces (treated with fibronectin) in various ratio to the curing agent with on polystyrene surface. They found that the growth rates are comparable; however, different cell types respond differently to different PDMS-to-curing-agent ratio [35, 47]. It was also previously found that even after an extensive curing, low molecular weight oligomers in PDMS remain uncrosslinked and soluble in many solvents [45, 48]. The implication of these leached oligomers to cell culture has not been extensively studied [17]. Common surface treatments on PDMS are also known to have low durability and may not be suitable for applications that takes a long culture time [17, 46].

To bridge the material gap between conventional cell culture and microfluidic technology, polystyrene-based microfluidic devices have been fabricated and studied [49-51]. The main challenge it faces is the fabrication step; to fabricate polystyrene-based microfluidic devices with similar pattern as PDMS-based ones, high pressure and temperature are often required [50, 51]. Other types of thermoplastic have also been explored for alternative materials, e.g., polymethyl methacrylate (PMMA) [52] and cyclo-olefin copolymer (COC) [53, 54]. However, a direct comparison of cell culture in devices made of different materials has yet to be studied.

## III. Drop-based microfluidics

### III.1. Methods for generating drops

Prior to microfluidics, water-in-oil emulsions have been used to isolate genes and perform transcription/translation reactions [55]. The demand of having monodispersity and performing high-throughput analysis has initially motivated the use of microfluidic devices to generate drops for compartmenting cells/genetic materials [2, 10]. Many drop-based microfluidics use junction geometry designed for generating drops. In this approach, the

single aqueous flow is broken up into drops as it intersects with the flow of the continuous phase [56-61]. The intersection between the aqueous and continuous phase can be of the shape of T-junction [56] (one channel of the continuous phase meets with one channel of the aqueous phase), cross junction or flow-focusing channel [62] (two channels of continuous phase "pinches" one channel of the aqueous phase flowing in the middle), or co-flow [61] (the channel of the aqueous phase lies within the channel of the continuous phase) (Figure 1A). One of the advantages of this system is the ability to control the size of the drops by varying the channel dimensions, the aqueous-phase flow rate, and the Capillary number of the continuous phase, which depends on the viscosity, flow velocity and interfacial tension [58, 60]. Surfactant is commonly used to alter the interfacial tension between the two phases to assist drop formation and stabilise the interface [18]. Another advantage is the possibility of generating monodisperse drops in a high-throughput manner, up to kilohertz range [63]. However, since the drop production is sensitive to the ratio of the flow rate between multiple channels, setting up the system can be laborious and result in some sample loss [64]. Moreover, since it is based on breaking up the aqueous-phase flow, even though a high number of drops can be produced, they all come from the same fluidic sample.

Some microfluidic techniques have been developed to generate drops with varying contents from different fluidic samples (Figure 1B) utilising an x-y-z stage [65-68] or a rotating device [69]. In these devices, different fluidic samples are provided, for example in a multi-well plate, and a capillary takes the fluids in from each well as demanded. This approach is often called the "on-demand" method. Despite having a relatively lower drop generation rate compared to the channel-junction methods, multiple samples can be processed in one device within the same trial, and it is possible to process a sample in

scarcity, for example if the reagent is expensive, or if the sample comes from a limited source.

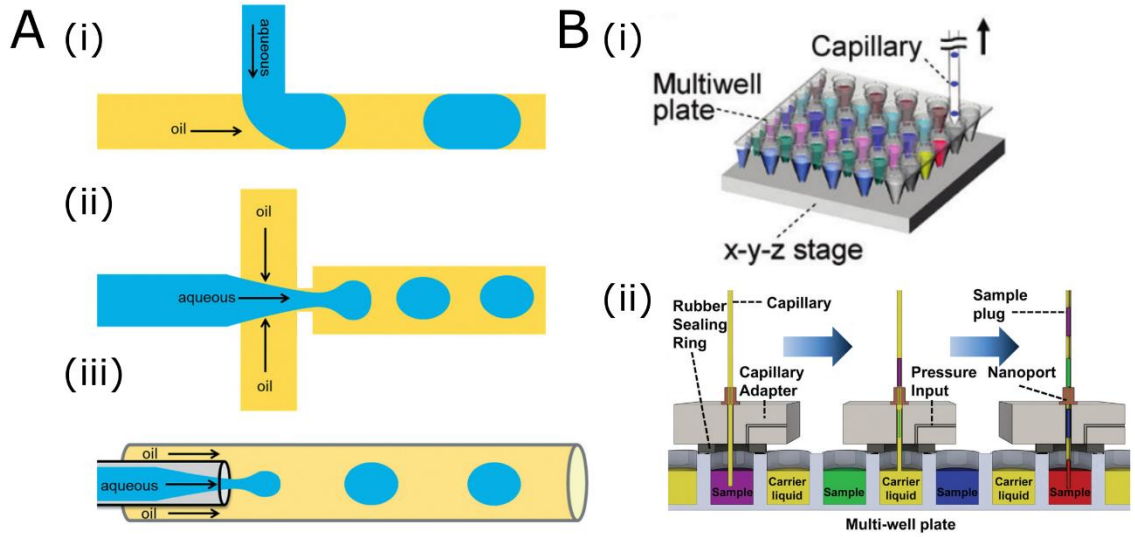


Figure 1 Methods to generate drops in microfluidic devices. (A) Drops are generated from a single aqueous sample by breaking up the aqueous phase when intersecting with the continuous (oil) phase. The common types of channel geometry used in this method are (i) T-junction, (ii) flow-focusing and (iii) co-flow devices [70]. Reprinted with permission from [70], published by The Royal Society of Chemistry. (B) Drops can also be generated from multiple samples pre-loaded in a multi-well plate, as shown in (i) DropLab [65] (reprinted with permission from [65], copyright (2010) American Chemical Society) and (ii) Serial-Sample-Loading (SSL) device [67] (reprinted with permission from [67]).

### III.2. Merging drops

After drops are generated, the subsequent process in an assay often includes adding reagents, drugs, or media to the drops. One strategy to do so is by generating another set of drops with different contents and then merging them in pairs with the drops containing the main sample. Specific channel geometry in microfluidic devices have been designed to merge pre-generated drops [4, 8, 71-73] based on varying the channel width. For example, Tan et al. (2004) [8] designed a "rectifier" channel geometry to alter the velocity of drops so that the distance between two flowing drops can be reduced until they touch each other and merge. A similar approach was taken by Niu et al. (2008) [71] but with the addition of

some pillars to assist merging (Figure 2A). When a drop enters the merging area, it decelerates due to the expansion of the channel width, allowing the next drop in line to catch up. The pair's interface is then disturbed by the pillars which induce merging.

Active elements have been used to merge two drops that are already in contact but have stable interfaces (Figure 2B-D). Electro-coalescence has been used to merge drops in many devices, as electric field can be easily switched on and off for on-demand merging. Priest et al. (2006) [74] embedded gold electrodes in their merging device to apply potential between a pair of drops which then would induce merging (Figure 2B). Other electro-coalescence devices utilise junction geometry and controlled flow rate to synchronise the flow of the drops [75, 76]. Drops separated by the carrier fluids have also been brought to contact using a trapping element before being electro-coalesced [76, 77].

Laser-induced heat was used as an alternative stimulus to merge surfactant-stabilised drops [78] (Figure 2C). This approach is based on the surfactant transport from the locally heated interface (i.e. Marangoni force). Surface acoustic wave have also been introduced to a pair of drops to assist merging from the resulted pressure wave [79]. A more recent method to merge stable drops was proposed by Akartuna et al. (2015) [80] which uses an additional channel injecting perfluorobutanol to locally destabilise surfactant (Figure 2D).

Overall, many strategies have been used to merge pairs of drops in contact. These strategies were developed mainly to destabilise the interface between the drops, to induce merging instead of forming bilayer. Using a less stabilizing surfactant, the drops can be merged only by bringing them into contact. In almost every merging method discussed above, drops are brought into proximity by using channel geometry to alter the drop velocity or to pair drops at a junction, and occasionally with the additional of flow rate control for synchronisation. It indicates that most of the merging methods rely on the specific design and fabrication of microfluidic channels.

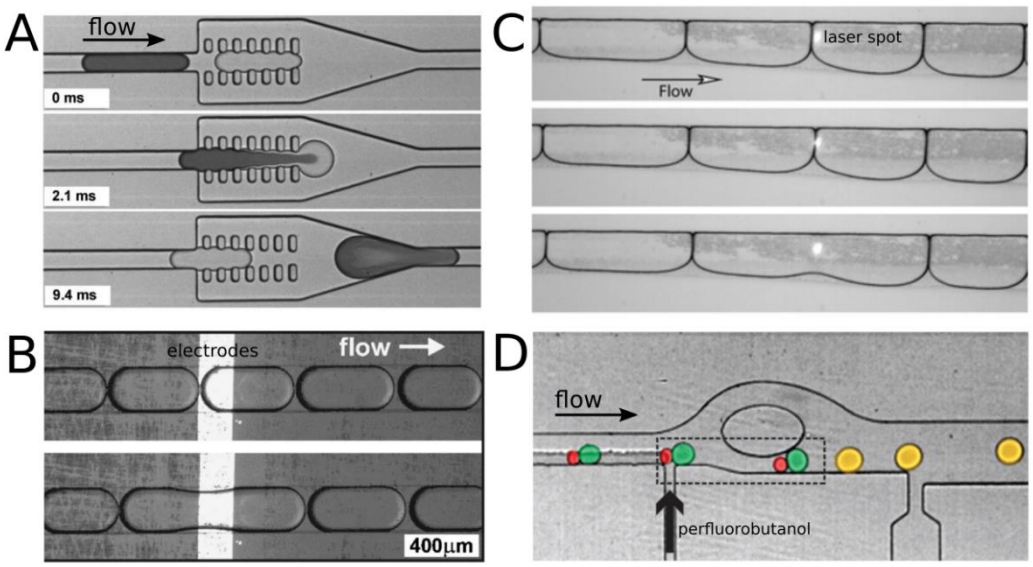


Figure 2 Methods for merging drops utilising (A) pillars in channel [71], (B) electrodes [74], (C) laser-induced heat [78], and (D) chemical induction [80]. Figure A, C, and D are reprinted with permission from [71, 78, 80], respectively, published by The Royal Society of Chemistry; B is reprinted from [74] with the permission of AIP Publishing.

### III.3. Injecting fluid into drops

Besides drop merging, fluidic transport in drop-based microfluidics can be in a form of injecting fluids into the pre-generated drops. An extra branch of micro-channel has connected to a main channel containing flowing drops in a microfluidic device for fluid addition. A PEEK Tee was used to create such junction [81] to deposit about 11 nl substrate solution into each reagent drop.

Picoinjection system is a similar approach using a nozzle-shaped channel and electrodes [82, 83] (Figure 3). In this approach, drops are streamed in the main channel and passing by the picoinjector nozzle. When the electrodes are activated, the temporary merging between the drop and the fluid from the picoinjector results in some fluidic transport into the drops. The amount of the injected fluid depends on the drop velocity and the pressure from the picoinjector. When the electrodes are not activated, there will be no merging

occurs, therefore the electrodes here act as an on/off switch. A simplified version of this approach omits the electrodes but instead charges the injected fluid [84].

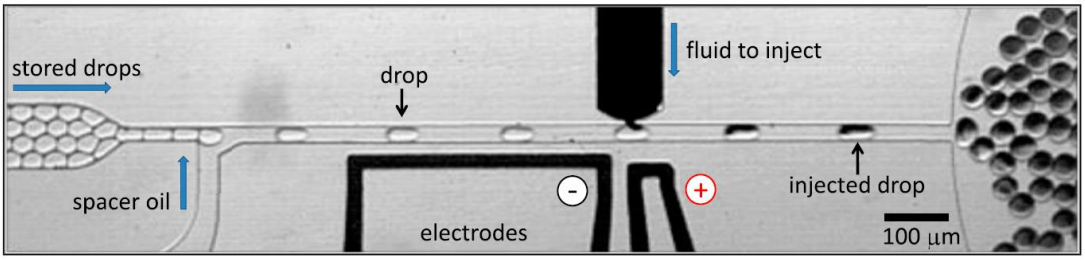


Figure 3 A picoinjector is designed to inject a small amount of fluid into pre-generated drops. The electrodes act as an on/off switch of the injection, and the amount of fluid injected into each drop is controlled by the injection pressure and flow rate of the drops [82]. Reprinted with permission from [82], copyright (2010) National Academy of Sciences.

## IV. Cell-based assays in microfluidic drops

### IV.1. Encapsulating cells in microfluidic drops

In many biological/biomedical applications, microfluidic drops are used as tiny "test tubes" to encapsulate single cells or a small population of cells. Previous studies involving cell/organism encapsulation in microfluidic drops are listed in Supplementary Table 1. Since drop-based microfluidics offers the possibility to manipulate small volumes, it enables the analysis of small cell populations and even at single-cell level. Small cell populations have been encapsulated in drops using T-junction drop generator [11, 12, 64, 85]. Single-cell encapsulation is often achieved by using T-junction or flow focusing devices [86-95]. Normally to achieve single-cell encapsulation, the sample needs to be in high dilution. If the encapsulation process is purely random, the distribution of cell number in drops will follow the Poisson statistics. It means that to minimise the presence of multiple cells in one drop, the majority of the drops would be empty [92]. To increase the efficiency of single cell encapsulation, cell-ordering devices have been designed [93-95].

### IV.2. Phenotypic screening and sorting

Separating sample of cells into drops enables screening and sorting of cell phenotypes through the measurement of the content of each drop. For example, Baret et al. (2009) [96] took inspiration from the common fluorescence-activated cell sorter (FACS) to design a microfluidic device capable to sort *E.coli* based on the enzymatic activity (Figure 4A). They started with a mix of *E.coli* expressing lacZ (encoding β-galactosidase) and an inactive mutant, and then encapsulate them in drops as single cells with fluorogenic β-galactosidase substrate. As a result, after incubation, the lacZ expressing cells appeared more fluorescent, which are then detected by a photomultiplier (PMT) upon laser excitation. The fluorescent drops were then collected by using a sorting device which uses electrodes that are programmed to be activated when receiving signal from the PMT. Similar principle have been used to sort bacteria from the environment which hydrolyse cellulosic biomass [97], *S.cerevisiae* with high xylose consumption [98], and L-lactate producing *E.coli* [98] by using fluorogenic cellobiohydrolas, pyranose oxidase and lactate oxidase, respectively, as the substrate to induce fluorescence. Since the cells are cultured separately, rare cells can be detected easier in microfluidic drops in compared to in bulk [99].

The principal of detecting rare cells using microfluidic drops have also been applied to detect bacterial mutant that are resistant to some antibiotics [100, 101], and drug-resistant cancer cells [102]. The ability to detect rare resistant cancer cells is important to prevent failure in chemotherapy. Conversely, drop-based microfluidics has also been used to analyse the toxicity of antibiotics in different concentrations and combinations [11, 64].

### IV.3. Long-term cell culture with growth monitoring

The time frame to monitor cell proliferation varies between cell types. Bacteria, for example *Escherichia coli* double every ~30 m [11], while algal cells *Chlamydomonas reinhardtii* every ~8 h [103] and mammalian cells such as HeLa take ~1 d [33, 104].

Different types of algal cells were cultured in microfluidic drops for up to 8 days from single cells to study the effect of pH, nitrate concentration and drop volume to the cell growth [103]. In this study, the drops were used to encapsulate single cells for studying cell heterogeneity in a population. Another study on algal cell growth involved a specific device for trapping drops for easy monitoring [105] up to 33 d. A drop trapping system "Dropspot" was also developed to monitor the proliferation of yeast cells [106] (Figure 4B). Meanwhile, mammalian cell proliferation has not been extensively studied in microfluidic drops beyond the viability measurement to demonstrate the biocompatibility of the device and surfactant [66, 107, 108].

### IV.4. Genetic screening

The development of genetic material amplification method through polymerase chain reaction (PCR) and the advance of Micro-Electro-Mechanical Systems (MEMS) have motivated the miniaturisation of the thermocyclers from the 1990s [109-111]. Many designs consisted of a micro-channel or capillary on several heating elements, so that the chemicals can flow and go through cycle of temperatures more rapidly due to reduced thermal mass (also called continuous-flow PCR) [110, 112, 113]. Fluorocarbon and surfactant was introduced in such system to separate 1-µl PCR reactions [114]. Meanwhile, water-in-oil emulsion has been used to compartment genetic materials [55] and later for PCR [115-118]. Combining these two concepts, integrated drop generator and thermocycling systems were developed in microfluidic devices [63, 119, 120].

Cells are now often encapsulated in drops before being lysed for genetic analysis [121]. Often after generating drops containing cells and the reagents, the drops are collected outside the device for thermal cycling [122-125]. For example, Jang et al. (2017) [122] designed a drop-based digital PCR to detect bacteria at a concentration lower than the minimum can be detected by a conventional PCR. A microfluidic device was used

to generate drops which would encapsulate the bacteria with primer and PCR mix before the drops were being collected off-device for thermal cycling (Figure 4C). The presence of bacteria was detected by fluorescence microscopy. The accumulation of fluorescent proteins in small volumes would make detection easier. Integrated thermocycler in a drop-based microfluidic device or connected to it has also been demonstrated in other studies [123, 126].

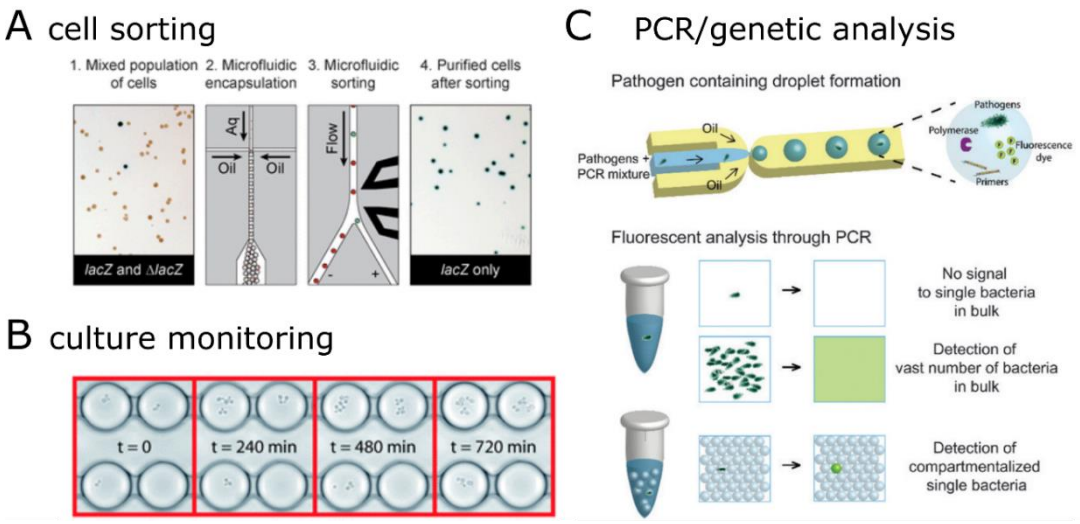


Figure 4 Some applications of drop-based microfluidics for cell-based assays. (A) Microfluidic drops encapsulate single *Escherichia coli* cells and the device sorts them based on their fluorescence expression [96]. Reprinted with permission from [96], published by The Royal Society of Chemistry. (B) *Saccharomyces cerevisiae* cells were cultured in drops starting from one or small number of cells per drop. Their growth was monitored for up to 15 h [106]. Reprinted with permission from [106], published by The Royal Society of Chemistry. (C) Drop-based PCR is used to identify *Escherichia coli* and *Salmonella* from a water sample [122]. Reprinted by permission from Springer Nature Customer Service Centre GmbH: Springer BioChip Journal [122] copyright (2017).

### IV.5. Genetic modification

Another application of drop-based microfluidics is to perform electroporation, which is a method to introduce genetic materials, drugs or dyes into cells using electric field. In this method, electric pulses are generated to induce formation of pores on cell membrane allowing foreign molecules to permeate [127]. Advantages of using microfluidic drops specifically to perform electroporation are the voltage needed is lower due to smaller dimensions, and it is possible to observe with microscope in real-time [127]. An example of

this device is shown in Figure 5 [128]. First, a T-junction generates drops containing cells and DNAs. The drops flow through a pair of gold electrodes on a microchannel. As voltage is applied, the DNAs are delivered to cells through membrane pores. Plasmid vectors that codes green fluorescence protein have been shown to be delivered into mammalian cells using this method [128]. Drop-based microfluidic systems with integrated electrodes have been reported to increase the efficiency of electroporation in yeast [129], algae [130] and mammalian cells [127, 128, 131].

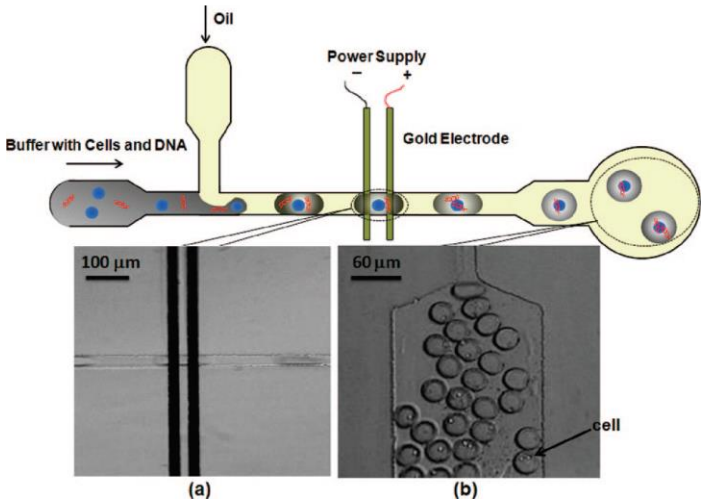


Figure 5 An example of drop-based electroporation device. Cells are co-encapsulated with DNA in drops and being pass through electrodes in a micro-channel. The applied voltage induces the formation of pores on the cell membrane, allowing the DNA to enter the cells. Reprinted with permission from [128]. Copyright (2009) American Chemical Society.

### IV.6. Sessile drop arrays

Sessile drops have also been used in microfluidics for cell-based assays. This method involves contact of the drops with at least one fluid (air or immiscible liquid) and one solid surface. This is particularly beneficial for adherent cells as it allows them to attach on the solid surface. List of previous studies which involve culturing cells in sessile drops are summarized in Table 3. As in other microfluidic systems, various solid materials have been used such as glass [132-134], PDMS [66, 135], and polystyrene [136, 137]. An immiscible liquid usually overlays the drops to prevent or limit evaporation, but sometimes humidified

air is used instead [134]. To stabilize drop arrays, the drops need to be anchored in a designated area on the solid surface. Hydrophilic surfaces are preferable for water-based drops to adhere on. Physical [66, 138] and wettability [139, 140] boundaries have been used to prevent the drops from sliding off or merging to each other. Wettability boundaries are created by treating the solid surface so that only the designated spots for the aqueous drops are hydrophilic and the rest of the surface hydrophobic. This way the drops tend to stay on the hydrophilic sites, at least up to a certain volume determined by the advancing contact angle. To create a wettability boundary pattern, surface modification techniques such as photolithography [139, 141-144] are usually involved.

Table 3 List of previous studies on mammalian cell encapsulation in sessile drop microfluidics

| Application | Device/surface type | Drop depositing method | Drop barrier | Drop size |
|---|---|---|---|---|
| Patterning cells for co-culturing tests [132] | Microscope glass slide | Manual pipetting | Mineral oil/silicone oil | 1 µl |
| Single cell encapsulation [133] | Microscope glass slide | Inkjet printing | Mineral oil | ~ 27 nl |
| 3D cell culture [136] | Petri dish | Purpose-built ejector | Cell culture media (hydrogel drops) | ~30 nl |
| Drug screening [139] | Superhydrophilic surface | Rolling fluid across pattered surface | Patterned hydrophobic barriers | 700 pl – 3 µl |
| Drug screening [134] | Glass surface with hydrophobic well walls | Syringe pump and PDMS nozzle | humidified air in chamber | 50 – 500 nl |
| Drug screening [66] | PDMS | Syringe pump and tubing system | FC-40 | 500 nl |
| Protein analysis in single cells [145] | Coverslip with silicone isolator | Syringe pump and tubing system | Oil (not specified) | 10 nl |
| Spheroid formation [135] (drops anchored sideways) | PDMS | Syringe pump and tubing system | FC-40 | 500 nl |
| Single cell isolation and growth monitoring [137] | Silanized petri dish | Syringe pump and tubing system | Mineral oil | 7 nl |
| Drug screening [144] | Glass with pillar arrays | Dipping-depositing with a pin | Mineral oil | 179 fl – 1 nl |
| Drug screening, organism response monitoring, genetic analysis [146] | Petri dish | Draw barrier with hydrophobic pin (reverse printing) | FC-40 | ~ 150 nl – 1.2 µl |

## IV.7. Biocompatibility assessment of microfluidic devices

The word “biocompatible” generally means not having a harmful or toxic effect on biological materials or living systems. It is usually defined for specific applications, for example, Roach et al. (2005) screened different surfactants to select one which is the most biocompatible for *in vitro* transcription/translation (IVTT) in drops [147]. For this specific application, a biocompatible surfactant is defined as the one that can minimize protein adsorption and denaturation at the interface. As a result, a biocompatible surfactant would not prevent the protein reaction from occurring within the aqueous phase rather than at the drop interface. In their screening, both tensiometry and fluorescence analysis was used. Biocompatible surfactants used in this study are expected to lower the interfacial tension to some point, independent whether proteins present or not, whilst if there are some protein adsorption or denaturation at the interface, there would be some further decrease in the interfacial tension when proteins are added. Fluorescently-labelled proteins are also used to visualize if there is protein adsorption to the interface [147].

For a similar application, Kaltenbach et al. (2012) proposed a method to quantify the biocompatibility of fluid and surfactant (or mixture of several surfactants) based on the gradient seen in plots of fluorescence intensity level versus droplet diameter [148]. This parameter is termed “concentration correlation coefficient” (CCC) in the unit of Relative Fluorescence Unit (RFU) per μm drop diameter. In their screening, seven fluid and surfactant combinations that had been used in other studies were measured, where “EA” surfactant (commercially available PEG-PFPE based surfactant) in HFE-7500 fluorinated liquid was shown to have the greatest CCC, meaning it was the best combination for preventing adsorption [148].

For applications involving living cells and organisms, biocompatibility is usually defined as the ability to maintain cell viability, growth, and/or gene expression comparable

to when using conventional cell culture techniques. There are different ways of measuring device compatibility to living cells, but in much of the microfluidics literature [87, 94, 149-154], cell viability numbers (ratio of the number of living cells to the total number of cells) of higher than 80-90% over the experimental time frame (can be from 1-2 hours to several days) are presented as the indication of the device having no harmful effect to the cells. Cell viabilities after being encapsulated in drops have been assessed using trypan-blue [149, 155], propidium iodide (PI) staining [152, 156], and fluorescent live/dead staining [108]. However, it is to be noted that especially in short time experiments, cells can maintain high viability even in sub-optimal condition. Cell proliferation can be a more accurate indicator of device biocompatibility because in order to perform cell division, a closer-to-ideal environment is usually required [157]. The methods for measuring cell proliferation that have been used in drop-based microfluidics studies are sample counting [11, 12, 105] and carboxyfluorescein diacetate (CFDA) staining [152, 158].

An example of drop-based microfluidic device biocompatibility assessment was performed by Clausell-Tormos et al. (2008) who especially focused on surfactant biocompatibility to mammalian cells. In their approach, HEK293T cells were incubated on a layer of FC-40 + different surfactants for up to two days [108]. Cell morphology was observed using microscopy after incubation. Carboxy-PFPE and poly-L-lysine-PFPE (PLL-PFPE) were found to mediate cell lysis, while polyethyleneglycol-PFPE (PEG-PFPE) and dimorpholinophosphate-PFPE (DMP-PFPE) showed biocompatibility, indicated by the normal visible cell morphology. In the same study, using DMP-PFPE surfactant, the viability of Jurkat and HEK293T cell lines inside picoliter and nanoliter sized droplets was observed for over 14 days using live/dead staining. The cell viability was more than 80% up to 3 days and then decreased gradually. However, in their method it is not possible to retrieve and count the total number of cells, therefore cell proliferation can only be estimated roughly

from the increase of recovered cell number (e.g., ratio of recovered cells to initial cell number of Jurkat cells in 660 pl drops increased from 29% to 55% from 1 h to 2 d) [108].

## V. Carrier fluids and surfactants

### V.1. Fluids and surfactants for carrying cells in drops

Various types of fluids have been used to carry cell-laden aqueous drops, including mineral oils, vegetable oils, silicone oils, fluorocarbons, and hydrocarbons [159]. Often surfactants are added to stabilize drops [160]. Generally, there are three parameters taken into account for choosing the fluid and surfactant type, which are drop stability, biocompatibility, and cross-contamination [18].

Fluorocarbon fluids are probably the most common carrier fluid in flowing-drop microfluidics. Fluorocarbon as the carrier fluid have been used with bacteria [152, 159, 161-163], yeast [106, 164, 165], mammalian cells [108, 166-168], and even multicellular organisms [108, 169]. The popular use of fluorocarbon may be attributed to its immiscibility with both oil and water [170] – allowing three immiscible fluids in the device, its capacity to dissolve gas [170], and its compatibility with poly-dimethyl-siloxane (PDMS), a common material of microfluidic devices [171]. Fluorocarbon also has been reported to inhibit cross-contamination better than silicone oil [159]. It is different from other types of carrier (usually, oils) in a way that it is denser than water.

A common surfactant used with fluorocarbon fluids to encapsulate cells is the diblock PEG-PFPE or triblock PFPE-PEG-PFPE copolymer, either home-made [150-152, 160, 172] or proprietary [173-178]. It is a non-ionic surfactant with PEG (polyethylene glycol) as the hydrophilic block and PFPE (perfluorinated polyethers) as the hydrophobic block. The use of two PFPE tails is to enhance the interfacial coverage [160]. Other PFPE-derived surfactants used in drop microfluidics are DMP-PFPE [108] and PFPE-Tris [107]. Another

frequently used fluorosurfactant is perfluorooctanol [130, 179, 180]. As an alternative to conventional surfactants, fluorinated silica nanoparticles have been used to stabilise microfluidic drops, which showed superiority to PEG-PFPE based surfactants in terms of retaining small molecules and assisting adherent cells attachment [181].

Silicone oils are usually used when thermostability is a requirement [182, 183]. Silicone oil AS 4 was used as the carrier of Mouse B lymphocyte drops to demonstrate the thermal manipulation method in a microfluidic chip [155]. Mineral oil – a hydrocarbon mixture – with 1-5% Span 80 have been used in several studies involving mammalian cells, including CHO-K1 [184], Jurkat [149], blood progenitor cells [158] and human breast cancer cells [185]. Pure hydrocarbons are widely used in drop-based microfluidics research [186-190], but only limited applications in these studies involve living cells. Tetradecane without surfactant was used as a carrier fluid when growing bacteria in 60 nl drops for up to 144 hours [12], while hexadecane + 1% Span80 was used when studying the response of *Caenorhabditis elegans* to neurotoxin within 2 hours [191].

### V.2. Protein adsorption to interfaces

Protein can behave like surfactant due to the presence of some hydrophobic and hydrophilic sites. However, the adsorption of protein to an interface is a more complex process which can possibly include protein unfolding and denaturation [192, 193]. When a low concentration protein solution adsorbs to an interface, the dynamic interfacial tension undergoes three different regimes: (1) induction regime, where the interfacial tension is similar to the pure fluid, (2) monolayer saturation, characterized by a sharp decrease in interfacial tension, and (3) interfacial gelation, where interfacial tension decreases at a slower rate while protein molecules at the interface rearrange themselves and build a gel-like network [194], as illustrated in Figure 6. In general, protein molecules are much larger and can cover wider surface area than surfactant molecules, hence fewer adsorbed protein

molecules are needed to fully cover an interface as a monolayer. It is suggested that this is one of the reasons why low molecular weight surfactants can decrease interfacial tension more than proteins [194].

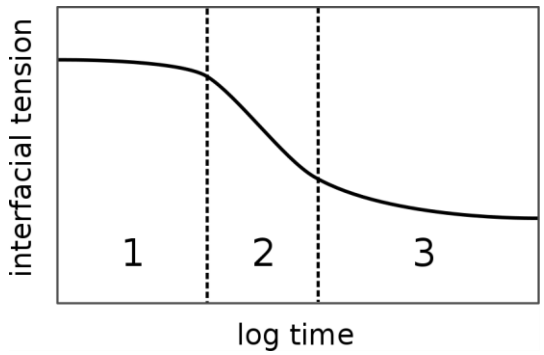


Figure 6 Sketch of typical dynamic interfacial tension due to protein adsorption at oil/water interface, plotted against time. The dashed lines separate the profile into three regimes: (1) induction, (2) monolayer saturation, and (3) interfacial gelation [194].

### V.3. Surfactant-protein interaction in microfluidic drops

Protein has been used to prevent molecule leakage from drops [195, 196]. In one study, it was observed that when using mineral oil + surfactant Abil EM 90 as the carrier fluid, fluorescein molecules were leaked to the neighbouring drops, and this leakage was reduced when bovine serum albumin (BSA) was added in the aqueous phase [195]. The reduction of molecule leakage was hypothesised to be the result of BSA barrier from its adsorption to the interface. However in a later study using fluorinated carrier fluid and resorufin dye molecules, it was speculated that the enhancing molecular retention came from the interaction between the dye and BSA molecules, which in turn alter the dye solubility [196].

Protein adsorption to the interface can be a disadvantage, for example, when the drops are used to compartmentalise reactions involving said protein. Roach et al. (2005) [147] screened different surfactants to find one that can inhibit protein (BSA and fibrinogen) adsorption to water/fluorinated liquid interface, as described above (Section IV.7).

## VI. Summary of the previous works

Microfluidics and especially drop-based microfluidics provides promising tools for cell-based assays; however, since the culture environment is different from the conventional cell culture, adaptations need to be applied. Challenges in adapting drop-based microfluidic systems for cell-based assays are summarized as the following.

1. Some cell types are sensitive to growth conditions, while some cells may appear more robust but still respond differently in sub-optimum conditions. There has not been any standard method in determining whether the condition in a microfluidic device is compatible for cell-based assays.
2. Materials used to fabricate microfluidic devices are usually different from those used in conventional cell culture; therefore, cells responses might be not comparable.
3. Small culture volume means large surface-to-volume ratio, which also means that any interfacial effects would be more dominant, e.g., adsorption of proteins to solid and liquid interfaces, toxicity effects from the materials.
4. Current techniques to generate drops and manipulate pre-generated drops usually rely on complex channel geometries and precise control of multiple inlets, which can take time to stabilize and cost some volume of the sample. This may affect cell condition and the quality of the assay.

The above points should be considered when designing a better microfluidic system for cell-based assays. Understanding the biology of cells and the properties of each component in the microfluidic system would be beneficial to address these challenges.

## VII. Objectives of thesis

This thesis aims to develop new drop-based microfluidic methods that are compatible for cell-based assays, especially with mammalian cells. In the field of microfluidics and

liquid-handling technology, this thesis is expected to present alternative methods which are versatile and accessible to be adapted in any biology laboratories. The objectives of works carried on for this thesis are:

1. To develop a novel passive drop-merging method within a single tube by exploiting fluid mechanics rather than channel geometry,
2. To assess the biocompatibility of fluids and surfactants used in the passive-merging method and demonstrate assays using mammalian cells,
3. To develop a method to perform assays in sessile drops on a Petri dish format, and assess the impact of cell-based reagents on pinning line and hence drop volume possible within a given footprint, and
4. To address the sessile drops on a Petri dish method for biocompatibility and adsorption of molecules.

## VIII. Proposed methods and overview of thesis

### VIII.1. Drops-in-drops in a Teflon tube

Techniques to manipulate pre-generated microfluidic flowing drops—e.g., transferring fluids between drops—have been previously developed. However, current microfluidic devices are usually complex and limited to one purpose. Therefore, the provision of accessible microfluidic technique which does not require specialised device fabrication method, and the use of a generic device that can perform different tasks, would open up many new applications. Drops-in-drops method is an alternative microfluidic method utilising a Teflon tube and fluid mechanics, rather than the more common approach of relying on the geometry of micro-scale channel networks. This method uses three or more immiscible fluids and the knowledge of their interfacial tension to create a specific

architecture. This method allows drop merging within a single channel and driven by laminar flow without other external forces (e.g., electric/heat) applied to the drops.

This method is described in detail in Paper 1, where applications including drug screening and protein crystallization are also demonstrated. The choice of fluids and surfactants used for this method is based on their interfacial tensions and biocompatibility. Screening of fluids and surfactants for this purpose is presented in Paper 2.

### VIII.2. Sessile drops on a tissue-culture-treated Petri dish

Analogue to multi-well plates used in conventional bio-assays, sessile drops have been used in microfluidics, i.e., by using arrays of drops of small volumes as reaction chambers that are attached to a surface. This technique allows large number of independent reactions on a surface, where the sample location can be defined and therefore simplifying the addition of reagents and readout. The provision of a surface for adherent cells to attach and proliferate is a key advantage of using sessile drops instead of flowing drops. In this thesis, the proposed method is based on depositing drops onto a surface of a Petri dish. This simple approach allows the user to skip the microfabrication process, resulting in a more straightforward and accessible technology while possibly retaining the volume and cost advantages of microfluidics.

In this method, the effect on the interface and pinning line of unmodified FBS was investigated. The contact lines of the sessile drops are pinned to the Petri dish surface by exploiting adsorption of molecules in cell-based reagents so that the advancing contact angle can be altered, and hence additional fluid can be added to a sessile drop without changing its footprint, as demonstrated in Paper 3. Paper 4 addresses the biocompatibility aspect of this method for long-term culture of mammalian cells.

# IX. Appendix

Supplementary Table 1 List of publications involving cell or organism encapsulation in microfluidic drops

| Aim of investigation | Cell name | Carrier fluid | Drop vol (nl) | Incubation time | Biocompatibility measure |
|---|---|---|---|---|---|
| ***Cell sorting/isolation*** | | | | | |
| Cultivate "unculturable" cells for microbiome study [197] | *Paenibacillus curdlanolyticus* and *Escherichia coli* | FC40 + 0.5% (w/v) RfOEG | 10 | 36 h | Off-device cell recovery |
| Design of sorting device [96] | *Escherichia coli* | HFE7500 + 2% (w/w) EA | 0.012 | | |
| Design of microfluidic analysis/screening platform for directed evolution [161] | *Escherichia coli* | HFE7500 + KryJeffa900 (Krytox157FSH+ Jeffamine) | 0.014 | 15 h | |
| *E.coli* detection system in water [198] | *Escherichia coli* | Mineral oil + 1% (w/w) Span80 | 0.52 | | |
| Screening of cellulolytic microorganisms [97] | *Bacillus subtilis, Escherichia coli*, soil bacteria | HFE7500 + 2% (w/w) EA | 0.02 | | |
| Genetic identification of environmental bacteria [199] | Environmental microorganisms | Mineral oil + 4% (v/v) Abil EM90 | 0.008 | | |
| Isolating cells based on chemotaxis reaction [200] | *Escherichia coli* | FC40 | 13 | | Off-device cell recovery |
| Design of rare cell detection system based on single cell encapsulation [98] | *Escherichia coli* and *Saccharomyces cerevisiae* | Fluorinated oil + EA (RainDance) | 6 | 4 d | Observe cell proliferation using microscopy |
| Isolating and monitoring cingle ciliates from water samples [177] | *Paramecium tetraurelia* | HFE7500 + 2% Picosurf 1, mineral oil | 160 | 8 h | |
| Heritable phenotype monitoring [201] | *Escherichia coli* | HFE7500 + 0.006% surfactant | 100 | | |
| Directed evolution [202] | *Saccharomyces cerevisiae* | FC40 + 1.8% (w/w) E2K0660 surfactant | 0.006 | 3 h | |
| Cell cultivation, genetic analysis [124] | *Saccharomyces cerevisiae* | Mineral oil + 2.5% (w/w) Span 80 | 0.1 | * | |
| Detecting and sorting rare cells [166] | Human periosteal cells | 1:2 (v/v) mixture of EGC1700 and FC-3283 + 10% (v/v) 1H,1H,2H,2H-perfluorooctanol | 0.375 | | |
| Design of cell detection system [156] | Mouse myeloma cells | Hexadecane + 1% Span80 | 40 | | |
| Design of separation system followed by droplet encapsulation [185] | Human breast cancer cells BT-474 and red blood cells | Mineral oil + 0-15% Span80 | 0.1 | 35 min | Cell staining with Propidium iodide (PI) |

| | | | | | |
|---|---|---|---|---|---|
| Design of colour based cell sorting system [203] | Her2 hybridoma and Jurkat | HFE7500 + 5% PEG surfactant | 0.001 | 9 h | |
| Design of ice valve and freezing cells inside droplets [155] | Mouse B lymphocytes | Silicone oil + 0.01% (w/w) Span80 | 0.113 | 7 d | Trypan blue staining |
| Detecting antibiotics from natural bacteria [204] | Enviromental bacteria, *Actinomycetales*, reporter: *Escherichia coli*, *Bacillus subtilis* | HFE7500 + 0.5% Picosurf 1 | 0.1 | 24 h | Measuring fluorescence intensity |
| ***Cell-cell interaction/co-culturing*** | | | | | |
| Co-culturing two types of algal cells [205] | *Chlamydomonas reinhardtii* | FC40 + 2.5% (w/w) EA | 0.057 | 17 d | Observe cell growth with microscopy |
| Co-cultivation of symbiotic bacteria [206] | *Escherichia coli* | HFE7500 + 2% (w/w) PEG-PFPE (RainDance) | 1 | | |
| Cell-cell communication study [162] | *Escherichia coli* | FC40 + 1% RainDance EA surfactant | 0.52 | | |
| Monitoring interaction of bacteria and macrophages [207] | *Escherichia coli* | FC40 + 1% (w/w) 008-fluorosurfactant | 0.003 | | |
| Co-encapsulation of dendritic cells and T cells [208] | Mouse bone marrow dendritic cells | Mineral oil + 1% (w/w) Span80 | 1 | 2.5 h | |
| Phenotypic screening on cell-cell interaction [209] | T cells, dendritic cells, RPMI-8226 | FC40 + 2% (w/w) 008-fluorosurfactant | 0.5 | 10 h | Calcein AM staining |
| Study virus-cell interaction [210] | RAW 264.7 | HFE7500 + 1% PEG-PFPE | 0.065 | 4 h | Off-device cell recovery |
| ***Design of new devices/fluidic techniques*** | | | | | |
| Cell sorting with magnetic nanoparticles [211] | *Chlorella sorokiniana* | FC40 + 5% (w/w) PEG-PFPE block copolymer | 2 | | |
| Demonstrating new technique of anchored drop merging [212] | *Dictyostelium discoideum* | QX100 (BioRad) | 0.5 | 30 min | Trypan blue staining |
| Demonstration of device fabrication technique [213] | *Escherichia coli* | 60% 20cSt PDMS oil + 40% DC5225C or mineral oil + 4.5% Span 80 + 0.4% Tween 80 + 0.05% Triton X-100 | 0.065 | | |
| Drop trapping and monitoring [214] | *Escherichia coli* | Mineral oil + 1.5% (w/w) Span80 | 0.065 | 45 min | |
| Assemble of nanoparticles in droplets [215] | *Escherichia coli* | FC40 + 1.8% (w/w) EA | 65.4 | | |
| Device for droplet storage and merging [216] | *Escherichia coli* | Mineral oil + 3% (w/w) Abil EM90 | 0.033 | 16 h | |
| Demonstrating drop generation using lab centrifuge [217] | *Escherichia coli* | HFE7500 + 2% ionic Krytox | 0.2 | | |

| | | | | | |
|---|---|---|---|---|---|
| Enhancement of fluorescence detection [218] | *Chlorella vulgaris*, NIH/3T3 | Soybean oil | 4 | | |
| Cell counting in droplets [176] | *Escherichia coli*, HL60, H1975 | HFE7500 + 2% (w/w) EA surfactant | 0.5 | 72 h | Calcein AM staining |
| Drop trapping for cell monitoring [106] | *Saccharomyces cerevisiae* | FC40 + 1.8% (w/w) fluorinated surfactant | 0.03 | 15 h | Monitor cell proliferation using microscopy |
| Design of droplet separation system by size to detect metabolic activity [165] | *Saccharomyces cerevisiae* | HFE7500 + 0.5% (w/w) EA | 0.14 | 12 h | |
| Dilution or washing step to decrease background noise [219] | *Saccharomyces cerevisiae* | HFE7500 + 1.8% (w/w) EA | 0.048 | | |
| Design of system interface between droplet and digital microfluidics [220] | *Saccharomyces cerevisiae* | HFE7500 + 0.5% (v/v) Picosurf | 20 | 24 h | Count cell numbers using microscopy |
| Design of sorting device [149] | Jurkat and red blood cells | Mineral oil + 5% (w/w) Span80 | 0.004 | | Trypan blue staining |
| Ordering cell for high efficiency in single cell encapsulation [92] | HL60 | FC40 + 1.8% (w/w) RainDance EA | 0.146 | | |
| Design of device for biological assays [184] | CHO-K1 cells | Mineral oil + 1.0% (w/w) Span80 | 0.062 | | Cell staining with trypan blue or PI |
| Demonstration of use of gas exchange on anchored droplets [221] | Red blood cells | FC40 + 0.5% DMP-PFPE | 10 | | |
| Design of device for producing gradients of concentration [222] | Leukemia cells | Mineral oil + 0.1% (w/v) Span 80 | 30 | | |
| Ordering cell for high efficiency in single cell encapsulation [93] | HL60 and K562 | FC40 + 1% (w/w) oil-phase surfactant | 0.073 | | |
| Plasma separation from whole blood sample [223] | Whole blood | Mineral oil | 1000 | | |
| Design of microfluidic system for droplet fusion and shrinkage [224] | Human promyelocytic leukemic HL60 | HFE7500 + 1% (w/w) surfactant | 4 | | Cell staining with calcein AM and PI |
| Inductively coupled plasma mass spectrometry [225] | Bovine/calf red blood cells | Perfluorohexane | 0.11 | | |
| Chip-free cell encapsulation method in picoliter droplets [154] | HL60 | Mineral oil + 10% Span 80 | 0.065 | 3 min | Trypan blue staining |
| Design of finger-powered PDMS-based device [226] | Bovine aortic endothelial cells | hexadecane + 5% (w/v) Span80 | 0.9 | | |
| Design of device to create immobilized drops [227] | HL60 | Mineral oil + 0.1% Span 80 | 0.26 | | |
| Efficient single cell encapsulation [94] | PC9 | HFE7500 + 2% modified Krytox | 0.024 | 12 h | Calcein AM staining |
| Design of droplet sorting system [228] | Human non-small lung cancer PC-9 | Mineral oil + 3% (v/v) Span80 + 2% (v/v) Abil EM90 | 0.08 | | |

| | | | | | |
|---|---|---|---|---|---|
| Single cell encapsulation [95] | K-562, blood cells | Ethyl oleate + 2% Abil EM90 | 0.03 | | |
| Optimizing picoinjection system [229] | *Escherichia coli* | HFE7500 + 2% (w/w) PicoSurf | 0.2 | * | |
| Design of device to break 200-400pl droplets into 2-5pl droplets [230] | *Escherichia coli* | Mineral oil + 1.0% (w/w) Span80 | 0.004 | | |
| ***Genetic screening (involving cell lysis)*** | | | | | |
| Single cell PCR [231] | *Synechocystis* | Mineral oil | 5000 | * | |
| Static drops for incubation and monitoring of cell population [180] | *Salmonella typhimurium, Escherichia coli* | FC40 + 17% (v/v) perfluorooctanol | 40 | 20 h | Measuring fluorescence intensity |
| Pathogen detection [232] | *Escherichia coli* | FC40 + 2% (w/w) EA | 0.001 | * | |
| Perform PCR in droplet with mini heating element [123] | *Lactobacillus brevis* | 500 cP silicone PDMS oil | 1000 | * | |
| Detection of pathogens [122] | *Escherichia coli, Salmonella* | EvaGreen generation oil | 0.5 | * | |
| Single-cell level genetic analysis [233] | *Escherichia coli* | HFE7500 + 5% fluorosurfactant (RAN biotechnologies) | 0.02 | * | |
| Single-cell screening/identification [234] | *Staphylococcus aureus, Streptomyces venezuelae, Escherichia coli* | Mineral oil + 3% (w/v) Abil EM180, HFE7500 + 2% (w/v) PicoSurf 2 | 0.03 | * | |
| Directed evolution [235] | *Escherichia coli* | HFE7500 + 0.7% (w/w) EA | 0.022 | * | |
| Single-cell sequencing [236] | *Escherichia coli, Bacillus subtilis,* SK-BR-3, HCT116 | HFE7500 + 2% (v/v) PicoSurf 1 | 0.03 | * | |
| Whole genome sequencing [175] | *Saccharomyces cerevisiae* | HFE7500 + 1%EA | 0.02 | 3 h | Off-device cell recovery |
| Single cell encapsulation [237] | Mouse mast cells and B lymphocytes | Silicone oil + 3% (w/w) Span 85 or Soybean oil | 0.1 | * | |
| Rare cell detection [238] | HEK293 | FC40 + EA surfactant | 0.1 | * | |
| Detection of low abundance protein marker [239] | PC3 | Mineral oil + 1% (w/w) Span80 | 1.8 | * | |
| Droplet-based RT-qPCR [240] | H2B-RFP MDCK cells | Mineral oil + 2% (w/w) Abil EM90 | 2 | * | |
| Single cell enzyme assay [241] | PC12 | Tetradecane + 2% Span 80 | 0.31 | * | |
| Static drop merging and PCR [242] | MDA-MB-231 | Mineral oil | 2 | * | |
| Design of device for performing high throughput RT PCR [168] | Human PC3 prostate cancer and Raji B-lymphocyte | FC40 + 5% PEG-PFPE amphiphilic block copolymer | 0.03 | * | |

| | | | | | |
|---|---|---|---|---|---|
| mRNA analysis with cell barcoding [243] | HEK293T and 3T3 | Bio-Rad droplet generation oil | 1 | * | |
| Single cell transcriptomics [174] | Mouse ES and human K562 | HFE7500 + 0.75% (w/w) EA | 5 | * | |
| Measuring multiple protease activities in single cells towards cancer diagnosis [244] | MDA-MB-231, PC-9 and K-562 | HFE7500 + 0.5% krytox (modified) | 0.034 | * | |
| Genetic analysis on fixed cells [245] | HEK293T, 3T3, *Drosophila melanogaster* | Bio-Rad droplet generation oil | 1 | * | |
| All in one device droplet microfluidic based PCR [125] | Jurkat, MCF7 | HFE7500 + 5% (w/w) 008-fluorosurfactant | 0.1 | * | |
| Leukemia cell sequencing [246] | Acute myeloid leukemia tumor cells, Raji | HFE7500/FC40 + 2-5% PEG-PFPE block copolymer | 0.01 | * | |
| RNA sequencing of disaggregated synovial tissue [247] | Cells from synovial tissue | Bio-Rad droplet generation oil | 1 | * | |
| Micro RNA detection [248] | Human breast and cancer cells | HFE7500 + 5% (v/v) PicoSurf 1 | 0.034 | * | |
| ***Genetic modification/electroporation*** | | | | | |
| Cell transfection in drops [130] | *Chlamydomonas reinhardtii* | FC70 + 5% perfluorooctanol | 0.07 | | Off-device cell recovery, SYTOX green nucleic acid staining |
| Cell transfection in drops [129] | *Saccharomyces cerevisiae* | Soybean oil | 0.014 | | |
| Cell transfection in drops [128] | Chinese hamster ovary (CHO) cells | hexadecane + 5% (w/w) Span80 | 0.41 | 1 h | Off-device cell recovery, SYTOX green nucleic acid staining |
| Cell transfection in drops [127] | HeLa cells | Silicone oil | 0.065 | | PI staining |
| Cell transfection in drops [151] | Chinese hamster ovary (CHO) cells | FC40 + 5% (w/w) PEG-PFPE block copolymer | 0.001 | 6 h | PI staining |
| Electrofusion of cells [249] | HL60 cells | HFE7500 + 1% (w/w) surfactant | 0.035 | | Calcein AM staining |
| Cell transfection in drops [250] | K562, THP-1, Jurkat | FC40 + 5% perfluorooctanol | 0.07 | 24 h | PI staining |
| ***Long-term cell culture and monitoring*** | | | | | |
| Monitoring growth of algal cells [103] | *Chlamydomonas reinhardtii, Chlorella vulgaris, Dunaliella tertiolecta* | FC40 + 2% (w/w) EA | 0.3 | 6 d | Monitor cell proliferation using microscopy |
| Growth kinetic study [105] | *Chlorella vulgraris* | Mineral oil + 2% Span 80 | 10 | 17 d | Count cell number in drops using microscopy |

| | | | | | |
|---|---|---|---|---|---|
| Quantifying growth and oil accumulation for biofuel application [251] | *Chlamydomonas reinhardtii*, *Botryococcus braunii* | Mineral oil + 2% Abil EM90 | 7.2 | 6 d | |
| Sample cultivation [85] | *Escherichia coli*, *Pseudomonas fluorescens* | Tetradecane | 60 | 144 h | |
| Design of bacterial culture system with electrode fusion [252] | *Escherichia coli* | Silicone oil KF-96L-1CS + 2% KF-6028 | 640 | 70 h | Measuring cell density using microscopy |
| Viability study in microfluidic droplet environment [12] | *Escherichia coli*, *Pseudomonas fluorescens*, *Rhodococcus rhodochrous*, *Saccharomyces cerevisiae* | Tetradecane | 80 | 6 d | Off-device cell recovery |
| Design of on-chip droplet incubation chamber [253] | *Fusarium verticillioides* | HFE7500 + 2% PEG-PFPE | 0.9 | 12.5 h | Observing growth with microscopy |
| Viability study in microfluidic droplet environment [108] | HEK293T and Jurkats | FC40 + 0.5% (w/w) DMP-PFPE | 0.66 | 14 d | Off-device cell recovery |
| Investigating effects of drop size on cell culture [254] | Chinese hamster ovary (CHO) cells | HFE7500 + 2% EA | 0.3 | 72 h | Trypan blue staining |
| Viability study in microfluidic droplet environment [169] | *Danio rerio* | PP9 | 11000 | 78 h | Observing growth with microscopy |
| Viability study in microfluidic droplet environment [108] | *Caernohabditis elegans* | FC40 | 660 | 9 d | Observing worm growth starting as eggs |
| ***New surfactant/encapsulation method*** | | | | | |
| Testing biocompatibility of silica nanoparticles for droplet stabilizing [181] | *Escherichia coli* | HFE7500 + FSiO2 nanoparticles | 0.065 | 24 h | Measure optical density (OD) |
| Protecting cells from hazardous environments [255] | *Escherichia coli* | Heavy mineral oil + PCPO | 0.014 | 1 h | Cell staining with pepsin |
| Investigating effects of DDA addition in absence or presence of cells in droplets [256] | *Escherichia coli* and *Chlorella vulgaris* | Soybean oil | 2 | 5 d | OD measurement and microscopy |
| Using BSA to prevent retention of small molecules in drops [195] | *Escherichia coli* | Mineral oil + 0.75% Abil EM90 | 0.002 | 25 h | |
| Biocompatible surfactant synthesis [160] | *Saccharomyces cereviciae* | FC40 + 1.8% (w/w) PEG-PFPE | 0.14 | 17 h | Monitor cell proliferation using microscopy |
| Using phospholipids for cell encapsulation [257] | HeLa | Oleic acid | 1 | 2 h | Trypan blue staining |
| Creating synthetic antigen presenting cells using drops with functionalized surfactant [153] | Jurkat | FC40 + PFPE-PEG-PFPE and PFPE-PEG-Gold | 0.014 | 9 h | Calcein AM and Ethidium homodimer-1 staining |

| | | | | | |
|---|---|---|---|---|---|
| Synthesis of a new type of surfactant [107] | human MSCs | HFE7500 + 2% PFPE-Tris | 0.5 | 4 d | Calcein AM staining |
| ***Phenotypic screening/drug screening*** | | | | | |
| Rapid detection and drug susceptibility of bacteria in samples [258] | *Straphylococcus aureus* | FC40 | 1500 | 7.5 h | |
| Measuring enzyme reaction of cells [259] | *Escherichia coli* | Mineral oil + 1.5% (w/w) Abil EM90 | 0.84 | | |
| Drop trapping for cell monitoring [163] | *Escherichia coli* | FC40 + surfactants + 16% (w/w) tridecafluoro octanol | 0.02 | 20 h | Monitor cell proliferation using microscopy |
| Monitor pH change during E.coli culture [260] | *Escherichia coli* | PP9 | 300 | 75 h | |
| Monitoring enzymatic activity [159] | *Escherichia coli* | FC70 + 5% (w/w) DMP-PFPE fluorosurfactant | 0.21 | 22 h | Observing growth with microscopy |
| Antibiotic resistance test at population level [11] | *Escherichia coli* | HFE7500 + 0.006% surfactant and mineral oil (spacer) | 100 | | |
| Magnetic-bead-based biosensor development [261] | *Escherichia coli* | Mineral oil + 1% (v/v) Span 80 | 1 | | |
| Drug screening of binary mixtures [262] | *Escherichia coli* | PP9 | 600 | 24 h | Gold and silver nanoparticles |
| Antibiotic screening in small volumes [64] | *Escherichia coli* | Hexadecane + 2% Span80 | 100 | | |
| High throughput assessment of photodynamic therapy photosensitizer efficacy [152] | *Escherichia coli* | FC40 + 1.8% custom synthesized PEG-PFPE | 0.14 | 5 d | SYTO-9 and PI staining |
| Droplet imaging and live image processing [178] | *Streptomyces puniceus* | HFE7500 + 0.5% Pico-Surf | 0.14 | 36 h | |
| Antibiotic effect on cell growth [263] | *Escherichia coli* | HFE7500 or PP9 | 254 | 52 h | Measuring fluorescence intensity |
| Drug (combined) screening [264] | *Escherichia coli* | PP9 | 450 | | |
| Studying effect of copper and zinc on *Streptomyces* [265] | *Streptomyces acidiscabies* E13 and *Streptomyces sp.* F4 | PP9 | 450 | 92 h | Measuring fluorescence intensity |
| Quantitative detection of cells expressing BlaC to diagnose TB [266] | *Escherichia coli* and BCG | HFE7500 + 2% (w/w) EA | 0.03 | 3 h | |
| Communication system between bacteria and cell free gene expresser [267] | *Escherichia coli* | FC40 + 2% EA | 0.034 | 7 h | |
| Phenotypic growth/antibiotic resistance screening [101] | *Escherichia coli* | FC40 + 5% PEG-di-(kytox-FSH amide) | 0.02 | 1 h | |
| Antimicrobial resistance screening [100] | *Escherichia coli* | FC40 + 2% (w/v) 008-fluorosurfactant | 0.5 | 3 h | Measuring cell density using microscopy |
| Studying specific cell genetic characteristic [172] | *Pseudomonas aeruginosa* | HFE7500 + 1.5% (w/w) PEG-PFPE | 0.002 | 48 h | |

| | | | | | |
|---|---|---|---|---|---|
| Using droplet size to detect bioactivity [268] | *Saccharomyces cerevisiae* | 52% (w/w) mineral oil + 48% perfluorohexyloctane + 0.5% Span 80 + 0.25% ArlacelP125 | 0.033 | 30 h | |
| Cell metabolism detection using osmotic pressure [164] | *Saccharomyces cerevisiae* | FC40 + 19mM Krytox-PEG600-Diblock | 0.023 | | |
| Cell screening/sorting of enzymatic activity [269] | *Aspergillus niger* | HFE7500 + 2.5% KryJeffD900 | 10 | 24 h | |
| Cell screening/sorting of enzymatic activity [270] | *Yarrowia lypolytica* | HFE7500 + 2.5% KryJeffD900 | 0.02 | | |
| Agglutination assay for blood typing and subtyping [179] | Red blood cells | Fluoroinert 3283 + 10% PFO | 40 | | |
| Detection of cell-surface protein biomarkers in single cell [271] | Human monocytic U937 | FC40 + 2% PEG-PFPE | 0.033 | 2 h | |
| Study the sickling of red blood cells by exchanging oxygen between oil phase and aqueous phase [167] | Red blood cells | FC40 + 0.5% DMP-PFPE | 7 | | |
| Detection of single-cell analyte secretion [272] | CD4 T cells | Mineral oil + 1%(w/w) Span 80 | 1.8 | | |
| Integrated droplet microfluidic module for cell assays [173] | 4E3 hybridoma | HFE7500 + 2% (w/w) EA | 0.66 | 6 h | |
| Drug screening in static drops [66] | A349 nonsmall lung cancer | FC40 | 500 | 11 d | Calcein AM and ethidium homodimer staining |
| Blood typing [273] | Human blood | Hexadecane | 320 | | |
| Antibiotic screening in small volumes [274] | OKT 9, H25B10, | HFE7500 + 1% PicoSurf 2 | 0.66 | 24 h | Calcein AM and ethidium homodimer staining |
| Quantitative cell-based assay in *Bombyx mori* [275] | *Bombyx mori* | HFE7500 + 0.5% (w/w) RainDance EA surfactant | 0.9 | 24 h | |
| Single cell phenotypic screening [276] | *Dunaliella tertiolecta, Phaeodactylum tricornutum* | FC40 + 2% PicoSurf 1 | 1 | 24 h | |
| Single cell flourescence detection system [277] | *Escherichia coli* | Light mineral oil + 1% (w/v) Span 80 | 0.3 | | |
| Single cell enzymatic activity screening [278] | *Escherichia coli* | HFE7500 + 0.5 % (w/w) Pico-Surf 2 | 0.125 | | |
| Single cell isolation and easy storage/monitoring [137] | *Escherichia coli, Pseudomonas aeruginosa, Mycobacterium , Blastococcus* | Mineral oil | 7 | | |
| Development of microfluidic cytometers [150] | 2C6 hybridoma cells | FC40 + 1.8% (w/w) PEG-PFPE | 0.33 | 6 h | Live-dead assays post incubation |
| Integrating single cell encapsulation with FACS [90] | HeLa | Hexadecane + 3% (v/v) Span80 | | | |

| | | | | | |
|---|---|---|---|---|---|
| Single cell screening with automated image analysis [87] | HEK293T | Fluorinated oil + 0.5% EA | 0.022 | 11 h | Calcein AM and Ethidium homodimer-1 staining |
| Detecting membrane protein on individual cell using aptamer and enzyme assisted amplification [279] | HeLa, CCRF-CEM, Ramos | Tetradecane + 2% Span 80 | 0.3 | | |
| Single cell measurement of telomerase expression and splicing [91] | Jurkat and K562 | Bio-Rad droplet generation oil | 5.9 | 2 d | Count cell numbers using microscopy |
| Determining lactate release in single cells for cancer cell biology [88] | K562 leukemia and U87 glioblastoma cancer cells | FC40 + 2% (w/w) 008-fluorosurfactant | 0.4 | | |
| Radiometric assay in drops [86] | Human breast adenocarcinoma cells | HFE7500 + 2% (w/w) 008-fluorosurfactant | 0.3 | | |
| Combinatorial antibiotic screening [280] | *S. aureus, P. aeruginosa, Escherichia coli* | HFE7500 + 0.5 – 2% (w/w) 008-fluorosurfactant | 1 | 7 h | Measuring fluorescence intensity |
| Screening antibiotic resistance [281] | *Escherichia coli* | HFE7500 + 6% (w/w) 60 nm F-$SiO_2$ nanoparticles | 0.075 | 1 h | Measuring fluorescence intensity |
| Single-cell level study of interferon in population [282] | Jurkat | HFE7500 + 3% (w/w) PicoSurf | 0.07 – 0.1 | 2 h | Fixable Viability Dye eFluor® 780 staining |
| Drop trapping for worm behaviour monitoring [191] | *Caernohabditis elegans* | Hexadecane + 2% Span80 | 20 | 2 h | Observe worm behaviour |

*cells were lysed in drops at the beginning stage of the assay

# Paper 1: Merging drops in a Teflon tube, and transferring fluid between them, illustrated by protein crystallization and drug screening

*Reproduced from Lab on a Chip, vol. 15, no. 18, pp. 3766-75, Aug 25 2015 [283] with permission from The Royal Society of Chemistry.*

A. Feuerborn,[a] A. Prastowo,[b] P. R. Cook,[a] and E. Walsh[b]

[a]Sir William Dunn School of Pathology, University of Oxford, South Parks Road, Oxford OX1 3RE, UK.

[b]Osney Thermo-Fluids Laboratory, Department of Engineering Science, University of Oxford, Osney Mead, Oxford OX2 0ES, UK. Email: edmond.walsh@eng.ox.ac.uk; Fax: +44 1865 288756; Tel: +44 1865 288731

**Abstract –** The ability to manipulate drops with small volumes has many practical applications. Current microfluidic devices generally exploit channel geometry and/or active external equipment to control drops. Here we use a Teflon tube attached to a syringe pump and exploit the properties of interfaces between three immiscible liquids to create particular fluidic architectures. We then go on to merge any number of drops (with volumes of micro- to nano-liters) at predefined points in time and space in the tube; for example, 51 drops were merged in a defined order to yield one large drop. Using a different architecture, specified amounts of fluid were transferred between 2-nl drops at specified rates; for example, 2.5 pl aliquots were transferred (at rates of ~500 fl/s) between two drops through inter-connecting nano-channels (width ~40 nm). One proof-of-principle experiment involved screening conditions required to crystallize a protein (using a concentration gradient created using such nano-channels). Another demonstrated biocompatibility; drugs were mixed with human cells grown in suspension or on surfaces, and the treated cells responded like those grown conventionally. Although most experiments were performed manually, moderate high-

throughput potential was demonstrated by mixing ~1,000 different pairs of 50-nl drops in ~15 min using a robot. We suggest this reusable, low-cost, and versatile methodology could facilitate the introduction of microfluidics into workflows of many experimental laboratories.

## I. Introduction

Droplet-based microfluidics allows manipulation of volumes down to femto-liters; it has applications in biomedicine – including single-cell diagnostics,[1-3] DNA amplification using the polymerase chain reaction (PCR)[4, 5] and the synthesis of nano-materials[6]. The underlying aim in many applications is to bring together and mix different water-soluble reagents. One challenge is to deliver such reagents to drops,[7] and various approaches are available to control the coalescence of a few drops either actively (e.g., using lasers or electrodes)[8] or passively (e.g., using channel geometry)[9]. For example, pico-injection has been applied to modify contents of pre-formed drops as they flow past a fixed point in a channel,[10] and to create new drops with slightly varying contents[11, 12]. Drops have also been merged as they flow through a PDMS channel by exploiting interfacial tensions between two[11, 13] (perhaps in association with a chemical method)[14] or three[15] immiscible liquids.

Several simplified methods for droplet merging have been proposed that do not utilise a preformed microchip. These include modular systems that allow many tubes/channels and T-junctions to be joined together easily,[16, 17] and a robot-driven capillary that first "prints" arrays of drops on a hydrophilic-patterned surface and then adds additional drops to specified locations (applied to single-cell RT-PCR)[18]. Whilst these methods alter drop contents in a "digital" way (i.e., by adding discrete volumes), there remains no "analogue" variant that allows continuous changes in drop content (i.e., by gradual advection into, or

out of, pre-formed drops) – aside from molecular diffusion through walls/fluids[19, 20] (where control is limited by the porosity of the wall to molecules of interest).

The use of multiple emulsions has a long history in microfluidics[15, 21-26]. Here, we exploit three or more phases to create fluidic architectures where individual drops have an aspect ratio (length to diameter) >1, and use them to merge drops, and transfer fluid between them. The approach is simple and versatile. It exploits interfacial tensions at the boundaries between immiscible fluids contained in a Teflon tube. Flow through the tube is driven by a syringe pump (or gravity), and interfacial tension is used to bring drops together, and transfer aqueous fluids gradually between pre-formed ones through fluidic nano-channels (~40-nm wide) at rates down to fl/s. We apply the first approach to confirm biocompatibility by testing drugs for their effects on human cells, and the second to screen conditions for crystallizing a protein. We also demonstrate moderate high-throughput capability by mixing ~1,000 pairs of 50-nl drops in ~15 min using a robot. We anticipate the general approach will prove useful in handling and manipulating small volumes.

## II. Methodology

Our approach utilizes at least three immiscible fluids, and different ones are used for different experiments. Interfaces between three such fluids are in equilibrium when the "Neumann triangle" is satisfied (as in Fig. 1Ai – where phase 1 is FC40 plus surfactant, phase 2 is water containing a red dye, and phase 3 is silicone oil). Then, the interfacial tension, $\gamma$, between any two fluids is less than the combination of interfacial tensions between the others ($\gamma_{1\text{-}2} < \gamma_{1\text{-}3} + \gamma_{2\text{-}3}$).[27, 28] However, drops-within-drops form if conditions no longer satisfy the Neumann triangle and $\gamma_{1\text{-}2} > \gamma_{1\text{-}3} + \gamma_{2\text{-}3}$ (which is achieved in this case by removing surfactant from phase 1). Now, fluid 3 forms the interface between fluids 1 and 2, so fluid 1 engulfs 3, and 3 engulfs 2 (Fig. 1Aii). The volumes of the immiscible drops are

independent of the inequality that leads to engulfment, which is sometimes recast as a spreading coefficient.[29] In most cases, surfactants (amphiphiles) are added to phase 3 to increase the inequality and so stabilize the chosen fluidic architecture. In all cases, the fluorocarbon "wets" the Teflon to create a continuous and protective film along the tube wall, so water-soluble molecules are unlikely ever to touch (or adhere to) the wall.

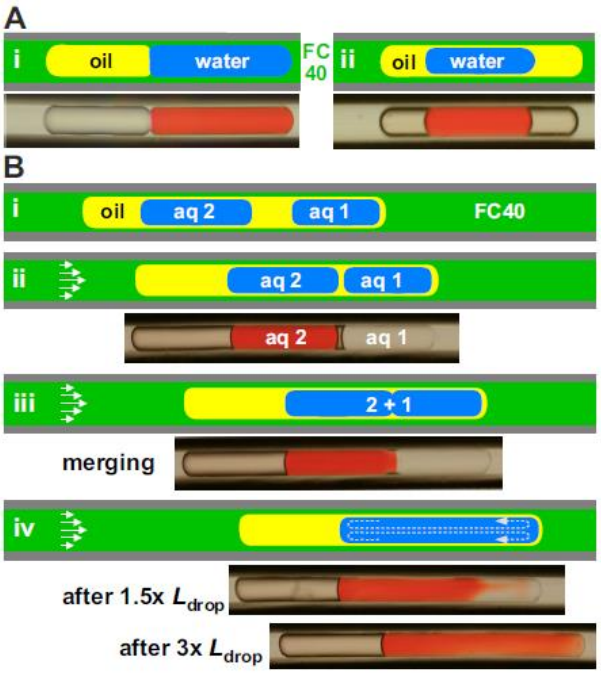


**Figure 1.** Drop merging and mixing (150-µm tubes). Schematics illustrate structures seen in movie frames below (some water drops contain red dye). (A) Structures depend on interfacial tension. (i) All three fluids are stably in contact (fluids – FC40 + 10% PFO, water + dye, 5-cSt silicone oil). (ii) If PFO is omitted, FC40 engulfs the oil, which engulfs water + dye. (B) Merging drops during flow (fluids – FC40, water ± dye, tetradecane + 1% Span80). (i) An oil drop engulfs two 10-nl aqueous drops. (ii) During flow (arrows illustrate parabolic velocity profile), relative velocities are: water drops > oil super-drop > bulk FC40. Then, as water-drop 1 cannot travel faster than the front of the oil super-drop, drop 2 soon catches it up. (iii) Drop 2 merges with 1. (iv) Vortices (curved arrows) mix contents (distance travelled indicated in drop lengths, $L_{drop}$).

We now illustrate the principle we will use to merge aqueous drops, beginning with a simple case involving a train of two drops (~10 nl) engulfed in one oil super-drop (~10 nl; Fig. 1Bi; Movie S1; all movies shown run in real time). Starting the pump connected to the tube causes laminar flow. Then drops closer to the centre-line move at a higher speed than

the engulfing fluid, and the relative mean velocities of fluids are: water > oil > FC40. Water-drop 1 is constrained from moving faster than the surrounding oil by the oil/FC40 interface. However, drop 2 is unconstrained and moves faster, and so catches up drop 1 (Fig. 1Bi,ii). The two drops merge as soon as they touch because the interface is unstable (Fig. 1Biii). Subsequently, vortices mix contents within ~4 drop lengths (Fig. 1Biv). Such "front-to-back" mixing is efficient, unlike the "side-by-side" mixing found in some microfluidic devices.[30]

## III. Materials and methods

### III.1. General reagents and equipment

FC40 and HFE7500 were from Acota, Abil®EM180 surfactant from Surfachem, and all other fluids from Sigma Aldrich unless otherwise stated. Where indicated, aqueous drops contained water-soluble dyes: 5 mg/ml Allura Red, 2 mg/ml toluidine blue, 6 mg/ml haematein (yellow), or 200 μM carboxy-fluorescein unless otherwise stated. Surfactant concentrations are given on a weight-to-weight basis. Teflon (poly-tetrafluoroethylene, PTFE) tubing (50-620 μm bore; Cole-Parmer/Zeus) was attached to a programmable syringe pump (Harvard PhD Ultra I/W) fitted with Hamilton air-tight glass syringes – with sizes ranging from 5 μl to 2.5 ml (Hamilton 800/1700 and 1000 series) – and blunt needles of appropriate gauge (i.e., 20-32). In some cases, bipartite tubes with thin and thick segments were used for high-throughput analyses. Then, the smaller segment allows manipulation of smaller volumes, whilst the larger one reduces the pressure drop (and so the possibility of leaks), minimizes the tube length required to store merged drops during multiplexing (as trains become shorter in the wider tube), and allows the use of lower-cost optics for detection of fluorescence/colour (as drops have a larger depth due to increased diameter). Conditions used for individual experiments are described in Electronic Supplementary Information.

### III.2. Interfacial tension measurement

Interfacial tensions were measured using the pendant-drop technique and a commercial system (First Ten Angstroms 1000). Drops were ejected from 16-30 gauge stainless-steel blunt needles (using a Harvard syringe pump or a Gilmont micro-meter syringe) into the less-dense fluid in a 2-ml cuvette. The manufacturer's software was used to calculate the interfacial tension for each image. Before using any new fluids, the system was calibrated; the interfacial tension of filtered water/air or FC40/air was measured and good agreement was found with established values of 72 and 16 mN/m.

### III.3. Static and dynamic interfacial tension

During flow, internal circulation in drops[31] can transport surfactant molecules from the front to the back of a drop along the interface. Hence, it will be the dynamic interfacial tension that should be used when determining the Neumann inequality. Unfortunately the dynamic interfacial tension is both difficult to measure directly, and varies – as we will demonstrate. Therefore, we select fluids for the fluidic architecture that give a strong Neumann inequality based on static interfacial tensions. Estimates of this inequality (using data in the literature)[32] demonstrate that this is easily achievable for most fluid combinations. For example, the equilibrium interfacial tension between fluorocarbon and water is ~45 mN/m, between fluorocarbon and oils is ~8 mN/m, and separating oil + surfactant and water is ~15 mN/m. The result is a strong inequality, so that fluorocarbon engulfs oil, and oil engulfs water (i.e., 45 > 15+8). This architecture is used for merging. When using surfactant-free fluids, the static interfacial tension is expected to be equal to the dynamic one, so that interfacial tensions from the pendant-drop method can be applied more definitively to the flowing system.

### III.4. Generation of arrays of drops

Carrier fluids (FC40, HFE7500, or FC40 + HFE7500, all ± surfactant), aqueous fluids (± additive), and separating fluids (tetradecane, dodecane, 5-cSt silicone oil, silicone oil AR20, sunflower oil, all ± surfactant) – which are called "oils" in the main text – were generally placed in separate wells of a 96-well plate. To avoid the need to overlay reagents with oil, drops were created by operating the syringe pump attached to a PTFE tube. Initially, the tube, syringe, and needles were all filled with FC40/HFE7500 ensuring no gas was present. The syringe pump was programmed to operate in "withdraw/stop mode". In withdrawal mode, the tip of the tube was immersed manually in the fluid until the required amount was loaded (flow rates 0.01-2 ml/h); then the pump was stopped, the tip moved to the next fluid, and withdrawal mode restarted. This sequence was repeated to produce the required fluidic architecture.

A "train" containing one aqueous drop engulfed in one oil "super-drop" can be prepared by filling a Teflon tube attached to the programmable pump with fluorocarbon, and dipping the tip of the tube successively into water and oil. Use of the custom "withdraw/stop" program provides precise control over drop sizes as fluids are loaded during "withdraw", and the tip is transferred to a new fluid during "stop". This program utilizes the software built in to the syringe pump to specify how long the "withdraw" and "stop" modes last. More aqueous drops can be engulfed in one oil super-drop by including extra dips into water and oil before the last into fluorocarbon (Fig. 1B, Fig. S1). Fluidic architectures are stably maintained when flow stops/restarts. Additional independent trains (separated by fluorocarbon) are prepared by repeating this simple process. As we shall see, each train then becomes an independent reaction vessel that utilizes only reagents in that train.

When loading tubes, aqueous reagents were initially covered with separating fluid to reduce the possibility of ingesting air into tubes, which then complicates flow patterns as

pumps start and stop (due to the compressibility of the air). However, the oil overlay was found to be unnecessary if tubes and syringes were originally filled with degassed fluorocarbon without air drops, and if no cavitation occurred when flow stopped and started. Consequently, use of a low-viscosity carrier was preferred as it reduced the pressure drop and enabled faster flow rates. Therefore, HFE7500 was often used, but it was replaced with FC40 to produce particular fluidic architectures and provide greater biocompatibility. Use of smaller syringes and larger-bore tubes also reduced the probability of air ingestion. For example, use of a 250-µl gas-tight syringe (Hamilton) connected to 350-µm diameter tube via a blunt needle led to no air ingestion, but a 2.5-ml syringe connected to the same tubing resulted in sporadic ingestion. For tube diameters between 100-200 µm, we used 50-100 µl syringes, and for 50-µm tubing 5-10 µl syringes. Although the tube is filled under sub-atmospheric pressure, ends of loaded tubes can easily be capped with a resin-filled blunt needle and operated under high pressure; however, the system is not conducive with closed-loop functionality.

For Figures 4-6, S2, and S3, tubes were loaded using stepper motors. The accuracy of drop generation depends on the drop size (the longer the better) and tube wall thickness (the smaller the better). For example, 100 drops (400 nl) were loaded into a train in a 350-µm diameter tube (using a 250-µl syringe); they had a maximum variation in volume of <4%. This variation was typically found with all syringe/tube combinations used.

Although most experiments were performed by manually dipping between reservoirs in a 96-well plate, a "robot" with three axis-positioning systems (Z-400, CNC Step, Germany) is used to demonstrate automated high-throughput potential.

### III.5. Measurement of drop velocity and length

Drop velocity and length were measured using two orthogonal LEDs/photodiodes spaced 1 m apart along a transparent PTFE tube (350 or 620-µm bore; photodiodes were

~0.5 m from tube ends; Fig. 2). As all fluids used in a single experiment had different refractive indices, photodiode voltage depends on the fluid in the light path. Times taken by drops to travel through one light beam and between beams were recorded, and drop length and inter-drop distance calculated using custom software, with sampling frequency of up to 500 Hz. To determine tube diameter, FC40/HFE7500 was pumped through a virgin tube at a known flow rate. The time taken for the leading FC40/HEF7500-air interface to travel between the two photodiodes was recorded, and diameter calculated using the continuity equation and known flow rate set on the syringe pump.

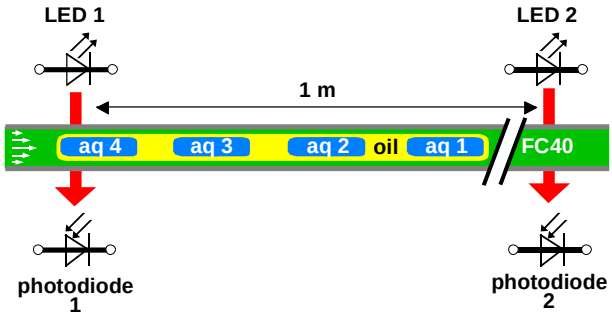


**Figure 2.** Experimental setup for measurement of drop length and velocity; photo-diode voltage reflects which fluid is in the light beam. Times taken by drops to travel through one light beam and between beams were recorded, and drop length and velocity calculated.

### III.6. Drop velocity and film thickness

The thickness of a film engulfing a drop (as in Fig. 3) may be estimated by implementing the assumptions of an inviscid ($\mu_1 \gg \mu_2$) or solid drop ($\mu_1 \ll \mu_2$), and applying continuity to the flow within a circular tube. For an inviscid drop, where $R$ = channel radius, $r$ = drop radius, $h$ = film thickness, $Q$ = flow rate, $U$ = mean velocity of fluids, we obtain:

$$\dot{Q}_{mean} = \dot{Q}_{film} + \dot{Q}_{drop}$$

The velocity in the film region is modelled as zero or a linear velocity profile (Couette flow) to determine the limits of the film thickness for the cases of inviscid or solid drops

respectively (Fig. 3ii). Equating flow rates at axial positions in carrier fluid (phase 1) and drop region (phase 2) yields:

$$\left[\pi R^2 U_{mean} = \pi (R-h)^2 U_{drop}\right]_{inviscid}$$

$$\left[\pi R^2 U_{mean} = \pi (R^2 - (R-h)^2)\frac{U_{drop}}{2} + \pi (R-h)^2 U_{drop}\right]_{Visc}$$

Solving these equations where $h << R$, provides

$$\left[\frac{h}{R}\right]_{\text{inviscid drop}} = \frac{1}{2}W$$

$$\left[\frac{h}{R}\right]_{\text{solid drop}} = W$$

$$W = \frac{U_{drop} - U_{mean}}{U_{drop}}$$

where $W$ is referred to as the excess velocity. These equations, or similar, have been derived by several authors for an inviscid[33, 34] and solid drop.[35] Therefore, when flow is induced in the capillary illustrated in Figure 3i, the distance between $x_f$ and $x_d$ reduces by $\Delta x$ which depends on film thickness. The film thickness, in the limits of an inviscid or solid drop, may be estimated by measuring the velocities of the drop and carrier fluid. For all cases where $\mu_1 \sim \mu_2$, it is expected to reside between these two limits. The same equations can then be applied to our new fluidic architecture illustrated in Figure 1B, where film thickness between water and oil phases may be estimated by measuring the mean velocity of both (assuming the carrier-fluid film surrounding the oil is unchanged over the length of the oil drop). The resultant film thicknesses, from the inviscid and solid drop equations, provide the limits of film thicknesses for any viscosity ratio between water and the engulfing oil drops.

The prediction of $h/R$, and hence excess velocity of the engulfed drops/bubbles, has been extensively studied[28,30-36] since the original experimental[36] and theoretical works;[37] most works identify the Capillary number [$Ca = \mu V/\gamma$] as the appropriate scaling parameter in such problems.

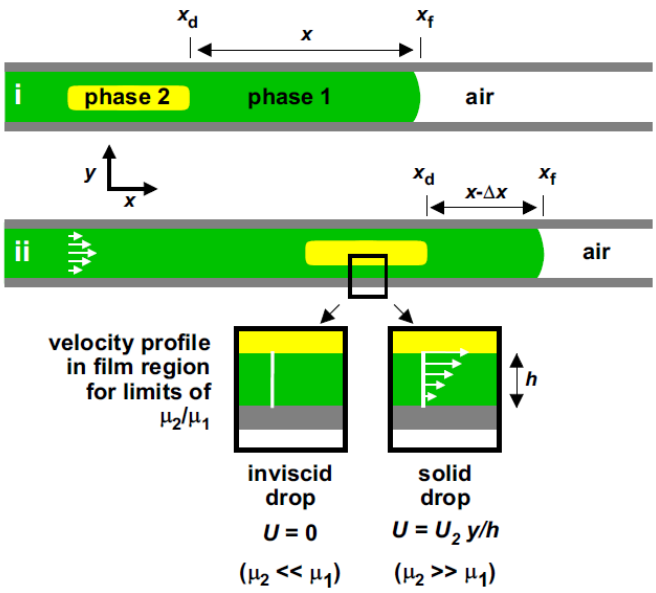


**Figure 3.** Schematic of immiscible fluids flowing in a circular capillary; (i) phase 2 (with leading interface at $x_d$) is engulfed by phase 1 (with leading interface at the air, $x_f$), which wets the wall. (ii) After flow, the distance between interfaces $x_f$ and $x_d$ has reduced due to the velocity of phase 2 (which is > phase 1). Also illustrated are the simplified velocity profiles in the film region between phase 2 and the wall, for an inviscid and solid drop.

## IV. Results and discussion

### IV.1. Relative drop velocities

To predict where and when two drops might merge in a train like that in Figure 1Bi, it is necessary to determine the excess velocity of drop 2 over drop 1. Sets of 10 trains containing two aqueous drops (each train as in Figure 1Bi) were created and the velocity of each drop recorded over a range of carrier-fluid velocities. The excess velocity of aqueous drops over the carrier-fluid velocity for each train is shown in Figure 4A. Across the ten trains the standard deviations range from 3-11% of the excess velocity between drops pairs (within the limits of carrier-fluid velocities of 5.5-0.46 mm/s).

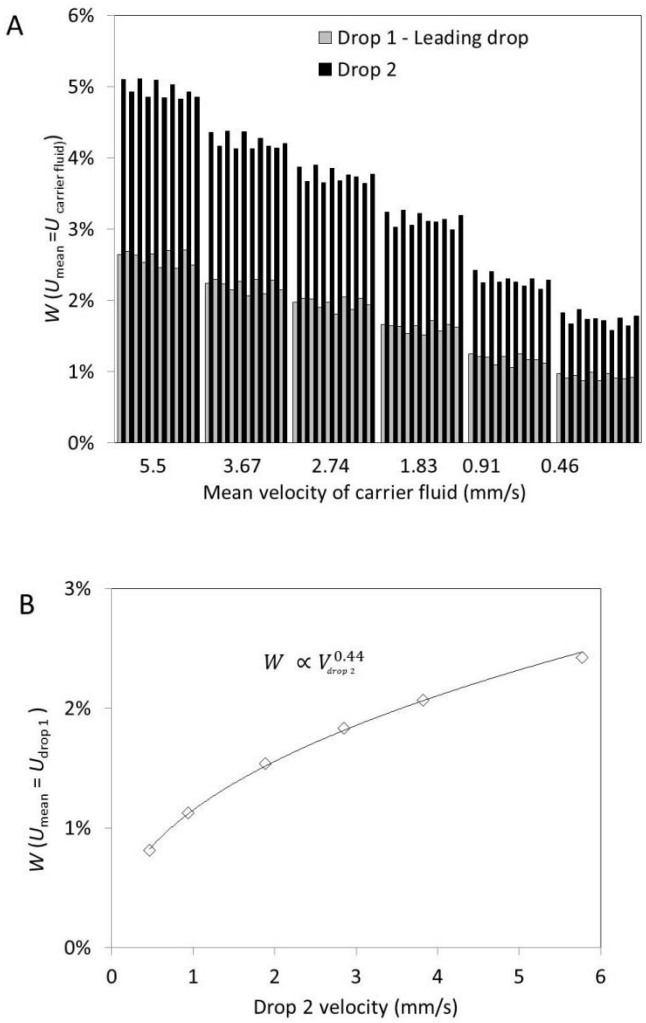


**Figure 4.** The effect of flow rate on the velocity excess, *W*, of each of two drops within sets of 10 trains in a 620-μm tube (fluids – FC 40, water, tetradecane + 1% Span80). Drop 1 and 2 are separated by a sufficient distance so they do not merge between photodiodes in Figure 2. (A) Velocity excess of all drops relative to velocity of carrier fluid. (B) Average excess velocity of drop 2 relative to 1 for different mean carrier-fluid velocities (diamonds, with line of best fit).

Thus, at one meter from the tube inlet in the experiment described in Figure 4, the distance between drop 1 and 2 reduces by 16 ± 1 mm (assuming an uncertainty of one standard deviation) at a carrier-fluid velocity of 1.83 mm/s. Considering a more realistic problem where the distance between drops is 2 mm at the inlet, the merge location is 128 ± 9 mm into the tube. Figure 4B shows the average excess velocity of drop 2 over 1 for various mean carrier-fluid velocities. The best-fit power law shows that $W \propto V_{drop}^{0.44}$, which for constant interfacial tension is in reasonable agreement with results for low capillary-number

flows[36] of $W \propto V_{drop}^{0.5}$. Therefore, drops can be merged and their contents mixed at predictable – and controllable – points in space (cm to meters) and time (seconds to days) by starting and stopping the syringe pump. The effects of gravity are mitigated by positioning tubes horizontally. We were unable to detect any change in drop size due to evaporation over several days. For conditions yielding different capillary numbers, different excess velocities will apply.

Many drops may be merged using trains with multiple aqueous drops; however the relative velocity of all drops needs to be known in order to predict where and when drops merge. Figure 5 illustrates how the excess velocity of drops 2-10 relative to drop 1 can be determined in trains with 10 drops (the first drop has an excess velocity of zero). When the separating oil contains surfactant, the velocity of each drop is dependent on its relative position in the train, which increases with drop position from the front. The cause of this increase is believed to be due to a continuously-varying surfactant concentration along each aqueous drop due to transport of surfactants around the drop interface. [The surfactant is attracted to the water interface due to the hydrophilic head group.] Internal circulation within the drop[38] then transfers surfactant from front to rear, whence it is transferred to the next separating compartment. Therefore, flow transforms an initially homogenous separating fluid into one that increases in surfactant concentration from the first to last separating compartment.

Consequently, the surfactant concentration of each drop varies with flow, and the interfacial tension (and hence Capillary number and excess velocity) is dynamic from two perspectives. Within each drop, circulation continuously redistributes surfactant along the interface of that drop; between drops, surfactant is transferred down the train. Such redistribution is evident from an increased turbidity of last separating compartment (as confirmed in Fig. 6B) – presumably due to micelle accumulation.

The distribution of drop velocities in Figure 5 suggests that velocity variations between successive drops will increase/decrease as surfactant concentrations in the separating fluid decrease/increase, and that saturation of the interface with surfactant will eventually limit the scale of the change. To confirm this, surfactant-free fluids were used to create trains with 10 aqueous drops. For the surfactant-free case (Fig. 5, black bars), the velocity of each drop remained constant irrespective of position in the train. This result points to future work where these fluidic architectures are used to filter or concentrate molecules of interest (as done with surfactant here).

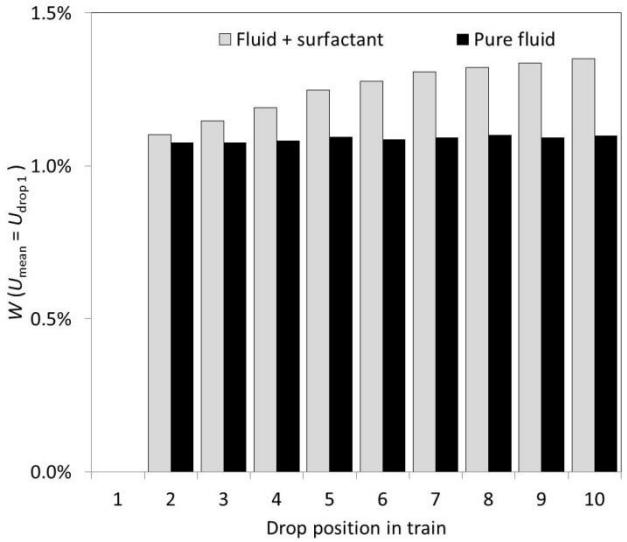


Figure 5. Velocity excess of each drop relative to the leading drop in a 10-drop train (350-□m tube; carrier-fluid velocity 5.8 mm/s). Grey bars: fluids – HFE 7500, water + dye, tetradecane + 1% Span80. Black bars: fluids – FC40, water + dye, 5 cSt silicone oil.

Based on measurements like those described above, surfactant-free fluids enable merging in sequential order from first to last irrespective of droplet spacing. However, when using surfactant within the separating fluid, drop-to-drop spacing may need to be altered to account for variation in relative drop velocity. By way of example, consider the 10-drop train and surfactant-laden separating fluid data of Figure 5. At one meter from the tube inlet, the distance between drop 1 and 2 reduces by 11 mm, while the distance between drop 1 and 3 reduces by 11.7 mm. Therefore, if the initial spacing between drops 2 and 3 was less than

0.7 mm, drops 2 and 3 would merge before drops 1 and 2. By controlling inter-drop distance and flow rates (and possibly the surfactant concentration in separating compartments), it is conceivable that trains can be designed where drops can be merged in any desired sequence.

We next demonstrate the sequential and ordered merging of 51 water drops one after another to give a single enlarged one using the architecture shown in Figure 6A. Here, a robot controls tube dipping. As each drop passes LED1, the voltage peaks (blue voltage trace in Figure 6A). As the train travels towards LED2, drop 2 merges with drop 1, then drop 3 with the now-enlarged leading water drop, and so on until all drops merge successively into one giant drop (red voltage trace in Figure 6A).

Thus far, we have mainly considered merging drops in one train. More drops can be merged using more trains (in series) and tubes (in parallel). In Figure 6B and Movie S2, four 1.35-m long tubes are attached to 4 syringes driven by one pump, and a robot dips tube ends into appropriate fluids to generate a series of trains. Such dipping has been used previously,[39] but then the tube tip passed directly from one aqueous reagent to another, and this could result in cross-contamination (see below). Each train contains two water drops carrying dye of the same colour, and drops have volumes of 40 and 60 nl; successive trains carry differently-coloured dyes. Flow again induces drops to merge, with drops of the same contents (colour) merging at approximately the same locations. The pairs of red and blue drops merge at slightly different points; this is due to the different dyes altering the interfacial tension of the water to slightly different degrees. This can be seen in greater detail in an analogous experiment illustrated in Figure S2 (which involves the merging of pairs of drops in 206 trains). Figure S3 also shows selected trains in a second tube with different contents run in parallel to the one illustrated in Figure S2. As the pump used can drive 10 syringes, drops in ~1,000 completely different trains can be prepared and mixed in ~15 min in this way (as in Movie S3).

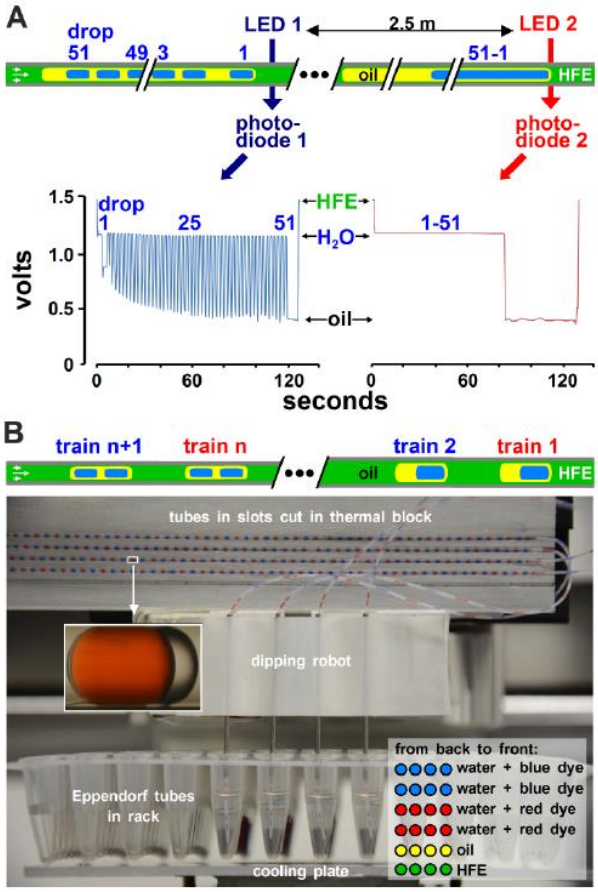


**Figure 6.** Multiplexed merging. (A) Merging 51 drops in one train (620-µm tube; fluids – HFE7500, water, tetradecane + 2.5% Span80). Photo-diode voltage reflects which fluid is in the light beam. Fifty-one 800-nl aqueous drops are engulfed in one oil super-drop; this train passes through the first light beam to yield the blue voltage trace. Voltage levels confirm that an oil super-drop engulfs 51 water drops (the space between drops 1 and 2 is greater than the others). Once the last of the oil passes LED1, drops merge one after another, and pass LED2 to yield the red voltage trace (which confirms all water drops have merged). A stereoscope was used to visually confirm that each drop was added to the enlarging first drop in their numerical order. (B) Merging hundreds of drop pairs in many trains (fluids – 75% FC40 + 25% HFE7500, water + red or blue dye, tetradecane + 1% Span80). Four bipartite tubes – made by joining 250- and 460-µm bore tubes (used for drop merging and storage, respectively) – are each attached to syringes driven by one pump (out of sight at top left); the other ends of the 4 tubes are dipped by a robot successively into appropriate fluids in Eppendorf tubes (arrangement shown at bottom right) on the cooling plate (not used here) to generate a series of trains (each with two 50-nl water drops + dye of the same color, as in the schematic above). Successive trains carry differently-colored dyes. Flow induces drops to merge by the time trains reach the thermal block (not used here; inset – magnification of merged drop). The number of drops that can be merged like this is limited only by fluid volume, syringe capacity, and tube length. See also Movie S2.

## IV.2. Transferring fluid between drops through nano-channels

A challenge in microfluidics is delivering reagents to drops with temporal control, which can be achieved by molecular diffusion through walls[19, 20] – but then control depends on wall porosity. Our system provides a simple way of transferring cargoes of interest. The two internal phases in Figure 1B are inverted when $\gamma_{1\text{-}3} > \gamma_{1\text{-}2} + \gamma_{2\text{-}3}$. This is achieved in Figure 7Ai using FC40 + 10% PFO (1H,1H,2H,2H perfluoro-1-octanol; phase 1), 1% TritonX100 in water (phase 2), and dodecane (phase 3). Here, an air drop restrains train speed, as air has the highest interfacial tension with FC40[37] and hence the lowest velocity. During flow, the oil drop (initially engulfed in aqueous drop 2) soon catches up aqueous drop 1 (Fig. 7Aii), and the two water drops merge. The resulting super-drop contains aqueous sub-compartments 1 and 2 connected by channels ("thin liquid films") around the oil. As flow continues, the oil drop continues to catch up the front of the super-drop; consequently, water flows back through the channels (Figure 7Aiii,iv; Movies S4 and S5). Rates of such advection (range fl/s – µl/s) depend on the velocity of the oil drop relative to the engulfing water drop – which is proportional to Capillary number (see Figure 4B).[36] Consequently, rates can be altered by varying tube diameter and/or Capillary number. When flow stops, there is little diffusional transfer between compartments as the aqueous channels are so long.

Discrete volumes can be delivered stepwise by such advection. Using the initial architecture in Figure 7Bi, flow backwards causes the oil drop to catch up the aqueous drop, creating an aqueous super-drop containing fluorescein (F) in one compartment and water in the other (Figure 7Bii). [At this stage, no fluorescein is detected in drop 2, so there is no net fluid flow from compartment F to 2. However for a non-circular channel this may not be the case, as it has been shown that a drop can travel faster or slower than the mean carrier-fluid velocity depending on surfactant levels.[40, 41]] In our case when flow is reversed, fluorescein

is carried through the connecting channels (Figure 7Biii). Now flow is again reversed for 60 s to mix the contents of 2 as it travels ~3 compartment lengths (Figure 7Biv). [This induces some fluorescein flow from 2 back to F, but relatively little is transferred because of prior dilution in the large volume of 2.] Cycles of 5-s flow in one direction and 60-s in the other deliver 2.5-pl aliquots of fluorescein (at ~500 fl/s) to compartment 2, and then mixes contents (Figure 7Bv). Even smaller aliquots can be delivered by reducing flow rates or increasing the interfacial tension (both altering the Capillary number) and/or varying tube diameter. Here, the connecting channel is a ring ~40 nm wide separating the oil and fluorocarbon. [The scale of the ring is calculated assuming $\text{viscosity}_{\text{oil}} >> \text{viscosity}_{\text{water}}$, (in the other limit where $\text{viscosity}_{\text{oil}} << \text{viscosity}_{\text{water}}$, film thickness would be expected to be half this value; see Experimental section).[35]] As ring width can be varied by changing tube diameter and *Ca*, this suggests that such nano-channels can be used to filter particles in this size range.

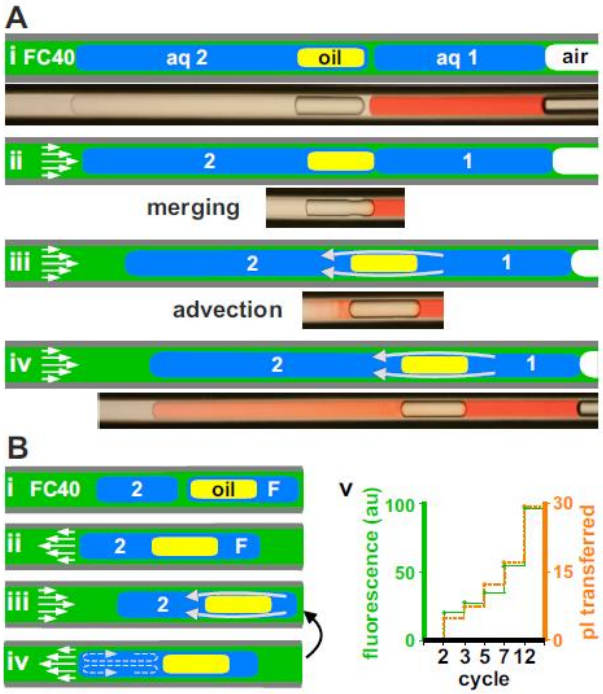


**Figure 7.** Transferring fluids between compartments through nano-channels (fluids – FC40 + 10% PFO, 1% TritonX100 in water ± red dye, oil indicated). (A) Example (150-µm tube). Schematics

illustrate structures seen in movie frames below. (i) Train: air drop, 20-nl drop 1 + red dye, aqueous super-drop 2 engulfing a dodecane drop. (ii) On flow (white arrows), the oil catches up 1, and 2 merges with 1; now, an aqueous channel (a ring around the oil) connects 2 with 1. (iii,iv) Oil advances; water flow (~300 pl/s) carries dye back from 1 to 2 (grey arrows). (B) Advection rates (50-µm tube). (i) Train: a 1.5-nl aqueous super-drop + carboxy-fluorescein (F) engulfs a 2-nl sunflower-oil drop, 2.5-nl water-drop 2. (ii) During flow to left, the oil catches up 2, drops merge, and aqueous channels now connect F to 2. (iii) Flow is reversed; advection (~500 fl/s; grey arrows) carries dye from F to 2. (iv) Reversing flow as 2 traverses three compartment-lengths and mixes contents (dashed grey arrows). A fluorescence micrograph is collected, before cycles iii to iv repeat (black arrow). (v) Fluorescence intensity (arbitrary units, au) in drop 2 after cycle number indicated (fl transferred calculated from shrinkage rate of F).

### IV.3. Cross-contamination

Although most bio-molecules are insoluble in fluorocarbons and oils, some might nevertheless diffuse between drops and/or adhere to walls and then dissociate to contaminate the next drop or train as it passes. Contamination could also occur when making a train with progressively more and more aqueous drops so the protecting fluorocarbon layer abutting the wall becomes so thin it eventually disappears (e.g., when making trains with more aqueous drops than in Fig. 6A). Then, only separating fluid would provide a barrier between the aqueous drops and the wall. [In such a case, the potential for cross contamination would be similar to that obtained with most existing two-phase microfluidic droplet-based networks.] Therefore, we assessed the level of such cross-contamination by monitoring the unwanted transfer of fluorescein or DNA (using sensitive fluorescence or PCR-based assays; Figs S3 and S4). Such experiments showed that if cross-contamination did occur, it did so at a level that can be neglected when carrying out the proof-of-principle applications now described.

## IV.4. Two applications

### *Crystallizing proteins*

Finding conditions permitting protein crystallization represent major bottlenecks in determining tertiary structure by X-ray crystallography. Crystals are usually obtained by screening different protein/precipitant concentrations to find ones suitable for crystal growth, and – because protein supply is often limited – microfluidic devices are sometimes used.[42] Here, we use lysozyme (L) as an example (Fig. 8). Serial protein dilutions are made using a train containing lysozyme in the first aqueous drop and precipitant in drops 2-6. Flow both generates one aqueous super-drop separated by oil drops into sub-compartments, and drives advection that carries protein back through the connecting nano-channels to create serial dilutions. After stopping the train, crystals form in compartments containing appropriate conditions. Here a water-based surfactant was added to carrier (and not water), so commercially-available preparations of precipitant could be used as supplied.

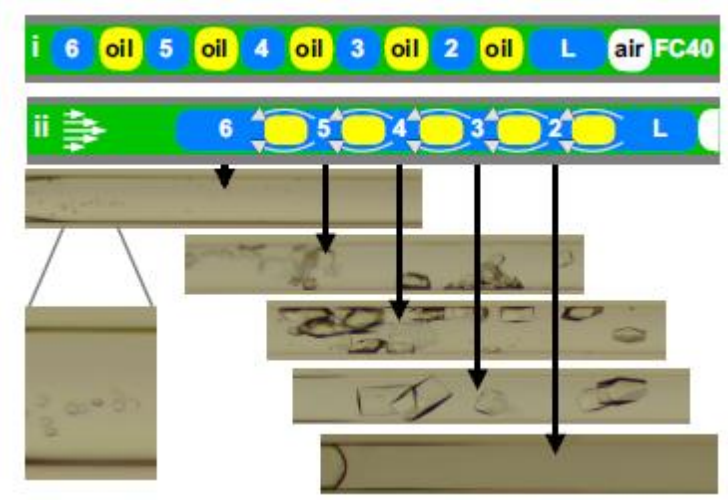


**Figure 8.** Screening crystallization conditions (150-μm tubes; fluids – FC40 + 5% PFO + 1% TritonX100, aqueous phase, tetradecane; schematics not to same scale as micrographs below). (i) Train: air drop to control train speed, water drop 1 (60 nl) contains lysozyme (L), and drops 2-6 (20 nl) precipitant. (ii) Flow (straight arrows) creates an aqueous super-drop engulfing 5 oil drops, and drives advection between compartments (curved arrows) to create a gradient in protein

concentration. After stopping flow and incubation (3 h), micrographs of compartments 2-6 are shown.

***Screening drugs for effects on human cells***

Screening scarce chemicals to see which might serve as useful drugs represents an attractive application for microfluidics. Therefore, we first screened fluids to see which might allow human cells to survive in drops-in-drops, and found suitable ones (using a threshold of >90% survival after 24 h, assessed using trypan-blue exclusion). As proof-of-concept, we compared the effects of mixing various drugs with cells grown conventionally in plates or in drops (using the fluidic architecture in Fig. 9A) – and obtained similar results.

For example, tumor necrosis factor α (TNFα) is a pro-inflammatory cytokine that can switch on expression of the green fluorescent protein (GFP) in a Jurkat line encoding a GFP-reporter gene under the control of a responsive promoter. This line is derived from a T lymphocyte and grows in suspension. When imaged in a tube under ultra-violet light, untreated cells are non-fluorescent; however, cells treated with TNFα for 20 h fluoresce green (Fig. 9Bi). When cells from similar trains are ejected from tubes and passed through a FACS (fluorescence activated cell sorter), intensities are found to be ~100-fold greater than those given by untreated cells; they are also similar to those in cells grown conventionally (Fig. 9Bii). TNFα had much the same effect when added to human embryonic kidney cells growing on the surface of dextran beads and which encoded a related GFP-reporter gene (Fig. S5A,B). This demonstrates that our approach can be used with both suspension and adherent cells.

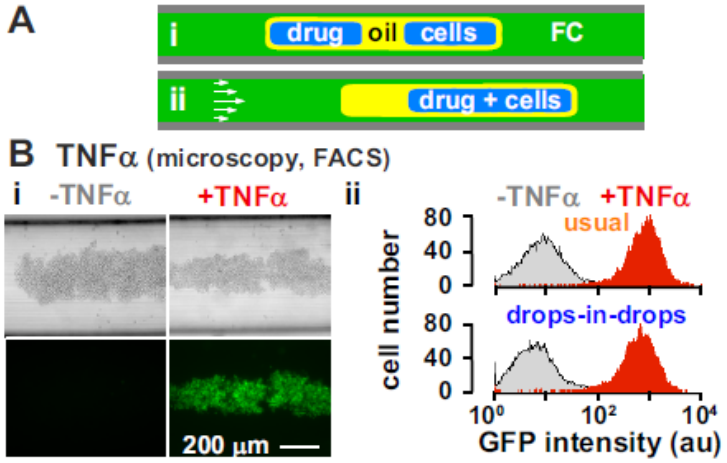


**Figure 9.** Drug screening: proof-of-principle. (A) Approach (FC is a mixture of fluorocarbons). (i,ii) Flow delivers drug to cells. (B) TNFα induces GFP expression in (initially non-fluorescent) NF-κB/Jurkat/GFP$^{TM}$ Reporter cells (560-µm tubes; fluids – 50% FC40 + 50% HFE7500, cells in growth medium ± TNFα, 5-cSt silicone oil + 0.25% AbilEM180). After merging delivers drug, tubes were incubated (37°C; 20 h). (i) Bright-field and fluorescence images of tubes containing cells treated ± TNFα (20 h). (ii) Cells were ejected from similar tubes, and GFP-intensities (au, arbitrary units) seen in $10^4$ cells analyzed using FACS. Cells grown conventionally in plates ("usual") provide controls.

The use of various other cell/drug combinations and readouts confirmed the potential of our device for drug screening; in all cases, cells in tubes behaved like their counterparts grown conventionally. For example: (i) TNFα increases levels of TNFAIP2 mRNA in HeLa cells growing on the surface of dextran beads (Fig. S5C).[43] (ii) DRB (5,6-dichloro-1-β-D-ribo-furanosyl-benzimidazole) – a protein kinase inhibitor that blocks elongation by RNA polymerase II – reduced levels of c-MYC mRNA in Jurkat cells in suspension (assessed using quantitative reverse-transcriptase PCR, qRT-PCR; Fig. S6A,B). (iii) Using the same cells, ionomycin plus PMA (phorbol 12-myristate 13-acetate) – a stimulant – increased those of IL2 mRNA (assessed using RT-PCR; Fig. S6C).[44] These results (obtained using different human cells growing in suspension or attached to surfaces, and both activators and inhibitors) – together with the multiplexing described earlier – provide proof-of-principle demonstrations that our device could be used for drug screening. They also confirm its versatility and biocompatibility.

## V. Conclusions

In summary, by exploiting interfacial tension and at least three immiscible fluids we have demonstrated a novel approach to enable the controlled coalescence of many drops. Using the same physical principle, we also demonstrate a new method for controlled transport of media through nano-channels between many drops. These new approaches for merging drops and advection between them are achieved using a single Teflon tube with no surface modification, and manual drop loading. Consequently, they can be replicated without requirement for a dedicated microfluidics laboratory. As many drops and trains can be created using a robot, manipulations are also scalable. By selecting appropriate fluids, we have demonstrated biocompatibility through two proof-of-concept applications – protein crystallisation and screening drugs for their effects on human cells growing in suspension or on surfaces. These novel approaches should find many other applications where small volumes of fluids are manipulated.

**Acknowledgements –** We thank Oreste Acuto for Jurkat cells, and the Medical Research Council (AF, PRC), the Indonesian Endowment Fund for Education (AP), the 7$^{th}$ Framework Marie Curie Career Integration grant contract No. 333848, and University of Oxford John Fell Fund (EW) for support.

## VI. Notes and References

(1) Wu, N.; Zhu, Y.; Brown, S.; Oakeshott, J.; Peat, T. S.; Surjadi, R.; Easton, C.; Leech, P. W.; Sexton, B. A., A PMMA microfluidic droplet platform for in vitro protein expression using crude E. coli S30 extract. *Lab on a Chip* **2009,** *9*, 3391-3398.

(2) Bennett, M. R.; Hasty, J., Microfluidic devices for measuring gene network dynamics in single cells. *Nat. Rev. Genet.* **2009,** *10* (9), 628-638.

(3) White, A. K.; VanInsberghe, M.; Petriv, O. I.; Hamidi, M.; Sikorski, D.; Marra, M. A.; Piret, J.; Aparicio, S.; Hansen, C. L., High-throughput microfluidic single-cell RT-qPCR. *PNAS* **2011,** *108* (34), 13999-14004.

(4) Hindson, C. M.; Chevillet, J. R.; Briggs, H. A.; Gallichotte, E. N.; Ruf, I. K.; Hindson, B. J.; Vessella, R. L.; Tewari, M., Absolute quantification by droplet digital PCR versus analog real-time PCR. *Nat. Meth.* **2013,** *10* (10), 1003-1005.

(5) Williams, R.; Peisajovich, S. G.; Miller, O. J.; Magdassi, S.; Tawfik, D. S.; Griffiths, A. D., Amplification of complex gene libraries by emulsion PCR. *Nat. Meth.* **2006,** *3* (7), 545-550.

(6) Hoang, P. H.; Park, H.; Kim, D. P., Ultrafast and Continuous Synthesis of Unaccommodating Inorganic Nanomaterials in Droplet- and Ionic Liquid-Assisted Microfluidic System. *J. Amer. Chem. Soc.* **2011,** *133* (37), 14765-14770.

(7) Blainey, P. C., The future is now: single-cell genomics of bacteria and archaea. *FEMS Microbio. Rev.* **2013,** *37* (3), 407-427.

(8) Fallah-Araghi, A.; Baret, J. C.; Ryckelynck, M.; Griffiths, A. D., A completely in vitro ultrahigh-throughput droplet-based microfluidic screening system for protein engineering and directed evolution. *Lab on a Chip* **2012,** *12* (5), 882-891.

(9) Bremond, N.; Thiam, A. R.; Bibette, J., Decompressing emulsion droplets favors coalescence. *Phys. Rev. Lett.* **2008,** *100* (2), 024501.

(10) Eastburn, D. J.; Sciambi, A.; Abate, A. R., Picoinjection Enables Digital Detection of RNA with Droplet RT-PCR. *Plos One* **2013,** *8* (4).

(11) Gu, S. Q.; Zhang, Y. X.; Zhu, Y.; Du, W. B.; Yao, B.; Fang, Q., Multifunctional Picoliter Droplet Manipulation Platform and Its Application in Single Cell Analysis. *Analytical Chemistry* **2011,** *83* (19), 7570-7576.

(12) Boedicker, J. Q.; Li, L.; Kline, T. R.; Ismagilov, R. F., Detecting bacteria and determining their susceptibility to antibiotics by stochastic confinement in nanoliter droplets using plug-based microfluidics. *Lab on a Chip* **2008,** *8* (8), 1265-1272.

(13) Hong, J.; Choi, M.; deMello, A. J.; Edel, J. B., Interfacial Tension-Mediated Droplet Fusion in Rectangular Microchannels. *BIOCHIP JOURNAL* **2009,** *3* (3), 203-207.

(14) Akartuna, I.; Aubrecht, D. M.; Kodger, T. E.; Weitz, D. A., Chemically induced coalescence in droplet-based microfluidics. *Lab on a Chip* **2015,** *15* (4), 1140-1144.

(15) Deng, N. N.; Sun, J.; Wang, W.; Ju, X. J.; Xie, R.; Chu, L. Y., Wetting-Induced Coalescence of Nanoliter Drops as Microreactors in Microfluidics. *Acs Appl Mater Inter* **2014,** *6* (6), 3817-3821.

(16) Baraban, L.; Bertholle, F.; Salverda, M. L. M.; Bremond, N.; Panizza, P.; Baudry, J.; de Visser, J. A. G. M.; Bibette, J., Millifluidic droplet analyser for microbiology. *Lab on a Chip* **2011,** *11* (23), 4057-4062.

(17) Trivedi, V.; Doshi, A.; Kurup, G. K.; Ereifej, E.; Vandevord, P. J.; Basu, A. S., A modular approach for the generation, storage, mixing, and detection of droplet libraries for high throughput screening. *Lab on a Chip* **2010,** *10* (18), 2433-2442.

(18) Zhu, Y.; Zhang, Y. X.; Liu, W. W.; Ma, Y.; Fang, Q.; Yao, B., Printing 2-Dimentional Droplet Array for Single-Cell Reverse Transcription Quantitative PCR Assay with a Microfluidic Robot. *Sci Rep-Uk* **2015,** *5*.

(19) Courtois, F.; Olguin, L. F.; Whyte, G.; Theberge, A. B.; Huck, W. T. S.; Hollfelder, F.; Abell, C., Controlling the Retention of Small Molecules in Emulsion Microdroplets for Use in Cell-Based Assays. *Anal. Chem.* **2009,** *81* (8), 3008-3016.

(20) Shim, J.; Patil, S. N.; Hodgkinson, J. T.; Bowden, S. D.; Spring, D. R.; Welch, M.; Huck, W. T. S.; Hollfelder, F.; Abell, C., Controlling the contents of microdroplets by exploiting the permeability of PDMS. *Lab on a Chip* **2011,** *11*, 1132-1137.

(21) Liang-Yin Chu; Andrew S. Utada; Rhutesh K. Shah; Jin-Woong Kim; Weitz, D. A., Controllable Monodisperse Multiple Emulsions. *Angew. Chem. Int. Ed.* **2007,** *46*, 8970-8974.

(22) Abate, A. R.; Weitz, D. A., Faster multiple emulsification with drop splitting. *Lab on a Chip* **2011,** *11* (11), 1911-1915.

(23) Wu, N.; Oakeshott, J. G.; Easton, C. J.; Peat, T. S.; Surjadi, R.; Zhu, Y., A double-emulsion microfluidic platform for in vitro green fluorescent protein expression. *J Micromech Microeng* **2011,** *21* (5), 1-7.

(24) Shah, R. K.; Shum, H. C.; Rowat, A. C.; Lee, D.; Agresti, J. J.; Utada, A. S.; Chu, L. Y.; Kim, J. W.; Fernandez-Nieves, A.; Martinez, C. J.; Weitz, D. A., Designer emulsions using microfluidics. *Mater Today* **2008,** *11* (4), 18-27.

(25) Zhao, C. X., Multiphase flow microfluidics for the production of single or multiple emulsions for drug delivery. *Adv Drug Deliver Rev* **2013,** *65* (11-12), 1420-1446.

(26) Li, E. Q.; Zhang, J. M.; Thoroddsen, S. T., Simple and inexpensive microfluidic devices for the generation of monodisperse multiple emulsions. *J Micromech Microeng* **2014,** *24* (1).

(27) Rowlinson, J., *Molecular Theory of Capillarity*. Clarendon Press Oxford, 1982.

(28) Guzowski, J.; Korczyk, P. M.; Jakiela, S.; Garstecki, P., The structure and stability of multiple micro-droplets. *Soft Matter* **2012,** *8* (27), 7269-7278.

(29) Guzowski, J.; Garstecki, P., Comment on "Wetting-induced formation of controllable monodisperse multiple emulsions in microfluidics" by N.-N. Deng, W. Wang, X.-J. Ju, R. Xie, D. A. Weitz and L.-Y. Chu, Lab Chip, 2013, 13, 4047. *Lab on a Chip* **2014,** *14* (8), 1477-1478.

(30) Tice, J. D.; Song, H.; Lyon, A. D.; Ismagilov, R. F., Formation of droplets and mixing in multiphase microfluidics at low values of the Reynolds and the capillary numbers. *Langmuir* **2003,** *19* (22), 9127-9133.

(31) King, C.; Walsh, E.; Grimes, R., PIV measurements of flow within plugs in a microchannel. *Microfluidics and Nanofluidics* **2007,** *3* (4), 463-472.

(32) Chen, D. L. L.; Li, L.; Reyes, S.; Adamson, D. N.; Ismagilov, R. F., Using three-phase flow of immiscible liquids to prevent coalescence of droplets in microfluidic channels: Criteria to identify the third liquid and validation with protein crystallization. *Langmuir* **2007,** *23* (4), 2255-2260.

(33) Howard, J. A.; Walsh, P. A., Review and extensions to film thickness and relative bubble drift velocity prediction methods in laminar Taylor or slug flows. *Inter. J. Multiphase flows* **2013,** *55*, 32-42.

(34) Aussillous, P.; Quere, D., Quick deposition of a fluid on the wall of a tube. *Physics of Fluids* **2000,** *12* (10), 2367-2371.

(35) Charles, M. E., The pipeline flow of capsules, Part 2: The concept of capsule pipelining. *Can. J. Chem. Eng.* **1963,** *41* (2), 46-51.

(36) Fairbrother, F.; Stubbs, A. E., Studies in Electro-endosmosis. *J. Chem. Soc.* **1935**, 527-529.
(37) Bretherton, F. P., The Motion of Long Bubbles in Tubes. *J. Fluid Mech.* **1961,** *10* (2), 166-188.
(38) Ratulowski, J.; Chang, H. C., Marangoni Effects of Trace Impurities on the Motion of Long Gas-Bubbles in Capillaries. *Journal of Fluid Mechanics* **1990,** *210*, 303-328.
(39) Du, W. B.; Sun, M.; Gu, S. Q.; Zhu, Y.; Fang, Q., Automated Microfluidic Screening Assay Platform Based on Drop Lab. *Anal. Chem.* **2010,** *82* (23), 9941-9947.
(40) Fuerstman, M. J.; Lai, A.; Thurlow, M. E.; Shevkoplyas, S. S.; Stone, H. A.; Whitesides, G. M., The pressure drop along rectangular microchannels containing bubbles. *Lab on a Chip* **2007,** *7* (11), 1479-1489.
(41) Baret, J. C., Surfactants in droplet-based microfluidics. *Lab on a Chip* **2012,** *12* (3), 422-433.
(42) Dowling, E. C.; Klabunde, C.; Patnick, J.; Ballard-Barbash, R.; International Cancer Screening, N., Breast and cervical cancer screening programme implementation in 16 countries. *J Med Screen* **2010,** *17* (3), 139-46.
(43) Papantonis, A.; Kohro, T.; Baboo, S.; Larkin, J.; Deng, B.; Short, P.; Tsutsumi, T.; Taylor, S.; Kanki, Y.; Kobayashi, M.; Li, G.; Poh, H.-M.; Ruan, X.; Aburatani, H.; Ruan, Y.; Kodama, T.; Wada, Y.; Cook, P. R., TNFa signals through specialized factories where responsive coding and micro-RNA genes are transcribed. *J. EMBO* **2012,** *31*, 4404-4414.
(44) Schwarz, E. M.; Salgame, P.; Bloom, B. R., Molecular Regulation of Human Interleukin-2 and T-Cell Function by Interleukin-4. *P. Nat. Acad. Sci. USA* **1993,** *90* (16), 7734-7738.

## VII. Supplementary Information

### Methods

### Merging 51 drops

For Figure 6A, 51 800-nl aqueous drops were engulfed in one super-drop of tetradecane + 2.5% Span80, which – in turn – was engulfed by HFE7500; this train passes (flow 2 ml/h) through LED1/photo-diode1 to yield the blue voltage trace (data collected at 100 Hz). Once the last of the oil passes LED1, flow is increased to 6 ml/h, and water drops merge one after another. Flow is reduced to 2 ml/h when the front of the oil travels 2.5 m to reach LED2/photo-diode2 (which gives the red voltage trace). The two LED/photo-diode

systems yield slightly different voltage differences between HFE7500 and oil, so differences were equalized.

**Imaging**

All images (other than those of cells; below) were collected using a camera (Olympus D7100 DSLR) connected to an epi-fluorescent microscope (Olympus IX53; 1.25X, 4X, 10X, 25X objectives) with translation stage and overhead illuminator (Olympus IX3 with filters) for bright-field images, and LED wavelength-specific sources (CoolLED) for fluorescent images. Image processing, analysis and illustrations were prepared using Matlab and/or CorelDraw. For several images, the PTFE tube was immersed in water to improve contrast with the walls of the tube. All movies were collected at video rates and play in real time.

**Assessing cross-contamination**

Cross-contamination between drops/trains was assessed using fluorescein and imaging (Figure S3) or using DNA and quantitative PCR (qPCR; Figure S4). In the latter case, drops ± DNA (100 ng/µl of plasmid pcDNA3; Invitrogen) were loaded manually (flow rate 0.05 ml/h) into a 150-µm tube using a rack and pinion (to give the architecture in Figure S4 so that drops contain more accurate volumes than those obtained manually): 30 nl water (drop 1), 30 nl tetradecane + 1% Span80, 200 nl HFE7500, 30 nl water containing DNA (drop 2), 30 nl tetradecane + 1% Span80, 200 nl HFE7500, and so on. After creating a train with 13 aqueous drops, the pump withdrew a further 3 µl HFE7500, and then was stopped for 5 min. Drops were now ejected individually into different Eppendorf tubes (flow rate 0.05 ml/h) containing 4 µl water (with the tip of the150-µm tube just breaking the water-air meniscus, as monitored with a camera attached to a 25x lens). Next, the DNA content of each tube was measured using a kit (Platinum® SYBR® Green One-Step qRT-PCR kit; Life Technologies) according to the manufacturer's instructions for qPCR (i.e., using Platinum

Taq polymerase but no reverse transcriptase). PCR (25 µl) was performed using primers "pcDNA3 fw" and "rev" (Table S1), and a Mastercycler® realplex2 (Eppendorf) using temperatures of 95°C for 2 min, then 40 cycles of 95°C for 20 s + 62°C for 20 s + 72°C for 30 s, 72°C for 5 min, and finally those for the pre-programed melting-curve.

**Cells**

As $CO_2$ is used to maintain the pH of media during cell growth and Teflon is permeable to the gas, all fluorocarbons and oils used were pre-equilibrated in open vessels with 5% $CO_2$ in a conventional $CO_2$ incubator for >30 min; tubes were also placed in the incubator to allow cells to grow.

For Figure 9, NF-κB/Jurkat/GFP$^{TM}$ Reporter cells (System Biosciences, catalogue number TR850A-I) were used and maintained as described by the manufacturer. These cells grow in suspension and were derived by the supplier as follows. The human immunodeficiency virus was used to insert a GFP gene under the control of the minimal cytomegalovirus promoter downstream of four copies of the nuclear factor κB (NF-κB) consensus transcriptional-response element. Positively-transduced cells were selected using fluorescent activated cell sorting (FACS), and clonal populations stably retaining the provirus further selected; finally, a clone demonstrating a low GFP background, and a robust increase in GFP expression upon stimulation with TNFα was chosen. Two sets of 15 trains (Figure 9Ai) were generated in 2 tubes (fluids – 50% FC40 + 50% HFE7500, growth medium ± TNFα, 5-sSt silicone oil + 0.25% AbilEM180); each train contained one 1-µl drop with ~4,000 cells, plus a second 1-µl drop of medium + 20 ng/ml TNFα (PeproTech). An identical set without TNFα provided a control. After merging drops, tubes were plugged (by inserting metal plugs into free ends), placed in a conventional $CO_2$ incubator for 20 h, bright-field and GFP images of randomly-selected drops collected under water using a camera (AxioCam MRm) attached to a microscope (Zeiss Axioskop 40), and 30 merged

drops from 2 tubes ejected into 1 ml PBS. GFP intensity in individual cells was now analyzed using a fluorescence-activated cell sorter (FACSCalibur™, BectonDickinson; GFP expression assessed using the 488-nm argon-ion laser, scattered signal using channel FL-1 and 515-545 nm). Cells grown ± TNFα and treated conventionally in a plate provided a control.

For Figure S5B, HEK-293 reporter cells (NF-kB/293/GFP-Luc™ Transcriptional Reporter Cell Line; System Biosciences, catalogue number TR860A-I), were used; they were maintained as indicated by the manufacturer, and seeded on to Cytodex beads (Cytodex® 1 micro-carrier beads; Sigma Aldrich; ~20,000 cells/1 $cm^2$ micro-carrier surface), where they grow attached to the surface. These cells were derived by the supplier as follows: a lentiviral vector was used to insert a GFP gene (plus a luciferase reporter, but luciferase levels were not assessed here) under the control of the minimal cytomegalovirus promoter downstream of four copies of the NF-κB consensus transcriptional-response element, and positively-transduced cells that responded robustly to stimulation with TNFα selected as described above for the analogous Jurkat reporter line used in Figure 9. Trains were generated (fluids – 50% FC40 + 50% HFE7500, growth medium ± TNFα, 5-cSt silicone oil + 0.25% AbilEM180); each train contained one 1-µl drop with cells on Cytodex beads (as above), plus a second 1-µl drop medium + 20 ng/ml TNFα (PeproTech). An identical set without TNFα provided a control. After merging drops, tubes were plugged, incubated for 20 h (as above), and bright-field and GFP images of selected drops collected (as for Figure 9Bi).

For Figure S5C, Hela cells were maintained in DMEM high-glucose medium (Life Techologies) + 5% FBS, seeded on to Cytodex beads, grown overnight, and serum-starved (18 h) to accumulate cells in G1 phase in medium containing 0.5% FBS. Subsequently, 15 trains each composed of a 1-µl drop containing ~30-40 microcarrier beads with the cells

plus another 1-µl drop containing either TNFα (20 ng/ml; PeproTech) or medium only were loaded and merged, and sealed tubes incubated for 2.5 h – all as described for Jurkat cells. After incubation, merged drops from 5 similar trains were all ejected into 500 µl Direct-zol™ to lyse cells, and total RNA isolated using the Direct-zol™ MiniPrep kit (ZymoResearch). Levels of mRNA encoded by a gene responding to TNFα – TNFAIP2 – were now assessed using qRT-PCR as outlined above with primers "TNFAIP2 fw" and "rev" (Table S1). Results are averages given by the 3 sets of 5 trains. Three sets of RNA extracted from cells grown and treated conventionally on plates provided a control.

For Figure S6, standard Jurkat cells (a T-lymphocyte line which grows in suspension) were cultured routinely in RPMI 1640 (Sigma Aldrich) containing 10% FBS (Sigma Aldrich). Prior to incorporating cells into a 560-µm tube, the tube was filled with HFE7500, immediately loaded (flow rate 2 ml/h) successively with: 1 µl containing ~2,000 cells in RPMI 1640, 200 nl silicone oil (5 cSt) + 0.25% AbilEM180, 1 µl RPMI 1640 plus a drug (or DMSO as a control). Drops had merged in the first trains to be loaded prior to loading the last train, and flow was increased to 5 ml/h to ensure merging in all trains. Drugs (final concentrations given after merging drops) were 100 µM DRB (5,6-dichloro-1-β-D-ribofuranosyl-benzimidazole; Sigma Aldrich) – an inhibitor of RNA polymerase II – or ionomycin (1 µg/ml) + 62.5 ng/ml PMA – (phorbol-12-myristate-13-acetate; Sigma Aldrich) – inflammatory activators.[45] The free end of the tube was now inserted into a second syringe to pressurise the system, and the now-sealed tube placed in a $CO_2$ incubator for 4 h at 37°C. Next, merged drops were ejected individually into 12 µl "CellsDirect resuspension and lysis buffer" (CellsDirect™; Life Technologies), and the mixture incubated (10 min; 75°C) to lyse cells. Changes in levels of c-MYC and IL2 mRNAs were assessed (25-µl reactions) using qRT-PCR ("Platinum® SYBR® Green One-Step qRT-PCR" kit; Mastercycler® realplex2, Eppendorf) and the ΔΔCt method,[46] primers ("c-MYC fw" and

"rev", or "IL2 fw" and "rev"; Table S1), and the following temperatures – 50°C for 20 min, 95°C for 5 min, 40 cycles at 95°C for 15 s + 60°C for 30 sec, and finally the pre-programed cycle used for melting-curve analysis. All qRT-PCR runs contained a control lacking reverse transcriptase to assess amplification of genomic DNA, and expression levels were normalized relative to those of 5S rRNA (assessed using primers "5SrRNA fw" and "rev"; Table S1). Cells grown and treated conventionally provided a control.

**Shorthand notation**

The following shorthand notation can be used to describe the creation and evolution of fluidic architectures; it is exemplified first by reference to Figures 1Bi and iii.

1. 150-µm, FC40, tetradecane + 1% Span80, water ± Allura Red dye.

2. ( {[red] [ ] } )

3. Flow: ->

4. ( { [ red ] } )

Line 1 gives the internal diameter of the tube, and the fluids used as carrier, water, and separating fluid/oil. In line 2, () represents FC40, {} the oil super-drop, and [] one or other of the two water drops engulfed by the oil. After flow in the direction indicated in line 3, line 4 shows there is now only one water drop. Additional details can be included as required (e.g., an air drop can be indicated by <>).

**Notes for Electronic Supplementary information**

[45] A. J. M. Howden, V. Geoghegan, K. Katsch, G. Efstathiou, B. Bhushan, O. Boutureira, B. Thomas, D. C. Trudgian, B. M. Kessler, D. C. Dieterich, B. G. Davis and O. Acuto, *Nat. Methods*, 2013, **10**, 343-346.

[46] K. J. Livak and T. D. Schmittgen, *Methods*, 2001, **25**, 402-408.

## Figures

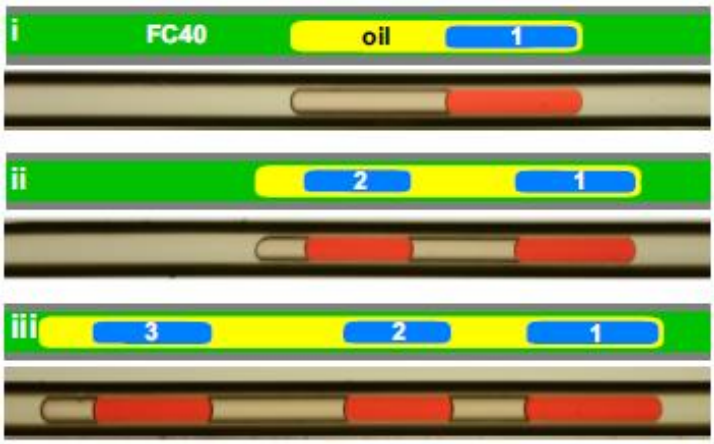


**Figure S1.** Trains with 1, 2 and 3 carriages. Schematics (with micrographs below) of tubes containing carrier fluid (FC40) surrounding a ~10-nl oil super-drop (tetradecane + 1% Span 80) engulfing 1-3 10-nl aqueous drops (the carriages in a train) containing red dye. A 150-µm tube was loaded by dipping it successively into wells containing: (i) carrier fluid (FC40), water, oil, water, and FC40, (ii) FC40, water, oil, water, oil, and FC40, and (iii) FC40, water, oil, water, oil, water, oil, and FC40. Fluid was drawn into the tube (0.05 ml/h) only when dipped below the surface of the fluid.

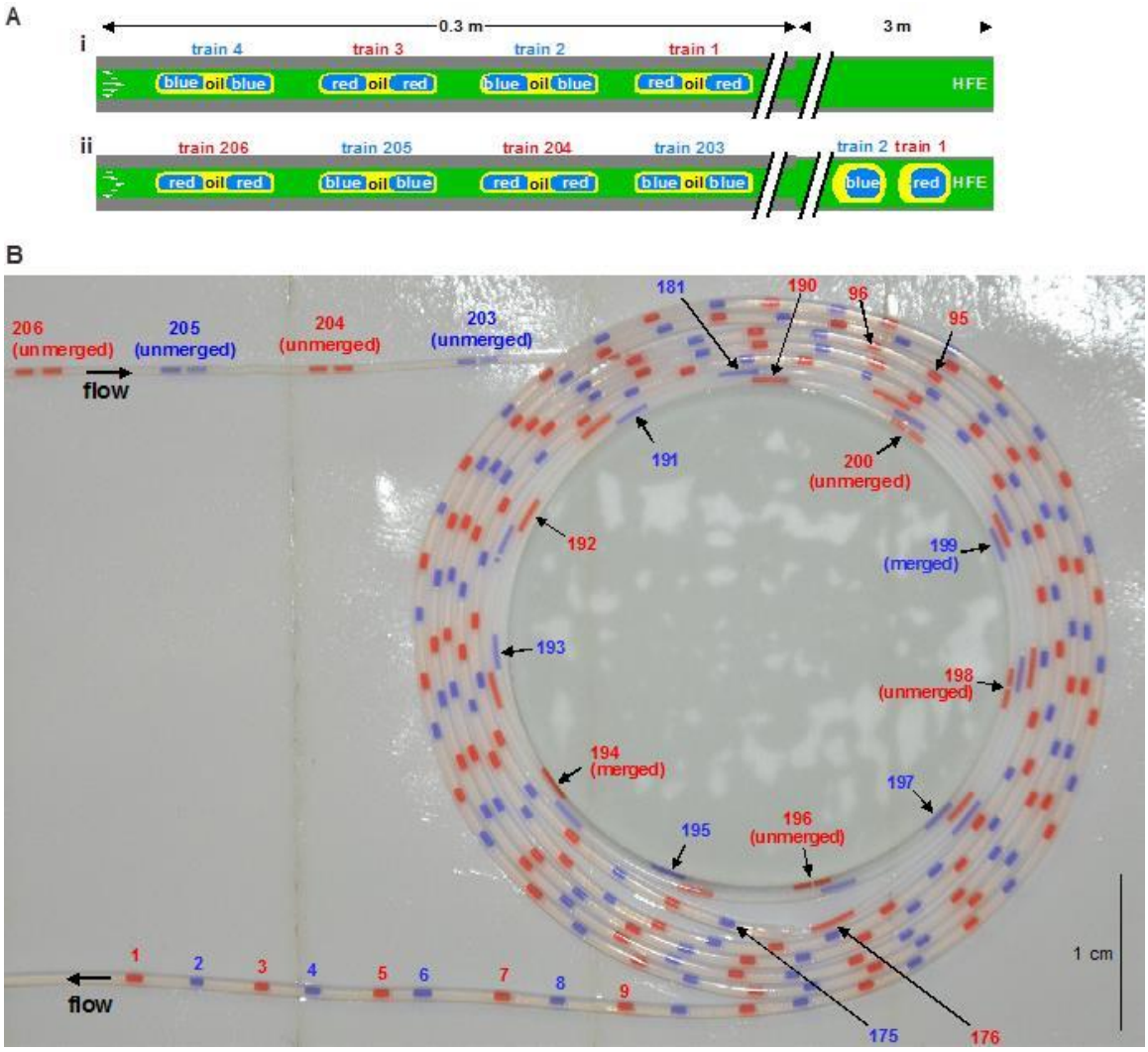


**Figure S2.** High-throughput demonstration of merging of 206 pairs of drops (fluids – 50% FC40 + 50% HFE7500, water + red or blue dye, tetradecane + 1% Span80). A bipartite tube was made by joining one tube (0.3 m) with a 250-µm bore to another with a 400-µm bore (3 m). All aqueous drops in a train are merged in the thinner segment, and merged drops are "stored" in the wider segment. The wider end was attached to a syringe pump (flow rate of 0.1 ml/h for carrier fluid, 0.08 ml/h for aqueous drops, and 0.06 ml/h for separating fluid; total run-time ~2 h). The narrow end of the tube was dipped successively into appropriate wells in 96-well plates to load 206 trains. Each train contained one oil drop engulfing two 50-nl water drops (each containing the same dye); successive trains contained differently-colored dyes (i.e., red or blue). Results obtained with a second identical tube (with different contents) attached to a second syringe driven by the same syringe pump at the same time are presented in Figure S3.

(A) Fluidic architecture of the first 4 trains in the bipartite tube. (i) Structure after loading the first 4 trains. The first and third trains each contained two water drops + red dye, and the second and fourth trains two water drops + blue dye. Trains loaded subsequently continued this alternating pattern. To demonstrate the indexing potential for different 96-well plates, we loaded trains 95 and 96 with red

dye. Then, all odd-numbered trains from 1-95 carried red dye, and all even-numbered ones blue dye; from train 96, all even-numbered trains carried red dye and odd-numbered ones blue dye. Additional indexing could be included by varying volumes of separating fluid and/or drop numbers/colors. (ii) Structures just after loading train 206. Aqueous drops in trains 203-206 in both tubes have not yet merged; however, those in trains 1 and 2 have merged.

(B) Bright-field image of the bipartite tube after coiling it around a cylinder. Trains were loaded in the thin end (now at top left); the last train (i.e., 206) has just been loaded, and then the pump was stopped. As a result, the two red drops in trains 206, 204, 202 (which is not visible as it lies under other segments of the tube), and 198 remain unmerged; however, drops in train 196 were just about to merge, whilst those in train 194 have merged. The two blue drops in trains 205 and 203 also remain unmerged (train 201 is also not visible); however, drops in train 199 have merged. [The different dyes cause slight differences in interfacial tension that affect where drops in a train will merge.] Drops in all other trains have merged. Trains 176 and 175 lie on each side of the junction between the two segments with different bores; consequently, the (merged) aqueous drop is longer in train 176 than that in 175. Note the two index trains with red dye (95, 96). Drop architecture remained unchanged during storage at room temperature for 1 day.

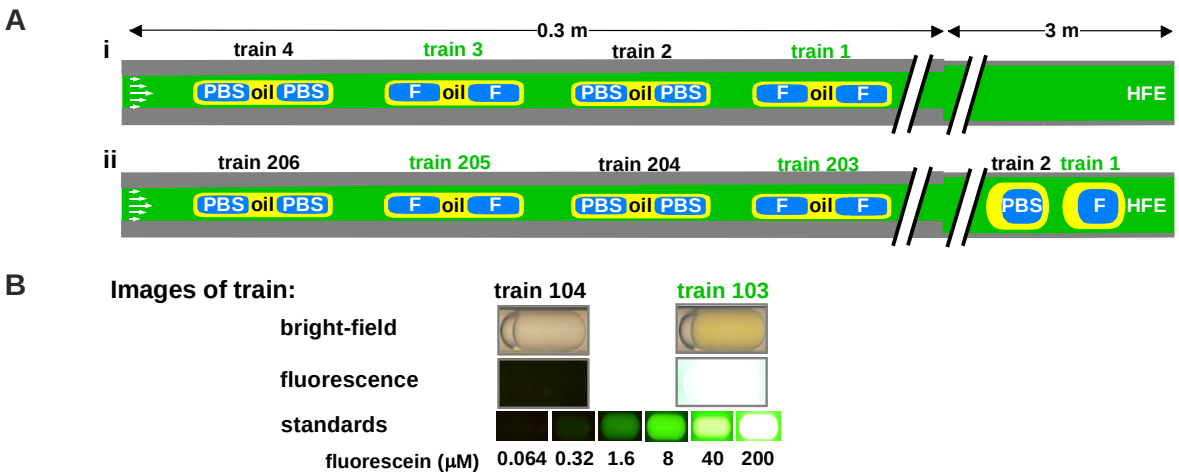


Figure S3. Negligible cross-contamination occurs during high-throughput merging of 206 pairs of drops (fluids – 50% FC40 + 50% HFE7500, PBS ± 200 μM carboxy-fluorescein, tetradecane + 1% Span80). A bipartite tube was made by joining one tube (0.3 m) with a 250-μm bore to another with a 400-μm bore (3 m). Almost all aqueous drops in a train are merged in the thinner segment, whilst merged drops "stored" in the wider segment. The wider end was attached to a syringe pump (flow rate of 0.1 ml/h for carrier fluid, 0.08 ml/h for aqueous drops, and 0.06 ml/h for separating fluid; total run-time ~2 h). The narrow end of the tube was dipped successively into the appropriate wells in 96-well plates to load 206 trains. Each train consisted of one oil drop engulfing two 50-nl drops carrying the same cargo (i.e., PBS or PBS + 200 μM carboxy-fluorescein); successive trains carried different cargoes (i.e., ± fluorescein). Results obtained with a second identical tube (with different contents) attached to a second syringe driven by the same pump at the same time are presented in Figure S2. (A) Fluidic architecture of the first 4 trains in the bipartite tube. (i) The first and third trains each contained two PBS drops with carboxy-fluorescein, and the second and fourth trains two PBS drops without. Subsequent trains in each tube continued this alternating pattern. (B) Bright-field and fluorescence images of trains 103 and 104 containing merged drops ± carboxy-fluorescein from the second tube (images collected 10 h after stopping flow). Fluorescence images of drops containing a dilution series of carboxy-fluorescein are included for reference. Trains containing only PBS have no detectable fluorescence. Selected trains were re-checked for any detectable fluorescence transfer after 4 days, but none was detected. Therefore, if cross-contamination occurs between trains, it does so at a level of less than one part in 625. This confirms that cross-contamination is negligible from train-to-train in the tube, and from well-to-well during loading (when the tube end is dipped hundreds of times between PBS ± fluorescein during loading). Note also that here the tube end was not "washed" in FC40 between dipping into different fluids, but such washing dips could be included if necessary.

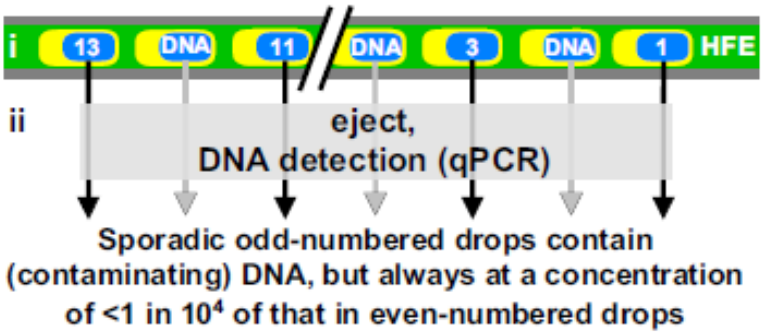


**Figure S4**. Assessing cross-contamination using PCR (150-µm tube; fluids – 50% HFE7500 + 50% FC40, water ± DNA, tetradecane + 1% Span80). (i) A set of 13 trains. Each train contains one 30-nl oil super-drop engulfing a 30-nl water drop (with 200 nl HFE7500 between oil super-drops); even-numbered water drops contain 3 ng DNA (~5 x$10^8$ molecules) whilst odd-numbered drops contain no DNA. Once loaded, flow was first stopped for 5 min to give DNA time to exchange between drops and/or bind to the tube wall (if it were able to do so), and then reversed so that individual aqueous drops could be ejected into different micro-centrifuge tubes. The tip of the 150-µm tube was "washed" by dipping for 1-2 s in FC40 after loading each train, and after ejecting each water drop. (ii) The amount of DNA in each ejected aqueous drop was assessed using qRT-PCR. All even-numbered drops contained the expected high concentration of DNA, whilst most odd-numbered drops contained no DNA detectable after 40 cycles. However, sporadic odd-numbered drops did contain DNA, but always at a concentration that was <1 in $10^4$ of that in even-numbered drops. Analysis of similar sets of trains on different days gave substantially similar results, indicating that sporadic contamination at a low level does occur (as in any laboratory conducting molecular biology). Levels can, of course, be reduced by including additional "washes" in FC40 between individual samples during loading and ejection. Therefore, we suggest that contamination levels should be assessed prior to the use of any new application.

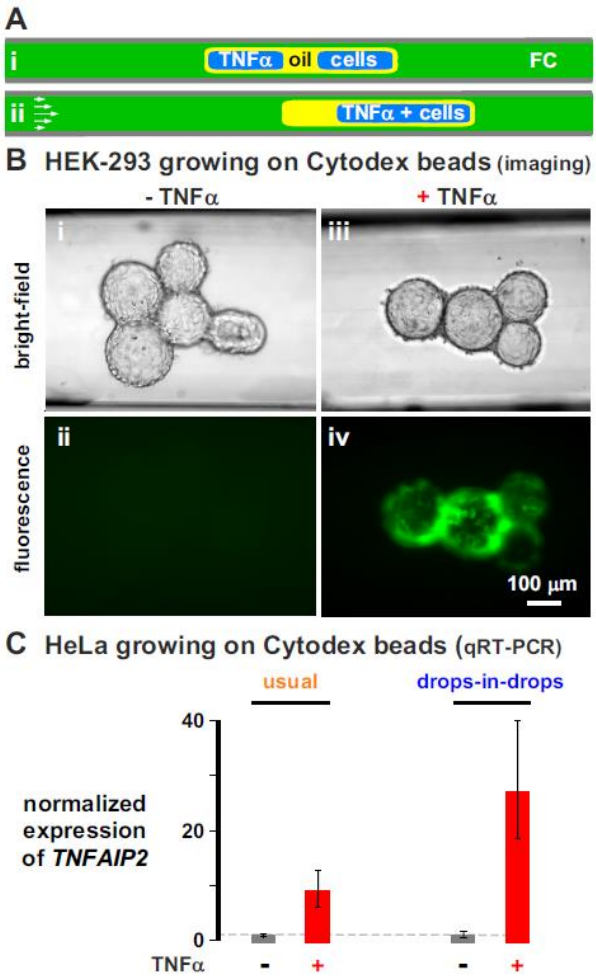


**Figure S5.** The effects of TNFα on gene expression in different cells growing on the surface of Cytodex beads (560-µm tubes). FC is fluorocarbon. Fluids: HFE7500 for (B) and 50% FC40 + 50% HFE7500 for (C), growth media, 5-cSt silicone oil + 0.25% AbilEM180. (A) Approach. (i) Initially, one oil drop engulfs 2 aqueous drops; the first contains cells on beads, and the second growth media ± TNFα. (ii) Flow then induces the two aqueous drops to merge and mix. Tubes are now incubated at 37°C. (B) HEK-293 cells encoding an NF-κB-responsive *GFP*-reporter gene. Tubes containing cells on Cytodex beads were grown ± TNFα for 20 h, before bright-field and fluorescence images of the tubes were collected. (i, ii) In the absence of TNFα, only background levels of fluorescence are seen associated with the 5 beads in the field. (iii,iv) TNFα induces bright (GFP) fluorescence in the cells growing on the 4 cells in the field. (C) Comparison of HeLa cells grown conventionally on the surface of plates ("usual") with those grown on beads in tubes ("drops-in-drops"). *TNFAIP2* is an endogenous gene that responds to TNFα. After incubation (2.5 h), drops were ejected from tubes, and levels of *TNFAIP2* mRNA assessed using quantitative RT-PCR (qRT-PCR; values are averages ± maximum and minimum values from 5 drops or plates normalized first relative to the unchanging levels of 5S RNA, and then relative to the control without TNFα). TNFα increases *TNFAIP2* expression in cells grown in both ways, despite the very different environments.

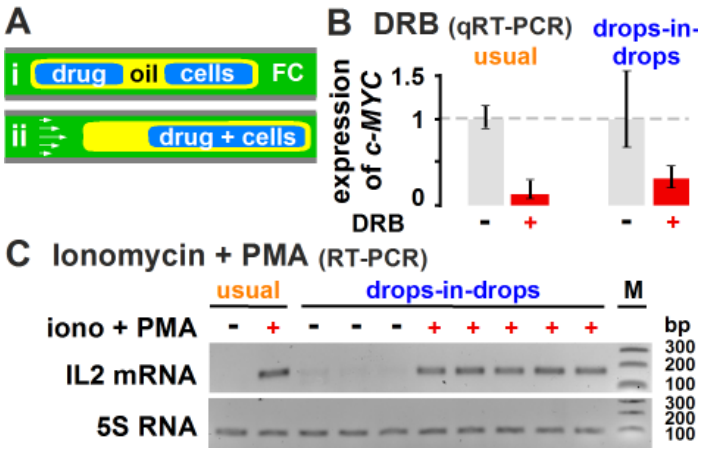


**Figure S6.** Effects of an inhibitor and an activator on mRNA levels in Jurkat cells growing in suspension (560-µm tubes). (A) Approach. Fluids: fluorocarbon (FC; HFE7500; growth medium ± cells or drug; 5-cSt silicone oil + 0.25% AbilEM180). Cells grown conventionally in plates ("usual") provide controls. (i,ii) Flow delivers drug to cells. Tubes are now incubated (37°C) for 4 h before the merged drop is ejected and its contents analyzed. (B) An inhibitor: DRB reduces levels of c-MYC mRNA (analyzed using quantitative RT-PCR; averages ± maximum and minimum values from 5 drops normalized first to the unchanging levels of 5S RNA, and then to the untreated control). (C) An activator: ionomycin and PMA increase levels of IL2 mRNA in individual drops but not those of 5S RNA used as a control (assessed using RT-PCR and gel electrophoresis; intensities of 171- and 90-bp bands reflect IL2 mRNA or 5S RNA levels; M shows 100-, 200-, 300-bp markers).

**Table S1.** Sequences of oligonucleotides used for PCR.

| PCR | | sequence (5' to 3') |
|---|---|---|
| pcDNA3 fw | | gtgtaggtcgttcgctccaa |
| pcDNA3 rev | | gcgtcagaccccgtagaaaa |
| IL2 fw | | tgtcacaaacagtgcacctact |
| IL2 rev | | agttctgtggccttcttggg |
| TNFAIP2 fw | | cagaattggcaggtacccca |
| TNFAIP2 rev | | cgtgtctacagtggcgatga |
| c-MYC fw | | ctgggaggagacattggttgaac |
| c-MYC rev | | agaagccgctccacatacag |
| 5srRNA fw | | tacggccataccaccctgaa |
| 5srRNA rev | | gcggtctcccatccaagtac |

## Statement of Authorship

| | | |
|---|---|---|
| Title of Paper | Merging drops in a Teflon tube, and transferring fluid between them, illustrated by protein crystallization and drug screening | |
| Publication Status | ☑ Published<br>❑ Accepted for Publication | ❑ Submitted for Publication<br>❑ Unpublished and unsubmitted work written in a manuscript style |
| Publication Details | Feuerborn, A., Prastowo, A., Cook, P. R., & Walsh, E. (2015). Merging drops in a Teflon tube, and transferring fluid between them, illustrated by protein crystallization and drug screening. Lab on a Chip, 15(18), 3766-3775. | |

### Student Confirmation

| | | | |
|---|---|---|---|
| Student Name: | Aishah Prastowo | | |
| Contribution to the Paper | Prepared experiments, collected data, and interpreted data for all cell-based experiments, produced Fig. 9 and Fig. S5, edited manuscript | | |
| Signature |  | Date | 8/11/2018 |

### Supervisor Confirmation

By signing the Statement of Authorship, you are certifying that the candidate made a substantial contribution to the publication, and that the description described above is accurate.

| | | |
|---|---|---|
| Supervisor name and title:<br>Edmond Walsh - Associate Professor of Engineering Science | | |
| Supervisor comments | | |
| Signature 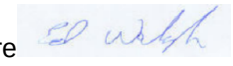 | Date | 23/11/18 |

# Paper 2: Biocompatibility of fluids for multiphase drops-in-drops microfluidics



Aishah Prastowo[1] · Alexander Feuerborn[2] · Peter R. Cook[2] · Edmond J. Walsh [1,a)]

[1] Osney Thermo-Fluids Laboratory, Department of Engineering Science, University of Oxford, Osney Mead, Oxford OX2 0ES, UK

[2] Sir William Dunn School of Pathology, University of Oxford, South Parks Road, Oxford OX1 3RE, UK

**Abstract** – This paper addresses the biocompatibility of fluids and surfactants in the context of microfluidics and more specifically a drops-in-drops system for mammalian cell based drug screening application. In the drops-in-drops approach three immiscible fluids are used to manipulate the flow of aqueous microliter-sized drops, and enable merging of drops containing cells with drops containing drugs within a Teflon tube. Preliminary drug screening tests showed that commonly used fluids and surfactant combination in the microfluidics literature resulted in significant variability in gene expression levels for Jurkat cells based on a four hour drug exposure experiment. This result stresses the need for further investigations into potential fluids and surfactants combinations that can be used in microfluidic systems for medium- to long-term drug screening applications. Through testing a range of fluids/surfactants commonly used in cell-based microfluidics, the results herein identify a fluid combination, HFE-7500 and 5-cSt silicone oil + 0.25% Abil EM180, which enabled the drops-in-drops approach while also demonstrating gene expression levels

comparable with conventional drug screening approaches in terms of both magnitude and variability.

Keywords: Biocompatibility · Drops-in-drops · Drug screening · Mammalian cell · Toxicity · Surfactant

## I. Introduction

Drop-based microfluidics is expected to play an important role in drug discovery[1-4] through increased efficiency coupled to large-scale parallelization[5, 6]; then many compounds in many different concentrations[7, 8], can be screened in different cell types[9, 10]. It can also facilitate single cell analyses[11]. In all these cases, there would be a simultaneous reduction in volumes and cost. However, current microfluidic systems suffer from various drawbacks that are limiting wide acceptance[12]; for example, they often contain complicated network of channels that are difficult to fabricate[13, 14], they require sophisticated additional machinery[15, 16], and one chip design is usually limited to one specific application[13, 17].

An alternative microfluidic method utilising a Teflon tube and fluid mechanics, rather than the more common approach relying on the geometry of micro-scale channel networks, has recently been developed[18, 19]. This method exploits the interfacial tension between three or more immiscible liquids to create specific fluidic architectures. In this context, we consider the particular architecture of two aqueous drops engulfed within one oil drop, which is – in turn – surrounded by a fluorocarbon. As a result of the liquid films surrounding drops at different points within the system, the relative velocities of the two aqueous drops can be controlled; the two drops can be forced to merge, and their contents mixed (FIG. 1).

To create the required fluidic architecture in the three-phase system, fluids must have the appropriate interfacial tensions. This can be achieved when the interfacial tension

between the fluorocarbon (FC) and the aqueous phase ($\gamma_{FC/aq}$) is greater than the sum of the interfacial tension between fluorocarbon and oil ($\gamma_{FC/oil}$) plus that between oil and water ($\gamma_{oil/aq}$). In other words, $\gamma_{FC/aq} > \gamma_{FC/oil} + \gamma_{oil/aq}$, as defined by the Neumann triangle [20, 21]. This fluidic architecture, and the mechanism that drives the merging of the two aqueous drops, are illustrated in FIG. 1. The time needed for the second drop to catch up the first one depends on the initial spacing between drops (established when the two drops first enter the tube) and their relative motion thereafter[18]. This relative velocity is influenced by the thickness of the fluidic film surrounding the drops, which varies with Capillary number ($Ca = \eta U/\gamma$, where $\eta$ = carrier fluid viscosity and $U$ = average velocity)[22, 23].

Many fluid/surfactant combinations can be found that satisfy the Neumann triangle, and allow drops-in-drops to form and merge. However, for cell-based assays, these fluid/surfactant combinations must also be biocompatible. Surfactants are widely used for biological applications, and – and as many fluid/surfactant combinations are toxic to cells[24-26] – biocompatibility of the liquids used is a general problem. The definition of a biocompatible environment varies within the microfluidic literature, and few studies have focused on this in a rigorous way. One measure used to claim biocompatibility is the ability to grow cells after they have been through a microfluidic device[27-29]. However, most cells respond to a toxic environment by arresting growth, and then they may be able to "recover" from the sub-optimal environment when returned to a favourable one. Consequently, cell behaviour may differ inside and outside the device. In addition, several authors claim biocompatibility by citing a previous study using similar fluids. For example, several articles cite ref[30] to support proliferation within drops; however, the original authors (who counted the ratio of living and dead cells) only found "some degree of proliferation within the drops". Here, we define a biocompatible environment as one in which the gene expression levels of cells in drops are comparable to those found using the same cells growing in a conventional

tissue-culture flask. This definition has particular relevance in the case of a cell grown in suspension like the Jurkat cell – and immortalized line of human T lymphocytes – where assessment of cell morphology is more difficult than it is with adherent cells.

Here we initially utilised the fluid/surfactant concentrations employed by others for drop-based microfluidics using cells (i.e., HFE-7500 and tetradecane + Span 80)[29, 31-35] with our new approach. We used a low concentration of surfactant (i.e., 0.25% w/w Span 80) to minimise potential toxicity. To verify biocompatibility, we first measured levels of 5S ribosomal RNA (rRNA) in Jurkat cells, as this is commonly used as a control[36]. Levels (quantified using qRT-PCR) in cells from different drops were found to vary sporadically. This led us to examine the reason for this sporadic behaviour, and this was traced to the fluids/surfactants employed. We then went on to screen many fluid/surfactant combinations to see which affected cell viability and gene expression. We found that many commonly-used combinations had negative effects on cells over periods of a few hours. We also identified a fluid/surfactant combination (i.e., HFE-7500 as carrier fluid, 5-cSt silicone oil + 0.25% Abil EM180 as separating fluid, and cell-culture media as the aqueous fluid containing cells and/or drugs) that could be used in our system and which was biocompatible (assessed by comparing viability and expression levels using cells grown conventionally in micro-wells).

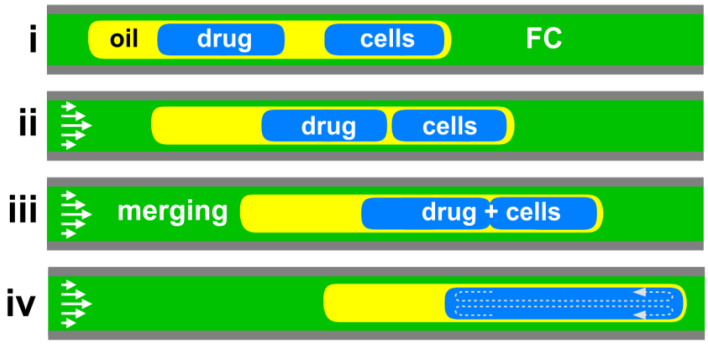


**FIG. 1** Merging drops-in-drops in a Teflon tube. (i) Initial structure of two aqueous drops – which contain cells or a drug – engulfed in one oil super-drop, which is engulfed in turn in a fluorocarbon

(FC). This structure spontaneously forms as the end of the tube (which is connected to a syringe pump acting in withdrawal mode, and which is pre-filled with fluorocarbon) is dipped successively into fluorocarbon, oil, growth medium containing cells, oil, growth medium containing the drug, and fluorocarbon. (ii) As a result of the oil film surrounding the aqueous drops and the parabolic laminar-flow profile, the engulfed aqueous drops containing cells moves faster than the oil. When the right-hand drop reaches the leading interface of the oil, it slows to travel at the velocity of the oil. With continued flow, the trailing left-hand drop containing the drug eventually catches up the leading one containing cells. (iii) Once the two aqueous drops touch, they merge. (iv) Internal vortices within the merged drop mix contents. This Figure was adapted from[18].

## II. Experimental methods

### II.1. Interfacial tension measurement

The interfacial tension between two immiscible fluids was measured using a commercial instrument (First Ten Angstroms) employing the pendant-drop method. Fluid with higher density was loaded in a syringe, a small drop was formed at the tip of the needle, and the drop was immersed in the second fluid contained in a transparent polystyrene cuvette. The interfacial tension was calculated using the manufacturer's software, a length scale (i.e., the width of the needle tip measured with a micrometre), and fluid density.

### II.2. Cell preparation

Jurkat or EL4 cells (mouse lymphoblasts) were cultured routinely in flasks in RPMI-1640 supplemented with 10% fetal bovine serum and 1% penicillin and streptomycin. They were used at 500 cells/μl for cell-viability assays (allowing cells to grow for up to 48 h), or 2000 cells/μl for drug-screening tests (for 4-h tests).

### II.3. Fluid and surfactant biocompatibility test

Different biocompatibility tests with different surface-to-volume ratios between aqueous drop and separating fluid were undertaken by overlaying the aqueous layer

containing cells with fluid in a 96-well plate (FIG. 3 A(i)) and using a Teflon tube containing an aqueous drops in two- or three-phase systems (FIG. 3 B(i), FIG. 3 C(i)).

The initial screen involved 150 μl separating fluid and cells in the same well of a 96-well plate (FIG. 3 A(i)); the non-adherant cells sediment under gravity to sit on the bottom of the well, or – if the separating fluid is the densest – on the interface between the two liquids. After incubating the plate at 37°C in 5% $CO_2$, the percentage of live cells was determined using trypan-blue exclusion and a hemocytometer after mixing equal volumes of cell solution and 0.4% trypan blue.

The fluids that had no effect on the viability in the initial screen were tested (FIG. 3 B(i)) by withdrawing drops into a Teflon tube (bore 560 μm) connected to a syringe pump (Harvard Ultra). The tube was filled with test fluid, 1 μl drops of cell solution were withdrawn into the tube at a flow rate of 2-5 ml/h, and the tube sealed at both ends and incubated at 37°C in 5% $CO_2$ for up to 48 h. Viability was assessed as before using trypan-blue exclusion by ejecting fluid from the tube at a flow rate of 2 ml/h until 10 drops were deposited into a drop of equal volume of trypan blue.

Biocompatibility was next tested using a static three-phase system in a Teflon tube containing the fluidic architecture to be used in a drug screen (FIG. 3 C(i)). In this screening also the selected separating fluids are mixed with surfactant: Span 80 (sorbitan monooleate), Abil EM90, and Abil EM180 (Cetyl PEG/PPG-10/1 Dimethicone). A tube filled with the fluorocarbon HFE-7500 was dipped successively into fluids contained in different wells in a 96-well plate; using a flow rate of 2-5 ml/h, the tube was dipped successively into cells (2 μl), separating fluid ± surfactant (1 μl), and HFE-7500 (5 μl). Finally, cells were incubated and viability was assessed as above.

The final biocompatibility test used conditions replicating those found in a drug screen – which involves flow down the tube to drive the merging of drops and delivery of drug to

cells. First, the tube was filled with HFE-7500, and – as fluid was withdrawn into the tube – the end was dipped successively into HFE-7500 (to load 5 μl), cells in medium (to load a 1 μl drop), separating fluid (to load 200 μl), cells in medium (another 1 μl drop), and then HFE-7500 (to load 5 μl). This creates a "train" of aqueous drops; repeating this process generates further trains separated by 5 μl carrier fluid.

To test the effect of fluid and surfactant on gene expression, a drop containing Jurkat cells and one containing 0.5% (v/v) dimethyl sulfoxide (DMSO) were merged (at least 10 pairs in one tube). The carrier fluid used was HFE-7500, and the separating oil was tetradecane + 0.25% Span80 or 5cSt silicone oil + 0.25% Abil EM180. Five drops were ejected from the tube immediately after loading and each was put into separate Eppendorf tubes containing 12 μl "CellsDirect resuspension and lysis buffer" (CellsDirect™; Life Technologies). The remaining drops in the tube were incubated at 37°C, 5% $CO_2$ for 4 h before being ejected individually into lysis buffer. This time was chosen because cells respond to one of the drugs used over this period[37]. As a control, 100 μl cells were plated in a well in a 96-well plate. 2 μl samples were taken from the plate after incubation for 0 and 4 h and mixed with lysis buffer following the same procedure used with samples from the drops-in-drops. Samples from both drops-in-drops and the control were lysed for 10 minutes at 75°C. The level of 5S rRNA in each sample was assessed using qRT-PCR (PCR cycles were 50°C for 20 min, 95°C for 5 min, and 40 cycles at 95°C for 15 s + 60°C for 30 sec).

### II.4. Proof-of-principle drug screening

To demonstrate the inhibition and activation of gene expression in Jurkat cells, the following drugs were used: 100 μM 5, 6-dichloro-1-β-D-ribofuranosyl-benzimidazole (DRB) as inhibitor, and 1 μg/ml ionomycin + 62.5 ng/ml phorbol 12-myristate 13-acetate (PMA) as activator. Jurkat cells and drugs or 0.5% (v/v) DMSO (as control) were taken into the tube using the same method as the previous test. The carrier fluid was HFE-7500 and the

separating oil was 5-cSt silicone oil + 0.25% Abil EM180. After incubation for 4 h, each sample was ejected into 12 µl lysis buffer, and treated as for the previous test. Levels of c-MYC mRNA and IL2 mRNA were also assessed using the ΔΔCt qRT-PCR method [38] and RT-PCR plus gel electrophoresis, respectively.

## III. Results and discussion

### III.1. Effects of tetradecane plus Span 80 on viability

HFE-7500 plus tetradecane/Span 80 plus growth medium had surface tensions satisfying the Neumann triangle. When 0.25% Span 80 (weight/weight) – an oil-soluble surfactant that significantly reduces the oil-media interfacial tension (i.e., from 17.7 to 1.88 mN/m) – is added to tetradecane, it has little effect on the interfacial tension between HFE-7500 and tetradecane. As this combination had a particularly suitable alignment of interfacial tensions for use in our assay, and the fluids had previously been used for applications in biology [29, 31-35], we explored its biocompatibility.

In our three-phase system, the carrier fluid HFE-7500 engulfs tetradecane and does not contact cells directly; therefore, the main fluid of concern for cell viability is tetradecane and Span 80, and their effects were investigated in two steps. First, as a quick screen, we incubated cells under a layer of tetradecane (with and without Span 80) in a 96-well plate. Viability (assess using trypan-blue exclusion) was >90% on exposure for 6 h to tetradecane, either on its own or with 0.25% or 1% Span 80. We then examined effects using the drops-in-drops structure in a tube, with and without drop merging. 0.25% Span 80 was used as the minimum amount of surfactant in tetradecane that facilitated a reliable merging. There was no significant impact of merging on cells viability (FIG. 2 B) using a level of 80% as a cut-off – a level that has been used in previous studies[39-41].

We then assessed levels of 5S rRNA in cells in drops-in-drops before and after 4 h incubation in the tube (using qRT-PCR). We first tested if loading and then immediately ejecting drops out of the tube affected cell number (and so 5S rRNA levels); it did not (in FIG. 2 D '0 h', cycle numbers for 'control' and 'drops-in-drops' are comparable). However, after incubation in the drops for 4 hours, levels fell (in FIG. 2 D '4 h', more PCR cycles are required for detection). This result points to a deterioration in cell function. Therefore, we screened other fluids and surfactants for their potential use in our approach.

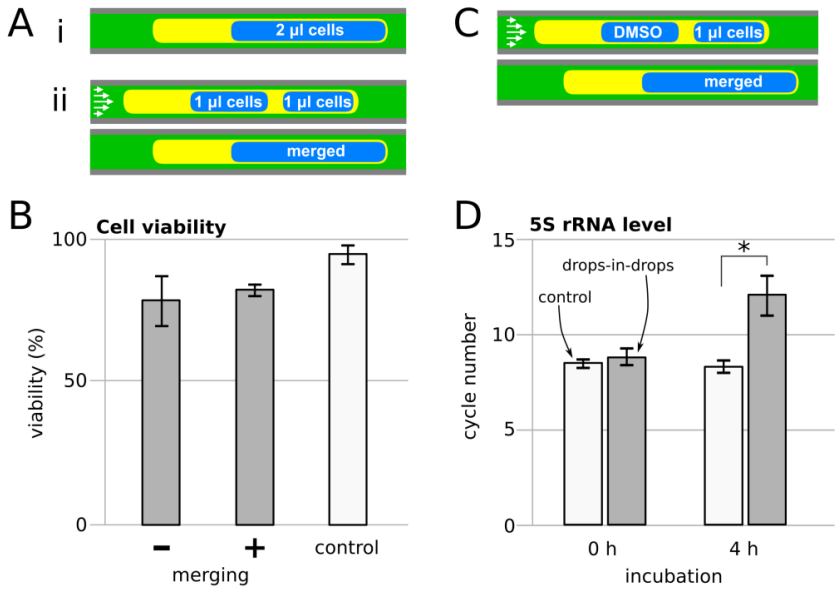


**FIG. 2** Effects of tetradecane and Span 80 on cell viability and levels of 5S rRNA (Jurkat cells). (A) Two approaches used to assess viability.: (i) no merging, static (2-µl drops in separating oil), and (ii) merging, dynamic (two 1-µl drops were loaded, and drops merged). (B) Viability (defined as the percentage of live cells in the population assessed using trypan-blue exclusion after 'no merging' or 'merging' followed by a 4-h incubation. The three phases were growth medium, tetradecane + 0.25% Span 80, and HFE-7500. 'Control': viability after 4 h for the same cells grown conventionally in a 96-well plate. (C) Approach used for gene expression analysis. A drop containing cells was merged with another containing DMSO (the drug carrier). (D) Levels of 5S rRNA (assessed using qRT-PCR; a low cycle number reflects high levels of 5S rRNA). Cells were either taken into tubes and ejected immediately ('0 h') or incubated in tubes for 4 h. 'Drops-in-drops': cells in the dynamic three-phase system (HFE-7500, growth medium, and either tetradecane + 0.25% Span 80). 'Control': the same cells grown conventionally in 96-well plate. Error bars: ± standard deviation, *: significantly different (two-sample t-test, $p<0.05$; *n* (control) = 3, *n* (drops-in-drops) = 7).

### III.2. Screening fluids for effects on viability

To explore alternative fluid/surfactant combinations that might be used to merge drops, we next listed the fluids/surfactants that had been used previously with mammalian cells in droplet-based microfluidics (TABLE I). In our three-phase system, one fluid must be cell-growth medium, and the second is likely to be either HFE-7500 or FC-40 (i.e., the two fluorocarbons used most frequently to carry aqueous drops in microfluidic systems). Here, we note that HFE-7500 stably maintains the desired architecture of drops-in-drops better than FC-40. The third fluid has to be immiscible with fluorocarbon and water – and so probably a hydrocarbon, silicone oil, or vegetable oil. Addition of surfactants to this third fluid allows interfacial tensions to be tuned to satisfy the Neumann triangle. However, surfactants are usually toxic to cells, and so the challenge is finding an appropriate combination of biocompatible fluids and surfactants.

**TABLE I.** Fluids and surfactants previously used in drop-based microfluidics with mammalian cells.

| Fluid | Surfactant | Cell type |
|---|---|---|
| *Fluorinated fluids* | | |
| FC-40 | PEG-PFPE block copolymer | 2C6 hybridoma[42], human U937[43], Chinese Hamster Ovary[44], human PC3, Raji B lymphocytes[45], HL60[46], HEK293T[47], K562, U87[48] |
| | DMP-PFPE block copolymer | HEK293T, Jurkat[30], Red blood cells[49, 50] |
| HFE-7500 | PEG-PFPE block copolymer | MDA-MB-231, PC9[51], Her2 hybridoma[32], RAW 264.7[52], mouse ES[53], K-562[51, 53] |
| FC-3283 | Perfluorooctanol (PFO) | Red blood cells[54], human periosteal cells[55] |
| *Hydrocarbon/silicone/vegetable oils* | | |
| Hexadecane | Span 80 | Chinese Hamster Ovary[56], mouse myeloma cells[57] |
| Tetradecane | Span 80 | PC12 [31], HeLa, CCRF-CEM, Ramos[35] |
| Mineral oil | Abil EM90 | MDCK[58] |
| | Span 80 | Jurkat, red blood cells[59], Chinese Hamster Ovary[60], leukemia cells[61], PC3[62], human breast cancer cells |
| | Abil EM90 + Span 80 | PC9[63] |
| Silicone oil | - | HeLa[64] |
| | Span 80 | Mouse B lymphocytes[39] |
| Soybean oil | - | Mouse mast cells and B lymphocytes[65] |
| Oleic acid | - | HeLa[66] |

To find which combinations might be appropriate, biocompatibility was assessed in several steps. First, two fluorocarbons and seven separating oil candidates without surfactant were screened using Jurkats and EL4 cells in a 96-well plate. Viability was quantified after incubation for 24 and 48 h (FIG. 3 A). As dodecane and olive oil gave less than 50% viability after 24 h (with a further reduction after 48 h), they were excluded from the next step.

The second step focused on the separating oil, leaving 5 candidates: silicone oil AR 20 (‘AR 20’), 5-cSt silicone oil (‘silicone oil’), mineral oil, tetradecane and hexadecane. Here the final environment was simulated using only two phases, the separating oil and cells in the aqueous phase. In the smaller volume where the surface-to-volume ratio is higher than in the first step, cells prove to be more sensitive as toxic effects were observed sooner (FIG. 3 B). All separating oils gave high viability during a short incubation of 4 h, but after 24 and 48 h some toxicity became apparent. For example, earlier we saw ~80% viability in tetradecane plus Span 80 after a 4-h incubation (FIG. 2 B); here, viability was higher without surfactant, but complete cell death was observed after 24 h (FIG. 3B). For the next step, only fluids giving high viability after the longest incubation period (i.e., mineral oil and 5-cSt silicone oil) were included, even though drug screening would be carried over a shorter period.

In the third test, 5-cSt silicone oil and mineral oil were tested for their suitability. Two 1-µl drops of cell culture media were initially separated by 200 nl oil in HFE-7500. First, a 1% weight-to-weight surfactant in oil was used, followed by serial dilution down to the lowest concentration giving reliable drop merging. As the two oils have different properties, different surfactant concentrations allow merging (e.g., 0.5% in mineral oil, and 0.25% in 5-cSt silicone oil). Next, Jurkats were incubated in a Teflon tube in 2-µl drops engulfed in separating fluid/surfactant (and HFE-7500 as the carrier), and viability measured (FIG. 3 C). Mineral oil + Span 80 proved particularly toxic. 5-cSt silicone oil with all surfactants gave

good viability, but Abil EM180 was selected as the detergent as it maintained drop architecture best during incubation.

As a final step, the effects of 5-cSt silicone oil + 0.25% Abil EM180 in a 3-phase system on levels of 5S rRNA were tested; cells in drops-in-drops behave like controls (FIG. 3 D).

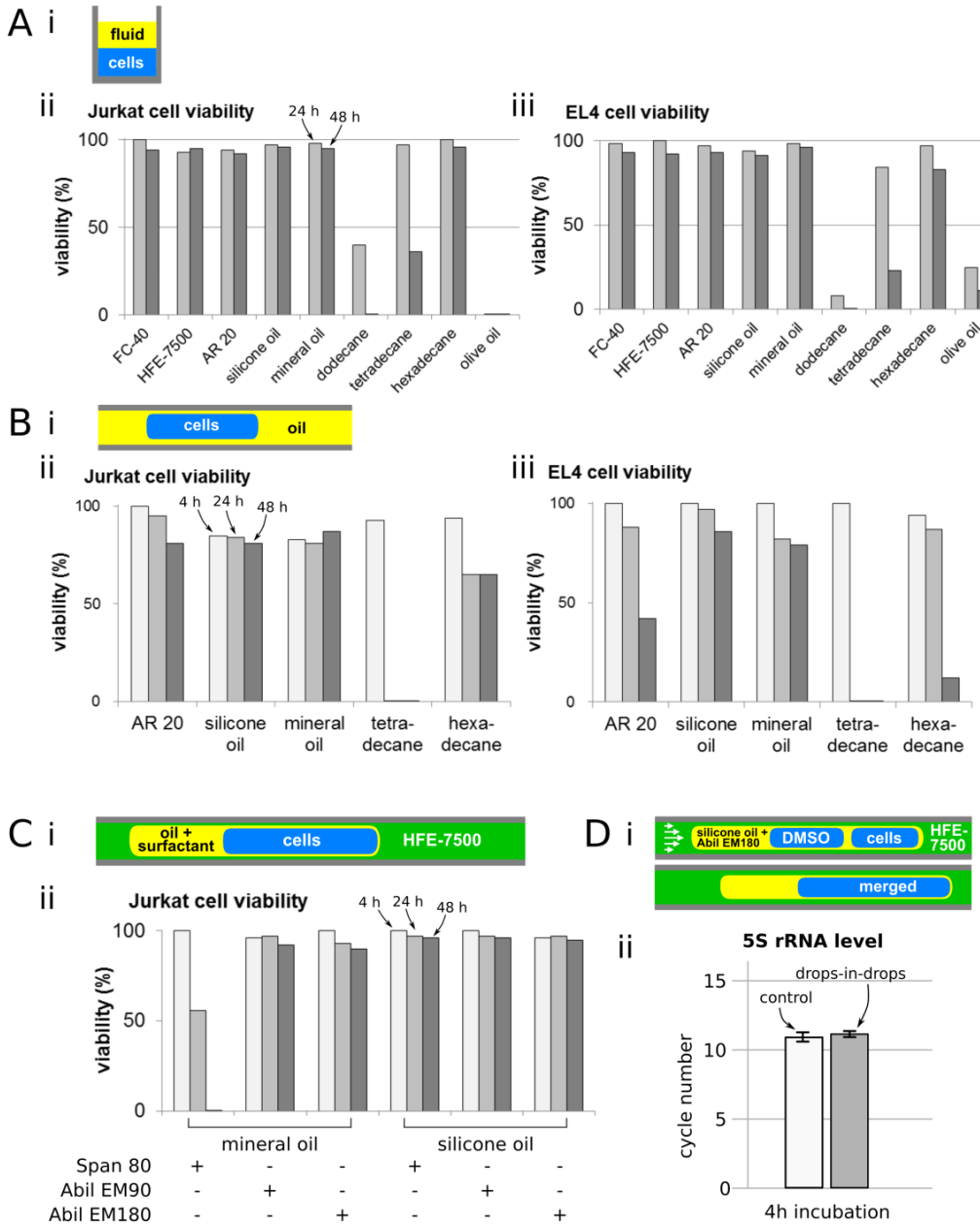


**FIG. 3** Effects of different fluids on viability of Jurkats and EL4. (A) Assay using an over-/under-lay in a 96-well plate (150 µl test fluid + 150 µl cells). (i) Cartoon illustrating approach (layers

inverted, depending on density). (ii-iii) Viability after incubation with different fluids. Dodecane and olive oil gave poor viability, and so were not used subsequently. (B) Assay using 1-µl drops in a two-phase system in a tube. (i) Cartoon illustrating approach. (ii–iii) Viability after incubation with different fluids. Mineral oil and silicone oil AR 20 advanced to the next screening round. (C) Assay using 3-phase system. (i-ii) Viability of Jurkats assessed at different times using a static 3-phase system in a tube. 2 µl aqueous drops were engulfed in the separating oil indicated, which – in turn – was engulfed in HFE-7500. (D) Gene expression test using selected fluid/surfactant combination. (i) Cartoon illustrating approach (HFE-7500 as carrier, 5-cSt silicone oil + 0.25% Abil EM180 as separating oil). (ii) 5S rRNA levels (assessed using qRT PCR; a low cycle number reflects a high level). After 4-h incubation, levels in cells in drops-in-drops are comparable to those in cells grown conventionally.

### III.3. A proof-of-principle drug screen

Having established which combination of fluids to use (i.e., HFE-7500, 5-cSt silicone oil + 0.25% Abil EM180, medium containing cells), we performed a proof-of-concept drug screen[18; supplementary information]. DRB (6-dichloro-1-β-D-ribofuranosyl-benzimidazole) is a general transcriptional inhibitor, and – when a drop containing it is merged with another containing Jurkats, levels of c-MYC mRNA (assessed by qRT-PCR) are repressed (in FIG. 4 A, more cycles are required, indicative of depression of levels). A drug pair – ionomycin plus phorbol 12-myristate 13-acetate (PMA) – initiate an inflammatory response, and this leads to an increase in levels of interleukin-2 (IL2) mRNA; when a drop containing the pair is merged with another containing cells, levels of IL2 mRNA (assessed using RT-PCR and gel electrophoresis) increase (in FIG, 4 B, the band indicative of IL2 mRNA appears). In both cases, cells in drops-in-drops behave like controls grown conventionally (FIG. 4A and B). These experiments show that HFE-7500 and 5-cSt silicone oil + 0.25% Abil EM180 can deliver both biocompatibility and the interfacial tensions necessary for the merging of drops in a Teflon tube – and so this combination is suitable for drug screening using our assay.

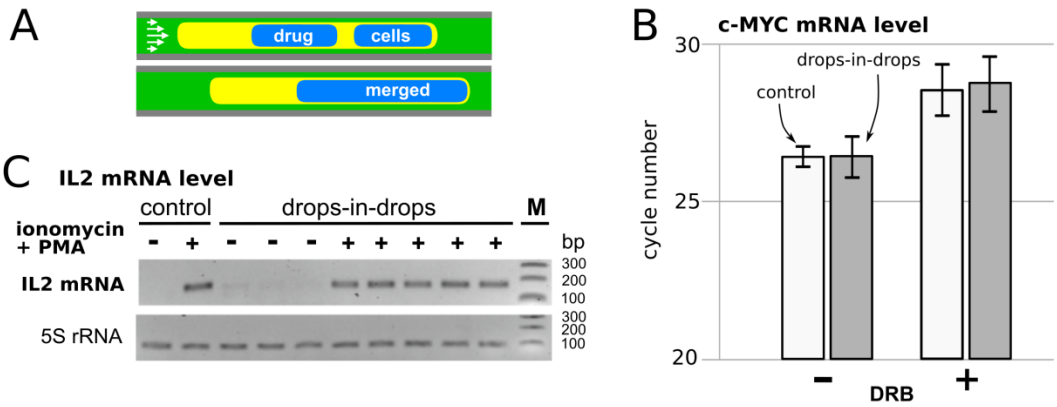


**FIG. 4** Jurkat cells in drops-in-drops respond to drugs like controls grown conventionally. (A) Schematic illustration of the drug screening (HFE-7500 as carrier, 5-cSt silicone oil + 0.25% Abil EM180 as separating oil). (B) Effects of DRB on c-MYC mRNA levels (assessed using qRT-PCR). DRB increases cycle number, indicating it reduces mRNA levels; conventional ('control') cells behave like those in drops-in-drops. (C) Effects of ionomycin + PMA on IL2 mRNA levels (assessed using RT-PCR and gel electrophoresis). 171-bp band indicative of IL2 mRNA is only seen after treatment with ionomycin and PMA; conventional ('control') cells behave like those in drops-in-drops. M: 100-, 200-, 300-bp markers. This Figure was adapted from[18].

## IV. Conclusion

Different fluids and surfactants commonly used in drop-based microfluidic system have been screened for their biocompatibilities. Genetic analysis showed that cell viability alone was a less reliable indicator for fluid and surfactant biocompatibility. For drops-in-drops applications involving mammalian cells, HFE-7500 as the carrier fluid and 5-cSt silicone oil + 0.25% Abil EM180 as the separating oil showed comparable performance in gene expression tests (4 h incubation time) to the conventional method. Therefore this fluid and surfactant combination is recommended for drug screening. Further works need to be done to assess cell proliferation in the tube for longer time period using this and/or other fluids. Although here we assume that the incompatibility comes from the fluid and surfactant which are in contact with cell media, there might also be contribution by the tube material[67, 68], hence the tube biocompatibility and alternative tube material could also be explored in

future works. Finally we suggest that results obtained with many fluid and surfactant combinations and cell-based microfluidics should be interpreted with caution.

**Acknowledgements** We thank Oreste Acuto for Jurkat cells, and the Medical Research Council, the Indonesian Endowment Fund for Education (LPDP), the 7th Framework Marie Curie Career Integration grant contract no. 333848, and University of Oxford John Fell Fund for support.



## V. References

(1) Dittrich, P. S.; Manz, A., Lab-on-a-chip: microfluidics in drug discovery. *Nat Rev Drug Discov* **2006,** *5* (3), 210-8.

(2) Kang, L.; Chung, B. G.; Langer, R.; Khademhosseini, A., Microfluidics for drug discovery and development: from target selection to product lifecycle management. *Drug Discov Today* **2008,** *13* (1-2), 1-13.

(3) Tsui, J. H.; Lee, W.; Pun, S. H.; Kim, J.; Kim, D. H., Microfluidics-assisted in vitro drug screening and carrier production. *Adv Drug Deliv Rev* **2013,** *65* (11-12), 1575-88.

(4) Dressler, O. J.; Maceiczyk, R. M.; Chang, S. I.; deMello, A. J., Droplet-based microfluidics: enabling impact on drug discovery. *J Biomol Screen* **2014,** *19* (4), 483-96.

(5) Gong, Z.; Zhao, H.; Zhang, T.; Nie, F.; Pathak, P.; Cui, K.; Wang, Z.; Wong, S.; Que, L., Drug effects analysis on cells using a high throughput microfluidic chip. *Biomed Microdevices* **2011,** *13* (1), 215-9.

(6) Miller, O. J.; El Harrak, A.; Mangeat, T.; Baret, J. C.; Frenz, L.; El Debs, B.; Mayot, E.; Samuels, M. L.; Rooney, E. K.; Dieu, P.; Galvan, M.; Link, D. R.; Griffiths, A. D., High-resolution dose-response screening using droplet-based microfluidics. *Proc Natl Acad Sci U S A* **2012,** *109* (2), 378-83.

(7) Hong, B.; Xue, P.; Wu, Y.; Bao, J.; Chuah, Y. J.; Kang, Y., A concentration gradient generator on a paper-based microfluidic chip coupled with cell culture microarray for high-throughput drug screening. *Biomed Microdevices* **2016,** *18* (1), 21.

(8) Churski, K.; Kaminski, T. S.; Jakiela, S.; Kamysz, W.; Baranska-Rybak, W.; Weibel, D. B.; Garstecki, P., Rapid screening of antibiotic toxicity in an automated microdroplet system. *Lab Chip* **2012,** *12* (9), 1629-37.

(9) Gao, Y.; Li, P.; Pappas, D., A microfluidic localized, multiple cell culture array using vacuum actuated cell seeding: integrated anticancer drug testing. *Biomed Microdevices* **2013,** *15*, 907-915.

(10) Yu, Z. T. F.; Kamei, K.-i.; Takahashi, H.; Shu, C. J.; Wang, X.; He, G. W.; Silverman, R.; Radu, C. G.; Witte, O. N.; Lee, K.-B.; Tseng, H.-R., Integrated microfluidic devices for combinatorial cell-based assays. *Biomed Microdevices* **2009,** *11*, 547-555.

(11) Rodriguez-Rodriguez, R.; Munoz-Berbel, X.; Demming, S.; Buttgenbach, S.; Herrera, M. D.; Llobera, A., Cell-based microfluidic device for screening anti-proliferative activity of drugs in vascular smooth muscle cells. *Biomed Microdevices* **2012,** *14*, 1129-1140.

(12) Sackmann, E. K.; Fulton, A. L.; Beebe, D. J., The present and future role of microfluidics in biomedical research. *Nature* **2014,** *507* (7491), 181-9.

(13) Friend, J.; Yeo, L., Fabrication of microfluidic devices using polydimethylsiloxane. *Biomicrofluidics* **2010,** *4* (2).

(14) Mazutis, L.; Gilbert, J.; Ung, W. L.; Weitz, D. A.; Griffiths, A. D.; Heyman, J. A., Single-cell analysis and sorting using droplet-based microfluidics. *Nat Protoc* **2013,** *8* (5), 870-91.

(15) Hansen, A. S.; Hao, N.; O'Shea, E. K., High-throughput microfluidics to control and measure signaling dynamics in single yeast cells. *Nat Protoc* **2015,** *10* (8), 1181-97.

(16) Kellogg, R. A.; Gomez-Sjoberg, R.; Leyrat, A. A.; Tay, S., High-throughput microfluidic single-cell analysis pipeline for studies of signaling dynamics. *Nat Protoc* **2014,** *9* (7), 1713-26.

(17) Fiorini, G. S.; Chiu, D. T., Disposable microfluidic devices: fabrication, function, and application. *BioTechniques* **2005,** *38*, 429-446.

(18) Feuerborn, A.; Prastowo, A.; Cook, P. R.; Walsh, E., Merging drops in a Teflon tube, and transferring fluid between them, illustrated by protein crystallization and drug screening. *Lab Chip* **2015,** *15* (18), 3766-75.

(19) Walsh, E.; Feuerborn, A.; Cook, P. R., Formation of droplet interface bilayers in a Teflon tube. *Sci Rep* **2016,** *6*, 34355.

(20) Guzowski, J.; Korczyk, P. M.; Jakiela, S.; Garstecki, P., The structure and stability of multiple micro-droplets. *Soft Matter* **2012,** *8* (27), 7269.

(21) Chen, D. L.; Li, L.; Reyes, S.; Adamson, D. N.; Ismagilov, R. F., Using three-phase flow of immiscible liquids to prevent coalescence of droplets in microfluidic channels: criteria to identify the third liquid and validation with protein crystallization. *Langmuir* **2007,** *23*, 2255-2260.

(22) Bretherton, F. P., The motion of long bubbles in tubes. *Journal of Fluid Mechanics* **1961,** *10* (02), 166-168.
(23) Bico, J.; Quéré, D., Liquid trains in a tube. *Europhysics Letters* **2000,** *51* (5), 546-550.
(24) Partearroyo, M. A.; Ostolaza, H.; Goni, F. M.; Barbera-Guillem, E., Surfactant-induced cell toxicity and cell lysis - a study using B12 melanoma cells. *Biochemical Pharmacology* **1990,** *40* (6), 1323-1328.
(25) Baret, J. C., Surfactants in droplet-based microfluidics. *Lab Chip* **2012,** *12* (3), 422-33.
(26) Pang, Z.; Al-Mahrouki, A.; Berezovski, M.; Krylov, S. N., Selection of surfactants for cell lysis in chemical cytometry to study protein-DNA interactions. *Electrophoresis* **2006,** *27* (8), 1489-94.
(27) Liu, W.; Kim, H. J.; Lucchetta, E. M.; Du, W.; Ismagilov, R. F., Isolation, incubation, and parallel functional testing and identification by FISH of rare microbial single-copy cells from multi-species mixtures using the combination of chemistrode and stochastic confinement. *Lab Chip* **2009,** *9* (15), 2153-62.
(28) Huang, M.; Bai, Y.; Sjostrom, S. L.; Hallstrom, B. M.; Liu, Z.; Petranovic, D.; Uhlen, M.; Joensson, H. N.; Andersson-Svahn, H.; Nielsen, J., Microfluidic screening and whole-genome sequencing identifies mutations associated with improved protein secretion by yeast. *Proc Natl Acad Sci U S A* **2015,** *112* (34), E4689-96.
(29) Martin, K.; Henkel, T.; Baier, V.; Grodrian, A.; Schon, T.; Roth, M.; Michael Kohler, J.; Metze, J., Generation of larger numbers of separated microbial populations by cultivation in segmented-flow microdevices. *Lab Chip* **2003,** *3* (3), 202-7.
(30) Clausell-Tormos, J.; Lieber, D.; Baret, J. C.; El-Harrak, A.; Miller, O. J.; Frenz, L.; Blouwolff, J.; Humphry, K. J.; Koster, S.; Duan, H.; Holtze, C.; Weitz, D. A.; Griffiths, A. D.; Merten, C. A., Droplet-based microfluidic platforms for the encapsulation and screening of Mammalian cells and multicellular organisms. *Chem Biol* **2008,** *15* (5), 427-37.
(31) Gu, S. Q.; Zhang, Y. X.; Zhu, Y.; Du, W. B.; Yao, B.; Fang, Q., Multifunctional picoliter droplet manipulation platform and its application in single cell analysis. *Anal Chem* **2011,** *83* (19), 7570-6.
(32) Hu, H.; Eustace, D.; Merten, C. A., Efficient cell pairing in droplets using dual-color sorting. *Lab Chip* **2015**.
(33) Schoeman, R. M.; Kemna, E. W.; Wolbers, F.; van den Berg, A., High-throughput deterministic single-cell encapsulation and droplet pairing, fusion, and shrinkage in a single microfluidic device. *Electrophoresis* **2014,** *35* (2-3), 385-92.
(34) El Debs, B.; Utharala, R.; Balyasnikova, I. V.; Griffiths, A. D.; Merten, C. A., Functional single-cell hybridoma screening using droplet-based microfluidics. *Proc Natl Acad Sci U S A* **2012,** *109* (29), 11570-5.
(35) Li, L.; Wang, Q.; Feng, J.; Tong, L.; Tang, B., Highly sensitive and homogeneous detection of membrane protein on a single living cell by aptamer and nicking enzyme

assisted signal amplification based on microfluidic droplets. *Anal Chem* **2014,** *86* (10), 5101-7.

(36) Tea, M.; Michael, M. Z.; Brereton, H. M.; Williams, K. A., Stability of small non-coding RNA reference gene expression in the rat retina during exposure to cyclic hyperoxia. *Molecular vision* **2013,** *19*, 501-508.

(37) Diehn, M.; Alizadeh, A. A.; Rando, O. J.; Liu, C. L.; Stankunas, K.; Botstein, D.; Crabtree, G. R.; Brown, P. O., Genomic expression programs and the integration of the CD82 costimulatory signal in T cell activation. *Proceedings of the National Academy of Sciences* **2002,** *99* (18), 11796-11801.

(38) Livak, K. J.; Schmittgen, T. D., Analysis of relative gene expression data using real-time quantitative PCR and the 2(-Delta Delta C(T)) Method. *Methods* **2001,** *25* (4), 402-8.

(39) Sgro, A. E.; Allen, P. B.; Chiu, D. T., Thermoelectric manipulation of aqueous droplets in microfluidic devices. *Analytical Chemistry* **2007,** *79*, 4845-4851.

(40) Du, G. S.; Pan, J. Z.; Zhao, S. P.; Zhu, Y.; den Toonder, J. M.; Fang, Q., Cell-based drug combination screening with a microfluidic droplet array system. *Anal Chem* **2013,** *85* (14), 6740-7.

(41) Qu, B.; Eu, Y. J.; Jeong, W. J.; Kim, D. P., Droplet electroporation in microfluidics for efficient cell transformation with or without cell wall removal. *Lab Chip* **2012,** *12* (21), 4483-8.

(42) Koster, S.; Angile, F. E.; Duan, H.; Agresti, J. J.; Wintner, A.; Schmitz, C.; Rowat, A. C.; Merten, C. A.; Pisignano, D.; Griffiths, A. D.; Weitz, D. A., Drop-based microfluidic devices for encapsulation of single cells. *Lab Chip* **2008,** *8* (7), 1110-5.

(43) Joensson, H. N.; Samuels, M. L.; Brouzes, E. R.; Medkova, M.; Uhlen, M.; Link, D. R.; Andersson-Svahn, H., Detection and analysis of low-abundance cell-surface biomarkers using enzymatic amplification in microfluidic droplets. *Angew Chem Int Ed Engl* **2009,** *48*, 2518-2521.

(44) Chen, F.; Zhan, Y.; Geng, T.; Lian, H.; Xu, P.; Lu, C., Chemical transfection of cells in picoliter aqueous droplets in fluorocarbon oil. *Anal Chem* **2011,** *83* (22), 8816-20.

(45) Eastburn, D. J.; Sciambi, A.; Abate, A. R., Ultrahigh-throughput Mammalian single-cell reverse-transcriptase polymerase chain reaction in microfluidic drops. *Anal Chem* **2013,** *85* (16), 8016-21.

(46) Edd, J. F.; Di Carlo, D.; Humphry, K. J.; Koster, S.; Irimia, D.; Weitz, D. A.; Toner, M., Controlled encapsulation of single-cells into monodisperse picolitre drops. *Lab Chip* **2008,** *8* (8), 1262-4.

(47) Juul, S.; Ho, Y.-P.; Koch, J.; Andersen, F. F.; Stougaard, M.; Leong, K. W.; Knudsen, B. R., Detection of single enzymatic events in rare or single cells using microfluidics. *ACS Nano* **2011,** *5* (10), 8305-8310.

(48) Mongersun, A.; Smeenk, I.; Pratx, G.; Asuri, P.; Abbyad, P., Droplet Microfluidic Platform for the Determination of Single-Cell Lactate Release. *Anal Chem* **2016,** *88* (6), 3257-63.

(49) Abbyad, P.; Tharaux, P. L.; Martin, J. L.; Baroud, C. N.; Alexandrou, A., Sickling of red blood cells through rapid oxygen exchange in microfluidic drops. *Lab Chip* **2010,** *10* (19), 2505-12.

(50) Abbyad, P.; Dangla, R.; Alexandrou, A.; Baroud, C. N., Rails and anchors: guiding and trapping droplet microreactors in two dimensions. *Lab Chip* **2011,** *11* (5), 813-21.

(51) Ng, E. X.; Miller, M. A.; Jing, T.; Chen, C. H., Single cell multiplexed assay for proteolytic activity using droplet microfluidics. *Biosens Bioelectron* **2016,** *81*, 408-14.

(52) Fischer, A. E.; Wu, S. K.; Proescher, J. B.; Rotem, A.; Chang, C. B.; Zhang, H.; Tao, Y.; Mehoke, T. S.; Thielen, P. M.; Kolawole, A. O.; Smith, T. J.; Wobus, C. E.; Weitz, D. A.; Lin, J. S.; Feldman, A. B.; Wolfe, J. T., A high-throughput drop microfluidic system for virus culture and analysis. *J Virol Methods* **2015,** *213*, 111-7.

(53) Klein, A. M.; Mazutis, L.; Akartuna, I.; Tallapragada, N.; Veres, A.; Li, V.; Peshkin, L.; Weitz, D. A.; Kirschner, M. W., Droplet barcoding for single-cell transcriptomics applied to embryonic stem cells. *Cell* **2015,** *161* (5), 1187-201.

(54) Kline, T. R.; Runyon, M. K.; Pothiawala, M.; Ismagilov, R. F., ABO, D blood typing and subtyping using plug-based microfluidics. *Anal Chem* **2008,** *80*, 6190-6197.

(55) Srisa-Art, M.; Bonzani, I. C.; Williams, A.; Stevens, M. M.; deMello, A. J.; Edel, J. B., Identification of rare progenitor cells from human periosteal tissue using droplet microfluidics. *Analyst* **2009,** *134* (11), 2239-45.

(56) Zhan, Y.; Wang, J.; Bao, N.; Lu, C., Electroporation of cells in microfluidic droplets. *Anal Chem* **2009,** *81*, 2027-2031.

(57) Kemna, E. W.; Segerink, L. I.; Wolbers, F.; Vermes, I.; van den Berg, A., Label-free, high-throughput, electrical detection of cells in droplets. *Analyst* **2013,** *138* (16), 4585-92.

(58) Mary, P.; Dauphinot, L.; Bois, N.; Potier, M. C.; Studer, V.; Tabeling, P., Analysis of gene expression at the single-cell level using microdroplet-based microfluidic technology. *Biomicrofluidics* **2011,** *5* (2), 24109.

(59) Chabert, M.; Viovy, J. L., Microfluidic high-throughput encapsulation and hydrodynamic self-sorting of single cells. *Proc Natl Acad Sci U S A* **2008,** *105* (9), 3191-6.

(60) Hufnagel, H.; Huebner, A.; Gulch, C.; Guse, K.; Abell, C.; Hollfelder, F., An integrated cell culture lab on a chip: modular microdevices for cultivation of mammalian cells and delivery into microfluidic microdroplets. *Lab Chip* **2009,** *9* (11), 1576-82.

(61) Sun, M.; Bithi, S. S.; Vanapalli, S. A., Microfluidic static droplet arrays with tuneable gradients in material composition. *Lab Chip* **2011,** *11* (23), 3949-52.

(62) Konry, T.; Smolina, I.; Yarmush, J. M.; Irimia, D.; Yarmush, M. L., Ultrasensitive detection of low-abundance surface-marker protein using isothermal rolling circle amplification in a microfluidic nanoliter platform. *Small* **2011,** *7* (3), 395-400.

(63) Jing, T.; Ramji, R.; Warkiani, M. E.; Han, J.; Lim, C. T.; Chen, C. H., Jetting microfluidics with size-sorting capability for single-cell protease detection. *Biosens Bioelectron* **2015,** *66*, 19-23.

(64) Xiao, K.; Zhang, M.; Chen, S.; Wang, L.; Chang, D. C.; Wen, W., Electroporation of micro-droplet encapsulated HeLa cells in oil phase. *Electrophoresis* **2010,** *31* (18), 3175-80.

(65) He, M.; Edgar, J. S.; Jeffries, G. D. M.; Lorenz, R. M.; Shelby, P.; Chiu, D. T., Selective encapsulation of single cells and subcellular organelles into picoliter-and-femtoliter-volume droplets. *Anal Chem* **2005,** *77*, 1539-1544.

(66) Tan, Y.-C.; Hettiarachchi, K.; Siu, M.; Pan, Y.-R.; Lee, A. P., Controlled microfluidic encapsulation of cells, proteins, and microbeads in lipid vesicles. *J. Am. Chem. Soc.* **2006,** *128*, 5656-5658.

(67) Panaro, N. J.; Lou, X. J.; Fortina, P.; Kricka, L. J.; Wilding, P., Surface effects on PCR reactions in multichip microfluidic platforms. *Biomedical Microdevices* **2004,** *6* (1), 75-80.

(68) Jiang, X.; Jeffries, R. E.; Acosta, M. A.; Tikunov, A. P.; Macdonald, J. M.; Walker, G. M.; Gamcsik, M. P., Biocompatibility of Tygon(R) tubing in microfluidic cell culture. *Biomed Microdevices* **2015,** *17* (1), 20.

## Statement of Authorship

| | | |
|---|---|---|
| Title of Paper | Biocompatibility of fluids for multiphase drops-in-drops microfluidics | |
| Publication Status | ☑ Published<br>❑ Accepted for Publication | ❑ Submitted for Publication<br>❑ Unpublished and unsubmitted work written in a manuscript style |
| Publication Details | Prastowo, A., Feuerborn, A., Cook, P. R., & Walsh, E. J. (2016). Biocompatibility of fluids for multiphase drops-in-drops microfluidics. *Biomedical microdevices*, *18*(6), 114. | |

### Student Confirmation

| | | | |
|---|---|---|---|
| Student Name: | Aishah Prastowo | | |
| Contribution to the Paper | Collected and interpreted data, produced figures, wrote the manuscript | | |
| Signature |  | Date | 8/11/2018 |

### Supervisor Confirmation

By signing the Statement of Authorship, you are certifying that the candidate made a substantial contribution to the publication, and that the description described above is accurate.

| | | |
|---|---|---|
| Supervisor name and title:<br>Edmond Walsh - Associate Professor of Engineering Science | | |
| Supervisor comments | | |
| Signature 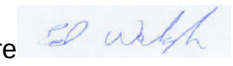 | Date | 23/11/18 |

# Paper 3: Contact-Line Pinning and Superhydrophobic Behavior of Sessile Drops Induced by Fetal Bovine Serum and Serum-Free Replacement

*This manuscript is under review in the journal Scientific Reports, submitted on 9 January 2019*

Aishah Prastowo[†], Peter R. Cook[‡], Edmond J. Walsh[†]*

†Osney Thermo-Fluids Laboratory, Department of Engineering Science, University of Oxford, Osney Mead, Oxford OX2 0ES, United Kingdom

‡Sir William Dunn School of Pathology, University of Oxford, South Parks Road, Oxford OX1 3RE, United Kingdom

*corresponding author

**Abstract –** Many bio-assays are performed using microplates with 96 wells, each with a working volume of tens to hundreds of microliters. Arrays of sessile drops (often covered with an immiscible liquid to prevent evaporation) have been used to scale down reaction volumes; then, the surface is usually patterned with hydrophilic and hydrophobic patches to ensure drop footprint does not change when growth medium is added. Here, fetal bovine serum, or a serum-free replacement, are added to cell-growth medium to stabilize pinning lines around footprints of drops sitting on virgin polystyrene Petri dishes. This increases the advancing contact angle beyond the 150° usually associated with superhydrophobic effects, and – in consequence – the maximum volume that can be contained without breaching pinning lines. Pinning lines also remain stable even when surfactants are added. Using this approach, a multi-step proof-of-concept drug screen is performed using living human cells and sub-microliter volumes.

## I. Introduction

Two dimensional (2D) arrays of nano- to micro-liter drops offer large reagent savings when used as miniaturised analogues of microplates in bioassays[1]; small volumes of reagents can be added through needles, capillaries[2, 3], or inkjet printers[4-6]. Drops are often anchored at specified locations by pre-patterning substrates (e.g., by surrounding hydrophilic spots with hydrophobic barriers[3, 7-13]) so the apparent advancing contact angle increases[14] and more volume can be added to drops without changing footprints (substrate areas in contact with drops). However, such pre-patterning requires specialised equipment[7, 10, 12] and is inflexible in terms of working area. Homogeneous surfaces like glass[5] and treated PDMS[4] have also been used but yield low contact angles with aqueous solutions which restricts working volumes[15]; moreover, PDMS may also leach toxins that reduce biocompatibility[16].

An approach to retain liquids that does not rely on the use of solid walls (as in microplates) or pre-patterned substrates has recently been developed[17]. A dispensing needle connected to a syringe pump deposits arrays of drops or draws fluidic circuits on a standard tissue-culture polystyrene Petri dish[16]; the aqueous pattern then remains pinned to the dish by interfacial tension. A transparent and immiscible fluorinated liquid, FC-40, overlays the drops/circuits to prevent evaporation. This overlay also increases the advancing contact angle so drops/circuits can hold more liquid without increase in footprint. As FC-40 is arguably one of the most bio-inert immiscible liquids known[18-20], this method is especially suitable for cell-based assays. Our initial purpose was to investigate the stability of pinning lines at the edge of the footprint where medium, FC-40, and substrate intersect.

Many eukaryotic cells are cultured in vitro, and so assayed in, media supplemented with 10% fetal bovine serum (FBS) – used because it contains low levels of potentially-harmful antibodies and high concentrations of growth factors[21, 22]. FBS is a natural product that contains a complex and variable mixture of proteins, lipids, vesicles, etc. Alternatively,

chemically-defined serum replacements (SRs) have been used, but their precise chemical compositions are usually withheld. Surfactants, which FBS or SR might contain, can possibly alter equilibrium contact angles – either decreasing[23, 24] or increasing[25, 26] them. We also know that proteins can increase pinning-line stability[27, 28], and create hydrophilic patterns on hydrophobic substrates to anchor sessile drops[29]. Our intention was to examine what effects FBS and SR had on working volumes confined within arrays of sessile drops.

Our studies yield the following results. First, 10% FBS or SR stabilize pinning lines by substantially increasing the advancing contact angle (e.g., with FBS, the advancing contact angle increases from ~60° to >120°); this significantly increases the range of volumes that can be accommodated within a given footprint. Second, such increases are time and temperature dependent. For example, addition of FBS to a drop of medium followed by incubation at 37°C can yield contact angles exceeding 150° – values given by drops of water sitting on ultra- or superhydrophobic substrates (usually textured surfaces)[30, 31]. This has another significant practical consequence: superhydrophobic-like effects can be generated simply by adding serum to the aqueous phase without the need for complex and expensive modification of substrate roughness. We also go on to use arrays of these sessile drops in a proof-of-concept cell-based drug screen to demonstrate biocompatibility of the platform.

## II. Results

### II.1. Serum stabilizes the pinning line

We first investigate how shapes of drops under FC-40 – initially containing 1 μl or 200 nl – change as different liquids are added. Before addition of liquids and after deposition on the substrate in air, drops of distilled water yield equilibrium contact angles of ~55°, while cell culture medium Dulbecco's Modified Eagle's Medium (DMEM) ± serum gives ~40-43° (Figure S1A). Depositing drops under FC-40 yields higher contact angles (e.g., 55°

for distilled water in air, compared with 78° under FC-40; Figure S1A). As FC-40 is significantly denser than water (density 1.86 g/ml), buoyancy effects will tend to drive water upward through the fluorocarbon. If effects of gravity are negligible (so buoyancy effects are also negligible), drops are shaped like spherical caps, and – when extra liquid is added to a drop (Figure 1A) – the extra volume can be accommodated by increasing footprint area or contact angle. If effects of gravity are significant, the shape will deviate from that of a spherical cap: the aqueous phase will tend to rise or flatten depending on the density of the overlaying fluid. In the case of denser FC-40, drop height will increase.

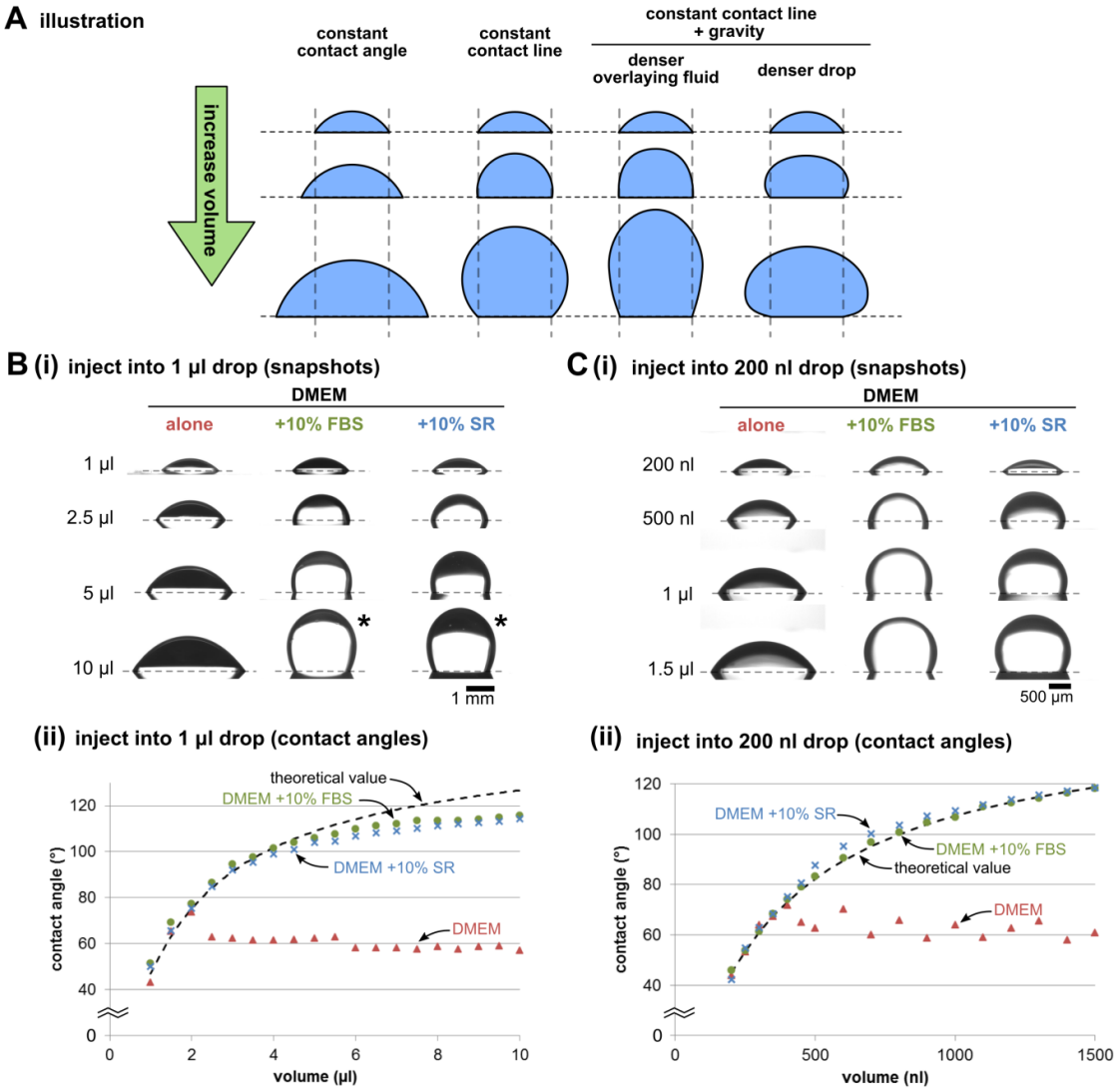


**Figure 1.** Serum stabilizes pinning lines. Dashed lines provide visual guides to the base line of each drop; below these lines are reflections. (A) Four ways drop shape might change as the volume of a

sessile drop (with/without an overlaying liquid) increases. (B) Drops of DMEM ± 10% FBS or SR were deposited in air, overlaid with FC-40, and the same aqueous fluid added in increments (~2 min between increments). *: cap geometry no longer that of a spherical cap. Drops (initially 1 µl), with 500 nl increments up to 10 µl. (i) Images. With DMEM, the pinning line is unstable, and drop width increases progressively. With 10% FBS or 10% SR, pinning lines are stable (so footprint width remains unchanged), and final shapes are no longer spherical caps (as buoyancy increases drop height and reduces drop width). (ii) Contact angles. Dotted line: the theoretical angle calculated assuming unchanging footprint. With DMEM (triangles), the angle remains constant as the footprint enlarges. With DMEM + 10% FBS (circles) or 10% SR (crosses), the footprint remains constant, and angles increase. (C) A same experiment as (B) but using initial volume of 200 nl and 50-100 nl volume increments. (i) Images. Changes are as for larger drops in (B); except shapes are always those of spherical caps. (ii) Contact angles. With DMEM (triangles), the angle again remains constant (experimental error increases as drops are smaller). With DMEM + 10% FBS (circles) or SR (crosses), measured contact angles are close to the theoretical over the whole range.

With 1 µl drops, the maximum contact angles obtained with DMEM + 10% FBS or SR are larger than those obtained with DMEM (Figure 1B). One µl drops of DMEM in air have contact angles of ~43°, and after overlaying FC-40 and adding more medium, the contact angle increases to ~75° at 2 µl (Figure 1Bi). Above this value, footprint area increases as the advancing contact angle stays at ~60° (Figure 1Bii). Similar results are observed when using water instead of DMEM, except that the advancing contact angle is higher (~80°; Figure S1B). With FBS or SR, drop volume may be increased while the footprint is unchanged and contact angle increases up to at least 10 µl (Figure 1Bi, ii). Above around 5 µl, the contact angle becomes progressively lower than that calculated assuming spherical-cap geometry (indicated by '*' in Figure 1Bi and departure from the 'theoretical' curve in Figure 1Bii); instead, the drop is taller and the contact angle is always below 120°. We conclude that the effect of gravity distorts drop shape from that of a spherical cap. These results show that FBS and SR stabilize pinning lines and increase the working range of volumes accommodated by a footprint of constant area.

Capillary length can be used to estimate when the effect of gravity starts to become apparent (Supplementary Methods). Since the drop is pinned and has large contact angle hysteresis, height of the drop is taken as the characteristic length instead of the base radius. Equilibrium interfacial tension of FC-40 and DMEM + 10% FBS was ~20 mN/m, and the density difference is 0.86 g/ml. Therefore, the capillary length is ~1.54 mm. For a sessile drop with footprint created by 1 μl medium and spherical cap height of 1.54 mm, the total volume is 5.01 μl. This is consistent with our observation that above 5 μl drop shape deviates from that of a spherical cap.

Subtly different effects are obtained by adding more liquid to drops of initial volume 200 nl (Figure 1C) – serum yields a constant footprint despite the increase in volume (unlike the serum-free case). However, now the maximum contact angle reaches ~120° at the largest volume shown here, and the measured contact angle follows values calculated using spherical-cap geometry up to at least 1.5 μl. This indicates that these drops are small enough that buoyancy effects are insignificant. For drops with this footprint size, to get the height of the capillary length, the volume needs to be ~3 μl, well above tested volumes.

**II.2. Pinning as a function of incubation time and temperature**

We next investigated the effects on pinning lines of flowing media into drops at different rates. A 1 μl drop of DMEM + 10% FBS was deposited in air, overlaid with FC-40, more DMEM + 10% FBS added, and contact angles measured as volumes increased (Figure 2Ai). When extra medium is added slowly (at 10 nl/s), the drop retains its initial footprint. However, with higher flow rates, (100 nl/s, 1 μl/s), inertia causes footprint area to increase and contact angles reach ~80°; angles then remain constant (Figure 2Ai). The higher advancing contact angle compared to the previous one of ~60° (Figure 1) is presumably because drop shape has not yet reached equilibrium by the time of measurement (as fluid is continuously injected). When the same flow rates are applied to a drop pre-incubated for 30

min, the contact angle increases progressively, and the pinning line remains unchanged (Figure 2Aii). These results prompted investigation of the effects of varying time and temperature between drop deposition and adding more liquid.

We first varied pre-incubation time (using an injection rate of 100 nl/s – a rate sufficient to destabilize pinning lines of an un-incubated drop; Figure 2Ai).With essentially no pre-incubation at room temperature (i.e., addition after 5 min), the contact angle increases up to ~80°, and then the footprint expands as drop volume increases (Figure 2Bi) – as found before (Figure 2Ai). In contrast, on addition after 10 min, the contact angle increases up to ~100° before falling back to ~80° as the volume increases (Figure 2Bi). With 30 or 60 min, pinning lines remain fixed, and contact angles increase as volume increases (Figure 2Bi). This points to pre-incubations at room temperature of 5-30 min progressively stabilizing pinning lines. We next repeated this experiment using pre-incubations at 37°C (Figure 2Bii). Now, the pinning line is partially stabilized by pre-incubation for only 5 min, and completely stabilized after 10 min (Figure 2Bii), indicating the higher temperature accelerates stabilization of pinning lines. When the tests are repeated with DMEM plus only 1% FBS; in general, longer incubation times are required to stabilize pinning lines (compare Figure 2 and Figure S2). Since the stabilization is temperature, time, and concentration dependent, we hypothesized that it is induced by a diffusion-driven adsorption process of serum components to the pinning lines[32, 33].

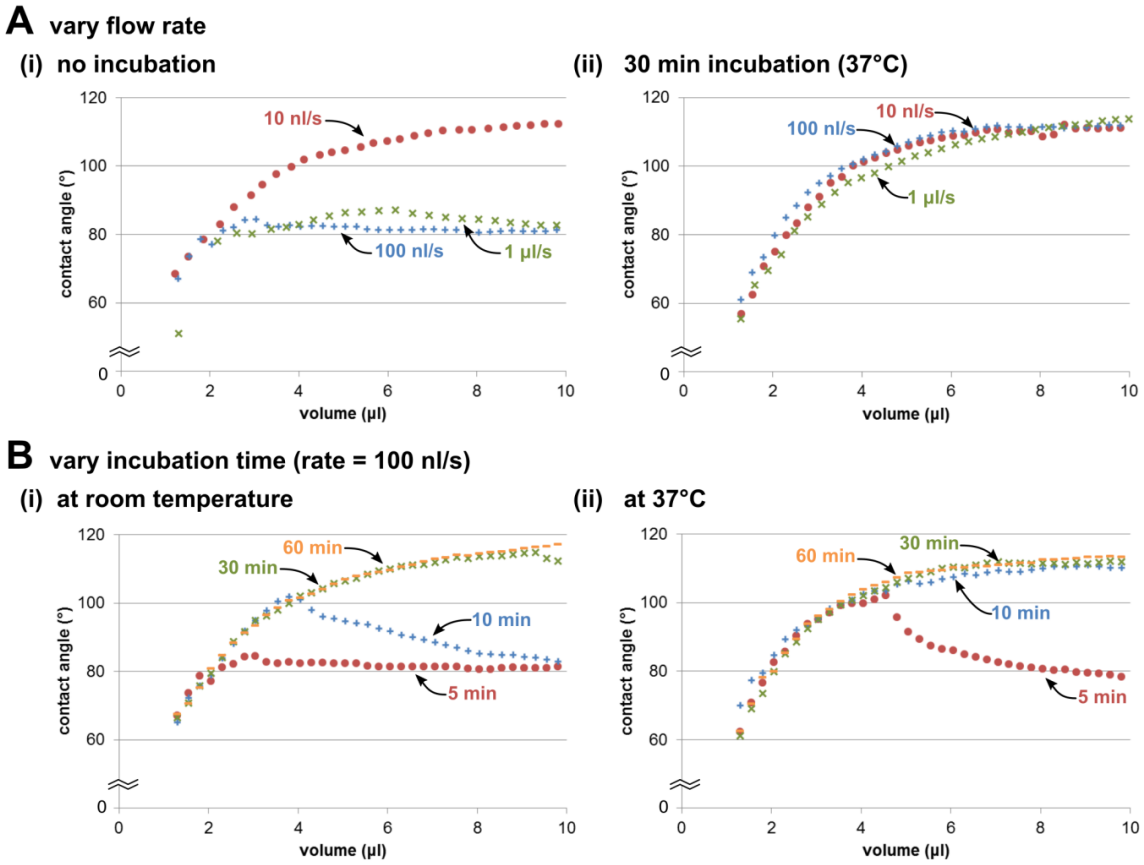


**Figure 2.** The stability of pinning lines around sessile drops depends on rate of injection, and incubation time and temperature. Drops (1 µl; DMEM + 10% FBS) were deposited, incubated for times and temperatures indicated, imaged as more medium was injected continuously into them, and contact angles determined. (A) Effects of flow rate. (i) Injection immediately after deposition. (ii) Drops were pre-incubated (37°C; 30 min) prior to injection. (B) Effect of incubation time and temperature on pinning (injection rate 100 nl/s). (i) Drops were pre-incubated at room temperature for 5-60 min prior to injection. (ii) Drops were pre-incubated (37°C; 5-60 min); higher temperature and longer incubation time stabilize pinning lines.

### II.3. Advancing contact angles and superhydrophobic effects

We aimed to measure the maximum contact angle that can be supported by serum-stabilized drops under FC-40; however, buoyancy effects complicate analysis. For example, after creating a 100 nl drop of DMEM + 10% FBS and injecting liquid slowly into it, footprint diameter remains constant as the contact angle first increases to ~128°, and then decreases to ~80° as extra volume is accommodated in the upper part of the ballooning drop (Figure 3Ai). Next, the balloon pinches off to float to the surface, and the contact angle rises

again (Figure 3Ai). As a result, it is difficult to determine the true value of the advancing contact angle – we can only conclude that it is >128°. An identical measurement was also performed using DMEM + 20% SR (Figure 3Aii). Now, the pinning line breaks when the contact angle reaches ~125°, and thereafter the diameter increases as the drop finds its new equilibrium contact angle (Figure 3Aii). We conclude this is the true value of the advancing contact angle under these conditions.

To obtain the real value of the advancing contact angle of a drop containing DMEM + 10% FBS under FC-40, we first loaded a footprint created by a 100 nl drop with 2 µl medium (above this volume, some of the drop detaches; Figure 3Ai), and incubated it at 37°C for 20 h to stabilize the pinning line. The drop was then slowly pushed/pulled manually by a needle. Figure 3B and Movie S1 show the drop can be pushed around without detaching; it remains stuck to the substrate through the pinning line formed by the original 100 nl drop. Pushing the drop to the left or right reveals an advancing contact angle close to 180°, pulling it up gives an angle of 90°, and – when the needle is retracted – the drop and its footprint return to their initial shapes. Therefore, the maximum contact angle is nearly 180°. As superhydrophobic states are generally defined by contact angles >150°[13, 32, 34], this means that serum addition followed by incubation provides a simple way of mimicking these states.

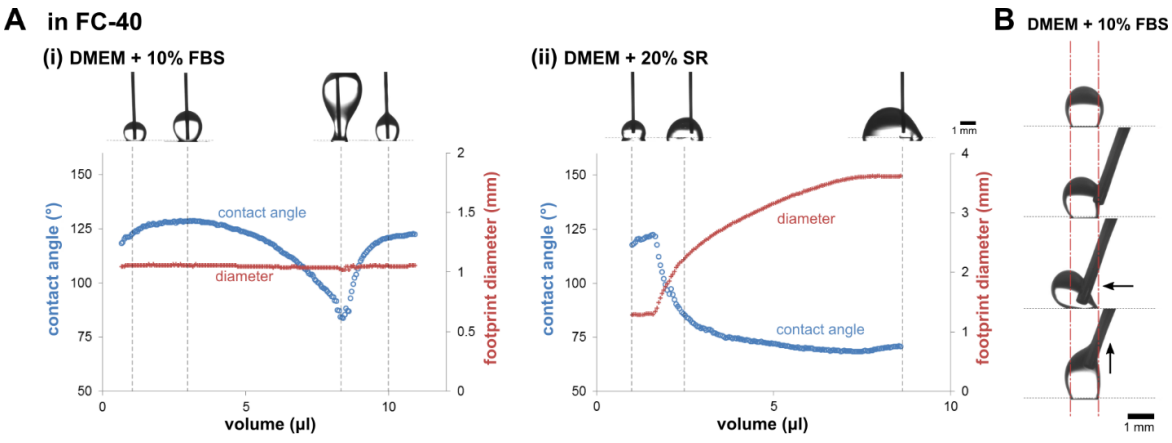

**Figure 3.** Advancing contact angles at serum-stabilized pinning lines. (A) 500 nl drops of DMEM + 10% FBS or 20% SR on a footprint created by 100 nl drop of the same liquid (diameter ~1.1 mm) were incubated (20 h, 37°C). More medium is injected at 10 nl/s. Images of drops are shown above representative points in the graph. (i) With DMEM + 10% FBS, as medium is added, footprint diameter remains constant throughout as the contact angle peaks at ~128° before decreasing as the buoyancy effect deforms drop shape. As the volume approaches ~9 µl, some of the drop detaches and floats to the surface to leave ~500 nl on the footprint. Thereafter, the contact angle increases; as the needle has been wetted, this also affects drop shape and lowers the contact angle. The volume indicated on the axis is the total including that of a detached part of the drop. (ii) With DMEM + 20% SR, the increase in volume initially increases contact angles; however, as the volume approaches ~2 µl, the pinning line breaks and the contact angle decreases to a new equlibrium while footprint diameter increases. (B) Measuring the advancing contact angle with the push/pull method (images from Movie S1). A 2 µl drop of DMEM + 10% FBS on a footprint created by 100 nl of the same liquid was incubated (20 h, 37°) and imaged. Pushing the drop manually to the left with a needle reveals a contact angle of almost 180° whilst pulling it up gives one ~90° – all without change in footprint.

We next repeated the experiment using an immiscible overlay – tetradecane – that has a density (0.76 g/ml) lower than media. Now, buoyancy forces act downwards, so the ballooning pinch-off cannot occur. The footprint was loaded with 500 nl, incubated for 20 h to stabilize the pinning line, and more medium injected. With DMEM + 10% FBS or 20% SR, as the volume increases, the apparent footprint diameter increases, and the apparent contact angle rises to a plateau at ~150° (Figure S3A). When the push/pull experiment is repeated with this oil – an angle of ~180° is again seen (Figure S3B, Movie S2).

### II.4. Serum adsorption to water/FC-40 interface

We then investigated the effect of adsorption of serum components to the water/FC-40 interface, with consequential effects on the dynamic interfacial tension[35]. Our measurements show that 10% FBS in DMEM decreases interfacial tension (using FC-40) from an equilibrium value of ~40 mN/m to ~20 mN/m within minutes (Figure 4A), consistent with diffusion-driven adsorption of FBS components to the water/FC-40 interface.

After rapid adsorption, many proteins denature to form thin semi-rigid skin-like layers at interfaces over longer time-scales[33, 35-39]. Since FBS is rich in proteins and other interacting lipids/factors – we expected an elastic protein- and/or factor-rich skin to form at our interfaces. We incubated a drop of DMEM + 10% FBS under FC-40 at 37°C for different times before withdrawing liquid (Figure 4B,C). With 2 h pre-incubation, no elastic skin is obvious (Figure 4B, Movie S3); however, with 20 h pre-incubation, an elastic skin is visually observed as a depression in the interface is seen on pressing a needle tip into the surface (Figure 4Ci,ii; Movie S4). Once the tip penetrates and liquid is withdrawn, the "elastic" interface first "wrinkles"[40, 41] to leave a final residue that is large and obvious (Figure 4Ciii,iv; Movie S4). Such skin formation is suggested to enhance pinning stability and create the superhydrophobic effect in Figure 3B – the skin creates barrier that prevents contact of the liquid drop with the surface of the Petri dish beyond the original footprint.

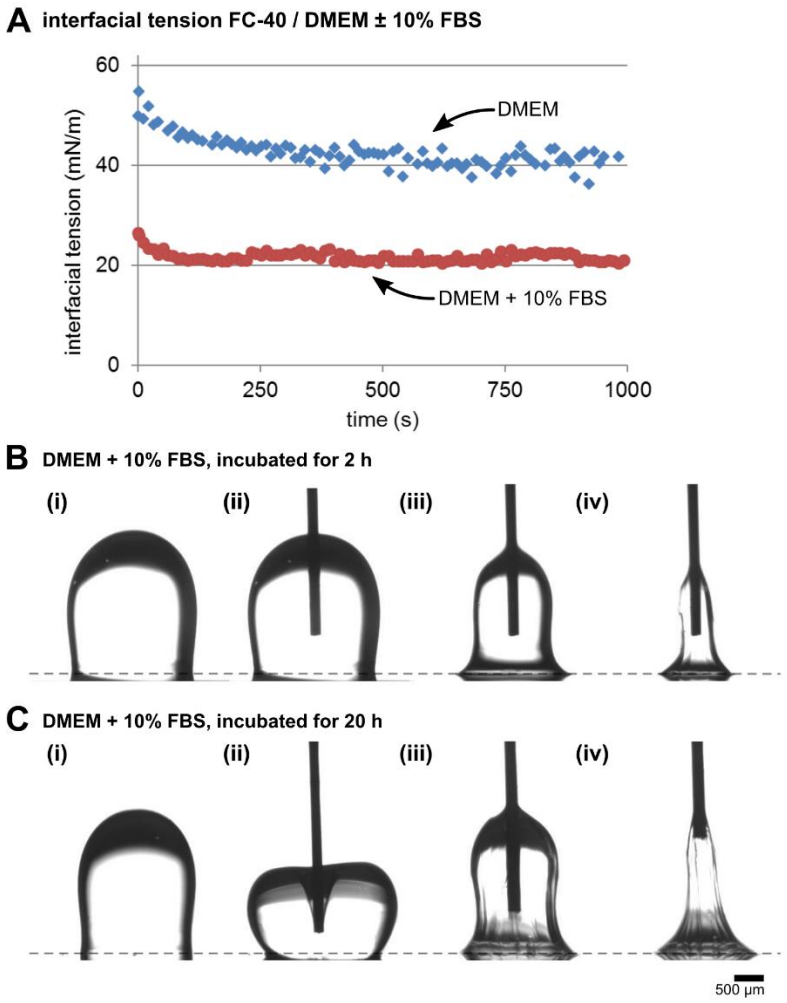


**Figure 4.** Serum adsorbs on the medium/FC-40 interface and forms an elastic skin. (A) Dynamic interfacial tension of FC-40 against DMEM ± 10% FBS measured using pendant drop method up to 1000 s. (B-C) Drops (10 µl on a footprint formed by 1 µl drop) of DMEM + 10% FBS under FC-40 were pre-incubated (2 or 20 h), liquid withdrawn (flow rate 100 nl/s) through a needle, and side-views collected (images from Movies S3-4). (B) DMEM + 10% FBS, 2 h pre-incubation. (i,ii) The needle easily penetrates the interface. (iii) As liquid is withdrawn, essentially no interfacial skin is visible, until (iv) nearly all liquid is removed (when vertical stress lines on the interface become visible). (C) DMEM + 10% FBS, 20 h pre-incubation. (i,ii) The needle initially fails to penetrate the strong elastic skin at the interface, deforming it. (iii, iv) After penetration and as liquid is removed, many wrinkles in the interface can be seen.

### II.5. Pinning lines stabilized by FBS can withstand the effects of surfactants

After pre-incubating drops of DMEM + 10% FBS under FC-40 at 37°C, we find that pinning lines sometimes survive when surfactants are added, and that effects depend on

surfactant concentration, drop volume, and incubation time (Figure S4). These results show that pre-incubation can allow pinning lines to withstand effects of surfactants; in general, the longer the incubation time, the more stable the pinning line. This indicates that this platform can accommodate complete cell-based assays rather than just culturing/drug treatment as was the original intention of this research.

### II.6. Using serum-pinned drops for cell-based assays

We next demonstrate that serum-pinned drops can support normal cell growth. FC-40 is freely permeable to $O_2$ and $CO_2$; consequently, cells in drops in Petri dishes filled with fluorocarbon can be grown in standard $CO_2$ incubators just like their counterparts grown conventionally[17]. In this case, an array of identical 1 μl drops of DMEM + 10% FBS each containing ~100 HEK cells were formed, and the final volume adjusted to 1 – 5 μl; cells are now grown for 4 days and imaged daily (Figure 5Ai). Contact-line pinning ensures all drops have the same footprints despite variations in volume. All drops initially had the same cell number; however, cells proliferated at different rates depending on drop volume (Figure 5Aii). Thus, cells in 5 μl drops grew like their counterparts cultured conventionally in flasks (not shown) to reach confluency by day 4. In contrast, cells in 1 μl drops initially grew as well, but growth rate declines after day 2. These results show that cells grow normally in large-volume drops, but growth rate soon declines in small-volume drops.

We next examined whether growth declined due to media exhaustion. We tested the same cells cultured in 500 nl on footprints created by 200 nl drops. We observed limited proliferation (Figure 5Bi, compare top and bottom rows); however, cells proliferate at similar rates as conventional cultures when media is renewed daily (Figure 5Bi, compare two bottom rows; Figure S5). This confirms that cells rapidly exhaust media in small drops.

Finally, we performed a proof-of-concept drug screen. The HEKs used here encode a GFP reporter gene controlled by a promoter switched on by tumour necrosis factor alpha

(TNF-α); when exposed to the cytokine, cells fluoresce green. As expected, untreated cells are non-fluorescent and TNF-α induces green fluorescence (Figure 5Bii), as expected.

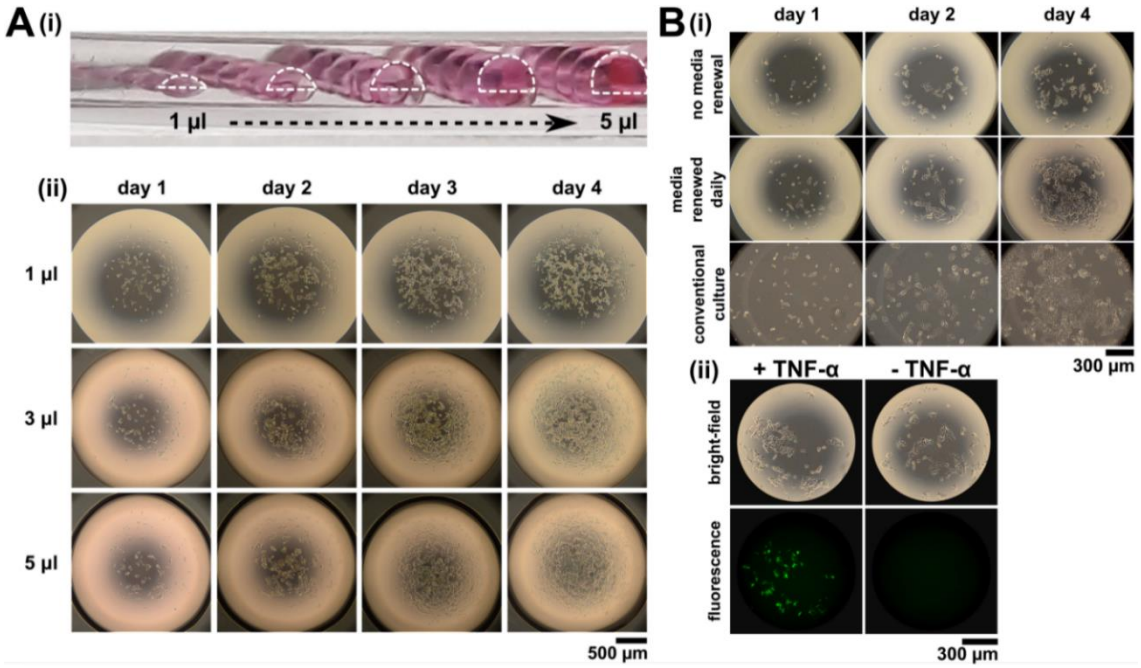


**Figure 5.** Cell-based assays in serum-pinned drops. (A) HEK cells cultured in 1-5 µl drops of DMEM + 10% FBS. (i) Side view of the rows of drops containing different volumes. All have the same footprint area created when the initial 1 µl DMEM + 10% FBS was deposited in air. The white dashed lines show the approximate outlines of the first drop on each row (reflections lie below). (ii) Phase-contrast images of cells growing in drops. All drops started with approximately the same cell number, but larger volumes yield higher cell confluencies. (B) Example cell-based assays in serum-pinned drops with sub-microliter volumes. (i) Cell proliferation. Top row: HEK cells cultured in 500 nl drops on footprints created by 200 nl DMEM + 10% FBS. Middle row: drops were prepared as in the top row, but each day 450 nl of medium was replaced with 450 nl fresh medium. (ii) Reporter cells respond normally by expressing GFP in response to TNF-α. Drops were prepared as in (Bi) but at day 2, 250 nl of medium were replaced with 250 nl DMEM + 10% FBS ± TNF-α (20 ng/ml); next, cells were grown for 20 h and bright-field and fluorescence images collected.

## III. Discussion

Pinning lines around sessile drops can be stabilized either by introducing physical or chemical heterogeneity into the substrate[42-44], or by adding particles to the liquid phase to achieve "self-pinning" [45-47]. We tested whether adding FBS or SR to drops (1 µl, 200 nl) of

standard growth medium sitting on standard tissue-culture dishes under FC-40 could self-pin drops, and found they could (Figure 1). Addition of 10% FBS increases the advancing contact angle from ~60° to at least ~120°, as the receding angle fell to <5°. Increase of contact-angle hysteresis will increase the range of working volumes that can be used with a drop without altering the footprint. We found that pinning-line stabilization is time- and temperature-dependent (Figure 2) due to adsorption of serum components at pinning lines[48].

FC-40 is denser than water, therefore buoyancy effects are inevitable and can complicate advancing contact angle measurement (Figure 3A). Therefore, we resorted to measuring the advancing contact angle by slowly pushing a stabilized drop using a needle and found a maximum contact angle of ~180°, well within the superhydrophobic range (Figure 3B). This extreme contact angle is also observed using another overlay, tetradecane, which is less dense than water (Figure S3B), and hence does not appear to be uniquely associated with fluorocarbons. Since the pinning relies on adsorption, the superhydrophobic-like behaviour is not immediately induced on drop deposition; rather, pinning increases with time and temperature as an elastic skin forms (Figure 4B,C). A previous study has shown that an elastic interfacial skin can enhance contact-line pinning[49]. Such pinning lines can even withstand the effects of surfactants (Figure S4).

As there is batch-to-batch variability in FBS components, we tested whether SR – where components are more defined – yields similar results; we found it could. However, pinning was not as effective as that given by 10% FBS (Figure 3Aii). Therefore, FBS remains our preferable stabilizing agent. Finally, we used serum-pinned micro-drops in a proof-of-concept drug screen. Cells grew and responded to a cytokine, TNF-α, as expected (Figure 5Bii). We expect that many other cell-based assays can be performed in such drops efficiently and at low cost.

## IV. Methods

### IV.1. Contact-angle measurement

Contact angles were measured using software (FTA32) and hardware provided by First Ten Angstroms. A drop of distilled water, DMEM (high glucose, Sigma), DMEM + FBS (Gibco), or DMEM + KnockOut™ SR (Gibco) was ejected using a needle (33G blunt NanoFil™ needle, World Precision Instruments) connected to a syringe pump (Harvard Ultra) through a Teflon tube. This drop was first formed on the tip of the needle (in air) before transfer to the surface of a square cut from the base of a standard Corning® tissue-culture treated dish (D × H: 60 × 15 mm) which had been placed on two stacked microscope glass slides (fixed with adhesives) – to adjust the height of the drop and avoid optical distortion from being too close to the base – inside a rectangular Petri dish (Thermo Scientific™ Nunc™ Rectangular Dishes 4-well). Rectangular dish is used instead of directly using the round Petri dish also to avoid optical distortion. The drop was then overlaid with FC-40 (3M) or tetradecane (Aldrich). Extra liquid was injected into the drop with the needle through the overlay. Images from the side of the drop were captured and drop contact angle, volume, and footprint area calculated using FTA32 software based on the length scale calibration using needle-tip diameter. Theoretical values of the contact angle are calculated assuming spherical-cap geometry[50]. Detailed methodology is available in Supplementary Methods.

### IV.2. Cell-based assays

To test cell growth in 1 μl drops (6 × 6 array), 1 μl DMEM + 10% FBS was deposited on a standard Petri dish using an isoCell printer (iotaSciences Ltd) and overlaid with FC-40. The isoCell delivers/removes specified nanoliter volumes to/from specified drops in an array, and its software was adapted for the purpose described here. The dish was now incubated in a standard $CO_2$ incubator (37°C, 15 min), 1 μl removed (programming the pump

to remove the same volume of liquid as deposited results in leaving a thin film on the hydrophilic surface) and replaced with 1 μl human embryonic kidney (HEK) cells (NF-κB/293/GFP™ Transcriptional Reporter Cell Line, #TR860A-1, System Biosciences, 100 cells/μl, prepared as in Supplementary Methods). The dish was now returned to the incubator and left for ~1 h. Media was then added to drops 1 μl at a time to create final volumes of 1-5 μl, drops re-incubated, and images of cells collected daily.

To test growth in 200 nl drops (6 x 6 array), 200 nl DMEM + 10% FBS was deposited as above, overlaid with FC-40, incubated (37°C, 1 h), and 200 nl removed and replaced with 500 nl cells (100 cells/μl). Drops were then incubated, and images of cells collected as above. Here, media were renewed daily in half the drops by removing 450 nl media and adding 450 nl fresh media.

Drug screening was demonstrated using a 6 x 6 array of 1 μl drops and daily media renewal (as above). At day 2, after media renewal, 250 nl media was removed from a drop (and from another 8 replicates in the array) and replaced by 250 nl fresh medium plus TNF-α (20 ng/ml). 9 other drops in the array received only 250 nl fresh medium. The other 18 drops were not replenished daily and were used to monitor growth without interventions. Finally, the response to TNF-α was observed using fluorescence microscopy 20 h later.

**Acknowledgements**

We thank the Medical Research Council (award MR/K010867/1 to P.R.C. and a Confidence in Concept award MC_PC_15029 to E.W. and P.R.C.), the Indonesian Endowment Fund for Education (LPDP), the 7th Framework Marie Curie Career Integration grant (contract no. 333848 to E.W.), and the University of Oxford John Fell Fund for support.

## References


(1) Garcia-Cordero, J. L.; Fan, Z. H., Sessile droplets for chemical and biological assays. *Lab Chip* **2017,** *17* (13), 2150-2166.

(2) Du, G. S.; Pan, J. Z.; Zhao, S. P.; Zhu, Y.; den Toonder, J. M.; Fang, Q., Cell-based drug combination screening with a microfluidic droplet array system. *Anal Chem* **2013,** *85* (14), 6740-7.

(3) Zhu, Y.; Zhang, Y. X.; Liu, W. W.; Ma, Y.; Fang, Q.; Yao, B., Printing 2-dimentional droplet array for single-cell reverse transcription quantitative PCR assay with a microfluidic robot. *Sci Rep* **2015,** *5*, 9551.

(4) Leung, K.; Klaus, A.; Lin, B. K.; Laks, E.; Biele, J.; Lai, D.; Bashashati, A.; Huang, Y.-F.; Aniba, R.; Moksa, M.; Steif, A.; Mes-Masson, A.-M.; Hirst, M.; Shah, S. P.; Aparicio, S.; Hansen, C. L., Robust high-performance nanoliter-volume single-cell multiple displacement amplification on planar substrates. *PNAS* **2015,** *113* (30), 8484-8489.

(5) Liberski, A. R.; Delaney, J. T., Jr.; Schubert, U. S., "One cell-one well": a new approach to inkjet printing single cell microarrays. *ACS Comb Sci* **2011,** *13* (2), 190-5.

(6) Sun, Y.; Zhou, X.; Yu, Y., A novel picoliter droplet array for parallel real-time polymerase chain reaction based on double-inkjet printing. *Lab Chip* **2014,** *14* (18), 3603-10.

(7) Ueda, E.; Geyer, F. L.; Nedashkivska, V.; Levkin, P. A., DropletMicroarray: facile formation of arrays of microdroplets and hydrogel micropads for cell screening applications. *Lab Chip* **2012,** *12* (24), 5218-24.

(8) Kuster, S. K.; Fagerer, S. R.; Verboket, P. E.; Eyer, K.; Jefimovs, K.; Zenobi, R.; Dittrich, P. S., Interfacing droplet microfluidics with matrix-assisted laser desorption/ionization mass spectrometry: label-free content analysis of single droplets. *Anal Chem* **2013,** *85* (3), 1285-9.

(9) Popova, A. A.; Schillo, S. M.; Demir, K.; Ueda, E.; Nesterov-Mueller, A.; Levkin, P. A., Droplet-Array (DA) Sandwich Chip: A Versatile Platform for High-Throughput Cell Screening Based on Superhydrophobic-Superhydrophilic Micropatterning. *Adv Mater* **2015,** *27* (35), 5217-22.

(10) Popova, A. A.; Demir, K.; Hartanto, T. G.; Schmitt, E.; Levkin, P. A., Droplet-microarray on superhydrophobic–superhydrophilic patterns for high-throughput live cell screenings. *RSC Advances* **2016,** *6* (44), 38263-38276.

(11) Wu, H.; Chen, X.; Gao, X.; Zhang, M.; Wu, J.; Wen, W., High-Throughput Generation of Durable Droplet Arrays for Single-Cell Encapsulation, Culture, and Monitoring. *Anal Chem* **2018,** *90* (7), 4303-4309.

(12) Wu, H.; Wu, L.; Zhou, X.; Liu, B.; Zheng, B., Patterning Hydrophobic Surfaces by Negative Microcontact Printing and Its Applications. *Small* **2018**, e1802128.

(13) Chen, L.; Yang, G.; Wang, S., Air-grid surface patterning provided by superhydrophobic surfaces. *Small* **2012,** *8* (7), 962-5.

(14) Extrand, C. W., Contact angles and hysteresis on surfaces with chemically heterogeneous islands. *Langmuir* **2003,** *19*, 3793-3796.

(15) Barnes, G. T.; Gentle, I. R., *Interfacial science: an introduction*. Oxford University Press Inc.: New York, United States, 2011.

(16) Berthier, E.; Young, E. W.; Beebe, D., Engineers are from PDMS-land, Biologists are from Polystyrenia. *Lab Chip* **2012,** *12* (7), 1224-37.

(17) Walsh, E. J.; Feuerborn, A.; Wheeler, J. H. R.; Tan, A. N.; Durham, W. M.; Foster, K. R.; Cook, P. R., Microfluidics with fluid walls. *Nature Communications* **2017,** *8* (816).
(18) Prastowo, A.; Feuerborn, A.; Cook, P. R.; Walsh, E. J., Biocompatibility of fluids for multiphase drops-in-drops microfluidics. *Biomed Microdevices* **2016,** *18* (114).
(19) Lowe, K. C.; Davey, M. R.; Power, J. B., Perfluorochemicals: their applications and benefits to cell culture. *Trends Biotechnol* **1998,** *16* (6), 272-277.
(20) Lowe, K. C., Perfluorochemical respiratory gas carriers: benefits to cell culture systems. *Journal of Fluorine Chemistry* **2002,** *118*, 19-26.
(21) Yao, T.; Asayama, Y., Animal-cell culture media: History, characteristics, and current issues. *Reprod Med Biol* **2017,** *16* (2), 99-117.
(22) van der Valk, J.; Bieback, K.; Buta, C.; Cochrane, B.; Dirks, W. G.; Fu, J.; Hickman, J. J.; Hohensee, C.; Kolar, R.; Liebsch, M.; Pistollato, F.; Schulz, M.; Thieme, D.; Weber, T.; Wiest, J.; Winkler, S.; Gstraunthaler, G., Fetal Bovine Serum (FBS): Past - Present - Future. *ALTEX* **2018,** *35* (1), 99-118.
(23) Stoebe, T.; Lin, Z.; Hill, R. M.; Ward, M. D.; Havis, H. T., Surfactant-enhanced spreading. *Langmuir* **1996,** *12*, 337-344.
(24) Stoebe, T.; Lin, Z.; Hill, R. M.; Ward, M. D.; Davis, H. T., Enhanced spreading of aqueous filmd containing ethoxylated alcohol surfactants on solid substrates. *Langmuir* **1997,** *13*, 7270-7275.
(25) Zhong, X.; Duan, F., Surfactant-adsorption-induced initial depinning behavior in evaporating water and nanofluid sessile droplets. *Langmuir* **2015,** *31* (19), 5291-8.
(26) Zhong, X.; Duan, F., Dewetting transition induced by surfactants in sessile droplets at the early evaporation stage. *Soft Matter* **2016,** *12* (2), 508-13.
(27) Berejnov, V. V., Protein and ionic surfactants - promoters and inhibitors of contact line pinning. *arXiv preprint* **2007,** *arXiv:0704.0434*.
(28) Berejnov, V. V., Self-pinning protein-laden drops. *J Colloid Interface Sci* **2008,** *322* (1), 246-51.
(29) Ma, X.; Xu, W.; Chen, C.; Lu, Z.; Li, J., A microfabrication-free nanoliter droplet array for nucleic acid detection combined with isothermal amplification. *Analyst* **2015,** *140* (13), 4370-3.
(30) Barthlott, W.; Neinhuis, C., Purity of the sacred lotus, or escape from contamination in biological surfaces. *Planta* **1997,** *202*, 1-8.
(31) McHale, G.; Newton, M. I., Liquid marbles: topical context within soft matter and recent progress. *Soft Matter* **2015,** *11* (13), 2530-46.
(32) Huang, X. J.; Kim, D. H.; Im, M.; Lee, J. H.; Yoon, J. B.; Choi, Y. K., "Lock-and-key" geometry effect of patterned surfaces: wettability and switching of adhesive force. *Small* **2009,** *5* (1), 90-4.
(33) Gorter, E.; Grendel, F., On the spreading of proteins. *Trans Faraday Soc.* **1926,** *1926* (22), 477-483.
(34) Wang, S.; Jiang, L., Definition of Superhydrophobic States. *Advanced Materials* **2007,** *19* (21), 3423-3424.
(35) Beverung, C. J.; Radke, C. J.; Blanch, H. W., Protein adsorption at the oil/water interface: characterization of adsorption kinetics by dynamic interfacial tension measurements. *Biophysical Chemistry* **1999,** *81*, 59-80.
(36) Hughes, A. H.; F.R.S, E. K. R., On protein monolayers. *Proceedings of the Royal Society A* **1932,** *137* (831), 62-77.
(37) Campbell, R. A.; Ang, J. C.; Sebastiani, F.; Tummino, A.; White, J. W., Spread Films of Human Serum Albumin at the Air-Water Interface: Optimization, Morphology, and Durability. *Langmuir* **2015,** *31* (50), 13535-42.

(38) Hoffmann, H.; Reger, M., Emulsions with unique properties from proteins as emulsifiers. *Adv Colloid Interface Sci* **2014,** *205*, 94-104.
(39) McClements, D. J., Protein-stabilized emulsions. *Current Opinion in Colloid & Interface Science* **2004,** *9* (5), 305-313.
(40) Alexandrov, N. A.; Marinova, K. G.; Gurkov, T. D.; Danov, K. D.; Kralchevsky, P. A.; Stoyanov, S. D.; Blijdenstein, T. B.; Arnaudov, L. N.; Pelan, E. G.; Lips, A., Interfacial layers from the protein HFBII hydrophobin: dynamic surface tension, dilatational elasticity and relaxation times. *J Colloid Interface Sci* **2012,** *376* (1), 296-306.
(41) Knoche, S.; Vella, D.; Aumaitre, E.; Degen, P.; Rehage, H.; Cicuta, P.; Kierfeld, J., Elastometry of deflated capsules: elastic moduli from shape and wrinkle analysis. *Langmuir* **2013,** *29* (40), 12463-71.
(42) Forsberg, P. S.; Priest, C.; Brinkmann, M.; Sedev, R.; Ralston, J., Contact line pinning on microstructured surfaces for liquids in the Wenzel state. *Langmuir* **2010,** *26* (2), 860-5.
(43) Kalinin, Y. V.; Berejnov, V.; Thorne, R. E., Contact line pinning by microfabricated patterns: effects of microscale topography. *Langmuir* **2009,** *25* (9), 5391-7.
(44) Eral, H. B.; 't Mannetje, D. J. C. M.; Oh, J. M., Contact angle hysteresis: a review of fundamentals and applications. *Colloid and Polymer Science* **2012,** *291* (2), 247-260.
(45) Sangani, A. S.; Lu, C.; Su, K.; Schwarz, J. A., Capillary force on particles near a drop edge resting on a substrate and a criterion for contact line pinning. *Phys Rev E Stat Nonlin Soft Matter Phys* **2009,** *80* (1 Pt 1), 011603.
(46) Shmuylovich, L.; Shen, A. Q.; Stone, H. A., Surface morphology of drying latex films: multiple ring formation. *Langmuir* **2002,** *18*, 3441-3445.
(47) Weon, B. M.; Je, J. H., Self-pinning by colloids confined at a contact line. *Phys Rev Lett* **2013,** *110* (2), 028303.
(48) Rabe, M.; Verdes, D.; Seeger, S., Understanding protein adsorption phenomena at solid surfaces. *Adv Colloid Interface Sci* **2011,** *162* (1-2), 87-106.
(49) Leiske, D. L.; Monteux, C.; Senchyna, M.; Ketelson, H. A.; Fuller, G. G., Influence of surface rheology on dynamic wetting of droplets coated with insoluble surfactants. *Soft Matter* **2011,** *7* (17), 7747.
(50) Berthier, E.; Beebe, D. J., Flow rate analysis of a surface tension driven passive micropump. *Lab Chip* **2007,** *7* (11), 1475-8.

**Associated content**

**Supplementary information.** The following files are available as supplementary information of this manuscript:

Supplementary methods (PDF); images of sessile drops of different fluids on a Petri dish (Figure S1); graphs of pinning-line stability given by 1% FBS (Figure S2); graphs showing advancing contact angle measurements and superhydrophobic behaviour of drops under tetradecane (Figure S3); graphs showing that pinning lines made with DMEM + 10% FBS

can withstand addition of surfactants (Figure S4); graphs showing effects of initial medium volume and refeeding on the growth rate of HEKs cultured in drops with similar footprints (Figure S5); detailed information on how Movies S1-S4 were prepared.

Supplementary movies (with supplementary PDFs).

Movie S1: Super-hydrophobic behaviour of a DMEM + 10% FBS drop overlaid with FC-40 (AVI).

Movie S2: Super-hydrophobic behaviour of a DMEM + 10% FBS drop overlaid with tetradecane (AVI).

Movie S3: An elastic skin at the interface between a drop of DMEM + 10% and FC-40 (2 h pre-incubation) (AVI).

Movie S4: An elastic skin at the interface between a drop of DMEM + 10% and FC-40 (20 h pre-incubation) (AVI).

**Author information**

**Corresponding Author**

*email: edmond.walsh@eng.ox.ac.uk; phone: +44 (0) 1865 288731

**Author Contributions**

A.P., P.R.C. and E.J.W. designed experiments, analyzed data and wrote the manuscript. A.P. collected data and produced figures and movies.

**Notes**

The authors declare no competing interest.

## SUPPLEMENTARY METHODS

**Theoretical contact angle values.** To validate experimental data and determine when gravity influences drop shape, a comparison with the analytical solution for a spherical cap

is made. In the absence of gravity, the relationship between the measured quantities drop volume ($V$), contact angle ($\theta$) and footprint radius ($a$) is:

$$V = \frac{\pi(2 - 3\cos\theta + \cos^3\theta)}{3}\frac{a^3}{\sin^3\theta}$$

**Interfacial tension measurement.** Interfacial tension between two immiscible fluids was measured using pendant drop method[1, 2]. A small drop (~500 nl) was formed at the tip of a needle (outer diameter 0.3 mm), connected to a Teflon tube and syringe pump (Harvard Ultra) for volume and flow rate control. The drop was immersed in the second fluid which has been loaded in a transparent polystyrene cuvette. The interfacial tension was calculated using software and hardware provided by First Ten Angstroms, which requires a length scale to be defined (i.e. needle tip as measured with a digital caliper) and fluid density as provided by the manufacturer. Measurements were taken at room temperature.

**Capillarity length calculation.** Capillarity length describes a characteristic length beyond which the effect of gravity becomes dominant[3]. It is calculated from the interfacial tension ($\gamma$), liquid density ($\rho$) and gravity ($g$), as[3]:

$$l = \sqrt{\gamma/\rho g}$$

**Adding fluids to pre-deposited sessile drops.** Drops (1 µl or 200 nl) of Dulbecco's Modified Eagle's Medium (DMEM, high glucose, Sigma) were deposited on a sample of a Petri dish (Corning® tissue-culture treated dish, D × H 60 mm × 15 mm) cut from the base of the dish which had been placed on two stacked microscope glass slides (fixed with adhesives) inside a rectangular Petri dish (Thermo Scientific™ Nunc™ Rectangular Dishes 4-well). Drops were then overlaid with FC-40 (3M). For tests with no-serum drops, drops were used directly. For tests with serum-containing drops, liquid in the drop was removed (either 1 µl or 200 nl) to leave just the wetted area of the footprint, then replaced by an equal volume (either 1 µl or 200 nl) of DMEM + 10% fetal bovine serum (FBS, Gibco) or KnockOut™ serum replacement (SR, Gibco), and finally incubated (30 min, 37°C). To

monitor effects of adding more DMEM ± 10% FBS or SR, medium was injected (flow rate 20-50 nl/s) into drops in 50 – 500 nl increments (~2 min between increments) when images (side views) of drops were captured and the volume, contact angle, and base area of drops calculated. The drop was in an equilibrium state for all images.

To test effects of flow rate and incubation time, 1 µl drops of DMEM + 10% or 1% FBS were deposited on a substrate prepared as above, and overlaid with FC40. The dish was then incubated at room temperature for ~5 min, or 37°C for 30 min (for flow-rate test), or at room temperature or 37°C for 5, 30 and 60 min (for incubation-time test). The same fluid (media + serum) was then injected continuously into a drop (at 10 – 1000 nl/s) while being imaged as above. Tests were done in at least triplicates.

**Measurement of advancing contact angles and footprint diameters.** The advancing contact angle was measured on a drop with a footprint created by depositing 100 nl DMEM + 10% FBS in air prior to overlaying FC-40 or tetradecane (Aldrich). The dish was incubated at 37°C for ~1 h to stabilize the pinning line, 400 nl DMEM + 10% FBS added to the drop, the dish incubated (37°C, ~20 h), more DMEM + 10% FBS injected continuously into the drop (at 10 nl/s) up to the final volume of 25 µl, images (side views) collected, and angles and lengths measured.

**Serum adsorption to the water/FC-40 interface.** To demonstrate the formation of an interfacial skin by adsorbed serum at the interface with FC-40, 1 µl drops of DMEM + 10% FBS were deposited on a Petri dish surface as above, overlaid with FC-40, and incubated for a minimum of 1 h at 37°C to stabilize the pinning line. 9 µl of DMEM + 10% FBS was then injected to the drop (at 100 nl/s). Drops were then incubated (37°C, 2 or 20 h), liquid inside drops withdrawn (at 100 nl/s), and images recorded.

**Effects of surfactants.** RNA lysis buffer (Zymo Research), 1% (w/w) Triton™ X-100 (Sigma-Aldrich) in Dulbecco's Phosphate Buffered Saline (PBS, Sigma) and 1% (w/w)

Tween® 20 (Sigma-Aldrich) in PBS were used as surfactants. Drops (1 µl) of DMEM + 10% FBS were deposited on a surface cut from a Petri, incubated (37°C, 30 min to 16 h), 1 µl withdrawn at 1000 nl/s, surfactant (1 µl or 500 nl) injected into the residual liquid at 100 nl/s, drops incubated (room temperature, 1 h), and integrity of pinning lines scored.

**Cell preparation.** Human embryonic kidney (HEK) cells (NF-κB/293/GFP™ Transcriptional Reporter Cell Line, #TR860A-1, System Biosciences) were cultured conventionally in DMEM supplemented with 10% (v/v) FBS (Gibco) and 1% antibiotics (penicillin and streptomycin). This cell line, derived by the manufacturer, encodes a green fluorescence protein (GFP) reporter gene under the control of a promoter that is switched on by tumour necrosis factor alpha (TNF-α). Cells were prepared using standard procedures; they were washed with 5 ml PBS, incubated for 2-3 minutes with 1 ml cell-dissociation reagent (Gibco TrypLE Express Enzyme), cell clumps dissociated by pipetting the cell solution plus 9 ml media, cell concentrations determined using trypan blue (Trypan Blue Solution, 0.4%, Sigma) and a haemocytometer, and adjusted to achieve the desired concentration.

## SUPPLEMENTARY FIGURES

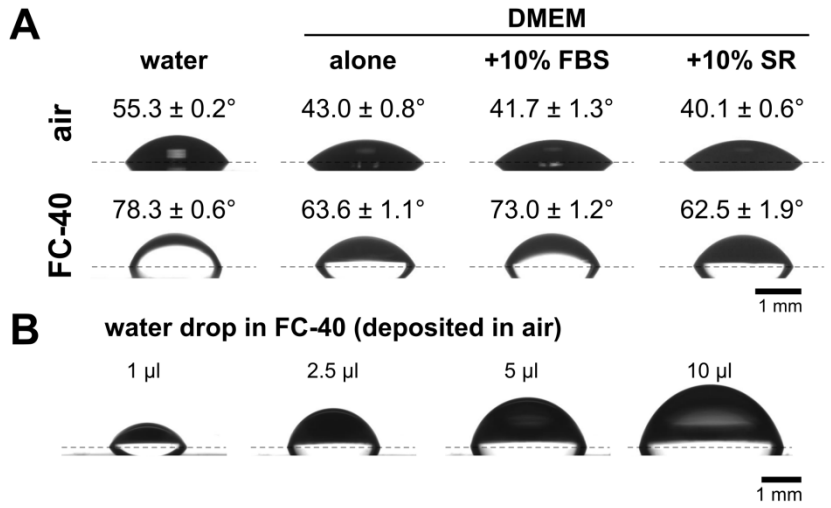


**Figure S1.** Images of sessile drops of different fluids on the surface of a standard Petri dish used for tissue culture. Dashed lines provide visual guides to the base line of each drop; below these lines are reflections. (A) Equilibrium initial contact angles of drops containing different liquids. A drop of each liquid (1 µl) was formed at the tip of a needle, transferred to a dish, and overlaid ± FC-40 ('air', 'FC-40'); images were collected, and contact angles measured (values are averages ± SD; *n* = 3). (B) The changing shape of a water drop as water is added. A water drop (1 µl) was deposited in air as in (A), and overlaid with FC-40; the volume was now gradually increased to 10 µl by injection. Images show the footprint area increases (left to right); the maximum/advancing contact angle was ~80°.

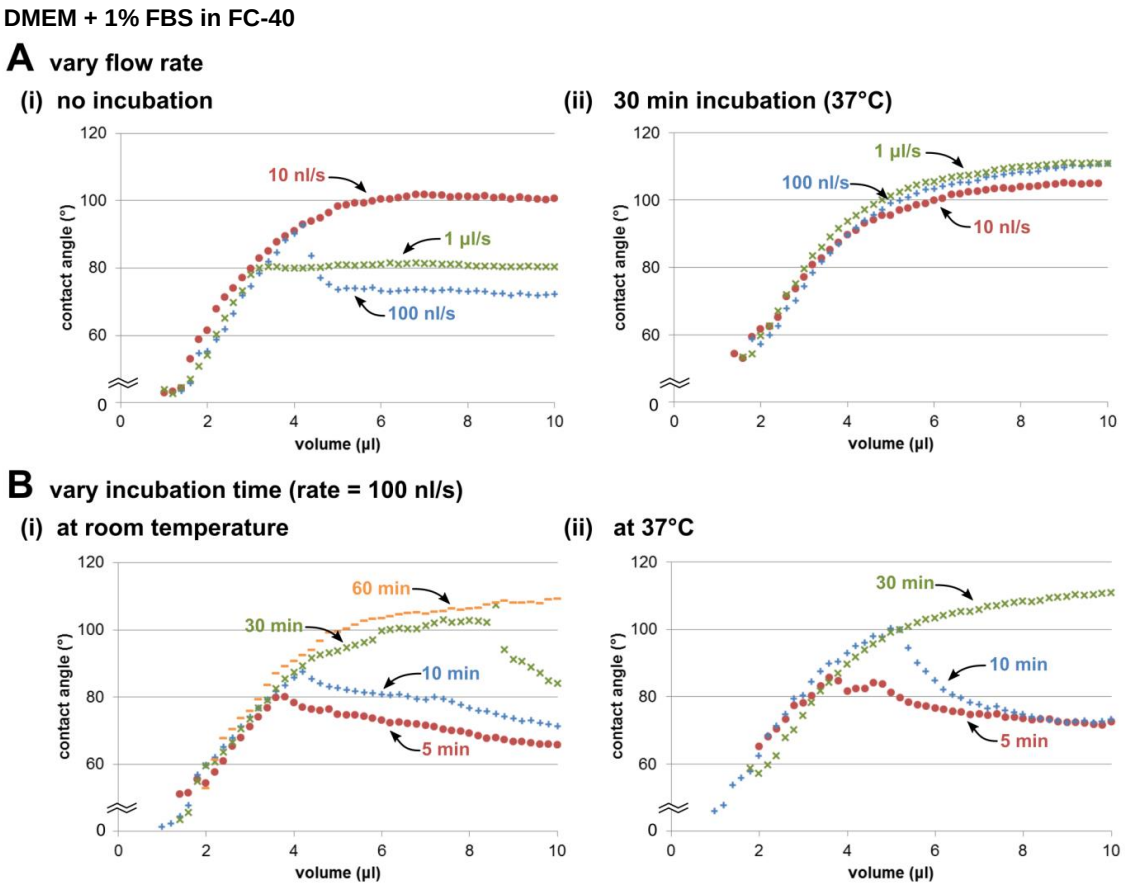


**Figure S2.** Reducing the concentration of FBS from 10% to 1% reduces pinning-line stability. Tests are as in Figure 3 but using 1% FBS instead of 10% FBS. Drops (1 µl; DMEM + 1% FBS) were deposited, incubated for times and temperatures indicated, imaged as more medium was injected continuously into them, and contact angles determined. (A) Effects of flow rate reflect results seen with 10% FBS. (i) Injection immediately after deposition. With 10 nl/s, the contact angle increases progressively (pinning lines remain unchanged, so drop volume increases). With 100 nl/s and 1 µl/s, pinning lines soon break (footprints increase in area), and contact angles remain roughly constant. (ii) Drops were pre-incubated (37°C; 30 min) prior to injection; this stabilizes pinning lines at all flow rates (so contact angles increase). (B) Effect of incubation time and temperature on pinning (injection rate 100 nl/s). (i) Drops are pre-incubated at room temperature for 5-60 min; longer incubation times yield more stable pinning lines. With 5 min, lines break when the drop contains ~2 µl; thereafter, the contact angle remains constant as the footprint progressively increases. With 10 min, lines break after ~4 µl; thereafter, the contact angle declines. With 30 min, lines break after ~8 µl. Finally, with 60 min, lines remain intact beyond 9 µl. (ii) Drops were pre-incubated (37°C; 5-60 min); the higher temperature stabilizes pinning lines. Compared to 10% FBS, a longer incubation time is required to stabilize pinning lines.

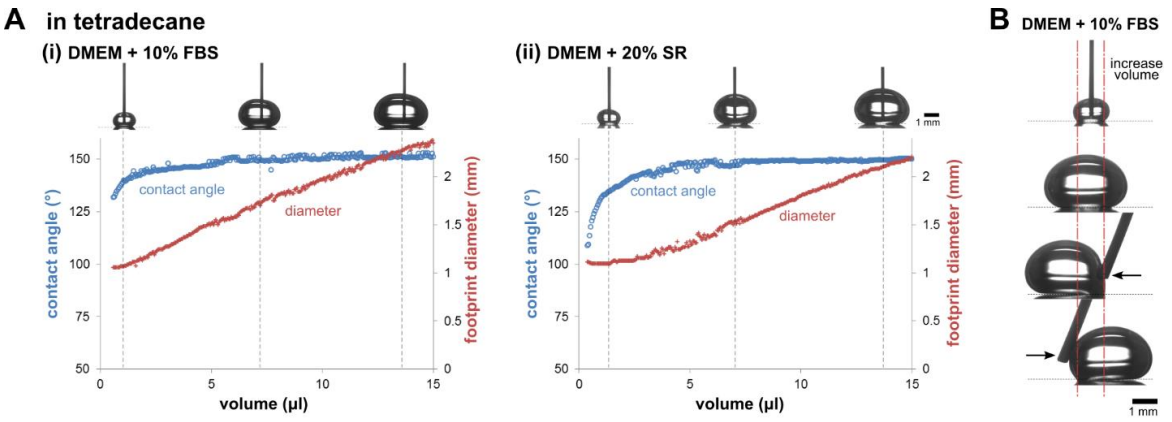


**Figure S3.** Advancing contact angles at serum-stabilized pinning lines and superhydrophobic effects under tetradecane. Drops (100 nl) containing DMEM + 10% FBS or 20% SR were deposited on a dish, overlaid with tetradecane (density less than medium), incubated (1 h, 37°C), injected with 400 nl of the same fluid, and re-incubated (20 h, 37°C). This results in a stable pinning line (diameter ~1.1 mm). (A) More medium is now injected at 10 nl/s. Images of drops are shown above representative points in the graph. With both both (i) DMEM + 10% FBS and (ii) DMEM + 20% SR, as medium is added, the apparent contact angle increases to a maximum of ~150° as footprint diameter gradually increases. (B) Superhydrophobic behaviour (images from Movie S2). 1st image: The drop with inserted dispensing tube. 2nd image: More medium is added to give a final volume of 15 µl, and the tube withdrawn; as medium is denser than tetradecane, the drop is flattened with an apparent contact angle of ~150°. 3rd and 4th images: When the drop is pushed using a needle, it is clear the original footprint/pinning line is retained, and the actual contact angle is ~180°; note the needle does not stick to the interface (unlike under FC-40).

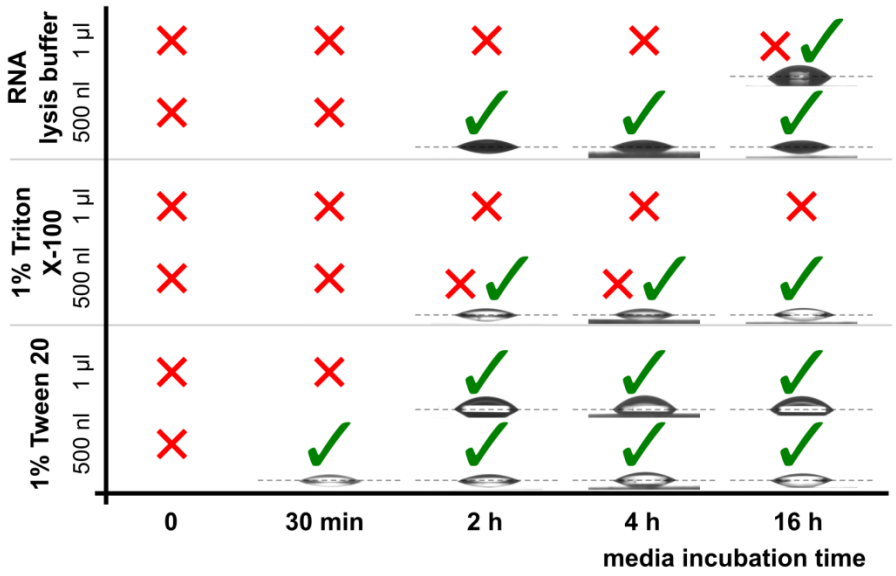


**Figure S4.** Pinning lines made with DMEM + 10% FBS can withstand the effects of strong surfactants. Drops (1 µl) of DMEM +10% FBS were deposited on a dish, overlaid with FC-40, incubated (0-16 h at 37°C), various detergents added (500 nl or 1 µl), and imaged. The experiment was repeated three times, with three drops. Crosses: In all replicates, detergent addition immediately breaks pinning lines and drops spread throughout the dish (no image shown). Ticks: in all replicates, pinning lines persist (images shown). Crosses and ticks: in some cases pinning lines persist (images shown) but in others they do not (so not shown).

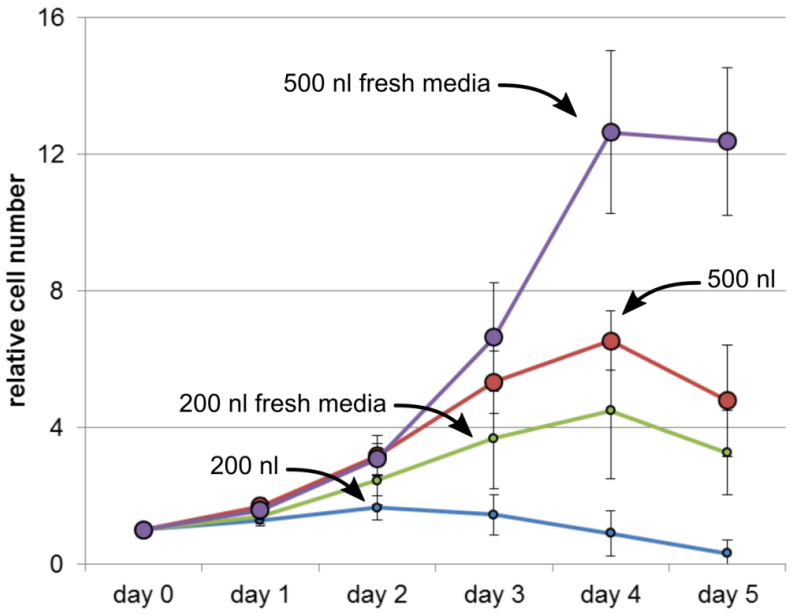


**Figure S5.** Effects of initial medium volume and refeeding on the growth rate of HEKs cultured in drops with similar footprints. 36 drops (200 nl DMEM + 10% FBS) each containing 26 ± 7 cells were deposited on a dish and incubated in a $CO_2$ incubator for 4 h to allow cells to attach. Drops were divided into 4 groups, each drop was imaged daily, and cell number per drop counted and expressed relative to the original cell number (error bars are the standard deviation; n = 4). Group 1 ('200nl'): No additional medium added on day 0, and cells not fed thereafter. Cells grow poorly in the small volume, and many die. Group 2 ('200 nl fresh media'): No additional medium added on day 0, but cells are fed daily on days 1-4 by removing 150 nl and replacing it with 150 nl fresh medium. Cells grow better, but numbers peak on day 4 as medium becomes exhausted. Group 3 ('500 nl'): 300 nl additional medium added on day 0, but cells not fed thereafter. Cells grow better than those in Groups 1 and 2, as more medium is initially present. Group 4 ('500 nl fresh media'). 300 nl additional medium was added on day 0, and cells fed daily on days 1-4 by removing 450 nl and replacing it with 450 nl fresh medium. After an initial lag, cells double every 24 h, but after day 4 there is insufficient medium to support growth of such numbers.

## SUPPLEMENTARY MOVIES

**Movie S1.** Super-hydrophobic behaviour of a DMEM + 10% FBS drop overlaid with FC-40.

A 100 nl drop (footprint diameter 1.1 mm) of DMEM + 10% FBS was deposited, overlaid with FC-40 (which is denser than the medium), 1.9 µl more medium added, and the drop incubated for 20 h at 37°C. During the movie (which runs in real time), the drop is pushed manually using a needle so the interface almost touches the substrate; this demonstrates that the contact angle can temporarily reach ~180° without breaking the pinning line.

**Movie S2.** Super-hydrophobic behaviour of a DMEM + 10% FBS drop overlaid with tetradecane.

A 100 nl drop (footprint diameter 1.1 mm) of DMEM + 10% FBS was deposited, overlaid with tetradecane (which is less dense than the medium), 400 nl more medium added, the drop incubated for 20 h at 37°C, and extra medium injected to obtain a final volume of 15 µl. During the movie (which runs in real time), the drop is pushed manually using a needle to show that the drop retains the original pinning line; this demonstrates that the actual contact angle is ~180°.

**Movie S3.** An elastic skin at the interface between a drop of DMEM + 10% and FC-40 (2 h pre-incubation).

A 1 µl drop of DMEM + 10% FBS drop was deposited, overlaid with FC-40, incubated for 1 h, 9 µl more medium added, and incubated for 2 h. During the movie (which runs in real time), a needle was first inserted into the drop and then used to withdraw liquid at 100 nl/s. Here, the needle penetrates the interface easily, and the interface wrinkles little when liquid is withdrawn (indicating an insubstantial interfacial skin).

**Movie S4.** An elastic skin at the interface between a drop of DMEM + 10% and FC-40 (20 h pre-incubation).

A 1 µl drop of DMEM + 10% FBS drop was deposited, overlaid with FC-40, incubated for 1 h, 9 µl more medium added, and incubated for 20 h. During the movie (which runs in real time), a needle was first inserted into the drop and then liquid was withdrawn at 100 nl/s. Here, the needle does not easily penetrate the interface, indicating formation of a strong interfacial skin. This skin is also clearly visible as the residue left after withdrawing most liquid.

## REFERENCES


(1) Drelich, J.; Fang, C.; White, C. L., Measurement of interfacial tension in fluid-fluid systems. *Encyclopedia of surface and colloid science* **2002,** *3*, 3158-3163.

(2) Yakhshi-Tafti, E.; Kumar, R.; Cho, H. J., Measurement of Surface Interfacial Tension as a Function of Temperature Using Pendant Drop Images. *International Journal of Optomechatronics* **2011,** *5* (4), 393-403.

(3) Gennes, P.-G. d.; Brochard-Wyart, F.; Quéré, D., *Capillarity and wetting phenomena: drops, bubbles, pearls, waves*. Springer Science+Business Media, Inc.: USA, 2010.

## Statement of Authorship

| | | |
|---|---|---|
| Title of Paper | Contact-line pinning and superhydrophobic behavior of sessile drops induced by fetal bovine serum and serum-free replacement | |
| Publication Status | ❑ Published<br>❑ Accepted for Publication | ☑ Submitted for Publication<br>❑ Unpublished and unsubmitted work written in a manuscript style |
| Publication Details | Submitted to *Analytical Chemistry* on 15 October 2018 | |

### Student Confirmation

| | | | |
|---|---|---|---|
| Student Name: | Aishah Prastowo | | |
| Contribution to the Paper | Collected and interpreted data, produced figures, wrote the manuscript | | |
| Signature |  | Date | 8/11/2018 |

### Supervisor Confirmation

By signing the Statement of Authorship, you are certifying that the candidate made a substantial contribution to the publication, and that the description described above is accurate.

| | | |
|---|---|---|
| Supervisor name and title:<br>Edmond Walsh - Associate Professor of Engineering Science | | |
| Supervisor comments | | |
| Signature 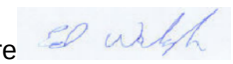 | Date | 23/11/18 |

# Paper 4: Biocompatibility of sessile drops as chambers for cell culture measured by HEK cells adhesion

**Abstract** – Sessile drop arrays (overlaid with an immiscible liquid to prevent evaporation) on a standard tissue-culture Petri dish have been employed as a platform to perform bio-assays in small volumes (microliters or less). To apply this approach for assays involving cell culture, it is essential to ensure that this system is biocompatible for assays involving cell culture; however, we observed that human embryonic kidney (HEK) cells do not attach and proliferate well when cultured in drops with high surface-to-volume ratio. Here, we investigate the effect of serum adsorption to solid/liquid and liquid/liquid interfaces on cell adhesion. We found that increasing the serum concentration in the drop or pre-exposing the drop footprint with medium plus serum could improve cell adhesion.

## II. Introduction

Arrays of sessile drops (often covered with an immiscible liquid to prevent evaporation) on a planar surface have been used to perform bio-assays in small volumes[1-6]. This method is expected to provide an efficient alternative to perform assays including those with cell culture. However, one of the challenges is to ensure that an adequate amount of nutrients is being delivered to the cells as molecules are not transported in the same manner as in conventional cultures[7-9].

In this study, we assess the biocompatibility of sessile drops overlaid with an immiscible liquid for cell-based assays, specifically the adherent human embryonic kidney (HEK) cells. Measuring biocompatibility with adherent cells is arguably more straightforward than suspension cells: it can be done by observing the morphological change, and the cell number can be easily counted under the microscope as they grow as 2D

monolayer. We found that FC-40 is a biocompatible overlay, as previously suggested[10]; however, we observed that HEK cells in sessile drops did not attach and proliferate to the surface as well as in conventional culture. We hypothesised that this is related to the serum adsorption to the interfaces[11-14]. We observed that cell adhesion in drops can be improved by increasing serum concentration in the medium, suggesting that standard serum concentration used in macro-scale culture is not adequate to promote cell adhesion and growth in smaller drops.

We then study the effects of serum adsorption to the interfaces by pre-incubating drops with serum at different time periods. The results show that pre-exposing drop footprint with serum-containing medium can improve cell adhesion, especially during the initial contact of cells with surface of the Petri dish. We found that adsorption of serum components to the solid surface happens over incubation time, therefore saturating the drop footprint with serum prior to seeding cells could possibly be beneficial for cell culture.

## III. Experimental methods

### III.1. Cell culture and preparation

Suspension cells: Jurkat (NF-κB/Jurkat/GFP™ Transcriptional Reporter Cell Line, #TR850A-1) were cultured in flasks in RPMI-1640 (Sigma) media supplemented with 10% Fetal Bovine Serum (FBS, Gibco). Before using them for experiments, 5 ml cell solution was centrifuged at 500 g for 5 m, and the supernatant was discarded. The cell pellet was then diluted to get 500 cells per µl.

Adherent cells: HEK (NF-κB/293/GFP™ Transcriptional Reporter Cell Line, #TR860A-1) were cultured in flasks in DMEM (Sigma) supplemented with 10% FBS. The cells were sub-cultured every 2-3 days by dissociating them with Gibco TrypLE Express Enzyme and then splitting them in 1:10 ratio. For experiments, first cells were washed with

5 ml PBS and then incubated for 2-3 minutes with 1 ml trypsin. The cell clumps were then dissociated by pipetting the cell solution plus 9 ml media. Cell concentration was then adjusted for experiments.

### III.2. Biocompatibility measurement of the overlaying liquids

The following liquids were screened for their bicompatibilities as the overlays: FC-40, HFE-7500, silicone oil AR 20, 5-cSt silicone oil, hexadecane, tetradecane, dodecane, mineral oil and olive oil (Aldrich). 2 µl drops containing HEK cells or Jurkat cells were deposited on a surface of a standard Corning® tissue-culture treated dish (D × H 60 mm × 15 mm) or 6-well plate using a micro-pipette, then overlaid with one type of liquid per dish/well. The dishes/plates were then incubated at 37°C, 5% $CO_2$. The morphology of HEK cells was observed under a microscope after 24 h incubation. For measuring Jurkat cell viability, first the overlaying liquid was taken out, leaving the sessile drops on the bottom of the plate or dish. Ten drops from the same overlaying liquid were taken out using a pipette and mixed as one sample in a 1.5 ml Eppendorf tube. In the tube the drops merged and were separated from the residual overlaying liquid. The sample was then mixed with an equal volume of trypan blue and the cell viability was determined using a haemocytometer.

### III.3. Depositing drops

Drops were deposited using a Teflon tube connected to a syringe pump controlling liquid injection and withdrawal. The movement was controlled using a programmed 3D traverse system (Stepcraft), or a printer (iotaSciences Ltd). The syringe and tube were pre-filled with 70% ethanol. A small air-gap separates ethanol and the sample, and the liquid was loaded into the tube by withdrawing a desired volume of sample from a microwell-plate. The tube moved to the pre-determined locations on the surface of a Petri dish before sample was ejected out to create a drop or drop arrays. Drops were overlaid with FC-40 (3M) prior to incubation to limit evaporation.

To test the effect of serum concentration on cell adhesion, 200 nl drops of DMEM + 10% or 30% FBS containing ~160 cells were deposited on a Petri dish, overlaid with FC-40 and then incubated at 37°C. Images were captured after 24 h incubation.

### III.4. Calculation of drop surface-to-volume ratio

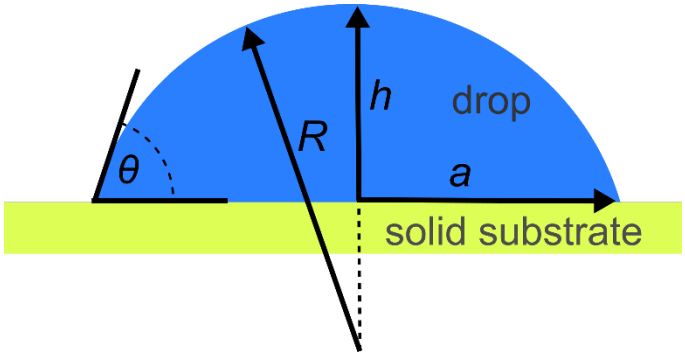


Figure 1 Illustration of a sessile drop on a solid substrate. R, θ, a and h denote drop geometrical dimensions for sphere/curvature radius, contact angle, base radius, and height, respectively.

The shape of a drop resting on a surface – neglecting the gravity effect – can be assumed as the cap of a sphere (Figure 1). As a spherical cap, the relationship of the drop's volume and surface area can be obtained from trigonometric in terms of $\theta$, drop height ($h$), base radius ($a$) and the effective sphere radius (radius of curvature, $R$)[15].

$$R = \frac{h^2 + a^2}{2h} \tag{1}$$

$$h = (1 - \cos\theta)R \tag{2}$$

$$a = R\sin\theta \tag{3}$$

The volume of a spherical cap is[15, 16]

$$V = \frac{\pi}{6}h(3a^2 + h^2) \tag{4}$$

and can be expressed in terms of contact angle as[15]

$$V = \frac{\pi(2 - 3\cos\theta + \cos^3\theta)}{3}\frac{a^3}{\sin^3\theta} \tag{5}$$

Equation (5) could also be written in the following form for $a$,

$$a = \left(\frac{3\sin^3\theta}{\pi(2 - 3\cos\theta + \cos^3\theta)}V\right)^{\frac{1}{3}} \tag{6}$$

The base area of the drop (solid/liquid interface) is simply an area of a circle with radius *a*,

$$A_{base} = \pi a^2 \tag{7}$$

Combining Equation (6) and (7) results in

$$A_{base} = \pi\left(\frac{3\sin^3\theta}{\pi(2 - 3\cos\theta + \cos^3\theta)}V\right)^{\frac{2}{3}} \tag{8}$$

$$A_{base} = f(\theta)\, V^{\frac{2}{3}} \tag{9}$$

While the cap surface area (liquid/liquid interface) of the drop is

$$A_{cap} = \pi(a^2 + h^2) \tag{10}$$

$$= \pi a^2\left(1 + \frac{(1 - \cos\theta)^2}{\sin^2\theta}\right)$$

$$= A_{base}\left(1 + \frac{(1 - \cos\theta)^2}{\sin^2\theta}\right)$$

Therefore, it can also be expressed as

$$A_{cap} = g(\theta)\, V^{\frac{2}{3}} \tag{11}$$

The surface (base)-to-volume ratio of the drop is then

$$\frac{A_{base}}{V} = \frac{f(\theta)\, V^{\frac{2}{3}}}{V} = f(\theta)V^{-\frac{1}{3}} \tag{12}$$

$$\frac{A_{base}}{V} \propto V^{-\frac{1}{3}} \tag{13}$$

And the surface (cap)-to-volume ratio of the drop is

$$\frac{A_{cap}}{V} = \frac{g(\theta)\, V^{\frac{2}{3}}}{V} = g(\theta)V^{-\frac{1}{3}} \tag{14}$$

$$\frac{A_{cap}}{V} \propto V^{-\frac{1}{3}} \tag{15}$$

with the functions of the contact angle as the following

$$f(\theta) = \pi^{\frac{1}{3}} \left( \frac{3 \sin^3\theta}{2 - 3\cos\theta + \cos^3\theta} \right)^{\frac{2}{3}} \quad (16)$$

$$g(\theta) = f(\theta) \left( 1 + \frac{(1 - \cos\theta)^2}{\sin^2\theta} \right) \quad (17)$$

From Equation (13) and (15) we could see that the drop surface-to-volume ratio, both when considering the cap surface area and the base area, is proportional to $V^{-1/3}$. These equations are used to plot surface-to-volume ratio *vs* volume in Figure 4.

### III.5. Varying drop surface-to-volume ratio

To test cell adhesion in drops with various surface-to-volume ratio, we deposited 200, 500 and 1000 nl drops of DMEM on a Petri dish, overlaid them with FC-40, removed medium, deposited 200 nl DMEM + 10% FBS containing cells in on the footprint, incubated at 37°C for~3 h (to allow cells to attach and drops to stabilize), then appropriate amount of medium was added to get final volumes of 200, 500 and 1000 nl in each variation of footprint area. The concentration of the cell sample was adjusted to get 100 cells/drop or 72 cells/mm$^2$ footprint area. Images were captured after 24 h incubation.

### III.6. Pre-exposing drop footprint with serum

To test the effect of serum adsorption to cell adhesion, 200 nl drops of DMEM + 10% FBS were deposited, overlaid with FC-40, then appropriate amount of medium was added to get final volumes of 200, 500 and 1000 nl. The drops were then incubated at 37°C for 2 h or 2 d before all liquid removed, and 200 nl of DMEM + 10% FBS containing 100 HEK cells were deposited into each footprint. As a control, cells are also cultured conventionally on a Petri dish with a total volume of 4 ml and in drops as above with footprint created by DMEM without serum. Images were captured after 1, 4 and 24 h incubation.

## IV. Results and discussion

### IV.1. Biocompatibility of overlaying liquids

Mineral oil, silicone oil and fluorocarbon have been used previously to prevent evaporation of sessile drops for cell culture[1, 17, 18]. To identify the biocompatible ones, nine liquids were screened to overlay 2 µl sessile drops containing HEK cells. As in conventional culture, cells are expected to attach to the surface within the first few hours and after 24 h most of them should have flattened into their intact morphology. Visual observation with microscopy reveals that after one day of incubation, cells do not attach well under some liquids. Cells appear flattened (an indication of adhesion) when the drops were overlaid with FC-40, HFE-7500, silicone oil AR 20 (‘AR 20’), hexadecane and 5-cSt silicone oil (Figure 2). Meanwhile, cells remain round when overlaid with mineral oil, tetradecane, dodecane and olive oil (Figure 2), so these overlays are considered toxic.

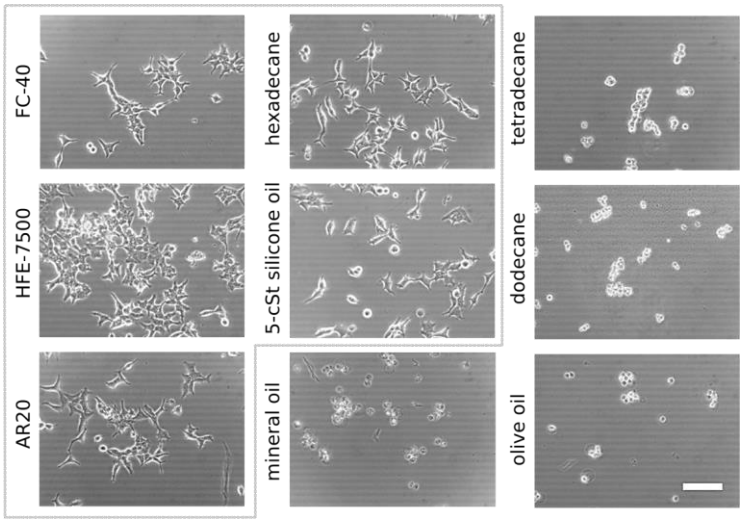


Figure 2 HEK cells morphology after 24 h incubation in 2 µl sessile drops overlaid with liquids of the corresponding labels. Intact shown exhibited by the cells covered with FC-40, HFE-7500, AR20 silicone oil, hexadecane and 5-cSt silicone oil. Cells remained in their round morphology (and even showed signs of cell death) when overlaid with mineral oil, tetradecane, dodecane and olive oil. The pictures captured a small area within the drop base area; hence the local cell density may vary across different images. Scale bar = 100 µm

To confirm these results, we measured biocompatibility using Jurkat cells. Due to their suspension nature, these cells stay round in culture; therefore, it is more difficult to visually observe the toxic effects of the liquids. However, these cells can easily be recovered from the drops without detaching them from the surface with dissociation reagents. This way, cell viability can be measured by counting the number of live and dead cells from the cell sample. Cell viabilities after 24 h and 48 h incubation are shown in Table 1. These results agree with the HEK cells results – four overlaying liquids preventing adhesion are also toxic to Jurkat cells, whilst the rest of the liquids gave high viability after 24 h (all >90% except for HFE-7500 which was >80%). After 48 h, only FC-40 gives 90% viability, while with other liquids, the viability decreased. Therefore, we concluded that FC-40 is the most biocompatible overlay and used this liquid to overlay drops in the subsequent experiments.

Table 1 Jurkat cell viability in 2 µl sessile drops overlaid with different liquids. Viability number is presented as the number of counted live cells divided by the total counted cells. When all cells were found dead at 24 h, viability measurements for the corresponding experimental condition were not performed for the further time point.

| Overlay | 24 hours (% viability) | 48 hours (% viability) |
|---|---|---|
| FC 40 | 95 | 90 |
| HFE 7500 | 83 | 70 |
| Silicone oil AR 20 | 99 | 71 |
| 5-cSt silicone oil | 91 | 70 |
| Mineral oil | 0 | |
| Hexadecane | 97 | 44 |
| Tetradecane | 0 | |
| Dodecane | 0 | |
| Olive oil | 0 | |

## IV.2. Cell culture in drops overlaid with FC-40

Fetal bovine serum (FBS) is commonly used to supplement cell medium to provide essential nutrients for the cells including growth factors[19, 20]. Lack of serum prevents cell adhesion as seen in conventional culture condition (Figure 3, far left), while with serum (10% FBS as recommended by the manufacturer) cells attach to the surface after being

seeded (Figure 3, second from left). In Figure 2, HEK cells in DMEM + 10% FBS are seen attaching well in a 2-µl drop overlaid with FC-40, however, when using smaller volume (200 nl), the morphology of the cells 24 h after seeded resembles the FBS-free condition (Figure 3, second from right). Interestingly, when the FBS concentration in the drop is increased to 30%, cells appear attached (Figure 3, far right).

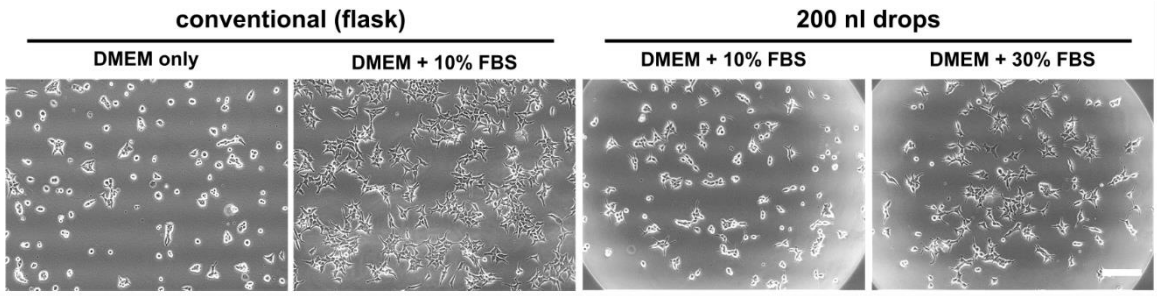


Figure 3 HEK cells cultured conventionally in flask without (far left) and with (second from left) 10% FBS in the cell medium, and in 200 nl drops with 10% (second from right) and 30% FBS (far right). Scale bar = 100 µm.

The poor adhesion of cells in 200 nl drops (corresponding with the higher surface-to-volume ratio compared to 2-µl drops or flask culture) with 10% FBS (a standard concentration in conventional culture) and the improvement given by increasing the concentration lead to hypotheses on the effect of serum adsorption to the interface[11-14]. The first possibility is that some components of the serum are adsorbed to the overlaying liquid and thus reducing the serum concentration in the drop. The second possibility is that the total amount of serum components in the drop may not be enough to adsorb to the solid surface, therefore preventing the cell from attaching and subsequently proliferating in a normal rate. Figure 4 shows that for drops with contact angle 45°, reducing the volume would result in a sharp increase of surface-to-volume ratio, especially for ~400 nl and below, both for the liquid/liquid and solid/liquid interfaces.

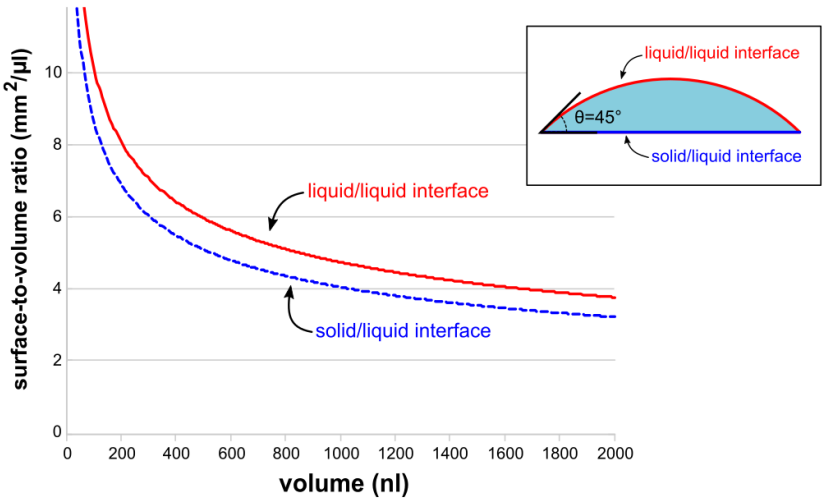


Figure 4 Surface-to-volume ratio of drops plotted against drop volume based on spherical cap geometry (see inset) with contact angle 45°.

### IV.3. Cell culture in drops with various surface-to-volume ratio

To test effects of drop surface-to-volume ratio on cell adhesion, we the cultured HEK cells in drops with different volumes and footprint areas. Table 2 lists the surface-to-volume ratio of drops in this test. Note that the footprint areas here correspond to the footprint areas of drops with labelled volume, deposited in air. Figure 5A shows 100 cells seeded to each drop, captured after 24 h incubation. The worse cell adhesion is in the drop with largest surface-to-volume ratio, i.e., 200 nl on '1000 nl' footprint, indicated by mostly round cells. More cells are progressively attached as the footprint area decreased, however, as in Figure 3 (second from right), 200 nl on '200 nl' footprint is still not an ideal culture condition. Increasing the volume to 500 nl or 1000 nl on this smallest footprint improves overall cell adhesion, indicated by more flattened cells. In these drops, the cells also appear to grow in clusters as in the ideal conventional culture (Figure 3, second from left). Cells in 1000 nl on '1000 nl' footprint drop also exhibit a high percentage of flattened cells, however as the footprint area is larger, they appear sparser.

Table 2 Surface-to-volume ratio of drops with various footprint area and volume. (*) footprint area created by a spherical cap drop of the corresponding volume with 45° contact angle.

| **Surface-to-volume ratio of liquid/liquid interface ($mm^2/\mu l$)** | | Footprint area* | | |
|---|---|---|---|---|
| | | 200 nl | 500 nl | 1000 nl |
| Volume | 200 nl | 8.08 | 13.08 | 20.31 |
| | 500 nl | 4.86 | 5.95 | 8.44 |
| | 1000 nl | 3.92 | 3.93 | 4.72 |
| **Surface-to-volume ratio of solid/liquid interface ($mm^2/\mu l$)** | | Footprint area* | | |
| | | 200 nl | 500 nl | 1000 nl |
| Volume | 200 nl | 6.90 | 12.70 | 20.15 |
| | 500 nl | 2.76 | 5.08 | 8.06 |
| | 1000 nl | 1.38 | 2.54 | 4.03 |

In Figure 5B, the cell density (number of cells per footprint area) was kept constant 72 cells/$mm^2$. Here, in 200 nl on '1000 nl' footprint drop, now more total cell number was seeded, and more cell attached, however a significant percentage of cells are still round. Again, the adhesion is progressively improved, on each footprint area, as the volume is increased. However, it is also clear that cells in larger-volume drops with their corresponding footprint area (i.e., 200 nl on '200 nl', 500 nl on '500 nl', and 1000 nl on '1000 nl' footprint) have better adhesion. These results confirm that in general cells attach better when cultured in lower surface-to-volume ratio.

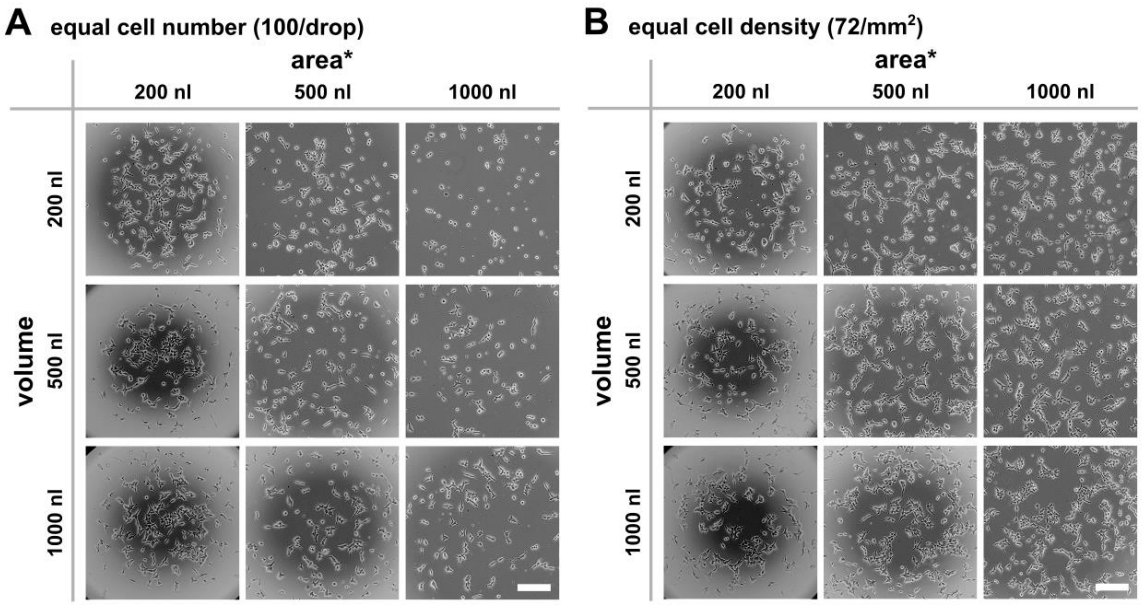


Figure 5 HEK cells cultured in sessile drops of different surface-to-volume ratio. In columns, the area (*) represented as volume means the footprint area (the contact area of a drop with the solid surface) created by a DMEM + 10% FBS drop of the corresponding volume in air. (A) Each drop has approximately initial cell concentration 500 cells/μl, or equal to 100 cells/drop. (B) Each drop has approximately initial cell density 72 cells/mm$^2$. The cells attach to surface better when surface-to-volume ratio was lower (e.g., 200 nl drops on '200 nl' *vs* '1000 nl' footprint area). Scale bar = 200 μm.

### IV.4. Effects of serum adsorption on cell adhesion

Next, we tested effects of serum adsorption on cell adhesion by pre-exposing footprints of 200 nl drops with medium plus serum before using them for culturing cells in 200 nls. Figure 6A shows the illustration of the test. 200, 500 and 1000 nl DMEM + 10% FBS were deposited on a footprint of 200 nl drop and incubated for 2 h (to test the transient condition) or 2 d (assuming the adsorption has reached equilibrium here). All liquids were then removed, and equally 200 nl cell-containing media were deposited to each footprint. As controls, cells were also seeded conventionally on a petri dish ('usual') and on a footprint created by 200 nl DMEM drop without serum. After 1 h incubation, only a small percentage (less than 10%) of cells in the 'usual' control is already not round, and less so in the 'drop' control (Figure 6Bi-ii). Meanwhile, in drops which footprints have been exposed to serum,

this number is increased with the medium volume and incubation period. We suggest that the amount of serum components adsorbed to the solid surface affect cell adhesion, especially early after cell seeding. This is evident from the fact that the 'usual' control exhibited low cell adhesion within this short time period, as cells in this case were seeded to a virgin Petri dish surface despite being exposed to comparably abundant serum.

After 4 h incubation, more serum components have been adsorbed to the solid surface, and cells continue to attach. Now, in the 'usual' control, ~70% cells already show signs of adhesion. In contrast, only ~50% do in the 'drop' control. We suggest this is due to lack of serum components adsorbed to the solid surface, and some might get adsorbed to the water/FC-40 interface. This percentage is again higher when the footprint has been pre-exposed to serum. For example, 70% or more flattened cells are observed in drops which footprints have been pre-exposed with 500 and 1000 nl DMEM + 10% FBS for 2 h or 2 d. When only 200 nl medium was used in the pre-exposure step, there is a big difference on the percentage of flattened cells between 2 h and 2 d exposure – suggesting that within 2 h the serum components have not yet reached equilibrium adsorption.

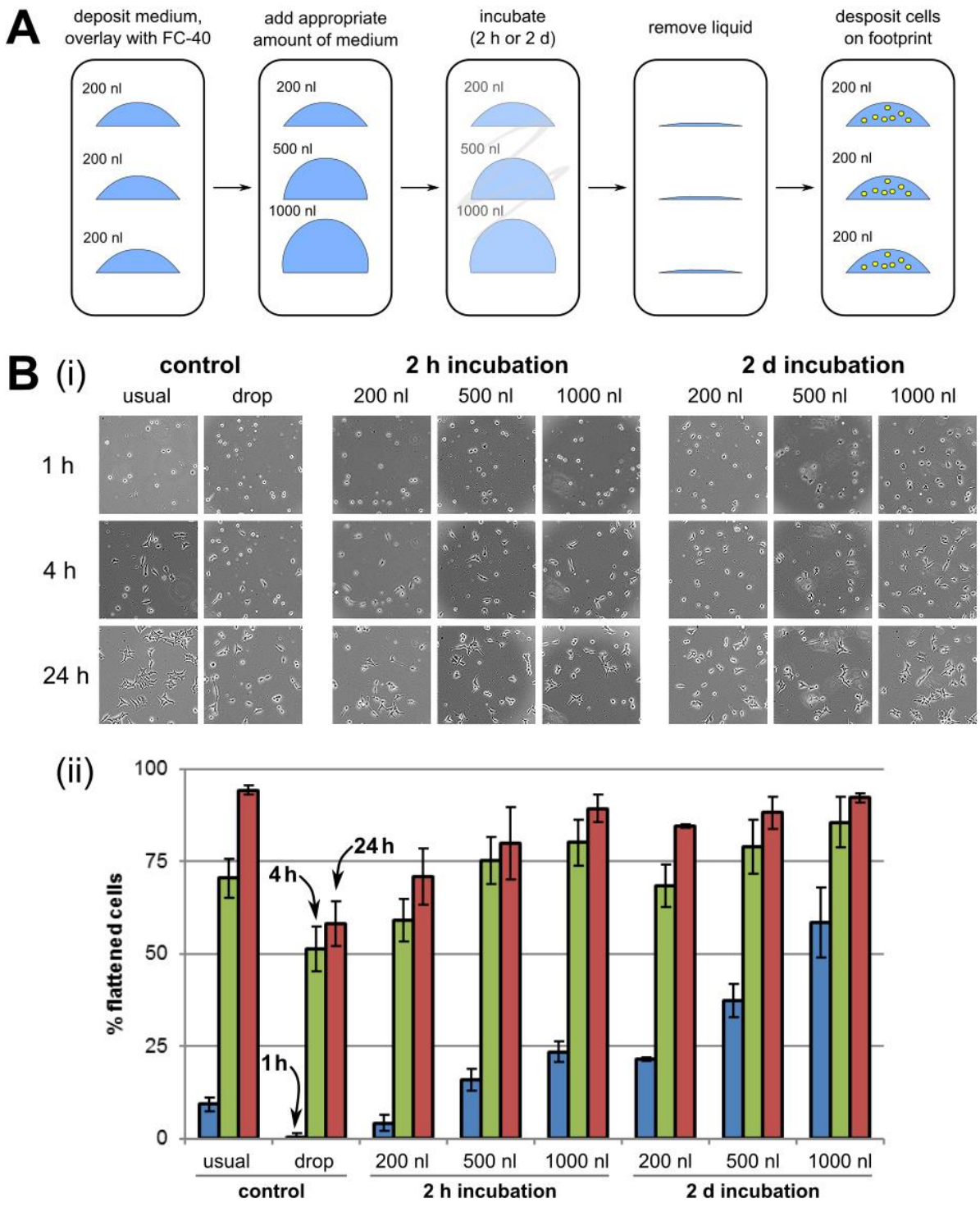


Figure 6 Measurement of cell adhesion in drops which footprints have been exposed to medium plus serum. (A) The illustration of the test. First, 200 nl drops of DMEM + 10% FBS were deposited, overlaid with FC-40, and more medium added to get 200, 500 and 1000 nl drops. These drops were then incubated at 37°C for 2 h or 2 d. All liquids were removed prior to depositing 200 nl medium containing HEK cells. (B) Results. (i) Representative images of cells in the drops in each condition. The controls: 'usual' is from cells cultured conventionally in a petri dish and 'drop' is from cells

cultured in drops without pre-exposure with serum. (ii) Percentage of flattened cells in drops, from the ratio of cells that do not appear round with the total number of cells in a drop. Error bar: standard deviation (n=3).

After 24 h, ~94% cells have been flattened in the 'usual' control. It is normal to have some cells in round state as they proliferate. We can also see in Figure 6Bi that the cells grow in clusters, indicating proliferation. Meanwhile, only less than 60% appear flattened in the 'drop' control. The maximum ratio of flattened cells is shown in drops is ~90%, which is observed in drops which footprints have been pre-exposed with 1000 nl DMEM + 10% FBS for 2 h and 2 d, and 500 nl for 2 d. The similar end profile suggests that in these cases, the water/FC-40 interface has been saturated, and cell adhesion is driven by the amount of serum components adsorbed at the solid interface from the pre-exposure step plus the ones in the medium which carry cells. However, cells in these drops still do not attach as well as the 'usual' control, which also confirmed by the images (Figure 6Bi), presumably because of the small culture volume (limited nutrients, higher local concentration of signal molecules, waste accumulation). A common strategy for this problem is exchanging medium more often[21], which we expect can improve cell growth here, and it is evident that further work needs to be undertaken to understand cell culture behaviour in such systems.

## V. Conclusion

We assessed biocompatibility of sessile drops, covered with FC-40, on a Petri dish for HEK cell culture. We observed that cells in drops do not attach well to the surface compared to conventional culture in flask. Cells in 200 nl drops attach better to the surface when serum (FBS) concentration in the medium is increased from 10% to 30%. Cell adhesion can also be improved by pre-exposing the drop footprint with medium plus serum in standard concentration (10% FBS). We suggest that poor cell adhesion in small drops is related to serum adsorption to interfaces – in drops with high surface-to-volume ratio, the effects of

adsorption of serum components to the solid and liquid interfaces would be amplified. The correlation of serum adsorption in drops with cell adhesion and subsequent proliferation remains an open question; further research needs to be done to support this hypothesis and to optimize this sessile drop platform for cell-based assays.

## References


(1) Liberski, A. R.; Delaney, J. T., Jr.; Schubert, U. S., "One cell-one well": a new approach to inkjet printing single cell microarrays. *ACS Comb Sci* **2011,** *13* (2), 190-5.

(2) Wang, C.; Liu, W.; Tan, M.; Sun, H.; Yu, Y., An open-pattern droplet-in-oil planar array for single cell analysis based on sequential inkjet printing technology. *Biomicrofluidics* **2017,** *11* (4), 044106.

(3) Ueda, E.; Geyer, F. L.; Nedashkivska, V.; Levkin, P. A., DropletMicroarray: facile formation of arrays of microdroplets and hydrogel micropads for cell screening applications. *Lab Chip* **2012,** *12* (24), 5218-24.

(4) Popova, A. A.; Demir, K.; Hartanto, T. G.; Schmitt, E.; Levkin, P. A., Droplet-microarray on superhydrophobic–superhydrophilic patterns for high-throughput live cell screenings. *RSC Advances* **2016,** *6* (44), 38263-38276.

(5) Cole, R. H.; Tang, S. Y.; Siltanen, C. A.; Shahi, P.; Zhang, J. Q.; Poust, S.; Gartner, Z. J.; Abate, A. R., Printed droplet microfluidics for on demand dispensing of picoliter droplets and cells. *Proc Natl Acad Sci U S A* **2017,** *114* (33), 8728-8733.

(6) Popova, A. A.; Schillo, S. M.; Demir, K.; Ueda, E.; Nesterov-Mueller, A.; Levkin, P. A., Droplet-Array (DA) Sandwich Chip: A Versatile Platform for High-Throughput Cell Screening Based on Superhydrophobic-Superhydrophilic Micropatterning. *Adv Mater* **2015,** *27* (35), 5217-22.

(7) Walker, G. M.; Zeringue, H. C.; Beebe, D. J., Microenvironment design considerations for cellular scale studies. *Lab Chip* **2004,** *4* (2), 91-7.

(8) Mehling, M.; Tay, S., Microfluidic cell culture. *Curr Opin Biotechnol* **2014,** *25*, 95-102.

(9) Dusny, C.; Grunberger, A.; Probst, C.; Wiechert, W.; Kohlheyer, D.; Schmid, A., Technical bias of microcultivation environments on single-cell physiology. *Lab Chip* **2015,** *15* (8), 1822-34.

(10) Prastowo, A.; Feuerborn, A.; Cook, P. R.; Walsh, E. J., Biocompatibility of fluids for multiphase drops-in-drops microfluidics. *Biomed Microdevices* **2016,** *18* (114).

(11) Roach, L. S.; Song, H.; Ismagilov, R. F., Controlling nonspecific protein adsorption in a plug-based microfluidic system by controlling interfacial chemistry using fluorous-phase surfactants. *Analytical Chemistry* **2005,** *77*, 765-796.

(12) Beverung, C. J.; Radke, C. J.; Blanch, H. W., Protein adsorption at the oil/water interface: characterization of adsorption kinetics by dynamic interfacial tension measurements. *Biophysical Chemistry* **1999,** *81*, 59-80.

(13) Maldonado-Valderrama, J.; Fainerman, V. B.; Aksenenko, E.; Jose Gálvez-Ruiz, M.; Cabrerizo-Vílchez, M. A.; Miller, R., Dynamics of protein adsorption at the oil–water interface: comparison with a theoretical model. *Colloids and Surfaces A: Physicochemical and Engineering Aspects* **2005,** *261* (1-3), 85-92.

(14) Miller, R.; Fainerman, V. B.; Makievski, A. V.; Kragel, J.; Grigoriev, D. O.; Kazakov, V. N.; Sinyachenko, O. V., Dynamics of protein and mixed protein surfactant adsorption layers at the water fluid interface. *Advances in Colloind and Interface Science* **2000,** *86*, 39-82.
(15) Berthier, E.; Beebe, D. J., Flow rate analysis of a surface tension driven passive micropump. *Lab Chip* **2007,** *7* (11), 1475-8.
(16) Tadmor, R., Line energy and the relation between advancing, receding, and young contact angles. *Langmuir* **2004,** *20*, 7659-7664.
(17) Luong-Van, E.; Kang, R. K.; Birch, W. R., A novel technique for positioning multiple cell types by liquid handling. *Biointerphases* **2009,** *4* (2), 13-8.
(18) Du, G. S.; Pan, J. Z.; Zhao, S. P.; Zhu, Y.; den Toonder, J. M.; Fang, Q., Cell-based drug combination screening with a microfluidic droplet array system. *Anal Chem* **2013,** *85* (14), 6740-7.
(19) Yao, T.; Asayama, Y., Animal-cell culture media: History, characteristics, and current issues. *Reprod Med Biol* **2017,** *16* (2), 99-117.
(20) van der Valk, J.; Bieback, K.; Buta, C.; Cochrane, B.; Dirks, W. G.; Fu, J.; Hickman, J. J.; Hohensee, C.; Kolar, R.; Liebsch, M.; Pistollato, F.; Schulz, M.; Thieme, D.; Weber, T.; Wiest, J.; Winkler, S.; Gstraunthaler, G., Fetal Bovine Serum (FBS): Past - Present - Future. *ALTEX* **2018,** *35* (1), 99-118.
(21) Giulitti, S.; Magrofuoco, E.; Prevedello, L.; Elvassore, N., Optimal periodic perfusion strategy for robust long-term microfluidic cell culture. *Lab Chip* **2013,** *13* (22), 4430-41.

## Statement of Authorship

| | | |
|---|---|---|
| Title of Paper | Biocompatibility of sessile drops as chambers for cell culture measured by HEK cells adhesion | |
| Publication Status | ❑ Published<br>❑ Accepted for Publication | ❑ Submitted for Publication<br>☑ Unpublished and unsubmitted work written in a manuscript style |
| Publication Details | | |

### Student Confirmation

| | | | |
|---|---|---|---|
| Student Name: | Aishah Prastowo | | |
| Contribution to the Paper | Collected and interpreted data, produced figures, wrote the manuscript | | |
| Signature |  | Date | 8/11/2018 |

### Supervisor Confirmation

By signing the Statement of Authorship, you are certifying that the candidate made a substantial contribution to the publication, and that the description described above is accurate.

| | | |
|---|---|---|
| Supervisor name and title:<br>Edmond Walsh - Associate Professor of Engineering Science | | |
| Supervisor comments<br>This potential paper is not under consideration at any journal at date of signing. | | |
| Signature 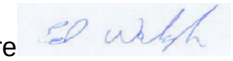 | Date | 23/11/18 |

# Discussion

## I. Overview of previous chapters

In the four papers in this thesis, new techniques for handling liquids in medium-scale drop-based microfluidic devices have been presented, and their biocompatibility issues addressed. Two approaches were presented: (1) three phase drops-in-drops microfluidics in a Teflon tube (Paper 1 and 2), and (2) sessile drop arrays on a Petri dish (Paper 3 and 4). Although the two approaches are fundamentally different, both are similar in a way that, unlike many other microfluidic devices, there are no pre-fabrication steps required, as Teflon tubes and tissue-culture Petri dishes are commercially available and to be used directly. Integrating drops-in-drops with sessile drop systems would result in a platform in which liquids can be prepared in a tube prior to being transferred to an empty dish or into pre-deposited drops on the dish. This integration step is not addressed in the thesis and is discussed in the future work section.

The drops-in-drops approach is expected to be an alternative of the more classical flowing drops approach in microfluidics: a Teflon tube is being used instead multiple channels in a polymer device, and the flow of the drops is being controlled by the fluid mechanics of three of more immiscible fluids in it. This way, the drops can be prepared in the tube in advance, and mass transfer can be timely controlled. Paper 1 elaborated this approach, and presented some applications including drug screening and protein crystallization. Paper 2 then addressed the biocompatibility issues of the system described in Paper 1. Genetic expression of mammalian cells in drops-in-drops system has been measured and analysed, which leads to the finding that cell viability alone is not a reliable measure for fluid biocompatibility. Several fluids and surfactants were then screened for their biocompatibility and suitability for drops-in-drops system for cell-based assays.

The sessile drop approach provides an easy way to monitor the content of the drops: arrays of drops are placed on a standard Petri dish, overlaid with an immiscible liquid to prevent evaporation, and anchored by fluid mechanics. In Paper 3, this approach is discussed along with the finding that fetal bovine serum (FBS) and serum replacement (SR) (commonly used to supplement cell culture media) stabilize pinning lines of drops. As a result, the advancing contact angles of the drops increase, and more volume can be added without changing the drop footprint. A large working volume is beneficial for many assays which require adding and subtracting liquids. Biocompatibility of the system is then assessed in Paper 4. Large surface-to-volume ratio of drops was found to negatively affect HEK cell adhesion and subsequently proliferation, which is predicted to be an effect of serum adsorption at the liquid/liquid interface (serum components cannot be accessed by the cells) and solid/liquid interface (cells need to attach to serum components adsorbed to the solid surface). One proposed strategy to improve cell adhesion is by pre-exposing drop footprints with serum-containing medium before seeding cells onto them.

## II. Challenges and limitations

The aim to develop new techniques for handling liquids as drops has been achieved in this study, however their implementation is still in the proof-of-principle stage. The challenges and limitations of the proposed approaches are discussed below.

### II.1. Biocompatible drops-in-drops advection

Although biocompatible fluids and surfactants for drops-in-drops merging have been identified in Paper 2, further works need to be done to identify biocompatible fluids and surfactants combination for fluid advection system. Fluidic architecture required for this approach consists of an oil drop ('oil') engulfed by an aqueous phase ('aq') within fluorocarbon ('FC') carrier, and the interfacial tensions ($\gamma$) need to satisfy $\gamma_{FC/oil} > \gamma_{FC/aq} +$

$\gamma_{aq/oil}$. One of the most straightforward ways to achieve this condition is by adding surfactants to the aqueous phase, however the ones that are strong enough to stabilize the architecture are toxic for cells, e.g., Triton X-100, as demonstrated in Paper 1. Screening wider range of water-soluble surfactants to find a combination that both is biocompatible and forms the desired structure is expected to address this issue. A biocompatible drops-in-drops system would open many applications in cell-based assays, e.g., to monitor cell response to gradual drug induction over time or to replenish medium for cell culture in long term.

### II.2. Drop generation frequency

Many studies in drop-based microfluidics boast the advantage of generating drops in high frequencies, often as high as kilo- or mega-hertz range [63, 92, 285]. This thesis proposes approaches in which drops are generated by withdrawing liquids into a tube (alternating between phases) or depositing liquids to a designated location on a Petri dish. Therefore, drop generation frequency depends not only on the liquid pumping rate but also mechanics of tube movement. In Paper 3 and 4, the cell printer deposited drops onto a Petri dish at a rate of ~1 drop/s, although this can be increased by adjusting the movement speed. However, conventional high-throughput microfluidic drop generators usually rely on branched channel and can only generate drops from one liquid sample. They are advantageous for single cell encapsulation, but adding another sample (e.g., drops containing drugs to be merged later with the cells) would greatly increase the complexity of the device. Drops-in-drops and the sessile drop systems target different applications – lower throughput, but higher flexibility in terms of the number and quantity of the samples. To increase frequency, the drop loading/depositing system can possibly be modified, for example using a rotating device [69] or several tubes in parallel [286].

### II.3. Cell culture in drops-in-drops

Although biocompatible fluids for drops-in-drops approach have been identified, there are still some problems with culturing cells for long-term in this device. For suspension cells, cells in high concentration tend to clump in a drop as it flows, which is often unfavourable. For adherent cells, some solid supports need to be introduced for cells to adhere (e.g., alginate beads), but this can complicate visual observation and add noise to the genetic measurements. To address these problems, further works need to be done to measure cell condition and growth in drops-in-drops, by considering cell concentration and flow rate among other factors. Alternatively, the drops-in-drops system can be used exclusively for sample preparation, before depositing them as sessile drops.

## III. Further work

Apart from addressing the above limitations, possible works for continuation of this thesis are discussed as the following.

### III.1. Integrating drops-in-drops and sessile drop systems

Both drops-in-drops and sessile drop platforms offer their own advantages; therefore, by integrating them, a more complete system can be developed for new applications. In previous studies, flowing drops in a microfluidic channel have been deposited on planar surfaces, such as dielectrophoretic surface [287], matrix-assisted laser desorption/ionization (MALDI) mass spectrometry [140], and digital microfluidic device [220]. Figure 1 shows an example of such integrated devices in which the PDMS-based flowing drop part of the platform generate picoliter drops (or separates pre-generated drops) and sorts them for ones containing tagged cells, determined by an optical detector [287]. Only positive drops are then deposited to the surface through a print nozzle for downstream analyses. This type of

integration can possibly be adapted to create an interface between drops-in-drops and sessile drop platforms.

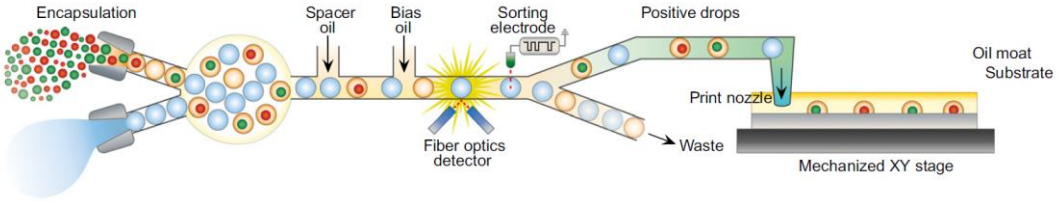


Figure 1 Example of an integrated device consisted of a PDMS-based flowing drop microfluidic system with sessile drop printer on a dielectrophoretic surface [287]. The PDMS device is placed on the printer head connected to a nozzle, generates drops using a T-junction channel and sorts the ones containing cells or specified molecules. The drops are deposited or printed on a specific location of the surface using a programmed x-y-z stage. The surface is overlaid with oil prior to printing. Reprinted with permission from [287], copyright (2017) National Academy of Sciences.

One important factor to consider in this integration step is, unlike in the example in Figure 1, drops-in-drop system employs three immiscible liquids. Consequently, there is one additional liquid which is not needed for the sessile drop system and can disrupt the drop depositing process. One possible way to solve this problem is by using a solid surface which strongly prefers the aqueous phase and the fluorocarbon, and at the same time repels the oil.

### III.2. Biocompatibility test with different cell types

In this thesis, only limited cell types were used in the biocompatibility studies, especially for the sessile drop system. As the images of cells can be easily captured in sessile drops, more intensive studies on cell morphology, proliferation and other behaviour can be performed. For example, in Paper 4 the quantification of cell adhesion is only based on whether the cells changed their shape or not, however in future works cell area can also be measured as an indicator for adhesion. There are also many other cell types with their different characteristics; testing biocompatibility with several other cell types could provide more information for future users of this technology.

### III.3. Adsorption of serum components to interfaces

Adsorption of serum components at solid and liquid interfaces has been suggested to affect sessile drop contact-line pinning (Paper 3) and cell adhesion in drops (Paper 4). However, the responsible molecules and mechanism have not been identified yet. To find serum components inducing contact-line pinning, sessile drops containing different well-defined proteins or protein combinations can be tested for their advancing contact angle. Serum and protein adsorption dynamics especially at liquid/liquid interface can be studied by measuring dynamic interfacial tension. Understanding the mechanism of serum components adsorption to solid and liquid interfaces, and also the contact line would be beneficial in designing a biocompatible sessile drop platform for assays involving cell culture.

# References


[1] G. M. Whitesides, "The origins and the future of microfluidics," *Nature,* vol. 442, no. 7101, pp. 368-73, Jul 27 2006.

[2] Y. Schaerli and F. Hollfelder, "The potential of microfluidic water-in-oil droplets in experimental biology," *Mol Biosyst,* vol. 5, no. 12, pp. 1392-404, Dec 2009.

[3] L. Mazutis and A. D. Griffiths, "Selective droplet coalescence using microfluidic systems," *Lab Chip,* vol. 12, no. 10, pp. 1800-6, Apr 24 2012.

[4] K. Liu, H. Ding, Y. Chen, and X.-Z. Zhao, "Droplet-based synthetic method using microflow focusing and droplet fusion," *Microfluidics and Nanofluidics,* vol. 3, no. 2, pp. 239-243, 2006.

[5] G. F. Christopher, J. Bergstein, N. B. End, M. Poon, C. Nguyen, and S. L. Anna, "Coalescence and splitting of confined droplets at microfluidic junctions," *Lab Chip,* vol. 9, no. 8, pp. 1102-9, Apr 21 2009.

[6] J. D. Tice, H. Song, A. D. Lyon, and R. F. Ismagilov, "Formation of droplets and mixing in multiphase microfluidics at low values of the Reynolds and the capillary numbers," *Langmuir,* vol. 19, pp. 9127-9133, 2003.

[7] W. Tanthapanichakoon, N. Aoki, K. Matsuyama, and K. Mae, "Design of mixing in microfluidic liquid slugs based on a new dimensionless number for precise reaction and mixing operations," *Chemical Engineering Science,* vol. 61, no. 13, pp. 4220-4232, 2006.

[8] Y. C. Tan, J. S. Fisher, A. I. Lee, V. Cristini, and A. P. Lee, "Design of microfluidic channel geometries for the control of droplet volume, chemical concentration, and sorting," *Lab Chip,* vol. 4, no. 4, pp. 292-8, Aug 2004.

[9] E. K. Sackmann, A. L. Fulton, and D. J. Beebe, "The present and future role of microfluidics in biomedical research," *Nature,* vol. 507, no. 7491, pp. 181-9, Mar 13 2014.

[10] B. Kintses, L. D. v. Vliet, S. R. Devenish, and F. Hollfelder, "Microfluidic droplets: new integrated workflows for biological experiments," *Current Opinion in Chemical Biology,* vol. 14, pp. 548-555, 2010.

[11] L. Baraban *et al.*, "Millifluidic droplet analyser for microbiology," *Lab Chip,* vol. 11, no. 23, pp. 4057-62, Dec 7 2011.

[12] K. Martin *et al.*, "Generation of larger numbers of separated microbial populations by cultivation in segmented-flow microdevices," *Lab Chip,* vol. 3, no. 3, pp. 202-7, Aug 2003.

[13] H. H. Caicedo and S. T. Brady, "Microfluidics: The Challenge Is to Bridge the Gap Instead of Looking for a 'Killer App'," *Trends Biotechnol,* vol. 34, no. 1, pp. 1-3, Jan 2016.

[14] S. Haeberle and R. Zengerle, "Microfluidic platforms for lab-on-a-chip applications," *Lab Chip,* vol. 7, no. 9, pp. 1094-110, Sep 2007.

[15] J. Friend and L. Yeo, "Fabrication of microfluidic devices using polydimethylsiloxane," *Biomicrofluidics,* vol. 4, no. 2, Mar 15 2010.

[16] F. Lapierre, N. R. Cameron, and Y. Zhu, "Ready… set, flow: simple fabrication of microdroplet generators and their use in the synthesis of PolyHIPE microspheres," *Journal of Micromechanics and Microengineering,* vol. 25, no. 3, p. 035011, 2015.

[17] E. Berthier, E. W. Young, and D. Beebe, "Engineers are from PDMS-land, Biologists are from Polystyrenia," *Lab Chip,* vol. 12, no. 7, pp. 1224-37, Apr 7 2012.

[18] J. C. Baret, "Surfactants in droplet-based microfluidics," *Lab Chip,* vol. 12, no. 3, pp. 422-33, Feb 7 2012.

[19] A. B. Theberge *et al.*, "Microdroplets in microfluidics: an evolving platform for discoveries in chemistry and biology," *Angew Chem Int Ed Engl*, vol. 49, no. 34, pp. 5846-68, Aug 9 2010.

[20] A. M. Streets and Y. Huang, "Chip in a lab: Microfluidics for next generation life science research," *Biomicrofluidics*, vol. 7, no. 01 1302, pp. 1-23, 2013.

[21] "Cell culture basic handbook," in "Includes transfection," Gibco™ Education, Thermo Fisher Scientific Inc.2016.

[22] R. I. Freshney, *Culture of Animal Cells: A Manual of Basic Technique and Specialized Applications*. Wiley-Blackwell, 2015, p. 758.

[23] A. A. Khalili and M. R. Ahmad, "A Review of Cell Adhesion Studies for Biomedical and Biological Applications," *Int J Mol Sci*, vol. 16, no. 8, pp. 18149-84, Aug 5 2015.

[24] J. A. Ryan, "Evolution of Cell Culture Surfaces," *BioFiles*, vol. 3, no. 8, p. 21, 2008.

[25] F. Grinnell and M. K. Feld, "Initial adhesion of human fibroblasts in serum-free medium: possible role of secreted fibronectin," *Cell*, vol. 17, pp. 117-129, 1979.

[26] A. S. G. Curtis and J. V. Forrester, "The competitive effects of serum proteins on cell adhesion," *J. Cell Sci.*, vol. 71, pp. 17-35, 1984.

[27] X. Zheng, H. Baker, W. S. Hancock, F. Fawaz, M. McCaman, and J. Erno Pungor, "Proteomic analysis for the assessment of different lots of Fetal Bovine Serum as a raw material for cell culture. Part IV. Application of proteomics to the manufacture of biological drugs," *Biotechnol. Prog.*, vol. 22, no. 1294-1300, 2006.

[28] P. J. Price and E. A. Gregory, "Relationship between in vitro growth promotion and biophysical and biochemical properties of the serum supplement," *In Vitro*, vol. 18, no. 6, pp. 576-584, 1982.

[29] F. Grinnell and M. K. Feld, "Adsorption characteristics of plasma fibronectin in relationship to biological activity," *J Biomed Mater Res,* vol. 15, no. 3, pp. 363-81, 1981.

[30] F. Grinnell and M. K. Feld, "Fibronectin adsorption on hydrophilic and hydrophobic surfaces detected by antibody binding and analyzed during cell adhesion in serum-containing medium," *The Journal of Biological Chemistry,* vol. 257, no. 9, pp. 4888-4893, 1982.

[31] M. Mehling and S. Tay, "Microfluidic cell culture," *Curr Opin Biotechnol,* vol. 25, pp. 95-102, Feb 2014.

[32] B. Zhang, M. C. Kim, T. Thorsen, and Z. Wang, "A self-contained microfluidic cell culture system," *Biomed Microdevices,* vol. 11, no. 6, pp. 1233-7, Dec 2009.

[33] P. J. Hung, P. J. Lee, P. Sabounchi, R. Lin, and L. P. Lee, "Continuous perfusion microfluidic cell culture array for high-throughput cell-based assays," *Biotechnol Bioeng,* vol. 89, no. 1, pp. 1-8, Jan 5 2005.

[34] C. Dusny, A. Grunberger, C. Probst, W. Wiechert, D. Kohlheyer, and A. Schmid, "Technical bias of microcultivation environments on single-cell physiology," *Lab Chip,* vol. 15, no. 8, pp. 1822-34, Apr 21 2015.

[35] S. Halldorsson, E. Lucumi, R. Gomez-Sjoberg, and R. M. Fleming, "Advantages and challenges of microfluidic cell culture in polydimethylsiloxane devices," *Biosens Bioelectron,* vol. 63, pp. 218-31, Jan 15 2015.

[36] S. Giulitti, E. Magrofuoco, L. Prevedello, and N. Elvassore, "Optimal periodic perfusion strategy for robust long-term microfluidic cell culture," *Lab Chip,* vol. 13, no. 22, pp. 4430-41, Nov 21 2013.

[37] R. A. Kellogg, R. Gomez-Sjoberg, A. A. Leyrat, and S. Tay, "High-throughput microfluidic single-cell analysis pipeline for studies of signaling dynamics," *Nat Protoc,* vol. 9, no. 7, pp. 1713-26, Jul 2014.

[38] G. M. Walker, H. C. Zeringue, and D. J. Beebe, "Microenvironment design considerations for cellular scale studies," *Lab Chip,* vol. 4, no. 2, pp. 91-7, Apr 2004.

[39] R. G. Harrison, "On the stereotropism of embryonic cells," *Science,* vol. 34, no. 870, pp. 279-281, 1911.

[40] A. Carrel and M. T. Burrows, "Cultivation of tissues in vitro and its technique," *The Journal of Experimental Medicine,* vol. 13, no. 3, pp. 387-396, 1911.

[41] K. Iijima, R. Suzuki, A. Iizuka, H. Ueno-Yokohata, N. Kiyokawa, and M. Hashizume, "Surface functionalization of tissue culture polystyrene plates with hydroxyapatite under body fluid conditions and its effect on differentiation behaviors of mesenchymal stem cells," *Colloids Surf B Biointerfaces,* vol. 147, pp. 351-359, Nov 1 2016.

[42] A. S. Curtis, "Adhesion of cells to polystyrene surfaces," *The Journal of Cell Biology,* vol. 97, no. 5, pp. 1500-1506, 1983.

[43] A. Carré and V. Lacarrière, "How substrate properties control cell adhesion. A physical-chemical approach," *Journal of Adhesion Science and Technology,* vol. 24, pp. 815-830, 2010.

[44] B. Huang, H. Wu, S. Kim, and R. N. Zare, "Coating of poly(dimethylsiloxane) with n-dodecyl-beta-D-maltoside to minimize nonspecific protein adsorption," *Lab Chip,* vol. 5, no. 10, pp. 1005-7, Oct 2005.

[45] K. J. Regehr *et al.*, "Biological implications of polydimethylsiloxane-based microfluidic cell culture," *Lab Chip,* vol. 9, no. 15, pp. 2132-9, Aug 7 2009.

[46] J. Leivo *et al.*, "A durable and biocompatible ascorbic acid-based covalent coating method of polydimethylsiloxane for dynamic cell culture," *J R Soc Interface*, vol. 14, no. 132, Jul 2017.

[47] J. N. Lee, X. Jiang, D. Ryan, and G. M. Whitesides, "Compatibility of mammalian cells on surfaces of poly(dimethylsiloxane)," *Langmuir*, vol. 20, no. 26, pp. 11684-91, Dec 21 2004.

[48] J. N. Lee, C. Park, and G. M. Whitesides, "Solvent compatibility of poly(dimetylsiloxane)-based microfluidic devices," *Anal Chem*, vol. 75, pp. 6544-6554, 2003.

[49] C. Y. Chan, V. N. Goral, M. E. DeRosa, T. J. Huang, and P. K. Yuen, "A polystyrene-based microfluidic device with three-dimensional interconnected microporous walls for perfusion cell culture," *Biomicrofluidics*, vol. 8, no. 4, p. 046505, Jul 2014.

[50] A. S. Johnson, K. B. Anderson, S. T. Halpin, D. C. Kirkpatrick, D. M. Spence, and R. S. Martin, "Integration of multiple components in polystyrene-based microfluidic devices part I: fabrication and characterization," *Analyst*, vol. 138, no. 1, pp. 129-36, Jan 7 2013.

[51] R. Tran *et al.*, "Simplified prototyping of perfusable polystyrene microfluidics," *Biomicrofluidics*, vol. 8, no. 4, p. 046501, Jul 2014.

[52] A. Toossi, H. Moghadas, M. Daneshmand, and D. Sameoto, "Bonding PMMA microfluidics using commercial microwave ovens," *Journal of Micromechanics and Microengineering*, vol. 25, no. 8, 2015.

[53] J. Steigert *et al.*, "Rapid prototyping of microfluidic chips in COC," *Journal of Micromechanics and Microengineering*, vol. 17, no. 2, pp. 333-341, 2007.

[54] P. M. van Midwoud, A. Janse, M. T. Merema, G. M. Groothuis, and E. Verpoorte, "Comparison of biocompatibility and adsorption properties of different plastics for

advanced microfluidic cell and tissue culture models," *Anal Chem,* vol. 84, no. 9, pp. 3938-44, May 1 2012.

[55] D. S. Tawfik and A. D. Griffiths, "Man-made cell-like compartments for molecular evolution," *Nature Biotechnology,* vol. 16, pp. 652-656, 1998.

[56] P. Garstecki, M. J. Fuerstman, H. A. Stone, and G. M. Whitesides, "Formation of droplets and bubbles in a microfluidic T-junction-scaling and mechanism of break-up," *Lab Chip,* vol. 6, no. 3, pp. 437-46, Mar 2006.

[57] A. Gupta, S. M. S. Murshed, and R. Kumar, "Droplet formation and stability of flows in a microfluidic T-junction," *Applied Physics Letters,* vol. 94, no. 16, p. 164107, 2009.

[58] Y.-C. Tan, V. Cristini, and A. P. Lee, "Monodispersed microfluidic droplet generation by shear focusing microfluidic device," *Sensors and Actuators B: Chemical,* vol. 114, no. 1, pp. 350-356, 2006.

[59] T. Ward, M. Faivre, and H. A. Stone, "Drop production and tip-streaming phenomenon in a microfluidic flow-focusing device via an interfacial chemical reaction," *Langmuir,* vol. 26, no. 12, pp. 9233-9, Jun 15 2010.

[60] C. A. Stan, S. K. Y. Tang, and G. M. Whitesides, "Independent control of drop size and velocity in microfluidic flow-focusing generators using variable temperature and flow rate," *Anal Chem,* vol. 81, pp. 2399-2402, 2009.

[61] K. Xu, C. P. Tostado, J.-H. Xu, Y.-C. Lu, and G.-S. Luo, "Direct measurement of the differential pressure during drop formation in a co-flow microfluidic device," *Lab on a Chip,* vol. 14, no. 7, p. 1357, 2014.

[62] Z. Nie *et al.*, "Emulsification in a microfluidic flow-focusing device: effect of the viscosities of the liquids," *Microfluidics and Nanofluidics,* vol. 5, no. 5, pp. 585-594, 2008.

[63] L. Mazutis *et al.*, "Droplet-based microfluidic systems for high-throughput single DNA molecule isothermal amplification and analysis," *Anal Chem,* vol. 81, pp. 4813-4821, 2009.

[64] K. Churski *et al.*, "Rapid screening of antibiotic toxicity in an automated microdroplet system," *Lab Chip,* vol. 12, no. 9, pp. 1629-37, May 7 2012.

[65] W.-B. Du, M. Sun, S.-Q. Gu, Y. Zhu, and Q. Fang, "Automated microfluidic screening assay platform based on DropLab," *Anal Chem,* vol. 82, pp. 9941-9947, 2010.

[66] G. S. Du, J. Z. Pan, S. P. Zhao, Y. Zhu, J. M. den Toonder, and Q. Fang, "Cell-based drug combination screening with a microfluidic droplet array system," *Anal Chem,* vol. 85, no. 14, pp. 6740-7, Jul 16 2013.

[67] T. D. Rane, H. C. Zec, and T. H. Wang, "A serial sample loading system: interfacing multiwell plates with microfluidic devices," *J Lab Autom,* vol. 17, no. 5, pp. 370-7, Oct 2012.

[68] H. Zec, T. D. Rane, and T. H. Wang, "Microfluidic platform for on-demand generation of spatially indexed combinatorial droplets," *Lab Chip,* vol. 12, no. 17, pp. 3055-62, Sep 7 2012.

[69] F. Gielen *et al.*, "A fully unsupervised compartment-on-demand platform for precise nanoliter assays of time-dependent steady-state enzyme kinetics and inhibition," *Anal Chem,* vol. 85, no. 9, pp. 4761-9, May 7 2013.

[70] N. Shembekar, C. Chaipan, R. Utharala, and C. A. Merten, "Droplet-based microfluidics in drug discovery, transcriptomics and high-throughput molecular genetics," *Lab Chip,* vol. 16, no. 8, pp. 1314-31, Apr 21 2016.

[71] X. Niu, S. Gulati, J. B. Edel, and A. J. deMello, "Pillar-induced droplet merging in microfluidic circuits," *Lab Chip,* vol. 8, no. 11, pp. 1837-41, Nov 2008.

[72] Y.-C. Tan, Y. L. Ho, and A. P. Lee, "Droplet coalescence by geometrically mediated flow in microfluidic channels," *Microfluidics and Nanofluidics,* vol. 3, no. 4, pp. 495-499, 2006.

[73] N. Bremond, A. Thiam, and J. Bibette, "Decompressing Emulsion Droplets Favors Coalescence," *Physical Review Letters,* vol. 100, no. 2, 2008.

[74] C. Priest, S. Herminghaus, and R. Seemann, "Controlled electrocoalescence in microfluidics: Targeting a single lamella," *Applied Physics Letters,* vol. 89, no. 13, p. 134101, 2006.

[75] D. R. Link *et al.*, "Electric control of droplets in microfluidic devices," *Angew Chem Int Ed Engl,* vol. 45, no. 16, pp. 2556-60, Apr 10 2006.

[76] K. Ahn, J. Agresti, H. Chong, M. Marquez, and D. A. Weitz, "Electrocoalescence of drops synchronized by size-dependent flow in microfluidic channels," *Applied Physics Letters,* vol. 88, no. 26, p. 264105, 2006.

[77] M. Zagnoni, G. Le Lain, and J. M. Cooper, "Electrocoalescence mechanisms of microdroplets using localized electric fields in microfluidic channels," *Langmuir,* vol. 26, no. 18, pp. 14443-9, Sep 21 2010.

[78] C. N. Baroud, M. R. de Saint Vincent, and J. P. Delville, "An optical toolbox for total control of droplet microfluidics," *Lab Chip,* vol. 7, no. 8, pp. 1029-33, Aug 2007.

[79] M. Sesen, T. Alan, and A. Neild, "Microfluidic on-demand droplet merging using surface acoustic waves," *Lab Chip,* vol. 14, no. 17, pp. 3325-33, Sep 7 2014.

[80] I. Akartuna, D. M. Aubrecht, T. E. Kodger, and D. A. Weitz, "Chemically induced coalescence in droplet-based microfluidics," *Lab Chip,* vol. 15, no. 4, pp. 1140-4, Feb 3 2015.

[81] T. Hatakeyama, D. L. Chen, and R. F. Ismagilov, "Microgram-scale testing of reaction conditions in solution using nanoliter plugs in microfluidics with detection by MALDI-MS," *Journal of the American Chemical Society,* vol. 128, pp. 2518-2519, 2005.

[82] A. R. Abate, T. Hung, P. Mary, J. J. Agresti, and D. A. Weitz, "High-throughput injection with microfluidics using picoinjectors," *Proc Natl Acad Sci U S A,* vol. 107, no. 45, pp. 19163-6, Nov 9 2010.

[83] D. J. Eastburn, A. Sciambi, and A. R. Abate, "Picoinjection enables digital detection of RNA with droplet RT-PCR," *PLOS One,* vol. 8, no. 4, p. e62961, 2013.

[84] B. O'Donovan, D. J. Eastburn, and A. R. Abate, "Electrode-free picoinjection of microfluidic drops," *Lab Chip,* vol. 12, no. 20, pp. 4029-32, Oct 21 2012.

[85] A. Grodrian, J. Metze, T. Henkel, K. Martin, M. Roth, and J. M. Kohler, "Segmented flow generation by chip reactors for highly parallelized cell cultivation," *Biosens Bioelectron,* vol. 19, no. 11, pp. 1421-8, Jun 15 2004.

[86] M. E. Gallina *et al.*, "Toward a Droplet-Based Single-Cell Radiometric Assay," *Anal Chem,* vol. 89, no. 12, pp. 6472-6481, Jun 20 2017.

[87] M. A. Khorshidi, P. K. Rajeswari, C. Wahlby, H. N. Joensson, and H. Andersson Svahn, "Automated analysis of dynamic behavior of single cells in picoliter droplets," *Lab Chip,* vol. 14, no. 5, pp. 931-7, Mar 7 2014.

[88] A. Mongersun, I. Smeenk, G. Pratx, P. Asuri, and P. Abbyad, "Droplet Microfluidic Platform for the Determination of Single-Cell Lactate Release," *Anal Chem,* vol. 88, no. 6, pp. 3257-63, Mar 15 2016.

[89] R. Hu *et al.*, "Encapsulation of single cells into monodisperse droplets by fluorescence-activated droplet formation on a microfluidic chip," *Talanta,* vol. 153, pp. 253-259, 2016.

[90] L. Wu, P. Chen, Y. Dong, X. Feng, and B. F. Liu, "Encapsulation of single cells on a microfluidic device integrating droplet generation with fluorescence-activated droplet sorting," *Biomed Microdevices,* vol. 15, no. 3, pp. 553-60, Jun 2013.

[91] R. Novak, K. Hart, and R. A. Mathies, "Single cell measurement of telomerase expression and splicing using microfluidic emulsion cultures," *Nucleic Acids Res,* Jul 21 2015.

[92] J. F. Edd *et al.*, "Controlled encapsulation of single-cells into monodisperse picolitre drops," *Lab Chip,* vol. 8, no. 8, pp. 1262-4, Aug 2008.

[93] E. W. Kemna, R. M. Schoeman, F. Wolbers, I. Vermes, D. A. Weitz, and A. van den Berg, "High-yield cell ordering and deterministic cell-in-droplet encapsulation using Dean flow in a curved microchannel," *Lab Chip,* vol. 12, no. 16, pp. 2881-7, Aug 21 2012.

[94] R. Ramji *et al.*, "Single cell kinase signaling assay using pinched flow coupled droplet microfluidics," *Biomicrofluidics,* vol. 8, no. 3, p. 034104, May 2014.

[95] G. Kamalakshakurup and A. P. Lee, "High-efficiency single cell encapsulation and size selective capture of cells in picoliter droplets based on hydrodynamic micro-vortices," *Lab Chip,* vol. 17, no. 24, pp. 4324-4333, Dec 5 2017.

[96] J. C. Baret *et al.*, "Fluorescence-activated droplet sorting (FADS): efficient microfluidic cell sorting based on enzymatic activity," *Lab Chip,* vol. 9, no. 13, pp. 1850-8, Jul 7 2009.

[97] M. Najah, R. Calbrix, I. P. Mahendra-Wijaya, T. Beneyton, A. D. Griffiths, and A. Drevelle, "Droplet-based microfluidics platform for ultra-high-throughput bioprospecting of cellulolytic microorganisms," *Chem Biol,* vol. 21, no. 12, pp. 1722-32, Dec 18 2014.

[98] B. L. Wang *et al.*, "Microfluidic high-throughput culturing of single cells for selection based on extracellular metabolite production or consumption," *Nat Biotechnol*, vol. 32, no. 5, pp. 473-8, May 2014.

[99] M. E. Vincent, W. Liu, E. B. Haney, and R. F. Ismagilov, "Microfluidic stochastic confinement enhances analysis of rare cells by isolating cells and creating high density environments for control of diffusible signals," *Chem Soc Rev*, vol. 39, no. 3, pp. 974-84, Mar 2010.

[100] P. Sabhachandani *et al.*, "Integrated microfluidic platform for rapid antimicrobial susceptibility testing and bacterial growth analysis using bead-based biosensor via fluorescence imaging," *Microchimica Acta*, vol. 184, no. 12, pp. 4619-4628, 2017.

[101] A. M. Kaushik, K. Hsieh, L. Chen, D. J. Shin, J. C. Liao, and T. H. Wang, "Accelerating bacterial growth detection and antimicrobial susceptibility assessment in integrated picoliter droplet platform," *Biosens Bioelectron*, vol. 97, pp. 260-266, Nov 15 2017.

[102] S. Sarkar, N. Cohen, P. Sabhachandani, and T. Konry, "Phenotypic drug profiling in droplet microfluidics for better targeting of drug-resistant tumors," *Lab Chip*, vol. 15, no. 23, pp. 4441-50, Dec 7 2015.

[103] J. Pan *et al.*, "Quantitative tracking of the growth of individual algal cells in microdroplet compartments," *Integr Biol (Camb)*, vol. 3, no. 10, pp. 1043-51, Oct 2011.

[104] M. Shamir, Y. Bar-On, R. Phillips, and R. Milo, "SnapShot: Timescales in Cell Biology," *Cell*, vol. 164, no. 6, pp. 1302-1302 e1, Mar 10 2016.

[105] A. Dewan, J. Kim, R. H. McLean, S. A. Vanapalli, and M. N. Karim, "Growth kinetics of microalgae in microfluidic static droplet arrays," *Biotechnol Bioeng*, vol. 109, no. 12, pp. 2987-96, Dec 2012.

[106] C. H. Schmitz, A. C. Rowat, S. Koster, and D. A. Weitz, "Dropspots: a picoliter array in a microfluidic device," *Lab Chip,* vol. 9, no. 1, pp. 44-9, Jan 7 2009.

[107] Y.-L. Chiu *et al.*, "Synthesis of fluorosurfactants for emulsion-based biological applications," *ACS Nano,* vol. 8, no. 4, pp. 3913-3920, 2014.

[108] J. Clausell-Tormos *et al.*, "Droplet-based microfluidic platforms for the encapsulation and screening of Mammalian cells and multicellular organisms," *Chem Biol,* vol. 15, no. 5, pp. 427-37, May 2008.

[109] P. Wilding, M. A. Shoffner, and L. J. Kricka, "PCR in a silicon microstructure," *Clin Chem,* vol. 40, no. 9, pp. 1815-1818, 1994.

[110] M. U. Kopp, A. J. d. Mello, and A. Manz, "Chemical amplification: continuous flow PCR on a chip," *Science,* vol. 280, no. 5366, pp. 1046-1048, 1998.

[111] Y. Zhang and P. Ozdemir, "Microfluidic DNA amplification--a review," *Anal Chim Acta,* vol. 638, no. 2, pp. 115-25, Apr 13 2009.

[112] N. Park, S. Kim, and J. H. Hahn, "Cylindrical compact thermal-cycling device for continuous-flow polymerase chain reaction," *Anal Chem,* vol. 75, pp. 6029-6033, 2003.

[113] L. J. Kricka and P. Wilding, "Microchip PCR," *Anal Bioanal Chem,* vol. 377, no. 5, pp. 820-5, Nov 2003.

[114] K. D. Dorfman, M. Chabert, J.-H. Codarbox, G. Rousseau, P. d. Cremoux, and J.-L. Viovy, "Contamination-free continuous flow microfluidic polymerase chain reaction for quantitative and clinical applications," *Anal Chem,* vol. 77, pp. 3700-3704, 2005.

[115] R. Williams, S. G. Peisajovich, O. J. Miller, S. Magdassi, D. S. Tawfik, and A. D. Griffiths, "Amplification of complex gene libraries by emulsion PCR," *Nat Methods,* vol. 3, no. 7, pp. 545-50, Jul 2006.

[116] A. Musyanovych, V. Mailander, and K. Landfester, "Miniemulsion droplets as single molecule nanoreactors for polymerase chain reaction," *Biomacromolecules,* vol. 6, pp. 1824-1828, 2005.

[117] T. Kojima, Y. Takei, M. Ohtsuka, Y. Kawarasaki, T. Yamane, and H. Nakano, "PCR amplification from single DNA molecules on magnetic beads in emulsion: application for high-throughput screening of transcription factor targets," *Nucleic Acids Res,* vol. 33, no. 17, p. e150, Oct 6 2005.

[118] F. J. Ghadessy, J. L. Ong, and P. Holliger, "Directed evolution of polymerase function by compartmentalized self-replication," *Proc Natl Acad Sci U S A,* vol. 98, no. 8, pp. 4552-7, Apr 10 2001.

[119] N. R. Beer *et al.*, "On-chip, real-time, single-copy polymerase chain reaction in picoliter droplets," *Anal Chem,* vol. 79, pp. 8471-8475, 2007.

[120] F. Sarrazin, K. Loubière, L. Prat, C. Gourdon, T. Bonometti, and J. Magnaudet, "Experimental and numerical study of droplets hydrodynamics in microchannels," *AIChE Journal,* vol. 52, no. 12, pp. 4061-4070, 2006.

[121] H. Yin and D. Marshall, "Microfluidics for single cell analysis," *Curr Opin Biotechnol,* vol. 23, no. 1, pp. 110-9, Feb 2012.

[122] M. Jang *et al.*, "Droplet-based digital PCR system for detection of single-cell level of foodborne pathogens," *BioChip Journal,* vol. 11, no. 4, pp. 329-337, 2017.

[123] A. G. Sciancalepore *et al.*, "Microdroplet-based multiplex PCR on chip to detect foodborne bacteria producing biogenic amines," *Food Microbiol,* vol. 35, no. 1, pp. 10-4, Aug 2013.

[124] Q. Zhang *et al.*, "Development of a facile droplet-based single-cell isolation platform for cultivation and genomic analysis in microorganisms," *Sci Rep,* vol. 7, p. 41192, Jan 23 2017.

[125] S. C. Kim, I. C. Clark, P. Shahi, and A. R. Abate, "Single-Cell RT-PCR in Microfluidic Droplets with Integrated Chemical Lysis," *Anal Chem,* vol. 90, no. 2, pp. 1273-1279, Jan 16 2018.

[126] A. C. Hatch, T. Ray, K. Lintecum, and C. Youngbull, "Continuous flow real-time PCR device using multi-channel fluorescence excitation and detection," *Lab Chip,* vol. 14, no. 3, pp. 562-8, Feb 7 2014.

[127] K. Xiao, M. Zhang, S. Chen, L. Wang, D. C. Chang, and W. Wen, "Electroporation of micro-droplet encapsulated HeLa cells in oil phase," *Electrophoresis,* vol. 31, no. 18, pp. 3175-80, Sep 2010.

[128] Y. Zhan, J. Wang, N. Bao, and C. Lu, "Electroporation of cells in microfluidic droplets," *Anal Chem,* vol. 81, pp. 2027-2031, 2009.

[129] C. Luo *et al.*, "Picoliter-volume aqueous droplets in oil: electrochemical detection and yeast cell electroporation," *Electrophoresis,* vol. 27, no. 10, pp. 1977-83, May 2006.

[130] B. Qu, Y. J. Eu, W. J. Jeong, and D. P. Kim, "Droplet electroporation in microfluidics for efficient cell transformation with or without cell wall removal," *Lab Chip,* vol. 12, no. 21, pp. 4483-8, Nov 7 2012.

[131] D. J. Im and S.-N. Jeong, "Transfection of Jurkat T cells by droplet electroporation," *Biochemical Engineering Journal,* vol. 122, pp. 133-140, 2017.

[132] E. Luong-Van, R. K. Kang, and W. R. Birch, "A novel technique for positioning multiple cell types by liquid handling," *Biointerphases,* vol. 4, no. 2, pp. 13-8, Jun 2009.

[133] A. R. Liberski, J. T. Delaney, Jr., and U. S. Schubert, ""One cell-one well": a new approach to inkjet printing single cell microarrays," *ACS Comb Sci,* vol. 13, no. 2, pp. 190-5, Mar 14 2011.

[134] Y. Zhou, Y. Pang, and Y. Huang, "Openly accessible microfluidic liquid handlers for automated high-throughput nanoliter cell culture," *Anal Chem,* vol. 84, no. 5, pp. 2576-84, Mar 06 2012.

[135] S. P. Zhao, Y. Ma, Q. Lou, H. Zhu, B. Yang, and Q. Fang, "Three-Dimensional Cell Culture and Drug Testing in a Microfluidic Sidewall-Attached Droplet Array," *Anal Chem,* vol. 89, no. 19, pp. 10153-10157, Oct 3 2017.

[136] F. Xu *et al.*, "A droplet-based building block approach for bladder smooth muscle cell (SMC) proliferation," *Biofabrication,* vol. 2, no. 1, p. 014105, Mar 2010.

[137] C. Y. Jiang *et al.*, "High-Throughput Single-Cell Cultivation on Microfluidic Streak Plates," *Appl Environ Microbiol,* vol. 82, no. 7, pp. 2210-8, 2016.

[138] W. W. Liu, Y. Zhu, Y. M. Feng, J. Fang, and Q. Fang, "Droplet-Based Multivolume Digital Polymerase Chain Reaction by a Surface-Assisted Multifactor Fluid Segmentation Approach," *Anal Chem,* vol. 89, no. 1, pp. 822-829, Jan 3 2017.

[139] E. Ueda, F. L. Geyer, V. Nedashkivska, and P. A. Levkin, "DropletMicroarray: facile formation of arrays of microdroplets and hydrogel micropads for cell screening applications," *Lab Chip,* vol. 12, no. 24, pp. 5218-24, Dec 21 2012.

[140] S. K. Kuster *et al.*, "Interfacing droplet microfluidics with matrix-assisted laser desorption/ionization mass spectrometry: label-free content analysis of single droplets," *Anal Chem,* vol. 85, no. 3, pp. 1285-9, Feb 5 2013.

[141] C. Wang, W. Liu, M. Tan, H. Sun, and Y. Yu, "An open-pattern droplet-in-oil planar array for single cell analysis based on sequential inkjet printing technology," *Biomicrofluidics,* vol. 11, no. 4, p. 044106, Jul 2017.

[142] A. A. Popova, K. Demir, T. G. Hartanto, E. Schmitt, and P. A. Levkin, "Droplet-microarray on superhydrophobic–superhydrophilic patterns for high-throughput live cell screenings," *RSC Advances,* vol. 6, no. 44, pp. 38263-38276, 2016.

[143] A. A. Popova, S. M. Schillo, K. Demir, E. Ueda, A. Nesterov-Mueller, and P. A. Levkin, "Droplet-Array (DA) Sandwich Chip: A Versatile Platform for High-Throughput Cell Screening Based on Superhydrophobic-Superhydrophilic Micropatterning," *Adv Mater,* vol. 27, no. 35, pp. 5217-22, Sep 16 2015.

[144] X. L. Guo, Y. Wei, Q. Lou, Y. Zhu, and Q. Fang, "Manipulating Femtoliter to Picoliter Droplets by Pins for Single Cell Analysis and Quantitative Biological Assay," *Anal Chem,* vol. 90, no. 9, pp. 5810-5817, May 1 2018.

[145] A. Salehi-Reyhani, E. Burgin, O. Ces, K. R. Willison, and D. R. Klug, "Addressable droplet microarrays for single cell protein analysis," *Analyst,* vol. 139, no. 21, pp. 5367-74, Nov 7 2014.

[146] C. Soitu *et al.*, "Microfluidic chambers using fluid walls for cell biology," *Proceedings of the National Academy of Sciences,* p. 201805449, 2018.

[147] L. S. Roach, H. Song, and R. F. Ismagilov, "Controlling nonspecific protein adsorption in a plug-based microfluidic system by controlling interfacial chemistry using fluorous-phase surfactants," *Analytical Chemistry,* vol. 77, pp. 765-796, 2005.

[148] M. Kaltenbach, S. R. Devenish, and F. Hollfelder, "A simple method to evaluate the biochemical compatibility of oil/surfactant mixtures for experiments in microdroplets," *Lab Chip,* vol. 12, no. 20, pp. 4185-92, Oct 21 2012.

[149] M. Chabert and J. L. Viovy, "Microfluidic high-throughput encapsulation and hydrodynamic self-sorting of single cells," *Proc Natl Acad Sci U S A,* vol. 105, no. 9, pp. 3191-6, Mar 4 2008.

[150] S. Koster *et al.*, "Drop-based microfluidic devices for encapsulation of single cells," *Lab Chip,* vol. 8, no. 7, pp. 1110-5, Jul 2008.

[151] F. Chen, Y. Zhan, T. Geng, H. Lian, P. Xu, and C. Lu, "Chemical transfection of cells in picoliter aqueous droplets in fluorocarbon oil," *Anal Chem,* vol. 83, no. 22, pp. 8816-20, Nov 15 2011.

[152] S. Cho *et al.*, "Droplet-based microfluidic platform for high-throughput, multi-parameter screening of photosensitizer activity," *Anal Chem,* vol. 85, no. 18, pp. 8866-72, Sep 17 2013.

[153] I. Platzman, J. W. Janiesch, and J. P. Spatz, "Synthesis of nanostructured and biofunctionalized water-in-oil droplets as tools for homing T cells," *J Am Chem Soc,* vol. 135, no. 9, pp. 3339-42, Mar 6 2013.

[154] H. Wang, W. Zhang, and Z. Dai, "A novel approach for encapsulating cells into monodisperse picolitre droplets actuated by microfluidic pulse inertia force," *Anal. Methods,* vol. 6, no. 24, pp. 9754-9760, 2014.

[155] A. E. Sgro, P. B. Allen, and D. T. Chiu, "Thermoelectric manipulation of aqueous droplets in microfluidic devices," *Analytical Chemistry,* vol. 79, pp. 4845-4851, 2007.

[156] E. W. Kemna, L. I. Segerink, F. Wolbers, I. Vermes, and A. van den Berg, "Label-free, high-throughput, electrical detection of cells in droplets," *Analyst,* vol. 138, no. 16, pp. 4585-92, Aug 21 2013.

[157] A. B. Pardee, "A restriction point for control of normal animal cell proliferation," *Proc Natl Acad Sci U S A,* vol. 71, no. 4, pp. 1286-1290, 1974.

[158] E. Tumarkin *et al.*, "High-throughput combinatorial cell co-culture using microfluidics," *Integr Biol (Camb),* vol. 3, no. 6, pp. 653-62, Jun 2011.

[159] P. R. Marcoux *et al.*, "Micro-confinement of bacteria into w/o emulsion droplets for rapid detection and enumeration," *Colloids and Surfaces A: Physicochemical and Engineering Aspects,* vol. 377, no. 1-3, pp. 54-62, 2011.

[160] C. Holtze *et al.*, "Biocompatible surfactants for water-in-fluorocarbon emulsions," *Lab Chip,* vol. 8, no. 10, pp. 1632-9, Oct 2008.

[161] T. Beneyton, F. Coldren, J. C. Baret, A. D. Griffiths, and V. Taly, "CotA laccase: high-throughput manipulation and analysis of recombinant enzyme libraries expressed in E. coli using droplet-based microfluidics," *Analyst,* vol. 139, no. 13, pp. 3314-23, Jun 3 2014.

[162] Y. Bai *et al.*, "Intra-species bacterial quorum sensing studied at single cell level in a double droplet trapping system," *Int J Mol Sci,* vol. 14, no. 5, pp. 10570-81, 2013.

[163] J.-u. Shim *et al.*, "Simultaneous determination of gene expression and enzymatic activity in individual bacterial cells in microdroplet compartments," *J. Am. Chem. Soc.*, vol. 131, pp. 15251-15256, 2009.

[164] T. W. Hofmann, S. Hanselmann, J. W. Janiesch, A. Rademacher, and C. H. Bohm, "Applying microdroplets as sensors for label-free detection of chemical reactions," *Lab Chip,* vol. 12, no. 5, pp. 916-22, Mar 7 2012.

[165] H. N. Joensson, M. Uhlen, and H. A. Svahn, "Droplet size based separation by deterministic lateral displacement-separating droplets by cell--induced shrinking," *Lab Chip,* vol. 11, no. 7, pp. 1305-10, Apr 7 2011.

[166] M. Srisa-Art, I. C. Bonzani, A. Williams, M. M. Stevens, A. J. deMello, and J. B. Edel, "Identification of rare progenitor cells from human periosteal tissue using droplet microfluidics," *Analyst,* vol. 134, no. 11, pp. 2239-45, Nov 2009.

[167] P. Abbyad, P. L. Tharaux, J. L. Martin, C. N. Baroud, and A. Alexandrou, "Sickling of red blood cells through rapid oxygen exchange in microfluidic drops," *Lab Chip,* vol. 10, no. 19, pp. 2505-12, Oct 7 2010.

[168] D. J. Eastburn, A. Sciambi, and A. R. Abate, "Ultrahigh-throughput Mammalian single-cell reverse-transcriptase polymerase chain reaction in microfluidic drops," *Anal Chem,* vol. 85, no. 16, pp. 8016-21, Aug 20 2013.

[169] A. Funfak, A. Brosing, M. Brand, and J. M. Kohler, "Micro fluid segment technique for screening and development studies on Danio rerio embryos," *Lab Chip,* vol. 7, no. 9, pp. 1132-8, Sep 2007.

[170] D. P. Curran, "Strategy-level separations in organic synthesis: from planning to practice," *Angew Chem Int Ed Engl,* vol. 37, pp. 1174-1196, 1998.

[171] J. N. Lee, C. Park, and G. M. Whitesides, "Sovent compatibility of poly(dimethylsiloxane)-based microfluidic devices," *Anal. Chem.*, vol. 75, pp. 6544-6554, 2003.

[172] T. Akiyama, K. S. Williamson, R. Schaefer, S. Pratt, C. B. Chang, and M. J. Franklin, "Resuscitation of Pseudomonas aeruginosa from dormancy requires hibernation promoting factor (PA4463) for ribosome preservation," *PNAS,* vol. 114, no. 12, pp. 3204-3209, 2017.

[173] B. El Debs, R. Utharala, I. V. Balyasnikova, A. D. Griffiths, and C. A. Merten, "Functional single-cell hybridoma screening using droplet-based microfluidics," *Proc Natl Acad Sci U S A,* vol. 109, no. 29, pp. 11570-5, Jul 17 2012.

[174] A. M. Klein *et al.*, "Droplet barcoding for single-cell transcriptomics applied to embryonic stem cells," *Cell,* vol. 161, no. 5, pp. 1187-201, May 21 2015.

[175] M. Huang *et al.*, "Microfluidic screening and whole-genome sequencing identifies mutations associated with improved protein secretion by yeast," *Proc Natl Acad Sci U S A,* vol. 112, no. 34, pp. E4689-96, Aug 25 2015.

[176] H. Lu *et al.*, "High throughput single cell counting in droplet-based microfluidics," *Sci Rep,* vol. 7, no. 1, p. 1366, May 2 2017.

[177] R. Illing, C. Burkart, D. Pfitzner, D. Jungmann, L. Baraban, and G. Cuniberti, "Ecotoxicity assessment using ciliate cells in millifluidic droplets," *Biomicrofluidics,* vol. 10, no. 2, p. 024115, Mar 2016.

[178] E. Zang *et al.*, "Real-time image processing for label-free enrichment of Actinobacteria cultivated in picolitre droplets," *Lab Chip,* vol. 13, no. 18, pp. 3707-13, Sep 21 2013.

[179] T. R. Kline, M. K. Runyon, M. Pothiawala, and R. F. Ismagilov, "ABO, D blood typing and subtyping using plug-based microfluidics," *Anal Chem,* vol. 80, pp. 6190-6197, 2008.

[180] K. Leung *et al.*, "A programmable droplet-based microfluidic device applied to multiparameter analysis of single microbes and microbial communities," *Proc Natl Acad Sci U S A,* vol. 109, no. 20, pp. 7665-70, May 15 2012.

[181] M. Pan *et al.*, "Fluorinated pickering emulsions impede interfacial transport and form rigid interface for the growth of anchorage-dependent cells," *ACS Appl Mater Interfaces,* vol. 6, no. 23, pp. 21446-53, Dec 10 2014.

[182] M. Nakano, J. Komatsu, S.-i. Matsuura, K. Takashima, S. Katsura, and A. Mizuno, "Single-molecule PCR using water-in-oil emulsion," *Journal of Biotechnology,* vol. 102, no. 2, pp. 117-124, 2003.

[183] T. Ohashi, H. Kuyama, N. Hanafusa, and Y. Togawa, "A simple device using magnetic transportation for droplet-based PCR," *Biomed Microdevices,* vol. 9, no. 5, pp. 695-702, Oct 2007.

[184] H. Hufnagel, A. Huebner, C. Gulch, K. Guse, C. Abell, and F. Hollfelder, "An integrated cell culture lab on a chip: modular microdevices for cultivation of mammalian cells and delivery into microfluidic microdroplets," *Lab Chip,* vol. 9, no. 11, pp. 1576-82, Jun 7 2009.

[185] A. Chen *et al.*, "On-chip magnetic separation and encapsulation of cells in droplets," *Lab Chip,* vol. 13, no. 6, pp. 1172-81, Mar 21 2013.

[186] H. Willaime, V. Barbier, L. Kloul, S. Maine, and P. Tabeling, "Arnold Tongues in a Microfluidic Drop Emitter," *Physical Review Letters,* vol. 96, no. 5, 2006.

[187] M. Toiya, V. K. Vanag, and I. R. Epstein, "Diffusively coupled chemical oscillators in a microfluidic assembly," *Angew Chem Int Ed Engl,* vol. 47, no. 40, pp. 7753-5, 2008.

[188] T. Thorsen, R. W. Roberts, F. H. Arnold, and S. R. Quake, "Dynamic Pattern Formation in a Vesicle-Generating Microfluidic Device," *Physical Review Letters,* vol. 86, no. 18, pp. 4163-4166, 2001.

[189] S. Punnamaraju, H. You, and A. J. Steckl, "Triggered release of molecules across droplet interface bilayer lipid membranes using photopolymerizable lipids," *Langmuir,* vol. 28, no. 20, pp. 7657-64, May 22 2012.

[190] S. Xu *et al.*, "Generation of Monodisperse Particles by Using Microfluidics: Control over Size, Shape, and Composition," *Angewandte Chemie,* vol. 117, no. 5, pp. 734-738, 2005.

[191] W. Shi, J. Qin, N. Ye, and B. Lin, "Droplet-based microfluidic system for individual Caenorhabditis elegans assay," *Lab Chip,* vol. 8, no. 9, pp. 1432-5, Sep 2008.

[192] L. Ter-Minassian-Saraga, "Protein denaturation in adsorption and water activity at interfaces: an analysis and suggestion," *Journal of Colloid and Interface Science,* vol. 80, no. 2, pp. 393-401, 1981.

[193] D. E. Graham and M. C. Phillips, "Proteins at liquid interfaces: I. Kinetics of adsorption and surface denaturation," *Journal of Colloid and Interface Science,* vol. 70, no. 3, pp. 404-414, 1979.

[194] C. J. Beverung, C. J. Radke, and H. W. Blanch, "Protein adsorption at the oil/water interface: characterization of adsorption kinetics by dynamic interfacial tension measurements," *Biophysical Chemistry,* vol. 81, pp. 59-80, 1999.

[195] F. Courtois *et al.*, "Controlling the retention of small molecules in emulsion microdroplets for use in cell-based assays," *Anal Chem,* vol. 81, no. 8, pp. 3008-3016, 2009.

[196] Y. Skhiri *et al.*, "Dynamics of molecular transport by surfactants in emulsions," *Soft Matter,* vol. 8, no. 41, p. 10618, 2012.

[197] W. Liu, H. J. Kim, E. M. Lucchetta, W. Du, and R. F. Ismagilov, "Isolation, incubation, and parallel functional testing and identification by FISH of rare microbial single-copy cells from multi-species mixtures using the combination of chemistrode and stochastic confinement," *Lab Chip,* vol. 9, no. 15, pp. 2153-62, Aug 7 2009.

[198] A. Golberg *et al.*, "Cloud-enabled microscopy and droplet microfluidic platform for specific detection of Escherichia coli in water," *PLoS One,* vol. 9, no. 1, p. e86341, 2014.

[199] K. Nakamura *et al.*, "Culture-independent method for identification of microbial enzyme-encoding genes by activity-based single-cell sequencing using a water-in-oil microdroplet platform," *Sci Rep,* vol. 6, p. 22259, 2016.

[200] L. Dong, D. W. Chen, S. J. Liu, and W. Du, "Automated Chemotactic Sorting and Single-cell Cultivation of Microbes using Droplet Microfluidics," *Sci Rep,* vol. 6, p. 24192, 2016.

[201] D. Cottinet *et al.*, "Lineage Tracking for Probing Heritable Phenotypes at Single-Cell Resolution," *PLoS One,* vol. 11, no. 4, p. e0152395, 2016.

[202] J. J. Agresti *et al.*, "Ultrahigh-throughput screening in drop-based microfluidics for directed evolution," *PNAS,* vol. 107, no. 9, pp. 4004-4009, 2010.

[203] H. Hu, D. Eustace, and C. A. Merten, "Efficient cell pairing in droplets using dual-color sorting," *Lab Chip,* Aug 27 2015.

[204] L. Mahler *et al.*, "Detection of antibiotics synthetized in microfluidic picolitre-droplets by various actinobacteria," *Sci Rep,* vol. 8, no. 1, p. 13087, Aug 30 2018.

[205] T. P. Lagus and J. F. Edd, "High-throughput co-encapsulation of self-ordered cell trains: cell pair interactions in microdroplets," *RSC Advances,* vol. 3, no. 43, p. 20512, 2013.

[206] J. Park, A. Kerner, M. A. Burns, and X. N. Lin, "Microdroplet-enabled highly parallel co-cultivation of microbial communities," *PLoS One,* vol. 6, no. 2, p. e17019, 2011.

[207] E. Hondroulis *et al.*, "A droplet-merging platform for comparative functional analysis of m1 and m2 macrophages in response to e. coli-induced stimuli," *Biotechnol Bioeng,* vol. 114, no. 3, pp. 705-709, Mar 2017.

[208] T. Konry, A. Golberg, and M. Yarmush, "Live single cell functional phenotyping in droplet nano-liter reactors," *Sci Rep,* vol. 3, p. 3179, 2013.

[209] S. Sarkar *et al.*, "Dynamic analysis of immune and cancer cell interactions at single cell level in microfluidic droplets," *Biomicrofluidics,* vol. 10, no. 5, p. 054115, Sep 2016.

[210] A. E. Fischer *et al.*, "A high-throughput drop microfluidic system for virus culture and analysis," *J Virol Methods,* vol. 213, pp. 111-7, Mar 2015.

[211] Y. J. Sung, J. Y. H. Kim, H. I. Choi, H. S. Kwak, and S. J. Sim, "Magnetophoretic sorting of microdroplets with different microalgal cell densities for rapid isolation of fast growing strains," *Sci Rep,* vol. 7, no. 1, p. 10390, Sep 4 2017.

[212] J. Tullis, C. L. Park, and P. Abbyad, "Selective fusion of anchored droplets via changes in surfactant concentration," *Lab Chip*, vol. 14, no. 17, pp. 3285-9, Sep 7 2014.

[213] T. D. Perroud *et al.*, "Isotropically etched radial micropore for cell concentration, immobilization, and picodroplet generation," *Lab Chip*, vol. 9, no. 4, pp. 507-15, Feb 21 2009.

[214] A. Huebner *et al.*, "Static microdroplet arrays: a microfluidic device for droplet trapping, incubation and release for enzymatic and cell-based assays," *Lab Chip*, vol. 9, no. 5, pp. 692-8, Mar 7 2009.

[215] J. H. Jung, T. J. Park, S. Y. Lee, and T. S. Seo, "Homogeneous biogenic paramagnetic nanoparticle synthesis based on a microfluidic droplet generator," *Angew Chem Int Ed Engl*, vol. 51, no. 23, pp. 5634-7, Jun 4 2012.

[216] E. Um, E. Rha, S. L. Choi, S. G. Lee, and J. K. Park, "Mesh-integrated microdroplet array for simultaneous merging and storage of single-cell droplets," *Lab Chip*, vol. 12, no. 9, pp. 1594-7, May 7 2012.

[217] N. Ahmed, D. Sukovich, and A. Abate, "Operation of Droplet-Microfluidic Devices with a Lab Centrifuge," *Micromachines*, vol. 7, no. 12, p. 161, 2016.

[218] Y. Y. Chen, Z. M. Chen, and H. Y. Wang, "Enhanced fluorescence detection using liquid-liquid extraction in a microfluidic droplet system," *Lab Chip*, vol. 12, no. 21, pp. 4569-75, Nov 7 2012.

[219] P. Mary, A. Chen, I. Chen, A. R. Abate, and D. A. Weitz, "On-chip background noise reduction for cell-based assays in droplets," *Lab Chip*, vol. 11, no. 12, pp. 2066-70, Jun 21 2011.

[220] S. C. Shih *et al.*, "A droplet-to-digital (D2D) microfluidic device for single cell assays," *Lab Chip*, vol. 15, no. 1, pp. 225-36, Jan 7 2015.

[221] P. Abbyad, R. Dangla, A. Alexandrou, and C. N. Baroud, "Rails and anchors: guiding and trapping droplet microreactors in two dimensions," *Lab Chip,* vol. 11, no. 5, pp. 813-21, Mar 7 2011.

[222] M. Sun, S. S. Bithi, and S. A. Vanapalli, "Microfluidic static droplet arrays with tuneable gradients in material composition," *Lab Chip,* vol. 11, no. 23, pp. 3949-52, Dec 7 2011.

[223] M. Sun, Z. S. Khan, and S. A. Vanapalli, "Blood plasma separation in a long two-phase plug flowing through disposable tubing," *Lab Chip,* vol. 12, no. 24, pp. 5225-30, Dec 21 2012.

[224] R. M. Schoeman, E. W. Kemna, F. Wolbers, and A. van den Berg, "High-throughput deterministic single-cell encapsulation and droplet pairing, fusion, and shrinkage in a single microfluidic device," *Electrophoresis,* vol. 35, no. 2-3, pp. 385-92, Feb 2014.

[225] P. E. Verboket, O. Borovinskaya, N. Meyer, D. Gunther, and P. S. Dittrich, "A new microfluidics-based droplet dispenser for ICPMS," *Anal Chem,* vol. 86, no. 12, pp. 6012-8, Jun 17 2014.

[226] K. Iwai, K. C. Shih, X. Lin, T. A. Brubaker, R. D. Sochol, and L. Lin, "Finger-powered microfluidic systems using multilayer soft lithography and injection molding processes," *Lab Chip,* vol. 14, no. 19, pp. 3790-9, Oct 7 2014.

[227] X. Huang *et al.*, "On-site formation of emulsions by controlled air plugs," *Small,* vol. 10, no. 4, pp. 758-65, Feb 26 2014.

[228] T. Jing, R. Ramji, M. E. Warkiani, J. Han, C. T. Lim, and C. H. Chen, "Jetting microfluidics with size-sorting capability for single-cell protease detection," *Biosens Bioelectron,* vol. 66, pp. 19-23, Apr 15 2015.

[229] M. Rhee *et al.*, "Pressure stabilizer for reproducible picoinjection in droplet microfluidic systems," *Lab Chip,* vol. 14, no. 23, pp. 4533-9, Dec 7 2014.

[230] E. Um, S.-G. Lee, and J.-K. Park, "Random breakup of microdroplets for single-cell encapsulation," *Applied Physics Letters,* vol. 97, no. 15, p. 153703, 2010.

[231] X. Shi, L. I. Lin, S. Y. Chen, S. H. Chao, W. Zhang, and D. R. Meldrum, "Real-time PCR of single bacterial cells on an array of adhering droplets," *Lab Chip,* vol. 11, no. 13, pp. 2276-81, Jul 7 2011.

[232] T. D. Rane, H. C. Zec, C. Puleo, A. P. Lee, and T. H. Wang, "Droplet microfluidics for amplification-free genetic detection of single cells," *Lab Chip,* vol. 12, no. 18, pp. 3341-7, Sep 21 2012.

[233] J. R. Haliburton, W. Shao, A. Deutschbauer, A. Arkin, and A. R. Abate, "Genetic interaction mapping with microfluidic-based single cell sequencing," *PLoS One,* vol. 12, no. 2, p. e0171302, 2017.

[234] S. S. Terekhov *et al.*, "Microfluidic droplet platform for ultrahigh-throughput single-cell screening of biodiversity," *PNAS,* vol. 114, no. 10, pp. 2550-2555, 2017.

[235] B. Kintses *et al.*, "Picoliter cell lysate assays in microfluidic droplet compartments for directed enzyme evolution," *Chem Biol,* vol. 19, no. 8, pp. 1001-9, Aug 24 2012.

[236] M. Hosokawa, Y. Nishikawa, M. Kogawa, and H. Takeyama, "Massively parallel whole genome amplification for single-cell sequencing using droplet microfluidics," *Sci Rep,* vol. 7, no. 1, p. 5199, Jul 12 2017.

[237] M. He, J. S. Edgar, G. D. M. Jeffries, R. M. Lorenz, P. Shelby, and D. T. Chiu, "Selective encapsulation of single cells and subcellular organelles into picoliter-and-femtoliter-volume droplets," *Anal Chem,* vol. 77, pp. 1539-1544, 2005.

[238] S. Juul *et al.*, "Detection of single enzymatic events in rare or single cells using microfluidics," *ACS Nano,* vol. 5, no. 10, pp. 8305-8310, 2011.

[239] T. Konry, I. Smolina, J. M. Yarmush, D. Irimia, and M. L. Yarmush, "Ultrasensitive detection of low-abundance surface-marker protein using isothermal rolling circle amplification in a microfluidic nanoliter platform," *Small,* vol. 7, no. 3, pp. 395-400, Feb 7 2011.

[240] P. Mary, L. Dauphinot, N. Bois, M. C. Potier, V. Studer, and P. Tabeling, "Analysis of gene expression at the single-cell level using microdroplet-based microfluidic technology," *Biomicrofluidics,* vol. 5, no. 2, p. 24109, Jun 2011.

[241] S. Q. Gu, Y. X. Zhang, Y. Zhu, W. B. Du, B. Yao, and Q. Fang, "Multifunctional picoliter droplet manipulation platform and its application in single cell analysis," *Anal Chem,* vol. 83, no. 19, pp. 7570-6, Oct 1 2011.

[242] K. Hettiarachchi, H. Kim, and G. W. Faris, "Optical manipulation and control of real-time PCR in cell encapsulating microdroplets by IR laser," *Microfluidics and Nanofluidics,* vol. 13, no. 6, pp. 967-975, 2012.

[243] E. Z. Macosko *et al.*, "Highly Parallel Genome-wide Expression Profiling of Individual Cells Using Nanoliter Droplets," *Cell,* vol. 161, no. 5, pp. 1202-14, May 21 2015.

[244] E. X. Ng, M. A. Miller, T. Jing, and C. H. Chen, "Single cell multiplexed assay for proteolytic activity using droplet microfluidics," *Biosens Bioelectron,* vol. 81, pp. 408-14, Jul 15 2016.

[245] J. Alles *et al.*, "Cell fixation and preservation for droplet-based single-cell transcriptomics," *BMC Biol,* vol. 15, no. 1, p. 44, May 19 2017.

[246] M. Pellegrino *et al.*, "High-throughput single-cell DNA sequencing of acute myeloid leukemia tumors with droplet microfluidics," *Genome Res,* vol. 28, no. 9, pp. 1345-1352, Sep 2018.

[247] W. Stephenson *et al.*, "Single-cell RNA-seq of rheumatoid arthritis synovial tissue using low-cost microfluidic instrumentation," *Nat Commun*, vol. 9, no. 1, p. 791, Feb 23 2018.

[248] S. Guo, W. N. Lin, Y. Hu, G. Sun, D. T. Phan, and C. H. Chen, "Ultrahigh-throughput droplet microfluidic device for single-cell miRNA detection with isothermal amplification," *Lab Chip*, vol. 18, no. 13, pp. 1914-1920, Jun 26 2018.

[249] R. M. Schoeman, W. T. E. van den Beld, E. W. M. Kemna, F. Wolbers, J. C. T. Eijkel, and A. van den Berg, "Electrofusion of single cells in picoliter droplets," *Sci Rep*, vol. 8, no. 1, p. 3714, Feb 27 2018.

[250] X. Li, M. Aghaamoo, S. Liu, D. H. Lee, and A. P. Lee, "Lipoplex-Mediated Single-Cell Transfection via Droplet Microfluidics," *Small*, vol. 14, no. 40, p. e1802055, Oct 2018.

[251] H. S. Kim, A. R. Guzman, H. R. Thapa, T. P. Devarenne, and A. Han, "A droplet microfluidics platform for rapid microalgal growth and oil production analysis," *Biotechnol Bioeng*, Jan 1 2016.

[252] M. Ito, H. Sugiura, S. Ayukawa, D. Kiga, and M. Takinoue, "A bacterial continuous culture system based on a microfluidic droplet open reactor," *Analytical Sciences*, vol. 32, pp. 61-66, 2016.

[253] J. Dai, H. S. Kim, A. R. Guzman, W.-B. Shim, and A. Han, "A large-scale on-chip droplet incubation chamber enables equal microbial culture time," *RSC Adv.*, vol. 6, no. 25, pp. 20516-20519, 2016.

[254] P. K. Periyannan Rajeswari, H. N. Joensson, and H. Andersson-Svahn, "Droplet size influences division of mammalian cell factories in droplet microfluidic cultivation," *Electrophoresis*, vol. 38, no. 2, pp. 305-310, Jan 2017.

[255] S. Chowdhuri, C. M. Cole, and N. K. Devaraj, "Encapsulation of Living Cells within Phospholipid Liposomes Formed by the Inverse-Emulsion Technique," *Chembiochem,* Feb 25 2016.

[256] Y.-Y. Chen and H.-Y. Wang, "Fabrication and characterization of polyelectrolyte microcarriers for microorganism cultivation through a microfluidic droplet system," *Biomicrofluidics,* vol. 10, no. 1, p. 014126, 2016.

[257] Y.-C. Tan, K. Hettiarachchi, M. Siu, Y.-R. Pan, and A. P. Lee, "Controlled microfluidic encapsulation of cells, proteins, and microbeads in lipid vesicles," *J. Am. Chem. Soc.,* vol. 128, pp. 5656-5658, 2006.

[258] J. Q. Boedicker, L. Li, T. R. Kline, and R. F. Ismagilov, "Detecting bacteria and determining their susceptibility to antibiotics by stochastic confinement in nanoliter droplets using plug-based microfluidics," *Lab Chip,* vol. 8, no. 8, pp. 1265-72, Aug 2008.

[259] A. Huebner *et al.,* "Development of quantitative cell-based enzyme assays in microdroplets," *Anal Chem,* vol. 80, no. 10, pp. 3890-3896, 2008.

[260] A. Funfak, J. Cao, O. S. Wolfbeis, K. Martin, and J. M. Köhler, "Monitoring cell cultivation in microfluidic segments by optical pH sensing with a micro flow-through fluorometer using dye-doped polymer particles," *Microchimica Acta,* vol. 164, no. 3-4, pp. 279-286, 2008.

[261] I. Sinn *et al.,* "Asynchronous magnetic bead rotation (AMBR) biosensor in microfluidic droplets for rapid bacterial growth and susceptibility measurements," *Lab Chip,* vol. 11, no. 15, pp. 2604-11, Aug 7 2011.

[262] A. Funfak, J. Cao, A. Knauer, K. Martin, and J. M. Kohler, "Synergistic effects of metal nanoparticles and a phenolic uncoupler using microdroplet-based two-

dimensional approach," *Journal of Environmental Monitoring,* vol. 13, no. 2, pp. 410-415, 2011.

[263] J. Cao, S. Schneider, R. Schultheiß, A. Schober, J. M. Köhler, and G. A. Groß, "“From microtiter plates to droplets” tools for micro-fluidic droplet processing," *Microsystem Technologies,* vol. 21, no. 3, pp. 539-548, 2013.

[264] J. Cao, J. Goldhan, K. Martin, and J. M. Köhler, "Investigation of mixture toxicity of widely used drugs caffeine and ampicillin in the presence of an ACE inhibitor on bacterial growth using droplet-based microfluidic technique," *Green Processing and Synthesis,* vol. 2, no. 6, 2013.

[265] J. Cao *et al.*, "Application of micro-segmented flow for two-dimensional characterization of the combinatorial effect of zinc and copper ions on metal-tolerant Streptomyces strains," *Appl Microbiol Biotechnol,* vol. 97, no. 20, pp. 8923-30, Oct 2013.

[266] F. Lyu, M. Xu, Y. Cheng, J. Xie, J. Rao, and S. K. Tang, "Quantitative detection of cells expressing BlaC using droplet-based microfluidics for use in the diagnosis of tuberculosis," *Biomicrofluidics,* vol. 9, no. 4, p. 044120, Jul 2015.

[267] M. Schwarz-Schilling, L. Aufinger, A. Muckl, and F. C. Simmel, "Chemical communication between bacteria and cell-free gene expression systems within linear chains of emulsion droplets," *Integrative Biology,* vol. 8, pp. 564-570, 2016.

[268] L. Boitard *et al.*, "Monitoring single-cell bioenergetics via the coarsening of emulsion droplets," *Proc Natl Acad Sci U S A,* vol. 109, no. 19, pp. 7181-6, May 8 2012.

[269] T. Beneyton *et al.*, "High-throughput screening of filamentous fungi using nanoliter-range droplet-based microfluidics," *Sci Rep,* vol. 6, p. 27223, Jun 7 2016.

[270] T. Beneyton, S. Thomas, A. D. Griffiths, J. M. Nicaud, A. Drevelle, and T. Rossignol, "Droplet-based microfluidic high-throughput screening of heterologous enzymes secreted by the yeast Yarrowia lipolytica," *Microb Cell Fact,* vol. 16, no. 1, p. 18, Jan 31 2017.

[271] H. N. Joensson *et al.*, "Detection and analysis of low-abundance cell-surface biomarkers using enzymatic amplification in microfluidic droplets," *Angew Chem Int Ed Engl,* vol. 48, pp. 2518-2521, 2009.

[272] T. Konry, M. Dominguez-Villar, C. Baecher-Allan, D. A. Hafler, and M. L. Yarmush, "Droplet-based microfluidic platforms for single T cell secretion analysis of IL-10 cytokine," *Biosens Bioelectron,* vol. 26, no. 5, pp. 2707-10, Jan 15 2011.

[273] S. Makulska, S. Jakiela, and P. Garstecki, "A micro-rheological method for determination of blood type," *Lab Chip,* vol. 13, no. 14, pp. 2796-801, Jul 21 2013.

[274] N. Shembekar, H. Hu, D. Eustace, and C. A. Merten, "Single-Cell Droplet Microfluidic Screening for Antibodies Specifically Binding to Target Cells," *Cell Rep,* vol. 22, no. 8, pp. 2206-2215, Feb 20 2018.

[275] J. C. Baret, Y. Beck, I. Billas-Massobrio, D. Moras, and A. D. Griffiths, "Quantitative cell-based reporter gene assays using droplet-based microfluidics," *Chem Biol,* vol. 17, no. 5, pp. 528-36, May 28 2010.

[276] M. Girault *et al.*, "An on-chip imaging droplet-sorting system: a real-time shape recognition method to screen target cells in droplets with single cell resolution," *Sci Rep,* vol. 7, p. 40072, Jan 6 2017.

[277] A. Huebner *et al.*, "Quantitative detection of protein expression in single cells using droplet microfluidics," *Chem Commun (Camb),* no. 12, pp. 1218-20, Mar 28 2007.

[278] J. Lim, J. r. m. Vrignon, P. Gruner, C. S. Karamitros, M. Konrad, and J.-C. Baret, "Ultra-high throughput detection of single cell β-galactosidase activity in droplets

using micro-optical lens array," *Applied Physics Letters,* vol. 103, no. 20, p. 203704, 2013.

[279] L. Li, Q. Wang, J. Feng, L. Tong, and B. Tang, "Highly sensitive and homogeneous detection of membrane protein on a single living cell by aptamer and nicking enzyme assisted signal amplification based on microfluidic droplets," *Anal Chem,* vol. 86, no. 10, pp. 5101-7, May 20 2014.

[280] A. Kulesa, J. Kehe, J. E. Hurtado, P. Tawde, and P. C. Blainey, "Combinatorial drug discovery in nanoliter droplets," *Proc Natl Acad Sci U S A,* vol. 115, no. 26, pp. 6685-6690, Jun 26 2018.

[281] F. Lyu *et al.*, "Phenotyping antibiotic resistance with single-cell resolution for the detection of heteroresistance," *Sensors and Actuators B: Chemical,* vol. 270, pp. 396-404, 2018.

[282] F. Wimmers *et al.*, "Single-cell analysis reveals that stochasticity and paracrine signaling control interferon-alpha production by plasmacytoid dendritic cells," *Nat Commun,* vol. 9, no. 1, p. 3317, Aug 20 2018.

[283] A. Feuerborn, A. Prastowo, P. R. Cook, and E. Walsh, "Merging drops in a Teflon tube, and transferring fluid between them, illustrated by protein crystallization and drug screening," *Lab Chip,* vol. 15, no. 18, pp. 3766-75, Aug 25 2015.

[284] A. Prastowo, A. Feuerborn, P. R. Cook, and E. J. Walsh, "Biocompatibility of fluids for multiphase drops-in-drops microfluidics," *Biomed Microdevices,* vol. 18, no. 114, 2016.

[285] J.-u. Shim *et al.*, "Ultrarapid generation of femtoliter microfluidic droplets for single-molecule-counting immunoassays," *ACS Nano,* vol. 7, no. 7, pp. 5955-5964, 2013.

[286] V. Linder, S. K. Sia, and G. M. Whitesides, "Reagent-loaded cartridges for valveless and automated fluid delivery in microfluidic devices," *Anal Chem,* vol. 77, pp. 64-71, 2005.

[287] R. H. Cole *et al.*, "Printed droplet microfluidics for on demand dispensing of picoliter droplets and cells," *Proc Natl Acad Sci U S A,* vol. 114, no. 33, pp. 8728-8733, Aug 15 2017.

# Appendix A: List of Measured Interfacial Tension

Below is a list of equilibrium interfacial tension of different fluids measured with pendant drop method. A small drop (~500 nl) of the heavy phase fluid (fluid with higher density) is formed at the tip of a needle connected to a Teflon tube and syringe pump (Harvard Ultra) for volume and flow rate control. The drop is then immersed in the light phase fluid (the one with lower density) loaded in a transparent polystyrene cuvette. The interfacial tension is calculated using software and hardware provided by First Ten Angstroms, which requires a length scale to be defined (i.e. needle tip as measured with a digital caliper) and fluid density as provided by the manufacturer. Measurements were taken at room temperature and after the system reaches equilibrium. Average value and the standard deviation are calculated from three independent single measurements or from three time points of one drop after reaching equilibrium in longer-term measurements.

| Heavy phase | Light phase | Interfacial tension (mN/m) |
|---|---|---|
| HFE-7500 | air | 16.01 ± 0.13 |
| | pure water | 35.80 ± 0.11 |
| | RPMI + 10% FBS | 24.25 ± 0.28 |
| | Tetradecane | 2.29 ± 0.09 |
| | Tetradecane + 0.25% Span 80 | 2.31 ± 0.05 |
| | Tetradecane + 1% Span 80 | 2.31 ± 0.03 |
| | 5 cSt silicone oil | <1 |
| | 5 cSt silicone oil + 0.25% Abil EM180 | <1 |
| FC-40 | air | 16.04 ± 0.28 |
| | pure water | 53.09 ± 0.26 |
| | DMEM | 41.10 ± 0.60 |
| | DMEM + 10% FBS | 21.24 ± 0.65 |
| | RPMI + 10% FBS | 33.37 ± 0.49 |
| | Tetradecane | 5.95 ± 0.15 |
| | Tetradecane + 0.25% Span 80 | 5.96 ± 0.15 |
| | Tetradecane + 1% Span 80 | 5.96 ± 0.14 |
| | 5 cSt silicone oil | 4.14 ± 0.13 |
| | 5 cSt silicone oil + 0.25% Abil EM180 | 4.01 ± 0.05 |
| HFE-7500 + FC-40 (1:1 ratio) | air | 16.12 ± 0.33 |
| | pure water | 49.51 ± 0.59 |

| | | |
|---|---|---|
| | RPMI + 10% FBS | 30.43 ± 0.36 |
| | Tetradecane | 3.93 ± 0.15 |
| | Tetradecane + 0.25% Span 80 | 3.91 ± 0.15 |
| | Tetradecane + 1% Span 80 | 3.84 ± 0.26 |
| | 5 cSt silicone oil | 1.71 ± 0.14 |
| | 5 cSt silicone oil + 0.25% Abil EM180 | 1.76 ± 0.09 |
| RPMI + 10% FBS | Tetradecane | 17.7 ± 0.40 |
| | Tetradecane + 0.25% Span 80 | 1.88 ± 0.22 |
| | Tetradecane + 1% Span 80 | 1.26 ± 0.06 |
| | 5 cSt silicone oil | 19.39 ± 1.09 |
| | 5 cSt silicone oil + 0.25% Abil EM180 | 5.69 ± 0.31 |

# Appendix B: Comments on the contact angle of a sessile drop immersed into a liquid

## I. General Young's equation

For a partially wetting liquid on a solid substrate at equilibrium, as sketched in Figure 1, equating the capillary forces at the contact line results in the following relation known as Young's equation [1-4],

$$\gamma_{LG} \cos\theta = \gamma_{SG} - \gamma_{SL} \tag{1}$$

where $\gamma_{LG}$, $\gamma_{SG}$ and $\gamma_{SL}$ are the interfacial tension of the liquid/gas, solid/gas and solid/liquid interfaces, respectively, and $\theta$ is the contact angle. Note that here gas could be replaced with a second liquid for the immersed drop case.

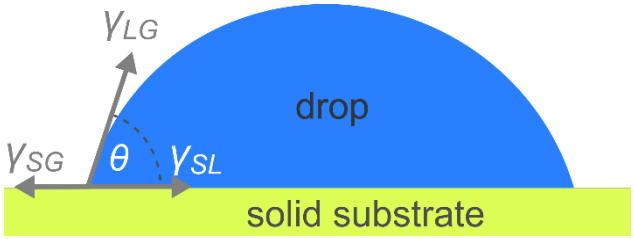


Figure 1 Illustration of a sessile drop on a solid substrate. Balance of interfacial tensions ($\gamma$) between the three phases – liquid/gas (*LG*), solid/gas (*SG*) and solid/liquid (*SL*) – forms a contact angle $\theta$ at the triple contact line, i.e. the intersection of the three interfaces.

## II. Young's equation for two liquids on a solid substrate

In the case of Paper 3 and 4, the sessile drop (liquid 1) on a solid substrate is immersed in a second liquid (liquid 2). Assuming the contact angles of liquid 1 and liquid 2 on the substrate (in air) are known, the contact angle of liquid 1 immersed into liquid 2 on the same substrate can be deducted from the above Young's equation [4]. Young's equations for each liquid are

$$\gamma_{L1,G} \cos\theta_{L1,G,S} = \gamma_{SG} - \gamma_{S,L1} \tag{2}$$

$$\gamma_{L2,G} \cos \theta_{L2,G,S} = \gamma_{SG} - \gamma_{S,L2} \quad (3)$$

Combining Equation (2) and (3) yields

$$\gamma_{L1,G} \cos \theta_{L1,G,S} - \gamma_{L2,G} \cos \theta_{L2,G,S} = \gamma_{S,L2} - \gamma_{S,L1} \quad (4)$$

For the case in which liquid 1 is immersed into liquid 2, liquid 2 replaces gas in Equation 1, therefore the Young's equation is

$$\gamma_{L1,L2} \cos \theta_{L1,L2,S} = \gamma_{S,L2} - \gamma_{S,L1} \quad (5)$$

Combining Equation 4 and 5 we could obtain the following equation [4],

$$\cos \theta_{L1,L2,S} = \frac{\gamma_{L1,G} \cos \theta_{L1,G,S} - \gamma_{L2,G} \cos \theta_{L2,G,S}}{\gamma_{L1,L2}} \quad (6)$$

$$\theta_{L1,L2,S} = \cos^{-1}\left(\frac{\gamma_{L1,G} \cos \theta_{L1,G,S} - \gamma_{L2,G} \cos \theta_{L2,G,S}}{\gamma_{L1,L2}}\right) \quad (7)$$

## III. Calculating liquid/liquid/solid contact angle for the case in Paper 3

For the case of sessile drops on polystyrene tissue culture Petri dish (PS) as in Paper 3 and 4, Table 1 lists the parameters to be used for estimating contact angles in FC-40. FC-40 contact angle is measured as approximately zero as it appears to completely wet the Petri dish surface.

Table 1 Parameters used to predict sessile drop contact angles in FC-40/on a Petri dish

| Liquid | Surface tension $\gamma_{LG}$ (mN/m) | Reference | Contact angle θ (°) | Reference |
|---|---|---|---|---|
| water | 72 | [5] | 55 | Paper 3 (SI) |
| DMEM | 72 | [6] | 43 | Paper 3 (SI) |
| DMEM + 10% FBS | 52 | [6] | 41 | Paper 3 (SI) |
| FC-40 | 16 | Appendix A | 0 | Measurement |

Table 2 presents the predicted liquid/liquid/solid contact angle based on calculation with Equation (7). The measured contact angles are taken from the Supplementary Information of Paper 3 (Figure S1).

Table 2 Calculated and measured contact angles of different liquids on a Petri dish surface, immersed in FC-40

| Liquid (immersed in FC-40) | Calculated $\cos^{-1}\theta$ | Calculated contact angle θ (°) | Measured contact angle θ (°) |
|---|---|---|---|
| water | 0.48 | 61 | 78 |
| DMEM | 0.89 | 27 | 64 |
| DMEM + 10% FBS | 1.10 | - | 73 |

In Table 2, the calculated values of the contact angle are well below the measured value. We suggest several reasons for this. First, since the drops are deposited after the Petri dish is filled with FC-40, the liquid has to displace the FC-40 to reach equilibrium. Therefore, the measured contact angle values are closer to the advancing contact angle values. This argument is supported by the fact that the measured water advancing contact angle is ~80° (Figure S1, Paper 3), close to the measured contact angle 78°. The calculated contact angle is an equilibrium value which is between the receding and advancing contact angle values. Second, as discussed in Paper 3, contact line pinning due to molecule adsorption can prevent spreading. Due to this pinning effect, the contact angle of DMEM + 10% FBS in air (Table 1) is presumably overestimated, which in turn affects the calculation of predicted contact angle in Table 2 (here the liquid is predicted to spread). Since contact line pinning prevents spreading, the measured contact angle of this liquid also becomes higher.

## References


[1] R. Tadmor, "Line energy and the relation between advancing, receding, and young contact angles," *Langmuir,* vol. 20, pp. 7659-7664, 2004.

[2] J. Berthier and K. Brakke, *The physics of microdroplets*. Wiley, 2012.

[3] P.-G. d. Gennes, F. Brochard-Wyart, and D. Quéré, *Capillarity and wetting phenomena: drops, bubbles, pearls, waves*. USA: Springer Science+Business Media, Inc., 2010.

[4] J. Berthier and P. Silberzan, *Microfluidics for Biotechnology* Second Edition ed. USA: Artech House, 2010.

[5] N. B. Vargaftik, B. N. Volkov, and L. D. Voljak, "International tables of the surface tension of water," *Journal of Physical and Chemical Reference Data*, vol. 12, no. 3, pp. 817-820, 1983.

[6] E. A. Vogler, "A thermodynamic model of short-term cell adhesion in vitro," *Colloids and Surfaces*, vol. 42, pp. 233-254, 1989.